UNIVERSIDAD DE GRANADA
DEPARTAMENTO DE BIOQUÍMICA
Y BIOLOGÍA MOLECULAR I
FACULTAD DE CIENCIAS

IDENTIFICATION OF NOVEL INFLAMMATORY SERUM BIOMARKER SIGNATURES ASSOCIATED WITH PANCREATIC CANCER AND MOLECULAR CHARACTERIZATION OF ANTITUMOUR AGENTS OVER PROLIFERATION AND APOPTOSIS IN VITRO

DETERMINACIÓN DE BIOMARCADORES SÉRICOS EN PACIENTES CON ADENOCARCINOMA DE PÁNCREAS Y CARACTERIZACIÓN MOLECULAR DE AGENTES ANTITUMORALES SOBRE EL CONTROL DE LA PROLIFERACIÓN CELULAR Y APOPTOSIS IN VITRO

CAROLINA TORRES PERALES

Editor: Editorial de la Universidad de Granada
Autor: Carolina Torres Perales
D.L.: GR 896-2014
ISBN: 978-84-9028-918-1

El doctorando, **Carolina Torres Perales** y los directores de la tesis **Dña. Ana Linares Gil** y **Dña. Sonia Perales Romero**, garantizamos, al firmar esta tesis doctoral, que el trabajo ha sido realizado por el doctorando bajo la dirección de los directores de la tesis y hasta donde nuestro conocimiento alcanza, en la realización del trabajo, se han respetado los derechos de otros autores a ser citados, cuando se han utilizado sus resultados o publicaciones.

Granada, a 14 de Noviembre de 2013

Director/es de la Tesis

Fdo.: Ana Linares Gil

Director/es de la Tesis

Fdo.: Sonia Perales Romero

Doctorando

Fdo.: Carolina Torres Perales

Este trabajo ha sido desarrollado dentro del grupo de investigación Metabolismo de SMC en la Aterosclerosis (CTS-168), perteneciente al Departamento de Bioquímica y Biología Molecular I de l Facultad de Ciencias de la Universidad de Granada. La investigación realizada ha sido financiada por el Ministerio de Educación mediante la concesión de una beca predoctoral de Formación de Profesorado Universitario (FPU) y a través de los proyectos "Estudio de correlación de la respuesta clínica a Gemcitabina y a Erlotinib en pacientes con adenocarcinoma de páncreas y la expresión génica por microarrays en células de tejido y de sangre periférica" (Ref.: H/OH-TRR-08/59) financiado por FIBAO y ROCHE Farma y "Determinación de biomarcadores en pacientes con adenocarcinoma de páncreas y expresión génica por microarrays. Estudio de correlación de la respuesta clínica a Gemcitabina y a Erlotinib" (Ref.: EC08/ 00009) financiado por el Instituto de Salud Carlos III.

La formación de tercer ciclo para la obtención de la tesis se ha realizado en el programa de doctorado de Bioquímica y Biología Molecular (113.99.2) de la Universidad de Granada.

A mi familia

A Curro

> *"Anyone who has never made a mistake has never tried anything new." - Albert Einstein*

CONTENTS:

ABBREVIATIONS

- 7-AAD: 7-amino-actinomycin D
- ACE: Angiotensin converting enzyme
- ADAMs: A disintegrin and metalloproteinase
- AIC: apoptosis inhibitory complex
- AIF: apoptosis-inducing factor
- ALDH: Aldehyde dehydrogenase
- Ang-1: Angiopoietin 1
- Ang-2: Angiopoietin 2
- ANOVA: analysis of variance
- APAF1: Apoptosis protease-activating factor-1
- APC: antigen-presenting cells
- ATCC: American Type Cell Culture
- ATM: Ataxia telangiectasia mutated
- AUC: area under the curve
- Bad: Bcl-2 antagonist of cell death
- Bak: Bcl-2 antagonistic killer
- Bax: Bcl-2 associated X protein
- Bcl-2: B cell lymphoma-2 protein
- BCL2A1: B-cell lymphoma 2-related protein A1
- BCL2A1: B-cell lymphoma 2-related protein A1
- Bcl-X_L: Bcl-extra long
- BMP: bone morphogenetic proteins
- BMP-2: Bone morphogenetic protein-2
- BNF-1: breast tumor novel factor 1
- BrdU: bromodeoxyuridine
- BSA: Bovine serum albumin
- CA: carcinoembryonic antigen
- CAC: centroacinar cell
- CAII: Carbonic anhydrase 2
- CCL2: chemokine (C-C motif) ligand 2
- CCL5: chemokine (C-C motif) ligand 5
- c-FLIP: Cellular FLICE (FADD-like IL-1β-converting enzyme)-inhibitory protein
- ChIP assay: chromatin immunoprecipitation assay
- Chk2: checkpoint kinase 2
- CI: combination index
- CI: Confidence interval
- cMV : cytomegalovirus immediate-early promoter
- Cp: crossing point
- CSF-1: colony stimulating factor 1
- Ct: cycle threshold
- CTGF: Connective tissue growth factor
- CTP-synthetase: cytidine triphosphate synthetase

- Cyt c: Cytochrome c
- dCDA: deoxycytidine deaminase
- dCK: deoxycytidine kinase
- dCMPDA: deoxycytidine monophosphate deaminase
- dCTD : deoxycytidine monophosphate deaminase
- dCTP: deoxycytidine triphosphate
- DF: Dilution factor
- dFdC: 2´-2´-difluorodeoxycytidine
- dFdCDP: 2´-2´-difluorodeoxycytidine diphosphate
- dFdCMP: 2´-2´-difluorodeoxycytidine monophosphate
- dFdCTP: 2´-2´-difluorodeoxycytidine triphosphate
- dFdU: difluorodeoxyuridine
- dFdUMP: 2´-2´-difluorodeoxyuridine monophosphate
- DC-HIL: Dendritic Cell–Heparin Integrin Ligand
- DI: DNA index
- DISC: death inducing signaling complex
- DMEM: Dulbecco's Modified Eagle medium
- DMSO: Dimethyl Sulfoxide
- DOPE: L-dioleoyl phosphatidylethanolamine
- E: PCR efficiency
- ECD: extracellular domain
- EDTA: Ethylenediaminetetraacetic acid
- EGFR: epidermal growth factor receptor
- EGTM: European Group of Tumor Markers
- EMT: epithelial-to-mesenchymal transition
- END: Endoglin
- ER: estrogen receptor
- ERBB-1: v-erb-b2 erythroblastic leukemia viral oncogene homolog 1
- ERK: extracellular signal-regulated kinase
- ESA: epithelial-specific antigen
- FACS: Fluorescence-activated cell sorting
- FADD: FAS-associated death domain protein
- FAP-1: Fas-associated phosphatase-1
- FBS: fetal bovine serum
- FC: fold change
- FGF: Fibroblast growth factor
- FGFR: fibroblast growth factor receptor
- FN1: fibronectin
- G418: Geneticin
- G6PD: glucose-6-phosphate dehydrogenase
- GBM: glioblastoma multiforme
- GDF: growth and differentiation factors
- GFAP : glial fibrillary acidic protein

- GFP: Green fluorescent protein
- GPNMB: Glycoprotein non-metastatic melanoma protein B
- GTE: Glucose/Tris/EDTA
- HA : hyaluronan
- HD: homozygous deletion
- HDM2: Human double minute 2
- HER-1: human epidermal growth factor receptor 1
- HER2/neu: heregulin/human epidermal growth-factor receptor 2
- HGFIN: Hematopoietic Growth Factor Inducible Neurokinin-1 type
- HR: hazard ratio
- IAP: inhibitor of apoptosis protein
- ICAM-1: Intercellular adhesion molecule-1
- ICD: intracellular domain
- IKK: IκB kinase complex
- IP samples: immunoprecipitated samples
- ITAM: Immunoreceptor Tyrosine-based Activation Motif
- LA: Luria Agar
- LAMP-1: lysosome-associated membrane protein
- LB: Luria Broth
- $LC_{50:}$ 50% lethal concentration
- LIF: Leukemia inhibitory factor
- LOOCV: Leave-one-out cross-validation
- LTR: retroviral long terminal repeats
- MAPK: mitogen-activated protein kinase
- MDM2: Mouse double minute 2
- MEK: MAP/ERK kinase
- MEKK: MEK kinase
- MIF: Müllerian inhibitory factor
- Mitf: microphthalemia-associated transcription factor
- MMLV: murine moloney leukemia virus
- MMP: matrix metalloproteinases
- MOMP: mitochondrial outer membrane permeabilization
- MTT: 3-(4,5-Dimethylthiazole- 2-yl)-2,5-diphenyltetrazolium bromide
- MUC4: Sialomucin complex SMC, an intramembrane ligand for ErbB2
- NACB: National academy of Clinical Biochemistry
- NICD: Notch intracellular domain
- NP40: Nonidep 40
- OD: optical density
- ORF: Open reading frame
- OS: overall survival
- OSM: Oncostatin M
- PA: phosphatidic acid
- PAI-1: plasminogen activator inhibitor 1 (serpine1)

- PAI-2: plasminogen activator inhibitor 2 (Serpinb2)
- PanIN: pancreatic intraepithelial neoplasia
- PBS: Phosphate buffered saline
- PC: phosphatidylcholine
- PCR: polymerase chain reaction
- PD: progressive disease
- PDAC: Pancreatic ductal adenocarcinoma
- Pdx1: transcription factor pancreatic and duodenal homeobox 1
- PE: phosphatidylethanolamine
- PI: prognosis index
- PI: propidium iodide
- PI3K: phosphatidylinositol 3-kinase
- PIPES: piperazine-N,N′-bis(2-hydroxypropanesulfonic acid
- PKD: polycystic kidney disease
- PMSF: phenylmethyldulfonyl fluoride
- PR: partial response
- pRS: retroviral silencing plasmid
- PS: phosphatidylserine
- PSC: pancreatic stellate cells
- PSC: Pancreatic stem cell
- R: relative expression ratio
- RAS: renin angiotensin system
- RGD : integrin-binding motif
- ROC: receiver operator characteristics curve
- SARA: SMAD anchor for receptor activation
- SC: Stem cell
- SCF: stem cell factor
- SD: stable disease
- SDS: sodium dodecyl sulfate
- Shh: Sonic Hedgehog
- SM: sphyngomielin
- Smac: second mitochondria-derived activator of apoptosis
- StD: standard deviation
- TBST: Tris-buffered Saline + Tween-20
- TE: Tris HCl/EDTA
- TEK: tyrosine kinase
- TF: Transcription factor
- TGF-α: transforming growth factor-α
- TGF-β: transforming growth factor β
- TIMP: tissue inhibitors of metalloproteinases
- Tm: melting temperature
- TNC : Tenascin
- TNF : Tumor necrosis factor

- TRAIL: TNF-related apoptosis inducing ligand
- UMK: uridine monophosphate kinase
- uPA: urokinase-type plasminogen activator
- VEGF: vascular endothelial growth factor
- VEGFR: vascular endothelial growth factor receptor
- WT: wild type
- β: Beta-coefficients

ABSTRACT /RESUMEN

Pancreatic ductal adenocarcinoma (PDAC) is the deadliest solid cancer and currently the fourth most frequent cause of cancer related deaths. PDAC is characterised by late diagnosis due to lack of early symptoms, extensive metastasis and high resistance to chemotherapy and radiation. Despite expanding research activities in the field of pancreatic tumour and vascular biology, there has been little substantial therapeutic progress regarding clinical endpoints over the past decades. Indeed, in contrast to the general trend of decreasing incidences for most cancers, the incidence and death rates for PDAC continue to increase.

In the 1990s, the introduction of the anti-metabolite, Gemcitabine improved clinical response in terms of pain reduction and weight loss. However, with a 5-year survival rate of 1–4% and an average survival period of 4–6 months, the prognosis of patients with PDAC remains extremely poor. Amongst the strategies to improve Gemcitabine therapy is its combination with targeted or cytotoxic agents. Notwithstanding, till date, only inhibition of the epidermal growth factor receptor (EGFR) has provided discrete clinically survival improvements. Erlotinib inhibits phosphorylation of the EGFR tyrosine kinase, blocking the downstream signalling, halting proliferation and tumour angiogenesis and inducing apoptosis.

Currently used therapies only slightly increase survival rates (mostly in small subsets of patients) and rarely result in long-term progression-free survival. Therefore, to substantially increase therapeutic response, the comprehensive elucidation of the mechanisms governing pancreatic cancer biology and chemotherapy resistance is mandatory. In this thesis, molecular mechanism related to proliferation, cell cycle alteration, differentiation, apoptosis and invasion were analyzed in vitro using pancreatic cancer cells and the before mentioned drugs.

As said before, amongst the reasons for this poor result highlight the delay in diagnosis, the cancer has almost always metastasized when detected and the development of drug-resistance to the available chemotherapy. Owing to the impact and the dramatic change that early diagnosis has in patient survival, better diagnostic tools for the detection and evaluation of this disease are urgently

needed. Thus, detection of early biomarkers and a better understanding of the response of PDAC patients to chemotherapy would be of critical importance in treating the disease. Serum is the preferred option to obtain specimens for testing malignant tumours as it can be taken via non-invasive methods and because, specifically the pancreas is difficult to access. For these reasons, serum-based cancer biomarkers constitute the easiest screening test.

Due to the increasing evidence of a link between cancer and inflammation we have focused in those inflammatory mediators that may constitute useful biomarkers for PDAC detection. We have speculated that altered levels of cytokines in the systemic circulation could be illustrative of their deregulation in the tumour microenvironment. Therefore serum protein predictive patterns based on cytokines could have great impact in the early prediction of new PDAC patients. Besides, serum cytokines levels in treated patients compared with non-treated patients could provide profiles of responses to therapy. Furthermore, the potential value of serum cytokines to predict clinical outcome in patients with PDAC and to establish a practical prognosis index was also analyzed in this work.

In the course of our evaluation, we have identified five cytokines that, being part of the tumour microenvironment, could enhance PDAC development and progression and they could represent novel perspectives for dealing with the disease. As patient sample size is small (just representative of the low incidence of this cancer), in vitro assays were carried out trying to validate the paramount role of one of this cytokines in PDAC. GPNMB/Osteoactivin was selected to analyze its implication in proliferation, cell cycle alteration, differentiation, apoptosis and invasion as it has recently related to poor prognostic in patients with breast cancer. Besides, it has been determined that Osteoactivin induces endothelial cell migration and subsequent angiogenesis. For the first time, the role of GPNMB/Osteoactivin in PDAC has been examined.

Our results show that GPNMB/Osteoactivin induces proliferation and abrogates apoptosis in pancreatic cancer cells. The major impact of GPNMB/Osteoactivin expression in pancreatic cancer cell is mediated by the enhancement of the

invasion. Due to its main membrane localization in cancer cells, GPNMB/Osteoactivin represents an interesting targeted therapy for cancer making Gpnmb/OA particularly attractive for antibody-based therapies because, as a target, it would be more readily accessible in cancer cells than in normal cells, thereby reducing potential complications owing to bystander effects.

El cáncer de páncreas (PDAC), pese a tener una incidencia de 2.68% entre todos los tipos de cáncer, representa la cuarta causa de muerte debida a cáncer a nivel mundial solamente precedido por los cánceres de pulmón y bronquios, próstata y colorectal en el caso de los hombres y por los cánceres de pulmón y bronquios, mama y colorectal en mujeres. 45.220 nuevos casos de PDAC se han estimado para el presente año en Estados Unidos de los cuales el 85% morirán de esta enfermedad. La alta agresividad del PDAC, menos del 5% de los pacientes con una esperanza de vida mayor de 5 meses, es debida principalmente al retraso en el diagnóstico, presentándose como una enfermedad metastásica e incurable en el momento de su detección, así como al escaso éxito de las terapias actuales. El desarrollo de la enfermedad es el resultado de un complejo proceso de acumulación de alteraciones genéticas y afectación de numerosas cascadas de señalización intracelulares lo que hace que sea una enfermedad altamente heterogénea.

En los años 1990s, la introducción del antimetabolito Gemcitabina mejoró la respuesta clínica de los pacientes. Sin embargo, el periodo de supervivencia medio continúa siendo de 4-6 meses. Entre las estrategias que se han estudiado para mejorar la terapia con Gemcitabina destacan sus combinaciones con otros agentes, especialmente con Erlotinib, un inhibidor del receptor EGFR. Esta combinación demostró mejoras discretas en la supervivencia de los pacientes.

Las terapias actuales como la Gemcitabina y el Erlotinib sólo consiguen pequeñas mejoras en la supervivencia. Por tanto, con el objetivo de mejorar la respuesta terapéutica de los pacientes con PDAC, son necesarios estudios moleculares que arrojen luz a los mecanismos que subyacen la progresión y la quimioresistencia del cáncer de páncreas. En esta tesis, el primer objetivo fue analizar los mecanismos moleculares relacionados con la proliferación, la alteración de la regulación del ciclo celular, la diferenciación, la inducción de la apoptosis y la invasión de células de cáncer de páncreas sometidas a las anteriormente citadas drogas. Con esta aproximación hemos determinado la implicación de numerosas rutas moleculares en la evasión de la acción de los agentes antitumorales.

El segundo objetivo de esta tesis doctoral es la determinación biomarcadores de diagnóstico, predictivos y de pronóstico para el PDAC. Dado el fuerte impacto que tiene el diagnóstico temprano en la supervivencia de los pacientes, la búsqueda de nuevas herramientas de diagnóstico para la detección y la evaluación de esta enfermedad mortal se han convertido en una necesidad urgente. La localización anatómica del páncreas hace muy difícil el acceso a este órgano. Un biomarcador ideal sería aquel que pudiera ser obtenido por métodos no invasivos. Las muestras de suero constituyen la opción más sencilla y preferida en la obtención de especímenes. De hecho, el único indicador de PDAC que se ha estado usando hasta la actualidad es el biomarcador sérico CA 19-9. Sin embargo, debido a que aparece alterado en otras patologías y a que su especificidad puede variar dependiendo del tamaño del tumor, recientemente se ha desaconsejado su empleo como prueba para el PDAC.

El cáncer de páncreas se caracteriza por una fuerte reacción desmoplástica y un microambiente constituido por grandes cantidades de matriz extracelular, proteínas, fibroblastos y células inflamatorias que por un lado constituyen una barrera que evitar la liberación adecuada de los agentes quimioterapéuticos al sitio de origen de la enfermedad y por otro, promueven la invasión y metástasis. Dada la relación con la inflamación, en nuestro grupo de investigación hemos analizado aquellos mediadores inflamatorios (citoquinas del suero) que podrían constituir biomarcadores útiles para el diagnóstico y pronóstico del PDAC utilizando un potente array de citoquinas (*RayBio*® *Human Cytokine Array*). Con esta aproximación, se determinaron 5 citoquinas que constituían un patrón diferencial de expresión entre pacientes diagnosticados con cáncer de páncreas e individuos sanos (marcadores de diagnóstico). A su vez, se estableció que 7 citoquinas podían ser consideradas como indicadores de respuesta/no respuesta a la quimioterapia en pacientes con adenocarcinoma de páncreas tratados con Gemcitabina en combinación con Erlotinib (marcadores de predicción). Por último, se determinó un índice de pronóstico que indica el riesgo relativo de muerte de cinco citoquinas cuando cambia su valor de expresión en una sola unidad (marcadores de pronóstico).

Como consecuencia del análisis de citoquinas anteriormente citado, hemos descrito a la citoquina GPNMB/Osteoactivin como un posible biomarcador de diagnóstico ya que está presente en el suero de pacientes de PDAC pero no en el de individuos sanos. Debido a su implicación en la agresividad de varios tipos de cánceres, especialmente el de mama, a que no existe información acerca de su papel en el PDAC y también debido a que presenta un patrón de expresión en membrana sólo en células cancerígenas lo que la convierte en una diana terapéutica ideal, ampliamos su estudio llevando a cabo análisis "in vitro" para determinar el papel de GPNMB/Osteoactivin en el desarrollo y progresión del cáncer de páncreas. Esto constituye el último de los tres grandes objetivos de esta tesis doctoral. Nuestros resultados han demostrado que GPNMB/Osteoactivin induce la proliferación e inhibe la apoptosis en células de cáncer de páncreas. El mayor impacto que tiene la expresión de GPNMB/Osteoactivin en células de cáncer de páncreas es mediado por la inducción de la invasión.

1

BACKGROUND

1.1 HISTOLOGY OF THE PANCREAS

1.1.1 Anatomy and physiology

The pancreas is a retroperitoneal organ that lies in an oblique position, behind the stomach, sloping upward from the c-loop of the duodenum to the spleen. In an adult, the pancreas weighs 75 to 100 g and is about 15 to 20 cm long. The fact that the pancreas is situated so deeply in the abdomen and is sealed in the retroperitoneum explains the poorly localized and sometimes ill-defined nature with which pancreatic pathology presents.

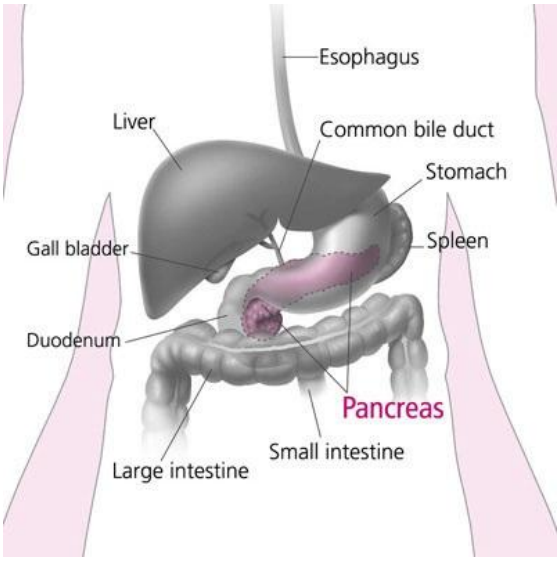

Figure 1.1 Localization of the pancreas and nearby organs.

The widest section is the head and the narrowest part is the tail. The middle section is called the body. The pancreas has a series of small tubes that drain into the pancreatic duct. The pancreatic duct joins the common bile duct and empties into the upper part of the small intestine, which is called the duodenum.

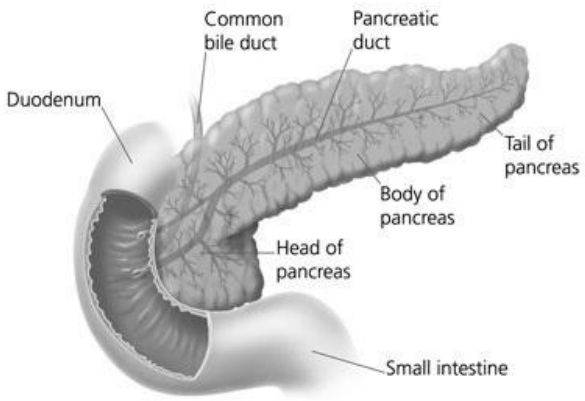

Figure 1.2 The pancreas is divided into several different subsections. The head of the pancreas is located nearest to the duodenum. The body of the pancreas is the largest section, located in the centre of the gland just below the stomach. The pancreas also has a tail, which is furthest from the duodenum.

The pancreas is a glandular organ and is comprised of two different functional units, exocrine and endocrine glands to regulate two major physiological processes: protein and carbohydrate digestion and glucose metabolism homeostasis, respectively. The exocrine pancreas accounts for about 85% of the pancreatic mass; 10% of the gland is accounted for by extracellular matrix and 4% by blood vessels and the major ducts, whereas only 2% of the gland is comprised of endocrine tissue. The endocrine and exocrine pancreas are sometimes thought of as functionally separate, but these different components of the organ are coordinated to allow an elegant regulatory feedback system for digestive enzyme and hormone secretion. This complex system regulates the type of digestion, its rate, and the processing and distribution of absorbed nutrients [1].

1.1.1.1 Exocrine Pancreas

The exocrine unit of the pancreas is composed of acinar cells which produce and secrete zymogens which pass through the duct and into the gastrointestinal tract which then add mucous and bicarbonate to the enzyme mixture. The centroacinar cells are found at the junction of the ducts and the acini.

The pancreas secretes approximately 500 to 800 ml per day of colorless, odorless,

alkaline, isosmotic pancreatic juice. Pancreatic juice is a combination of acinar cell and duct cell secretions. The acinar cells secrete amylase, proteases and lipases, enzymes responsible for the digestion of all three food types: carbohydrate, protein and fat. The acinar cells are pyramid-shaped, with their apices facing the lumen of the acinus. Near the apex of each cell are numerous enzyme-containing zymogen granules that fuse with the apical cell membrane [2].

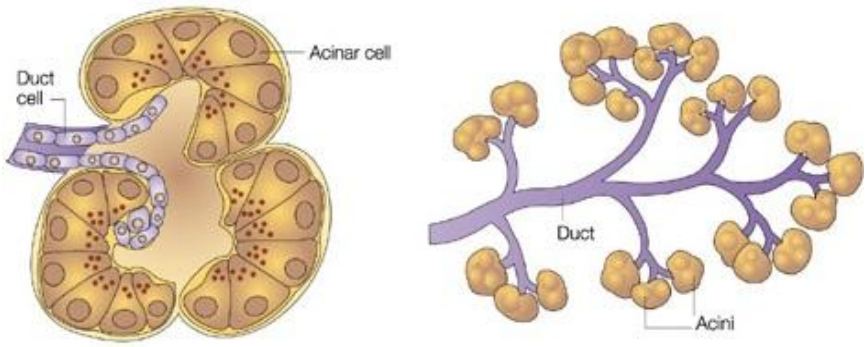

Figure 1.3 The exocrine pancreas consists of acinar and duct cells. The acinar cells produce digestive enzymes and constitute the bulk of the pancreatic tissue. They are organized into grape-like clusters that are at the smallest termini of the branching duct system. The ducts, which add mucous and bicarbonate to the enzyme mixture, form a network of increasing size, culminating in main and accessory pancreatic ducts that empty into the duodenum [3].

The centroacinar and intercalated duct cells secrete the water and electrolytes present in the pancreatic juice. About 40 acinar cells are arranged into a spherical unit called an acinus. Centroacinar cells are located near the center of the acinus and are responsible for fluid and electrolyte secretion. These cells contain the enzyme carbonic anhydrase, which is needed for bicarbonate secretion.

The acinar cells release pancreatic enzymes from their zymogen granules into the lumen of the acinus and these proteins combine with the water and bicarbonate secretions of the centroacinar cells. The pancreatic juice then travels into small intercalated ducts. Several small intercalated ducts join to form an interlobular duct. Cells in the interlobular ducts continue to contribute fluid and electrolytes to adjust the final concentrations of the pancreatic fluid. Interlobular ducts then join to form about 20 secondary ducts that empty into the main pancreatic duct.

Destruction of the branching ductal tree from recurrent inflammation, scarring, and deposition of stones eventually contributes to destruction of the exocrine pancreas and exocrine pancreatic insufficiency.

1.1.2 Endocrine Pancreas

The endocrine units or Islets of Langerhans are most numerous in the tail region of pancreas. The hormones they produce are secreted into the blood. The major endocrine cell types present are α, β, δ and PP cells which secrete glucagon, insulin, somatostatin and pancreatic polypeptide respectively.

1.2 NEOPLASMS OF THE PANCREAS

Due to the physiologic and cellular diversity of the pancreas, there is a spectrum of distinct pancreatic malignancies that possess histological and molecular features that recall the characteristics of the various normal cellular constituents [4]. Neoplasms of the pancreas are currently being classified based on that features together with the genetic and molecular changes underlying their development (obtained through the sequencing of more than 750.000.000 base pairs of DNA from 24 pancreatic cancers, has recently been completed, providing a unique understanding of the genetic changes, the so called pancreatic cancer genome project [5]). Molecular alterations often parallel these features, suggesting that molecular alterations can aid in diagnoses [6]. Pancreatic neoplasms encompass a wide array of clinical diseases, from benign cysts to deadly cancers and the genetic alterations underlying neoplasms of the pancreas are similarly diverse. Tumours arise in the pancreas with the features of the three major cell types of the pancreas: the acinar cells, endocrine cells and the pancreatic duct cells. Figure 1.4 summarizes the several types of pancreatic neoplasms. Pancreatic ductal adenocarcinoma (PDAC) is by far the most common pancreatic neoplasm, comprising around 90% of all pancreatic malignancies. Of these, 60% arises at the head of the pancreas while a 20% is located at neck and tail of the pancreas. The remaining is diffusely localized.

Pancreatic neoplasm	Histological features	Common genetic alterations
Ductal adenocarcinoma[a]	Ductal morphology; desmoplasia	*K-RAS*, *p16^{INK4a}*, *TP53*, *SMAD4*
Variants of ductal adenocarcinoma		
a. Medullary carcinoma	Poorly differentiated; intratumoral lymphocytes	*hMLH1*, *hMSH2*
b. Colloid (mucinous noncystic) carcinoma	Mucin pools	*MUC2 overexpression*
Acinar cell carcinoma	Zymogen granules	*APC*/β-*catenin*
Pancreatoblastoma	Squamoid nests, multilineage differentiation	*APC*/β-*catenin*
Solid pseudopapillary neoplasm	"Pseudo" papillae, solid and cystic areas, hyaline globules	*APC*/β-*catenin*, CD10 expression
Serous cystadenoma	Multilocular cysts; glycogen-rich epithelium	*VHL*
Pancreatic endocrine tumors	Hormone production	*MEN1*

Figure 1.4 Pancreatic neoplasm and associated genetic mutations[4].

1.3 PANCREATIC DUCTAL ADENOCARCINOMA

1.3.1 Epidemiology

Each year, the American Cancer Society estimates the numbers of new cancer cases and deaths expected in the United States in the current year and compiles the most recent data on cancer incidence, mortality and survival based on incidence data from the National Cancer Institute, the Centers for Disease Control and Prevention, and the North American Association of Central Cancer Registries and mortality data from the National Center for Health Statistics. For this year 2013, it has been estimated a number of 45.220 new cases of PDAC with an estimation of 38.460 deaths, which represents an 85% of patients dying due to the disease. Although PDAC accounts for only 2.68% of all cancers, it represents the fourth leading cancer-related death worldwide just remaining after lung and bronchus, prostate, and colorectum cancers in men and after lung and bronchus, breast, and colorectum cancers in women. In fact, together with the lung, pancreatic cancer has shown the least improvement [7].

1.3.2 Risk factors

A number of risk factors have been identified [8]. Pancreatic cancer is predominantly a disease of the elderly. Pancreatic cancer is rare before the age of 40 and the median age at diagnosis is 73 years. Smoking causes 20–25% of pancreatic cancer cases and is the most frequent cause of this tumour, yet it is the most preventable [9]. Only 5–10% of patients with pancreatic cancer have an underlying germline disorder, while the remaining cases seem to result from damage to genes occurred during life. Familial pancreatic cancer is defined in most studies as families in which a pair of first-degree relatives have been diagnosed with pancreatic tumours. Prospective analysis of families with this malignant disease shows that first-degree relatives of individuals with familial pancreatic cancer have a nine fold increased risk of this neoplasm over the general population. Familiar pancreatic cancer is usually related to mutation of the following genes: BRCA2, p16/CDKN2A, PRSS1, STK1/LKB1 and also with DNA

repair genes [10-12]. Chronic pancreatitis patients have up to 18-fold higher risk, and there is a relative risk of 1.8 in people with type II diabetes mellitus, compared to the general population [13].

1.3.3 Tumour initiation

As describe in section 1.1 the pancreas consists of three major compartments: acinar, islet and ductal. Although the histologic appearance of PDAC suggests a ductal origin, the frequent observation of premalignant acinar-to-ductal metaplasia in humans and mouse models suggest an acinar origin. A few investigators have even proposed that PDAC arises from islets of Langerhans, either from rare precursor cells or transdifferentiation of insulin-producing beta cells. Recent studies of pancreatic cancer have focused attention on yet another pancreatic cell type largely ignored for the past 40 years the centroacinar cell (CAC). This cell lies at the interface of the acinar structure and the ductal system and is continuous with both acinar and ductal lumens (Figure 1.5). Interest in the CAC reemerged with the finding that Notch signalling (a fundamental signalling system used by neighboring cells to communicate with each other in order to assume their proper developmental role) remains selectively active in these cells [14]. The Notch signalling pathway is widely used in development to regulate differentiation and in the embryonic pancreas, Notch is critical for maintaining pancreatic progenitor cells in an undifferentiated state. The persistence of Notch activity in CACs, coupled with their strategic location, identify this select adult population as a candidate stem cell (SC) for the exocrine pancreas and as such, as a potential source for the genesis of pancreatic cancer [15].

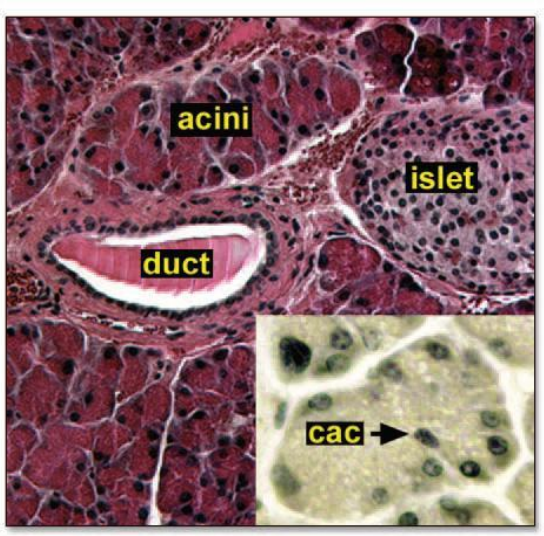

Figure 1.5 Pancreas histology. Histological section through a wild type mouse pancreas showing the islet, ductal, and acinar compartments. Inset shows one acinus in higher magnification with an arrow pointing to a centroacinar cell.

However, independently of the origin, a possible scenario for tumour initiation in solid organs is the malignant transformation of stem cells resident in the normal tissue. Somatic stem cells are intrinsically endowed with the capacity of self-renewal and would therefore only need to accumulate sequential mutations to undergo malignant transformation and give rise to a tumour. Normal stem cells undergo asymmetric cell division, with one daughter cell retaining self-renewal capacity and the other differentiating into a transit-amplifying cell, with limited proliferative potential; it is postulated that cancer stem cells divide in an identical manner[13].

All pancreatic cells, both from exocrine and endocrine lineages, are believed to originate from an initial cell progenitor expressing the transcription factor pancreatic and duodenal homeobox 1 (Pdx1). Pdx1 is a transcription factor necessary for pancreatic development and β-cell maturation. The process leading from the pancreatic stem cell to differentiated cell is depicted in Figure 1.6. The expression of this factor, together with the silencing of signalling mediated by Sonic hedgehog (Shh which plays a key role in regulating vertebrate organogenesis and also cell division of adult stem cells) in the surrounding mesenchymal tissue, initiates embryonic pancreas development. Pdx1 can be considered a critical

transcription factor in pancreatic commitment, although there are more actors implicated, since absence of this factor does not result in complete impairment of pancreas formation[16].

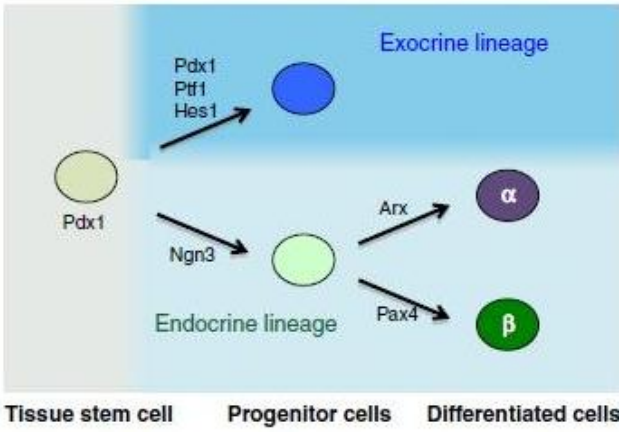

Figure 1.6 Development of the pancreas. Different transcription factors are responsible for the determination of cell fate during pancreas development. Cells that retain Pdx1 expression and initiate the expression of Ptf1 and Notch signalling progress towards an exocrine lineage. In contrast, the expression of Ngn3 determines an endocrine fate associated with differential expression of Arx and Pax4, which will then further differentiate these committed cells into α-cells and β-cell, respectively [17].

Different strategies are used to identify and isolate cancer stem cells from neoplasms. These strategies rely on characteristics associated with normal stem cells, including the expression of particular cell-surface markers, the capacity to efflux fluorescent dyes by multidrug transporters and the ability to clonally expand into spheres under specific culture conditions. So far, the most widely used strategies to identify cancer stem cells involve the evaluation of marker expression or efflux capacity [16]. For PDAC a number of distinct markers have been described. The first ones to be described were CD44, CD24, and epithelial-specific antigen (ESA) [18]. A second report showed that CD133 could also identify PCSCs [19]. In addition, cellular markers associated with drug resistance have been used to identify CSCs. Aldehyde dehydrogenase, ALDH, specifically ALDH1A1, is required for the synthesis of all-trans-retinoic acid, and high enzyme activity marks normal mouse pancreatic progenitor cells and normal human stem cells in several organ systems.

Despite the importance of CD44, CD133 and ALDH in identifying pancreatic CSCs, it is unclear whether these antigens are involved in regulating CSC function or merely serve as phenotypic markers. However, other pancreatic CSC markers have been identified that may be functionally relevant. For example, CXCR4 serves as the chemokine receptor for stromal cell-derived factor-1 (SDF-1, CXCL12). In addition, recent studies have shown that c-Met can identify as regulates PCSCs in a manner similar to findings in glioblastoma. Thus, several strategies have been used to identify pancreatic CSCs, and some of these may provide insights into regulatory factors and potential targeting strategies [20-22].

The CSC hypothesis is the subject of great interest within the field of PDAC as well as other malignancies, since it also provides a rationale for the phenomenon of high resistance to chemotherapy leading to relapse of disease after treatment. In this context, a thorough understanding of the biological characteristics of the subpopulation of CSC will be crucial for their identification and their tracking during treatment, representing a novel measure of treatment response. Additionally, increased understanding of the biology of the CSC could lead to the development of new treatments specifically directed against these cells as the putative root of PDAC [17].

1.3.4 The multistep model for pancreatic adenocarcinoma

PDAC is a genetic disease. The successive accumulation of mutations in key oncogenes and tumour suppressor genes leads to pancreatic cancer that once established is a quite complex, heterogeneous and genetically unstable disease. A multistep model for pancreatic adenocarcinoma has been proposed recently. In this model, well-defined, noninvasive ductal lesions are recognized as precursors of invasive cancer and have been classified under the nomenclature of pancreatic intraepithelial neoplasia or PanIN. Increasing evidence suggests that PanINs represent true neoplasms of the pancreatic ductal epithelium, accumulating histologic and genetic abnormalities in their progression toward invasive cancer[23].

The progression from minimally dysplastic epithelium (PanIN1A and B) to more severe dysplasia (PanIN2 and 3) and finally, to invasive carcinoma is paralleled by the successive accumulation of mutations that include the activation of the *k-ras* oncogene, inactivation of the tumour suppressor gene *cdkn2a/ink4a* and finally, inactivation of the tumour suppressor genes *tp53* and *dpc4/smad4* [24]. This sequence of events in pancreatic carcinogenesis is supported by studies in genetically engineered mouse models in which the targeted activation of the murine *kras* gene with concomitant inactivation of the *trp53* or *cdkn2a/ink4a* genes results in the development of pancreatic cancer identical to the cognate human disease [25-27].

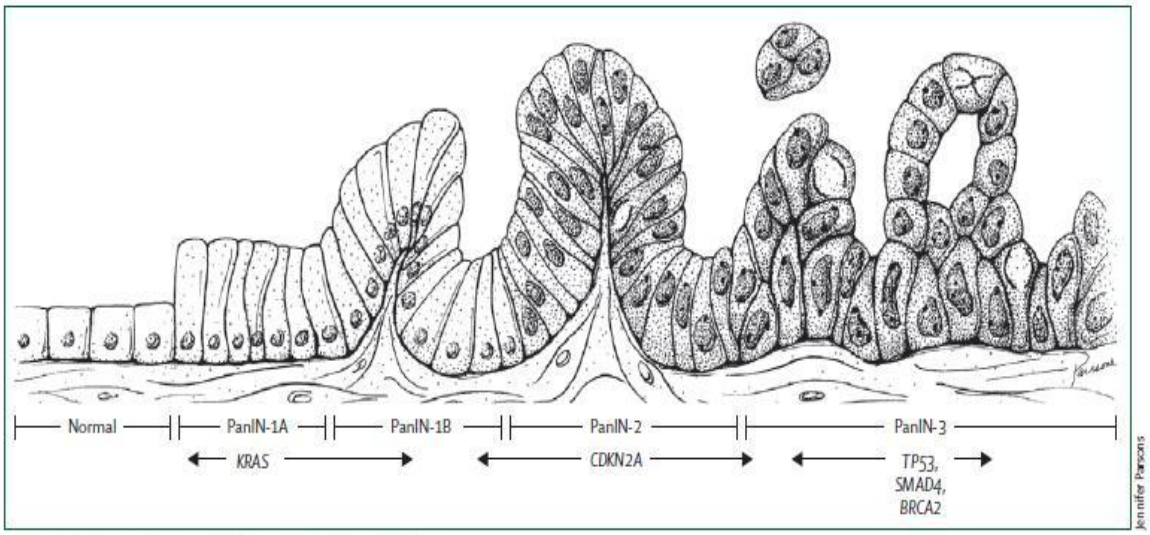

Figure 2: **PanIN progression model, showing genetic alterations**
PanIN=pancreatic intraepithelial neoplasia. Reprinted from reference 28, with permission of the American Association for Cancer Research.

Figure 1.7 From normal pancreatic epithelium to metastasis. The neoplastic progression is associated with genetic alterations involving oncogenes (Red), tumour suppressor (Blue) and genes that modulate tumour progression (Green)[28].

Almost all patients with fully established pancreatic cancer carry one or more of four genetic defects. 90% of tumours have activating mutations in the ***k-ras*** oncogene. Transcription of the mutant *k-ras* gene produces an abnormal Ras protein that is "locked" in its activated form, resulting in aberrant activation of proliferative and survival signalling pathways. Likewise, 95% of tumours have inactivation of the ***cdkn2a*** gene, with the resultant loss of the p16 protein (a

regulator of the G1–S transition of the cell cycle) and a corresponding increase in cell proliferation. ***Tp53*** is abnormal in 50 to 75% of tumours, permitting cells to bypass DNA damage control checkpoints and apoptotic signals and contributing to genomic instability. ***Dpc4*/smad4** is lost in approximately 50% of pancreatic cancers, resulting in aberrant signalling by the transforming growth factor β (TGF-β) cell- surface receptor [24, 29].

1.3.5 Signalling pathways altered in PDAC

It has been proposed that malignant cells must fulfill some of the following criteria: (1) self-sufficiency in growth signals, (2) insensitivity to antigrowth signals, (3) evasion of apoptosis, (4) limitless replicative potential, (5) angiogenesis, and (6) invasion and metastasis[30]. PDAC cells achieve these criteria by accumulating genetic mutations in signalling pathways.

Jones et al [5] recently provided the first clues to the genetic basis of pancreatic carcinogenesis at a global level. In this study, the authors subjected 24 human pancreatic tumours that were passaged in vitro as cell lines or in nude mice as xenografts to a large-scale genomic analysis of 20.661 genes. In this analysis, 1.562 somatic mutations, 198 homozygous deletions and 144 amplifications were identified, indicating the genetic complexity and diversity of PDAC. However, 69 gene sets were identified that were genetically altered in the majority of the 24 tumours and 31 of these sets could be grouped into 10 core signalling pathways (Figure 1.8).

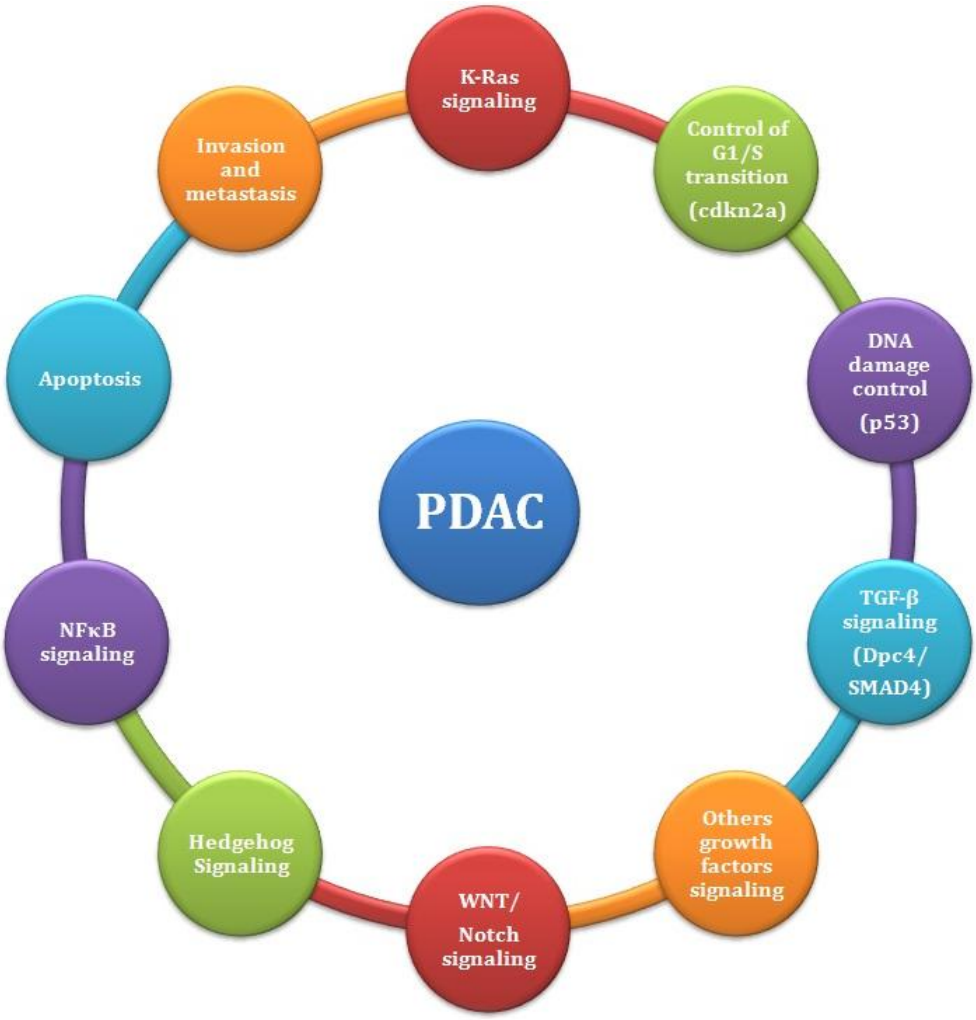

Figure 1.8 Core signalling pathways altered in pancreatic cancer.

While many of these genetic alterations have been validated in PDAC pathogenesis, major lingering questions center on how these mutations contribute to the tumour biological features of the neoplasms[4]. In the following subsections, we provide a summary of the current state of knowledge surrounding the PDAC signature mutations, their linked pathways and biological activities.

1.3.5.1 The K-RAS oncogene and its signalling pathways

K-RAS is a member of the RAS superfamily of GTPases and mediates a variety of cellular functions including proliferation, differentiation and survival [31-32]. Activating mutations of *k-ras* can be found in 30% of early neoplasms (including PanIN) but are present in almost 100% of advanced PDACs indicating a central role for *k-ras* mutations in tumorigenesis[33]. Direct evidence that activating *k-ras* mutations can induce PDAC comes from mouse models that express a constitutively active form of RAS in the pancreas. These mice develop PanIN lesions that progress to invasive PDAC [34]. Although RAS is a GTPase, its intrinsic activity is inefficient and requires GTPase activating proteins (GAPs) to promote GTP hydrolysis and attenuate downstream signalling. Activating *k-ras* point mutations at codon 12 (from GGT to GAT or GTT and more rarely CGT) results in substitution of glycine with aspartate, valine or arginine[35].

Although RAS is considered to be an attractive therapeutic target given its prominent role in the genesis of PDAC and many other human malignancies, specific biochemical properties of the protein have made this an elusive goal. Importantly, the hotspots of RAS mutations in human cancer are located near the bound nucleotide and decrease the intrinsic rate of GTP hydrolysis and make the molecule insensitive to GAPs. This results in a constitutively activated molecule that is essentially independent of growth factor stimulation. In contrast to the activating mutations of other oncogenes such as kinases, which increase their catalytic activity, the oncogenic mutations of RAS inhibit its enzymatic activity. Thus, rather than using the traditional paradigm of inhibiting an oncogene's enzymatic function (e.g., c-Kit, EGFR, HER2/Neu), an effective RAS antagonist would increase the GTPase activity of RAS or make it more sensitive to GAPs[4].

At the cellular level, mutant-activated RAS mediates several key aspects of oncogenesis, including deregulated cell growth, evasion of apoptosis, and induction of angiogenesis. These effects result from the integrated activities of multiple Ras signalling pathways, many of which are potential targets for cancer therapy [36-37]. Activated RAS utilizes several downstream effectors[38] but three

major downstream pathways and members of all of these pathways have been implicated in PDAC tumorigenesis: (1) the RAF/ERK pathway, (2) the phosphoinositide 3-kinase (PI3K) pathway, and (3) the RalGDS pathway (Figure 1.9) [39]. These downstream effectors activate several distinct signalling cascades, leading to activation of certain genes, such as those encoding growth factors (transforming growth factor α, TGF and vascular endothelial growth factor, VEGF), or changes in actin cytoskeleton by activating Rho family G proteins. Normally, these Ras-signalling cascades are only transiently activated because each normal Ras has low intrinsic guanine triphosphatase (GTPase) activity that gradually inactivates its own signalling function by hydrolyzing the bound GTP. More importantly, several distinct cytoplasmic GTPase-activating proteins (GAPs) stimulate the intrinsic GTPase activity of Ras, rapidly converting Ras from the active GTP form to the inactive GDP form. In this sense, the GAPs are attenuators of normal Ras. However, oncogenic mutations of *k-ras* not only reduce the intrinsic GTPase activity but also, more importantly, completely abolish the GAP-induced GTPase activation[38].

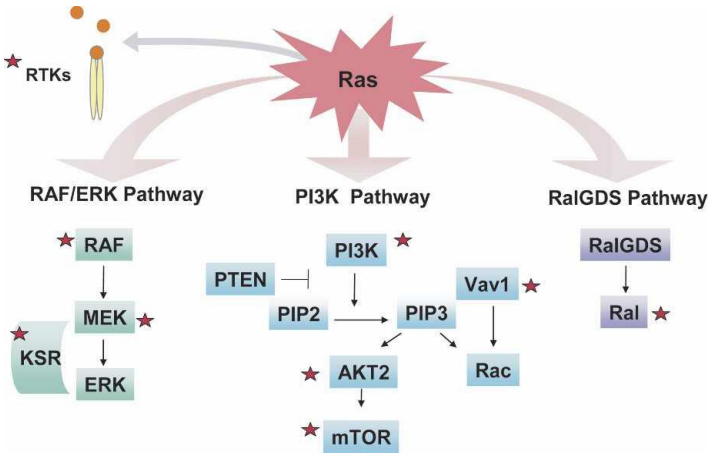

Figure 1.9 RAS signalling network. Ras uses a multitude of downstream effectors. Depicted here are three major signalling cascades that have been implicated in PDAC progression and maintenance: the Raf/Map Kinase (ERK) pathway, the PI3K pathway and the Ral GDS pathway.

Mitogen-activated protein (MAP) kinase cascades lie in a three-kinase-signalling module involved in transmitting membrane signals to the cell nucleus. MAPK

module consists of MAP kinase or extracellular signal-regulated kinase (ERK) activated by an MAP/ERK kinase (MEK or MAPKK) which, in turn, is activated by an MEK kinase (MEKK or MAPKKK). One such MEKK, which is the well-characterized downstream effector of Ras, is the serine–threonine kinase Raf-1. This protein is recruited by Ras-GTP to the plasma membrane, where is activated [38]. Once activated, RAF phosphorylates MEK, which, in turn, phosphorylates ERK. MAPK activation results in phosphorylation and activation of ribosomal S6 kinase and transcription factors, such as c-Jun, c-Myc, and c-Fos, resulting in the switching on of a number of genes associated with the cell cycle progression/cell division and a proliferative phenotype (Figure 1.10) [40]. Inhibition of MAPK, either through the use of dominant negatives or pharmacological inhibition of the upstream activator MEK, results in decreased proliferation of PDAC cell lines and cell cycle arrest [4].

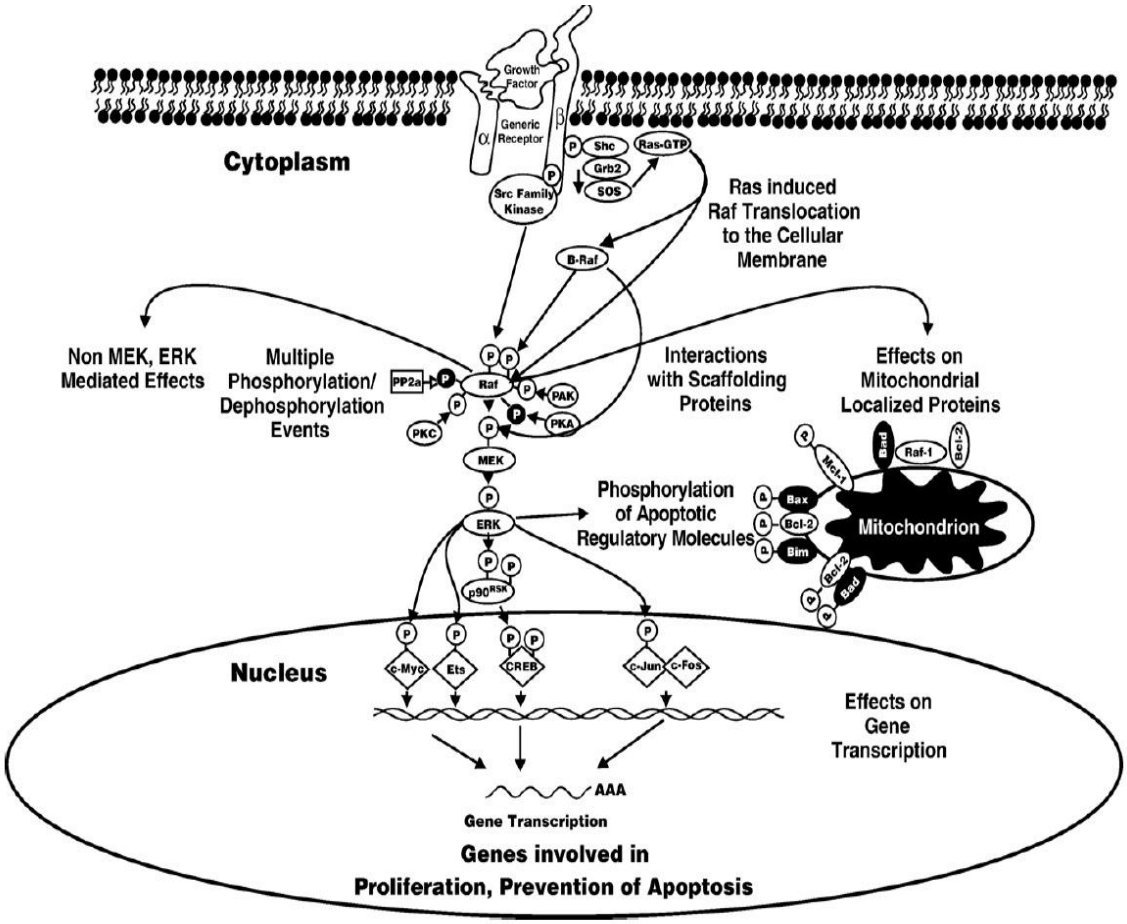

Figure 1.10 Overview of Raf/MEK/ERK Pathway. The Raf/MEK/ERK pathway is regulated by

Ras as well as various kinases. This pathway has diverse effects which can regulate the cell cycle progression, apoptosis or differentiation [41].

The PI3K/AKT pathway is uniformly activated in human PDAC and mouse models of Kras-driven pancreatic cancer[42]. The PI3K pathway can be activated by K-RAS and regulates multiple cellular events including cell proliferation and survival via several downstream effectors (Figure 1.11). PI3Ks are a family of heterodimeric lipid kinases composed of catalytic and regulatory subunits that, on stimulation, catalyze production of the second messenger phosphatidylinositol-3, 4, 5-triphosphate (PIP_3), which activates downstream kinases, such as PDK1 and AKT [43]. AKT is activated by a dual regulatory mechanism that requires both translocation to the plasma membrane and phosphorylation at Thr308 and Ser473. The generation of PIP3 on the inner leaflet of the plasma membrane, following PI3K activation, recruits AKT by direct interaction with its PH domain. At the membrane, another PH-domain-containing serine/threonine kinase named 3-phosphoinositide-dependent protein kinase-1 (PDK1) phosphorylates AKT on Thr308. Thr308 phosphorylation is necessary and sufficient for AKT activation; however, maximal activation requires additional phosphorylation at Ser473 by PDK2[44]. The main biological consequences of AKT activation that are relevant to cancer-cell growth can be catalogued loosely into three categories: survival, proliferation (increased cell number) and growth (increased cell size) [45-46].

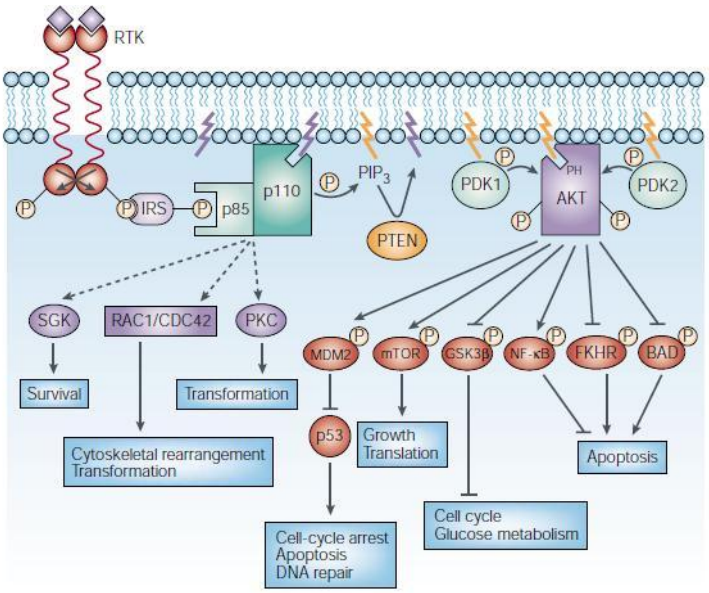

Figure 1.11 PI3K signalling. Activation of class IA phosphatidylinositol 3-kinases (PI3Ks) occurs through stimulation of receptor tyrosine kinases (RTKs) and the concomitant assembly of receptor–PI3K complexes. These complexes localize at the membrane where the p110 subunit of PI3K catalyses the conversion of PtdIns(4,5)P2 (PIP2) to PtdIns(3,4,5)P3 PIP3). PIP3 serves as a second messenger that helps to activate AKT. Through phosphorylation, activated AKT mediates the activation and inhibition of several targets, resulting in cellular growth, survival and proliferation through various mechanisms. Additionally, PI3K has been shown to regulate the activity of other cellular targets, such as the serum and glucocorticoid-inducible kinase (SGK), the small GTP-binding proteins RAC1 and CDC42, and protein kinase C (PKC), in an AKT-independent manner through poorly characterized mechanisms. The activity of these targets leads to survival, cytoskeletal rearrangement and transformation. GSK3β, glycogen synthase kinase-3β; NF-κB, nuclear factor of κB; PDK1/2, 3-phosphoinositide-dependent protein kinase 1/2.

While the RAF and phosphoinositol-3-kinase effector pathways are the best-studied and validated, recent studies have established the critical importance of Ral guanine nucleotide exchange factor (RalGEF) activation of the RalA and RalB small GTPases in cancer biology. The RalGDS pathway has been implicated in PDAC development downstream of K-RAS due to the fact that KRAS can activate the RAL exchange factor, and this activation enhances cellular transformation. Furthermore, RalA was shown to be activated in several PDAC cells lines being critical for supporting the anchorage independent and tumorigenic growth [39, 47-48].

1.3.5.2 p53

p53, originally identified as a protein associated with the simian virus 40 large T antigen in 1979 [49], guards genomic integrity via regulating numerous cellular processes, including cell cycle arrest, DNA repair, apoptosis and cellular senescence, in response to various stress signals. Mutation of the *p53* gene is the most common somatic alteration in human cancer. The level and activity of p53 protein are primarily regulated through posttranslational modifications. In normal cells, p53 is a short-lived protein which is continuously undergoing ubiquitination and subject to proteasomal degradation. Mouse double minute 2 (MDM2, HDM2 in human), one of the first characterized p53 targets, serves as a major E3 ubiquitin ligase for p53 degradation and thus forms a negative autoregulatory loop to maintain the low level of p53 expression in unstressed conditions (Figure 1.12). Upon genotoxic stresses, rapid phosphorylation of p53 at Ser15 by the Ataxia telangiectasia mutated (ATM), a serine/threonine protein kinase, and at Ser20 by the checkpoint kinase 2 (Chk2), results in dissociation of p53 from MDM2, leading to p53 stabilization and activation of its downstream processes [50].

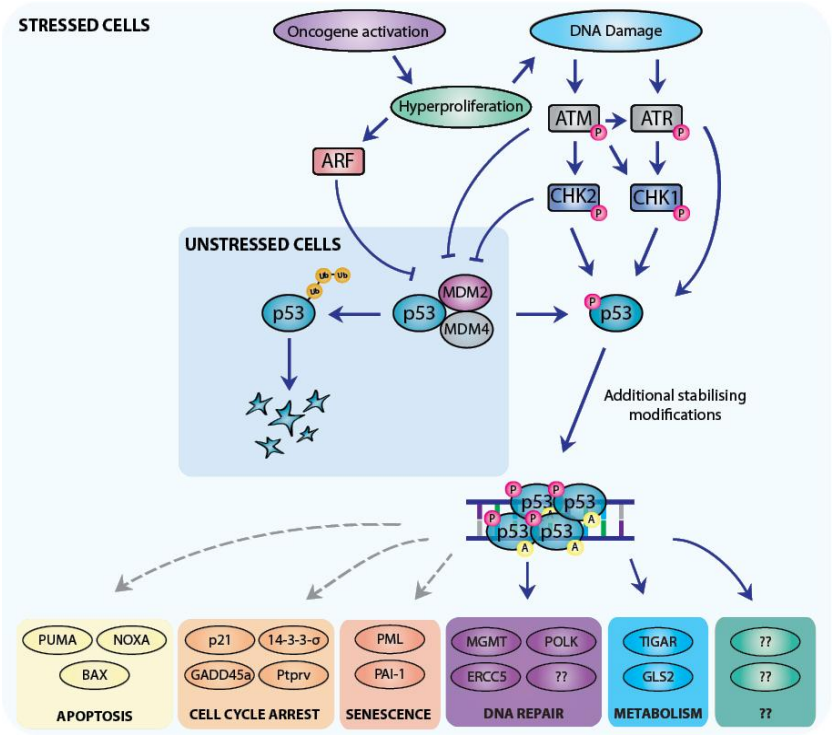

Figure 1.12 p53-mediated tumour suppression.

Loss of p53 function during carcinogenesis can lead to inappropriate cell growth, increased cell survival and genetic instability. This tumour suppressor gene is inactivated in 50 to 75% of infiltrating pancreatic adenocarcinomas, being rare in chronic pancreatitis [51]. *p53* gene mutations, predominantly through nonsense mutations [52] and overexpression of its product, are also frequent events in PDAC. The loss of *p53* means that two critical controls of cell number are deregulated in the majority of PDAC: cell division and cell death [53]. In addition, p53-induced growth arrest is also achieved by transactivation of p21. p53 binding to DNA stimulates production of the protein p21, which negatively regulates the complex consisting of cyclin D and the cell division-stimulating protein cyclin-dependent kinase-2, allowing time for repair to damaged DNA. If p53 mutates, it is not able to bind DNA, so p21 is not available and abnormal growth can occur. Cell lines that lack wild-type *p53* show a reduced or complete absence of *p21*. Loss of p21 activity has been observed in approximately 30%–60% of pancreatic tumour specimens [54].

The prognostic role of p53 expression in pancreatic adenocarcinoma remains controversial. Some studies have shown an association of p53 gene mutation with shorter survival in patients with pancreatic cancer, but most of the studies failed to document any significant correlation between those events [55-56].

1.3.5.3 Control of G1/S transition: CDKN2

The *cdkn2a* locus on chromosome 9q21 encodes 2 tumour suppressor genes, *p16ink4a* and *p14arf*.

The *p16ink4a* gene regulates cell-cycle progression by inhibiting cyclin D/CDK4/6 complexes, which in turn inhibit Retinoblastoma (Rb) phosphorylation. The retinoblastoma protein acts as the central control point for regulating cell cycle commitment (Figure 1.13). When cells are not stimulated to divide by growth factors, pRb kidnaps the transcription factor E2F involved in the cell cycle regulation and DNA synthesis, thereby restricting progression into S-phase. Upon growth factor stimulation, pRb releases E2F, allowing for the expression of S-phase critical genes.

The interaction of p14 ARF with MDM2 leads to p53 activation. In pancreatic cancer development, inactivation of *p16ink4a* seems to be of greater importance than inactivation of *p14arf* because germline and sporadic mutations have been identified that target *p16ink4a* and leave *p14arf* intact [57].

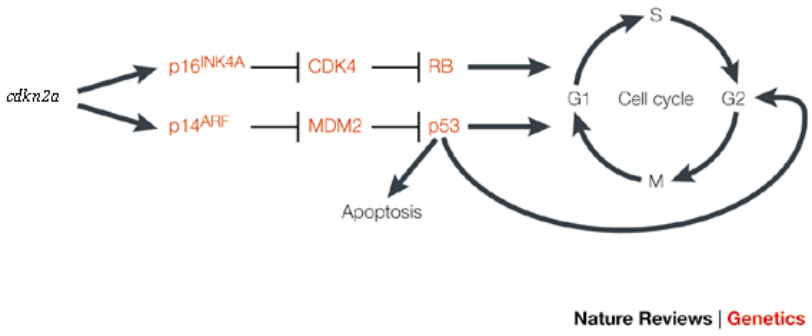

Figure 1.13 p16INK4A and p14ARF control the activity of retinoblastoma (RB) and p53. RB promotes cell-cycle arrest in G1 and regulates entry into the S phase of the cell cycle through its effects on E2F. p53 has several effects, including causing G1 and G2 arrest and promoting apoptosis. Loss of p53 function also promotes genomic instability [58].

In sporadic PDAC, loss of *p16ink4a* function by mutation, deletion or promoter hypermethylation occurs in 80% to 95% cases of PDAC [59]. *p16ink4a* loss occurs at one of the earlier stages of PanIN and is generally seen in moderately advanced lesions that show features of dysplasia. *p16ink4a* gene alterations may participate in the aggressiveness of PDAC. In the study by Ohtsubo et al, pancreatic tumour was significantly larger and the survival time significantly shorter in patients with p16 mutation compared with intact p16 [60]. Similarly, Hu et al. reported that loss of p16 expression in pancreatic cancer was associated with its pathologic grade and negatively correlated with patient survival [61].

1.3.5.1 Growth factors and their receptors

1.3.5.1.1 TRANSFORMING GROWTH FACTOR-B

The TGF-β family includes a large number of structurally and functionally related proteins. The members of the TGF-β family act as multifunctional regulators of a wide range of biological processes such as morphogenesis, embryonic development, adult stem cell differentiation, immune regulation, wound healing, inflammation and cancer. The first member of the family, TGF-β1, was discovered in 1983 because of its ability to stimulate the growth of cultured rat fibroblasts in soft agar. Thirty-three members of this family have been identified. These proteins cluster in several subfamilies, such as TGF-βs, bone morphogenetic proteins (BMPs), growth and differentiation factors (GDFs), Müllerian inhibitory factor (MIF), activins or inhibins [62].

Transforming growth factor-β (TGF-β) plays a complex role in tumorigenesis, since it has both tumour suppressive and oncogenic activities [63]. TGF-β signals through a heterotetrameric receptor complex comprising type II receptors (TβRII) and type I receptors (TβRI/ALK5), both serine/threonine kinases. Following ligand binding, the TβRII receptors activate TβRI receptors through direct phosphorylation.

Downstream of the receptors, the SMADs act as major transducers of the signal from the receptors to the nucleus. Members of the SMAD family are well conserved and can be classified into the following three groups: Receptor-associated SMADs (R-SMADs); Co-operating SMADs (Co-SMADs) and Inhibitory SMADs (I-SMADs)[62].

R-SMADs are directly phosphorylated on their carboxy(C)-terminus on two serine residues by the TβRI kinases, leading to R-SMAD activation. The unphosphorylated R-SMADs are transcriptionally inactive and can be sequestered in the cytoplasm by specific retention proteins, such as SARA (SMAD anchor for receptor activation),

endofin or ERBIN (Erbb2-interacting protein). Five different R-SMADs have been described in humans, which are substrates for activated TGF-β receptors (SMAD1, SMAD2, SMAD3, SMAD5 and SMAD8). SMAD2 and SMAD3 are substrates for receptors activated by TGF-βs and activins, whereas SMAD1, SMAD5 and SMAD8 mediate pathways activated by bone morphogenetic proteins (BMPs). The R-SMADs contain two highly conserved domains at the N- and the C-termini, termed Mad Homology (MH) 1 and MH2 domains, respectively, and are separated by a linker region of variable length. MH1 can interact with DNA and with other proteins. MH1 also possesses a nuclear localization signal. MH2, on the other hand, mediates homo or hetero-oligomerisation of the SMADs and the transactivation of the SMAD nuclear complexes. Located between the MH1 and MH2 domains is a highly variable linker region, which is enriched in proline residues and has serine/threonine residues that are acceptor sites for phosphorylation [64].

After phosphorylation of the R-SMAD, the phosphor-R-SMAD associates with SMAD4 (mammalian Co-SMAD). This SMAD complex translocates to the nucleus, where, in collaboration with other transcription factors, it binds and regulates promoters of different target genes. Two of these genes are I-SMADs: SMAD6 and SMAD7. The induced expression of these inhibitory SMADs produces a negative feedback regulation of TGF-β signalling[65]. Other genes regulated are related to proliferation, differentiation, migration and apoptosis (Figure 1.14).

In addition to Smad signalling, TGF-β also initiates non-Smad signalling from the TβRII/TβRI complexes, leading to the activation of pathways that are more commonly seen as effectors of receptor tyrosine kinase signalling, such as PI3K/Akt, Erk, and p38 MAPK, and Rho-GTPases pathways

TGF-β promotes the proliferation and transformation of fibroblasts and the epithelial-to-mesenchymal transition (EMT) a process by which advanced carcinomas lose their differentiated features and acquire a highly aggressive, invasive phenotype [66]. After prolonged signalling, the TGF-β receptors are degraded via the proteosomal and lysosomal pathways by a mechanism involving the recruitment to the activated receptor complexes of E3 ubiquitin ligases Smurf1

and Smurf2 by the inhibitory SMAD, SMAD7[67]. EMT is a major contributor to the aggressiveness of multiple cancers and pancreatic cancer in particular [66].

Genetic deregulation of TGF-β signalling pathway is commonly observed in pancreatic cancer. The alternative name of human SMAD4, i.e., DPC4 (deleted in pancreatic carcinoma, locus 4), suggests the close relationship of loss of this gene with pancreatic cancer. Several evidences support the role of SMAD4 as a tumour suppressor gene in pancreatic tumorigenesis. Although it is lost in other cancers too, loss of SMAD4 is more sensitive and specific to PDAC. It is inactivated in 55% of pancreatic cancers either by deletion of both alleles (35%) or by intragenic mutation in 1 allele coupled with the loss of the other alleles (20%)[51]. The expression level of SMAD4 protein is inversely associated with histopathological grades of pancreatic cancers [68-69].

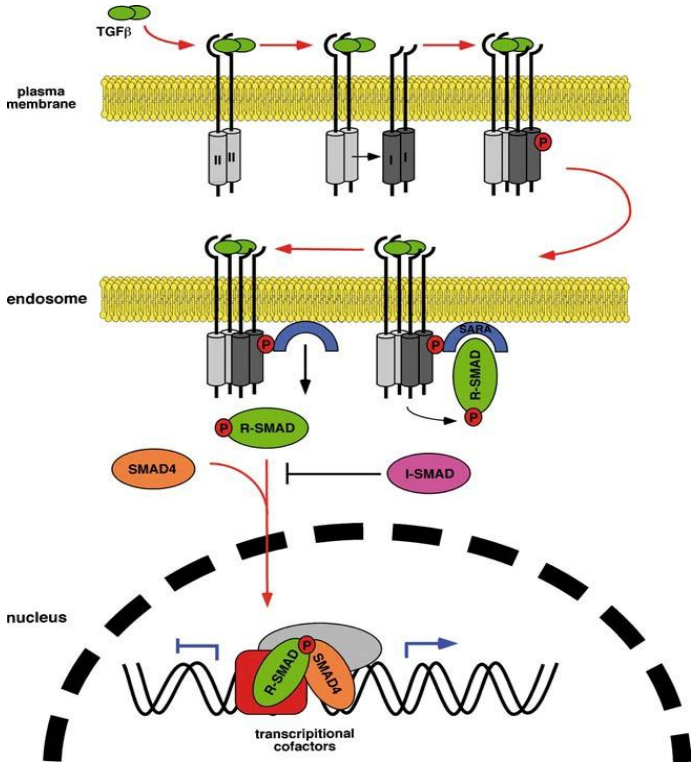

Figure 1.14 The TGF-β signalling pathway. Upon binding of dimeric TGF-β, the serine/ threonine receptor assembles as a heterotetramer consisting of TGF-β receptor II (TGFβRII) and TGF-β receptor I (TGFβRI) subunits. TGFβRII phosphorylates and activates TGFβRI which in turn phosphorylates and activates receptor bound SMAD proteins (R-SMADs). Activated R-SMADs bind to co-SMADs (SMAD4) and translocate into the nucleus where they

are able to enhance or suppress the expression of multiple genes in conjunction with transcriptional co-factors[39].

1.3.5.1.2 EPIDERMAL GROWTH FACTOR

The epidermal growth factor (EGF) family of receptor tyrosine kinases consists of 4 receptors, EGF-R (ErbB1), ErbB2 (HER 2/Neu), ErbB3 and ErbB4. The ligands, which are EGF family of growth factors, consist of multiple members, including EGF, TGF-β, amphiregulin, betacellulin, heparin-binding EGF-like growth factor (HB-EGF), epiregulin and heregulins[57].

EGFR is a 170kd glycoprotein, which is commonly expressed in normal and malignant tissues and is involved in cellular communication. The four receptors of the EGF family are composed of an extracellular domain, a hydrophobic transmembrane region and a tyrosine kinase-containing cytoplasmic region. The intracellular domain of EGFR is activated upon ligand binding triggering the EGF-mediated tyrosine kinase signal transduction pathway. EGF and TGF-α are believed to be the most important ligands for EGFR. Ligand binding with EGFR results in receptor homo- or heterodimerization at the cell surface followed by internalization of the dimerized receptor. After dimerization, phosphorylation of the intracytoplasmic EGFR tyrosine kinase domain occurs. Phosphorylated tyrosine kinase residues serve as binding sites for the recruitment of signalling molecules, such as K-RAS. These signalling molecules have the ability to phosphorylate other downstream molecules. The activation of downstream pathways promotes cellular proliferation, angiogenesis, development of metastases and reduces apoptosis [70].

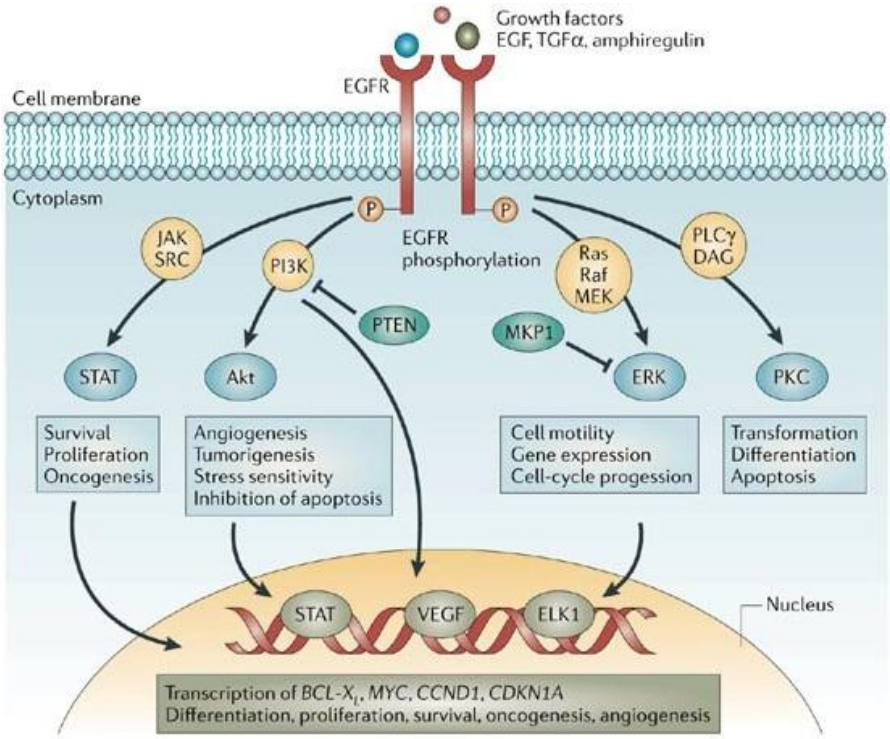

Figure 1.15 Signalling pathways activated by EGFR.

One of nuclear EGFR's main functions is to act as a transcriptional co-activator for various oncogenic genes. Since EGFR does not contain a DNA binding domain it must associate with other transcription factors in order to interact with genomic regions. EGFR has now been identified as a transcriptional co-activator for seven cancer promoting genes: cyclin D1, nitric oxide synthase (iNOS) B-Myb, Aurora Kinase A (Aurora-A), cyclooxygenase-2 (COX-2), c-Myc and breast cancer resistant protein (BCRP). Nuclear EGFR also plays essential roles in promoting both DNA replication and repair by associating with proliferating cell nuclear antigen (PCNA) and DNA dependent protein kinase (DNA-PK). Both DNA replication and repair are essential cellular processes necessary for cancer formation and progression [71].

Overexpressions of EGF and EGFR are a common feature of PDAC [72-73]. In normal human pancreatic tissue, EGF and EGFR immunoreactivities were present on the surface and in the cytoplasm of most ductal cells and many acinar cells [74]. In chronic pancreatitis tissues, the intensity of the immunohistochemical signal for EGF and EGFR was markedly increased. In PDAC, EGFR overexpression was found

significantly more often in tumours of advances clinical stages and was associated with shorter survival in pancreatic cancer patients[51].

1.3.5.1.3 VASCULAR ENDOTHELIAL GROWTH FACTOR

VEGF is the most potent angiogenic factor important in pancreatic tumour progression [75]. PDACs express high levels of vascular endothelial growth factor (VEGF). Recent studies indicate that suppression of VEGF expression attenuates pancreatic cancer cell tumorigenicity in a nude mouse model, and that VEGF can exert direct mitogenic effects on some pancreatic cancer cells. These findings suggest that cancer cell derived VEGF promotes pancreatic cancer growth in vivo via a paracrine angiogenic pathway and an autocrine mitogenic pathway [76].

VEGF promotes endothelial cell proliferation and survival by binding to the VEGFR-1 and VEGFR-2 endothelial cell transmembrane receptors [77]. VEGF is overexpressed by PDAC cells [78], whereas disruption of VEGF signalling by expression of soluble VEGF receptors, VEGF high-affinity binding chimeras, anti-VEGF antibodies or ribozymes strongly suppresses the tumorigenic growth of pancreatic cancer xenografts [79].

VEGF-A stimulates endothelial cell proliferation through binding to two related tyrosine kinase receptors, VEGFR-1 (flt-1) VEGFR-2 (flk-1/KDR), on the surface of endothelial cells, with most of the mitogenic effects taken to occur via VEGFR-2. VEGF-C, a regulator of lymphoangiogenesis, is also overexpressed in PDAC and may contribute to lymphatic spread and the lymph node metastasis common in this malignancy [80]. Tumour angiogenesis is often the consequence of an angiogenic imbalance in which pro-angiogenic factors predominate over anti-angiogenic factors. Furthermore, angiogenesis is essential for growth and metastasis of most solid malignancies, and VEGF-A is believed to be critical for tumour angiogenesis. Thus, secretion of bioactive VEGF-A by cancer cells may be directly involved in tumour progression[76].

1.3.5.1.4 FIBROBLAST GROWTH FACTORS

The fibroblast growth factors comprise a group of heparin-binding proteins that share similar structures. These factors are involved in a variety of functions, including angiogenesis and mitogenesis. There are 14 FGFs known with varying expression domains and targets. FGFs mediate their actions after binding to one of four FGF receptors (FGFRs) on the target cell. FGFRs are subject extensive alternative splicing and glycosylation, resulting in a multitude of affinities and specificities for various FGF ligands. Binding of FGFR leads to the activation of a number of signal transduction pathways via tyrosine phosphorylation. Multiple pathways are activated by FGFRs, including (1) the Ras-Raf1-MEK-MAPK pathway; (2) the phosphatidylinositol-3 kinase (PI3K) pathway; and (3) the phospholipase-C-gamma (PLC2γ)-phosphatidylinositol 4, 5-bisphosphate (PIP2) axis (Figure 1.16). These signalling cascades ultimately result in proliferative changes and effects on cellular differentiation. FGFs are upregulated in approximately 60% of all PDAC samples, and the degree of FGF expression correlates with advanced tumour stage and shorter patient survival at the time of diagnosis [81].

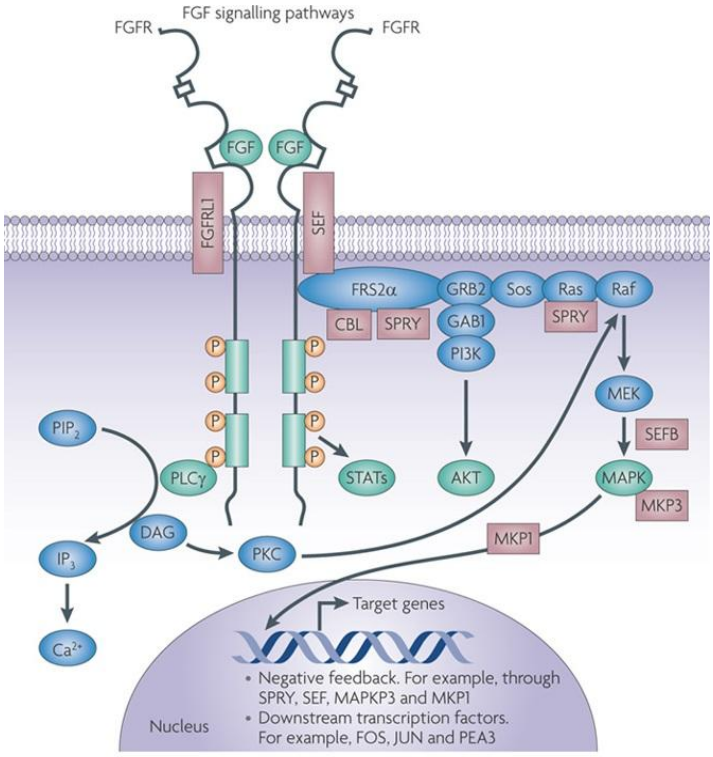

Figure 1.16 FGF signalling network. The signal transduction network downstream of fibroblast growth factor (FGF) receptors (FGFRs). Following ligand binding and receptor dimerization, the kinase domains transphosphorylate each other, leading to the docking of adaptor proteins and the activation of four key downstream pathways: RAS–RAF–MAPK, PI3K–AKT, signal transducer and activator of transcription (STAT) and phospholipase Cγ (PLCγ)[82].

1.3.5.2 Nuclear Factor Kappa B (NF-κB) signalling cascade

The NF-κB transcription factor may be another important downstream mediator of mutated K-RAS signalling in PDAC. Activation of this pathway occurs in response to a variety of cell stresses through stimulation by proinflammatory cytokines and growth factors, and is known to regulate the immune response, apoptosis, and many other processes.

NF-κB exists as a hetero and homodimeric protein complex of members of the so-called Rel-family. RelA/p65, RelB and c-Rel harbor a transactivation domain along with the Rel homology domain. The Rel homology domain, also present in NF-κB1 (p50/p105) and NF-κB2 (p52/p100), functions as an interacting site for Rel-family members and confers DNA binding. In contrast, through the transactivation domain p65, RelB and c-Rel regulate the expression of their target genes. The most abundant NF-κB form is the heterodimer of p65 and p50. In the so-called classical NF-κB pathway, p65/p50 is anchored in the cytoplasm by the inhibitor of κB (IκB-α) proteins. In response to NF-κB-activating stimuli, the IκB kinase complex (IKK) consisting of two catalytical kinases (IKKα and IKKβ), together with the regulatory component IKKγ/NF-κB essential modulator, is activated by phosphorylation. Once activated, IKK phosphorylates IκB, which is subsequently polyubiquitinated and degraded by the 26S proteasome. The NF-κB dimer then translocates to the nucleus and regulates the transcription of its target genes (Figure 1.17) [83].

Most primary pancreatic cancers and cell lines, but not normal pancreas specimens, show constitutive NF-κB activity [84-85]. Induction of NF-κB may directly involve K-RAS signalling since expression of a dominant-negative RAS allele abrogates NF-κB activity in PDAC cell lines [86]. Furthermore, the frequent overexpression and activation of members of the EFGR signalling pathway might contribute to NF-κB-dependent tumour progression and invasive phenotype of PDACs [87].

It has been described that constitutive NFκB activity plays a key role in the regulation of the proangiogenic factors, VEGF and IL-8 and in induction of

metastasis in pancreatic cancer cell lines [88]. The NF-κB pathway may also contribute to the prominent chemoresistance of PDAC. Among NF-κB target genes are well-defined antiapoptotic genes like Bcl-X_L, cIAP, Bcl-2 and c-Flip which are able to inhibit the apoptotic cascade at several points, conferring resistance against chemotherapeutic drugs and death receptor ligands. There is firm evidence that the death receptor ligands TRAIL (tumour necrosis factor-related apoptosis-inducing ligand) and Fas ligand induce NF-κB [89-90] and thereby inhibit their potential to eliminate pancreatic cancer cells [91].

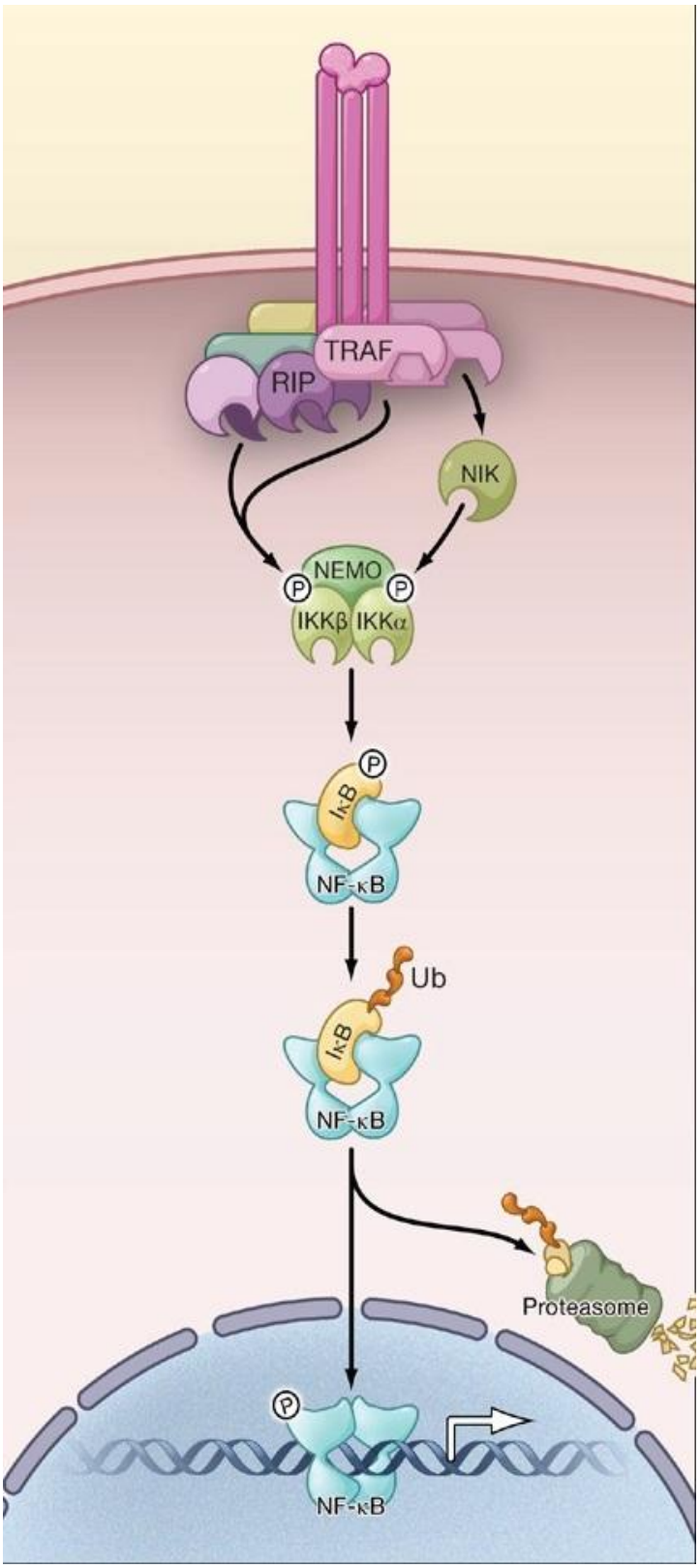

Figure 1.17 NF-κB Signalling Pathways [92].

1.3.5.3 Developmental signalling pathways in PDAC

1.3.5.3.1 HEDGEHOG

The hedgehog signalling pathway (Shh) is vital for embryonic development, particularly gastrointestinal patterning [93]. Shh is also active in a subset of cells in mature organs and may play a role in maintaining stem cell number and accurate patterning in the epithelia of the lungs, the skin and the digestive tract [94]. Deregulation of hedgehog signalling has also been observed in several human cancers, including small cell lung carcinomas, medulloblastomas, basal cell carcinomas and digestive tract tumour. In fact, activation of the hedgehog signalling pathway occurs in a majority of pancreatic ductal adenocarcinomas [95].

There are three mammalian hedgehog genes: Sonic (Shh), Indian (Ihh) and Desert (Dhh), all of which encode signalling molecules that undergo autocatalytic cleavage and double lipid modification to generate an active ligand. In the absence of hedgehog ligand, the hedgehog receptors, Patched1 and Patched2, are involved in repression of the hedgehog signalling molecule Smoothened (Smo). Upon ligand binding, Smo is released from inhibition, providing a signal for the dissociation of Gli transcription factors from an inhibitory complex that includes the serine/threonine protein kinase Fused (Fu) and Suppressor of Fused [Su (Fu)]. The Gli transcription factors translocate to the nucleus where they regulate the transcription of hedgehog responsive genes including Patched1 and Patched2 and Gli itself. Among the reported targets of hedgehog signalling are genes encoding cell cycle regulators as cyclin D, cyclin E, Myc, components of the epidermal-growth-factor pathway and genes related to angiogenesis (Figure 1.18).

It seems that Shh expression enhances the proliferation of pancreatic duct epithelial cells potentially through the transcriptional regulation of the cell cycle regulators cyclin D1 and p21. Furthermore, Shh protects pancreatic duct epithelial cells from apoptosis through the activation of MAPK and phosphatidylinositol 3-kinase signalling and the stabilization of Bcl-2 and Bcl-X_L. Significantly, Shh also

cooperates with activated K-Ras to promote pancreatic tumour development [96].

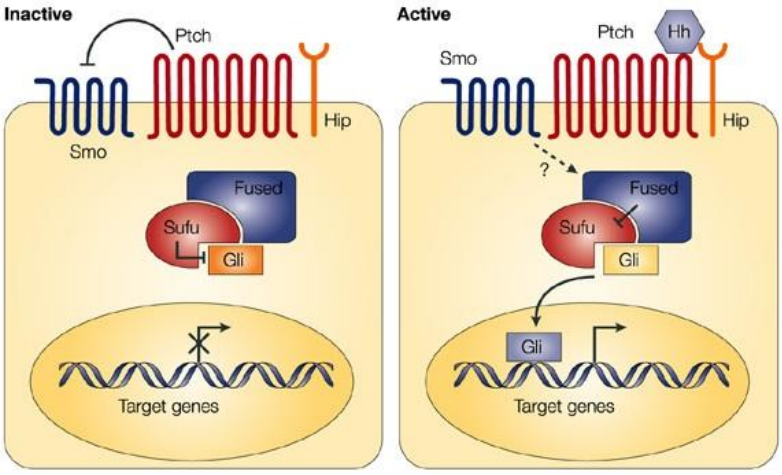

Figure 1.18 Sonic hedgehog signalling. In the absence of ligand, the Hh signalling pathway is inactive (left). In this case, the transmembrane protein receptor Patched (Ptch) inhibits the activity of Smoothened (Smo), a seven transmembrane protein. The transcription factor Gli, a downstream component of Hh signalling, is prevented from entering the nucleus through interactions with cytoplasmic proteins, including Fused and Suppressor of fused (Sufu). As a consequence, transcriptional activation of Hh target genes is repressed. Activation of the pathway (right) is initiated through binding of any of the three mammalian ligands, Sonic hedgehog, Desert hedgehog or Indian hedgehog (all are represented as Hh in the figure) to Ptch. Ligand binding results in de-repression of Smo, thereby activating a cascade that leads to the translocation of the active form of the transcription factor Gli to the nucleus. Nuclear Gli activates target gene expression, including Ptch and Gli itself, as well as Hip, a Hh binding protein that attenuates ligand diffusion. Other target genes that are important for the oncogenic function of the Hh pathway are genes that are involved in controlling cell proliferation (cyclin D, cyclin E, Myc and components of the epidermal-growth-factor pathway) and in angiogenesis (components of the platelet-derived-growth-factor and vascular-epithelial-growth-factor pathway)

1.3.5.3.2 NOTCH

Notch signalling pathway plays critical roles in the development and progression of PDAC. It is known that Notch signalling pathway, a ligand- receptor pathway, is involved in cell proliferation, apoptosis, migration, invasion, metastases, and angiogenesis in a variety of human cancers including PDAC [97]. As described in

section 1.3.3, the presence of active Notch signalling in centroacinar cells pointed them as candidate stem cells for the exocrine pancreas.

The mammalian Notch receptor family consists of four type I transmembrane receptors (termed NOTCH1–4), all of which have been implicated in human cancer. Notch proteins are synthesized as precursor forms that are cleaved by furin-like convertase (S1 cleavage) to generate the mature receptor, which is composed of two subunits. One of these subunits consists of the major portion of the extracellular domain (ECD) and the other subunit is composed of the remainder of the ECD, the transmembrane domain and the intracellular domain (ICD). These two subunits are held together by non-covalent interactions [98]. Notch signalling is initiated by the engagement of a Notch ligand to a Notch receptor, which is mediated by cell-to-cell contact. There are five known Notch ligands in mammals, jagged 1 (JAG1), JAG2, Delta-like 1 (DLL1), DLL3 and DLL4, which are collectively referred to as DSL proteins. Like the Notch receptors, the DSL proteins are type I transmembrane proteins. On binding to the Notch receptor, the ligand induces a conformational change, exposing the S2 cleavage site in the ECD to the metalloproteinase known as ADAM17. Following S2 cleavage, Notch undergoes a third cleavage (S3 cleavage) that is mediated by the presenilin–γ-secretase complex, which is composed of presenilin 1 (PSEN1), PSEN2, nicastrin (NCSTN), presenilin enhancer 2 (PEN2) and anterior pharynx-defective 1 (APH1). The S3 cleavage results in the release of the active NICD from the plasma membrane and its subsequent translocation into the nucleus.

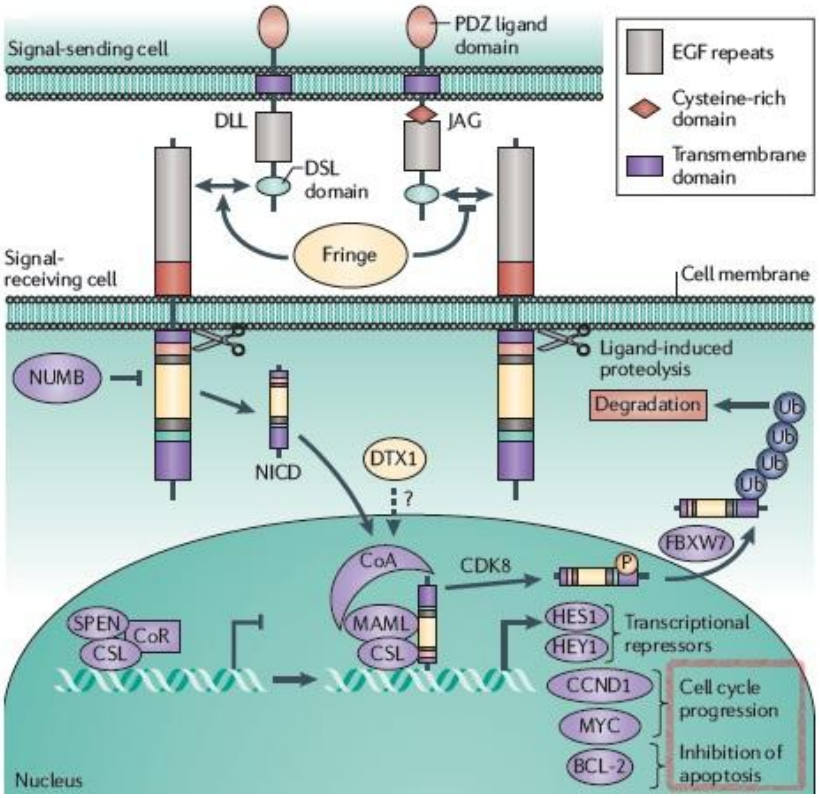

Figure 1.19 Notch signalling is activated by interaction between the ligand-expressing cell and the Notch-expressing cell, followed by proteolytic cleavage that releases the Notch intracellular domain (NICD). On activation of Notch, the NICD recruits the co-activator (CoA), mastermind-like 1 (MAML1) and others and thus converts the CSL-repressor complex into a transcriptional activator complex and drives the transcription of target genes [97].

Recent studies have demonstrated that Notch drives tumorigenesis mostly by promoting cell cycle progression and inhibiting apoptosis. These effects are thought to be the result of the transcriptional regulation of key components of the cell cycle and the tumour surveillance machinery [99]. As well as influencing tumour initiation, Notch is also important for aspects of tumour progression, including angiogenesis, EMT-driven metastatic growth and the maintenance of cancer stem cells [100].

A number of studies have shown that the Notch gene is abnormally activated in many human malignancies including pancreatic cancer. It has been reported that the Notch signalling pathway is frequently altered by upregulated expression of Notch receptors and their ligands in many human malignancies such as cervical,

lung, colon, head and neck, renal carcinoma, acute myeloid lymphomas and pancreatic cancer [101]. In pancreatic adenocarcinoma, interaction between Notch and RAS–MAPK signalling has been implicated in the initiation of tumours. NOTCH1 is induced by KRAS signalling and this results in dedifferentiation or in the inhibition of differentiation in the exocrine pancreas, leading to the formation of pancreatic intraepithelial neoplasia (PanIN) [102].

Recently, it has been shown that Notch signalling pathway targeted therapies suppressed tumour progression and metastatic spread in pancreatic cancer [103].

1.3.5.4 Apoptosis

Apoptosis or programmed cell death is a central regulator of normal tissue homeostasis [30]. Physiologically, apoptosis is essential for the elimination of redundant, damaged and infected cells. In particular, apoptosis represents a fundamental anti-neoplastic mechanism preventing tumorigenesis of normal cells. Almost all neoplastic changes during the transformation of a normal cell to a cancer cell, like DNA-damage, oncogene activation or cell cycle deregulation, are potent inducers of the programmed cell death pathway. Therefore, overcoming the apoptotic failsafe is observed in many cancers[104]. These mechanisms of anti-apoptotic protection are commonly found in cancer but some are more typically for PDAC. In PanIN 1 and 2 lesions, no apoptotic cells could be detected, arguing for the contribution of anti-apoptotic mechanisms quite early in the carcinogenesis of PDAC ensuring the survival of premalignant cells under oncogenic stress conditions [105].

Execution of apoptosis relies on a group of cysteine proteases, the caspases. Caspases are synthesized as proforms and become activated by cleavage next to aspartate residues. Since caspases cleave and activate each other, an amplification mechanism through a protease cascade exists, assuring proper execution of apoptotic cell death [106]. In addition, caspases cleave numerous substrates, like nuclear lamins, inhibitors of DNase or cytoskeletal proteins, ultimately leading to the typical morphological alterations of apoptosis.

There are two alternative pathways to initiate apoptosis and both finally activate the executioner caspases 3, 6 and 7. The first pathway is called intrinsic or mitochondrial pathway, because the mitochondria takes the key position by initiating apoptosis. The exact mechanism of initiation by different apoptotic stimuli is still not entirely clear, but involves an imbalance of pro- and anti-apoptotic members of the BCL-2 protein family [107]. This imbalance finally leads to the activation of the pro-apoptotic BCL-2 family members BAX and/or BAK and the perturbation of the integrity of the outer mitochondrial membrane [108]. This induces the release of Cytochrome C and other apoptotic regulators, like apoptosis-

inducing factor (AIF), Smac (second mitochondria-derived activator of apoptosis)/DIABLO (direct inhibitor of apoptosis protein (IAP)-binding protein with low PI), endonuclease G or Omi/HtrA2 from the intermembraneous space of mitochondria. In the cytosol, Cytochrome C, APAF-1 and the initiator procaspase-9 are forming the apoptosome multiprotein complex and activate the initiator caspase 9. This induces the cleavage of the executioner caspases, like caspase-3. Furthermore, the potent endogenous inhibitors of caspases, the inhibitor of apoptosis proteins (IAPs) are neutralized by Smac/DIABLO or Omi/HtrA2 (Figure 1.20).

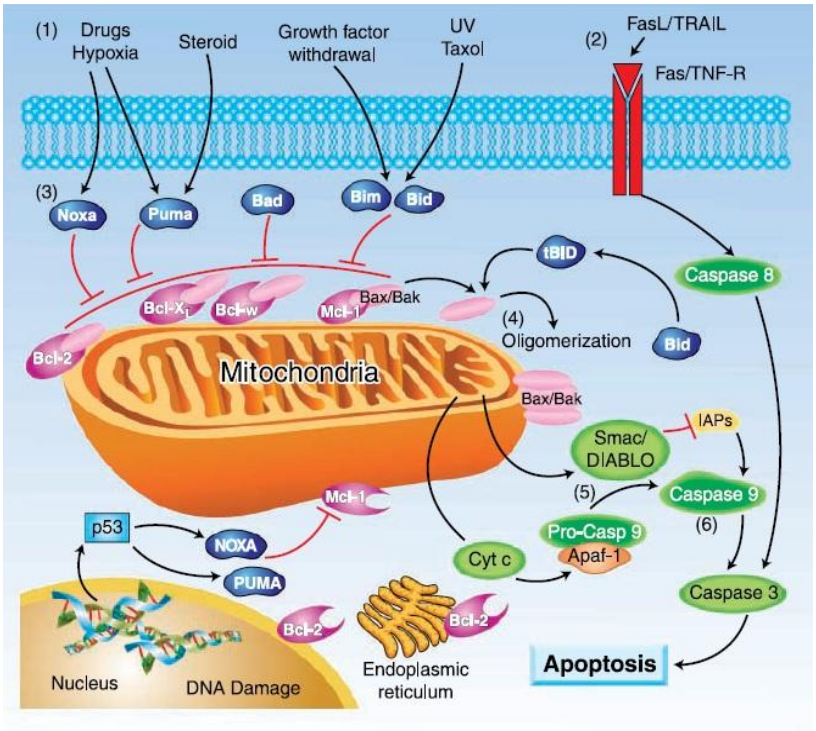

Figure 1.20 The apoptotic pathway to cell death from the perspective of the Bcl-2 family of proteins. 1. The intrinsic pathway is initiated by various signals, principally extracellular stimuli. 2. The extrinsic pathway is activated by Fas ligand or TRAIL, subsequently activating caspase-8. Caspase-8 transforms Bid into truncated Bid. In addition, caspase-8 initiates a cascade of caspases activation. 3. BH3-only proteins (Bim, Bid, Bad, Noxa, and Puma) engage with anti-apoptotic Bcl-2 family proteins to relieve their inhibition of Bax and Bak to activate them. 4. Next, Bax and Bak are oligomerized and activated, leading to mitochondrial outer membrane permeabilization. 5. Once mitochondrial membranes are permeabilized, cytochrome c and/or Smac/DIABLO is released into the cytoplasm, wherein they combine with an adaptor molecule, apoptosis protease-activating factor 1(APAF1) and an inactive

initiator caspase, procaspase-9, within a multiprotein complex called the apoptosome. Smac/DIABLO inhibits inhibitors of apoptosis proteins to activate caspase-9. 6. Caspase-9 activates caspase-3, which is the initiation step for the cascade of caspases activation. Intrinsic and extrinsic pathways converge on caspase-3.

The second pathway is called the extrinsic pathway and is mediated by different death receptors on the cell surface (Figure 1.21). These receptors are members of the tumour-necrosis factor (TNF) receptor superfamily, including the TNF-, FAS-(APO-1, CD95) and TRAIL-(TNF-related apoptosis inducing ligand) receptors. They share a common intracellular domain, which is called death domain. Activation of the receptors after extracellular binding of the specific ligands (TNF-α, FAS-L and TRAIL) initiates the recruitment of FADD (FAS-associated death domain protein), procaspase 8 and 10 to the death domain, which are forming the DISC (death inducing signalling complex). At the DISC, the initiator caspase 8 is activated.

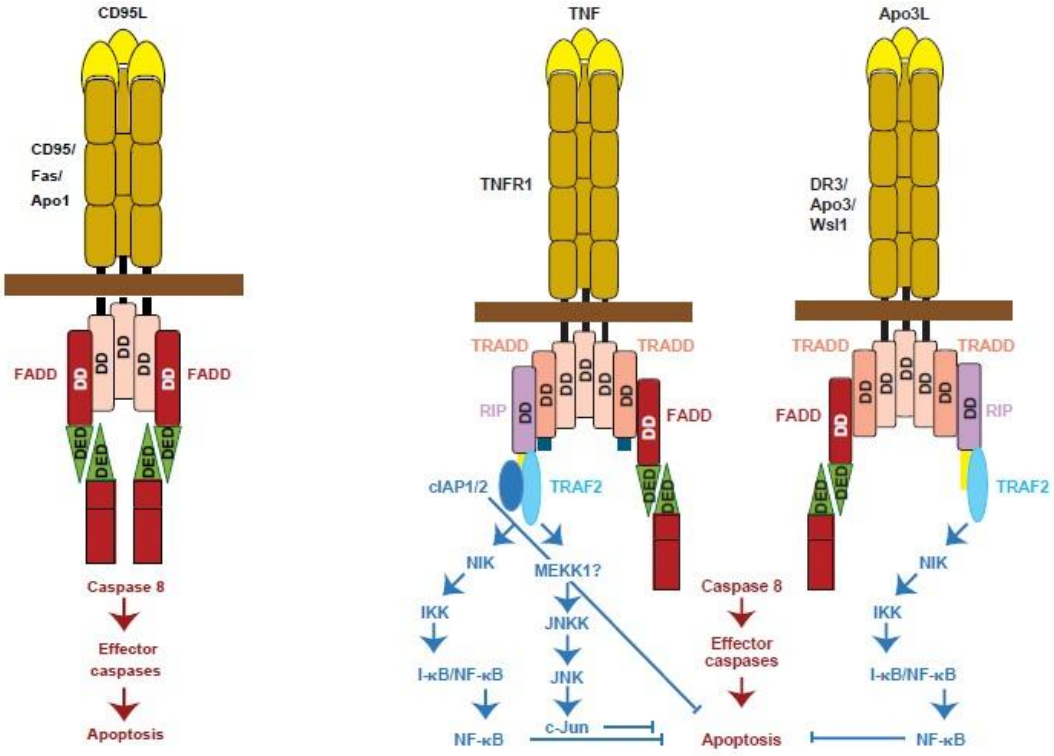

Figure 1.21 Engagement of death receptors by their cognate ligands triggers the recruitment of different adaptor proteins. Distinct pathways originate from the adaptor proteins. A classic proapoptotic pathway is initiated when the adaptor proteins recruit large amounts of the initiator caspases 8 and 10, resulting in their autoactivation. Active caspases 8 and 10 initiate a signalling cascade that results in activation of the effector caspases (caspases 3, 6,

and 7) either by directly processing the effector caspases themselves or by engaging the mitochondrial death pathway mediated by the cleavage of the BH3-only protein Bid. The release of proapoptotic proteins from the mitochondria, such as cytochrome c and Smac/DIABLO, ultimately promotes effector caspase activation and apoptosis. Several noncytotoxic signalling pathways can also originate from the association of adaptor proteins with the receptor, which generally results in the activation of MAPK- and/or NF-κB-mediated survival signals[109].

In type I cells the activated initiator caspases are sufficient to induce executioner caspases directly. In contrast type II cells need the signal enhancing-effect of mitochondria to induce apoptosis. Here, caspase 8 cleaves the pro-apoptotic BH3-only BCL-2 family member BID, which translocates to the mitochondrial membrane and induces the release of apoptogenic factors from the mitochondria. Pancreatic carcinoma cells are type II cells [110-111]. The type I/II concept, is a good example of the crosstalk between extrinsic and intrinsic apoptotic signalling and demonstrates the complexity of apoptosis [112].

Like other cancer cells, PDAC cells have evolved resistance mechanisms especially acting on the death receptor level and resulting in an impaired initiation of apoptosis by TNF-α, FasL and TRAIL[113]. In addition, PDAC cells gain protection against the mitochondrial pathway of apoptosis by overexpression of Bcl-family proteins (Bfl1, BCL-XL, MCL-1) [112] or by blocking activation of caspases for example by the overexpression of caspase inhibitors (cIAP, XIAP1, survivin), the epigenetic downregulation of procaspase gene expression or the direct caspase inhibition by cysteine nitrosylation [114].

Analyses of the expression of DISC-interacting proteins revealed that all apoptosis-resistant PDAC cells overexpress the TRAF2 protein. Furthermore, more than 90% of clinical specimens of pancreatic tumours showed strong upregulation of TRAF2-expression. High TRAF2 expression protects cells from FAS-mediated apoptosis also leading to constitutive upregulation of NF-κB and AP-1 activity and, in consequence, to the overexpression of urokinase-type plasminogen activator (uPA), matrix metalloproteases (MMP)-2/-9, IL8 and enhanced invasiveness. TRAF2 overexpression does not only block apoptosis induction by CD95 but

converts this death receptor into a mediator of invasiveness [90]. The Fas-associated phosphatase-1 (FAP-1) is overexpressed in PDAC tumour cells, protecting them from apoptosis by inhibiting FAS-induced caspase 8 activation [115].

Investigation of death receptor-induced non-apoptotic signalling in PDAC cells revealed that TRAIL-R also mediates activation of PKCs, JNK, p38, ERK1/ERK2 and of the transcription factors NF-κB and AP-1. Notably, PKC, ERK1/2 and NF-κB pathways inhibit apoptosis and in parallel induce the expression of inflammation and invasiveness promoting proteins like IL-8, MCP-1, MMPs and uPA. These proteins enhance the migration and invasion of apoptosis-resistant PDAC cells in an in vitro assay.
Pancreatic tumour cells secrete TNFα, which can induce the pro-inflammatory non-apoptotic signalling cascade. Previously, it has been shown that overexpression of TNFα confers invasive properties in a cell type–dependent manner in nude mice. A variety of tumour-promoting effects of TNFα was further shown in vitro and included protection against physiologic and pharmacologic apoptosis inducers, induction of angiogenic factors, enhancement of tumour cell motility, activation of oncogenic pathways and triggering of epithelial to mesenchymal transition. Again, the NF-κB pathway is regularly and robustly activated by TNFα and mediates many of the protumoural effects of TNFα [116].

Thus, activation of NF-κB leads either to the upregulation of anti-apoptotic genes or to the down-regulation of apoptotic genes. Another prevalent mechanism by which activated NF-κB induces chemoresistance in PDAC is the increased expression of cellular inhibitors of apoptosis (cIAP1, cIAP2, TRAF1, TRAF2, survivin) or the increased expression of the prosurvival bcl-2 homologue Bfl-1/A1 or of Bcl-X_L. Besides, NF-κB mediates resistance to chemotherapeutic drugs in PDAC cells represents the direct inactivation of caspases by nitric oxide (NO) [117].

In addition, cellular FLICE-inhibitory protein (cFLIP) is highly expressed in PDAC tumours. cFLIP is a master anti-apoptotic regulator and resistance factor that

suppresses TNF-α, Fas-L and TRAIL induced apoptosis, as well as apoptosis triggered by chemotherapy agents in malignant cells. c-FLIP binds to FADD and/or caspase 8 or 10 and TRAIL receptor 5 (DR5) and forms an apoptosis inhibitory complex (AIC). This interaction in turn prevents death-inducing signalling complex (DISC) formation and subsequent activation of the caspase cascade. c-FLIP(L) and c-FLIP(S) are also known to have multifunctional roles in various signalling pathways, as well as activating and/or upregulating several cytoprotective and pro-survival signalling proteins including Akt, ERK, and NF-κB[118]. Consistent with this finding, FADD expression seems to be reduced in PDAC tumour tissue [119].

At the level of the mitochondria, deregulated expression of members of the BCL2 protein family causes apoptotic resistance in PDAC[39]. The two anti-apoptotic BCL2-family members BCL-X_L and MCL-1 are upregulated in PDAC. Conversely, the proapoptotic BAX protein is reduced in approximately 50% of PDAC [120-121].

1.3.6 Invasion and metastasis: Role of tumour microenvironment in PDAC

Cancer invasion and metastasis are landmark events that transform a locally growing tumour into a systemic, metastatic and live-threatening disease [122]. Invasion is defined as the ability of cancer cells to degrade and adhere to the basement membrane. Adhesion molecules, such as integrins mediate direct cell-cell recognition and cell-matrix interactions and are essential for tumour cell migration and for basement membrane penetration. In pancreatic cancer, expression of integrins α6β1 and αvβ3 have previously been associated with invasion in cell lines and tissues [123]. The invasive potential of cancer cell depends on three aspects: alteration of cellular adhesions, ECM proteolytical degradation and migration of tumour cells [124].

Metastasis occurs when invading tumour cells engage with blood and lymph vessels, penetrate basement membranes and endothelial walls, and disseminate through the vessel lumen to colonize distant organs. Like cells in primary tumours, cells in metastases also proliferate, invade and enter blood vessels, leading to secondary metastasis [122].

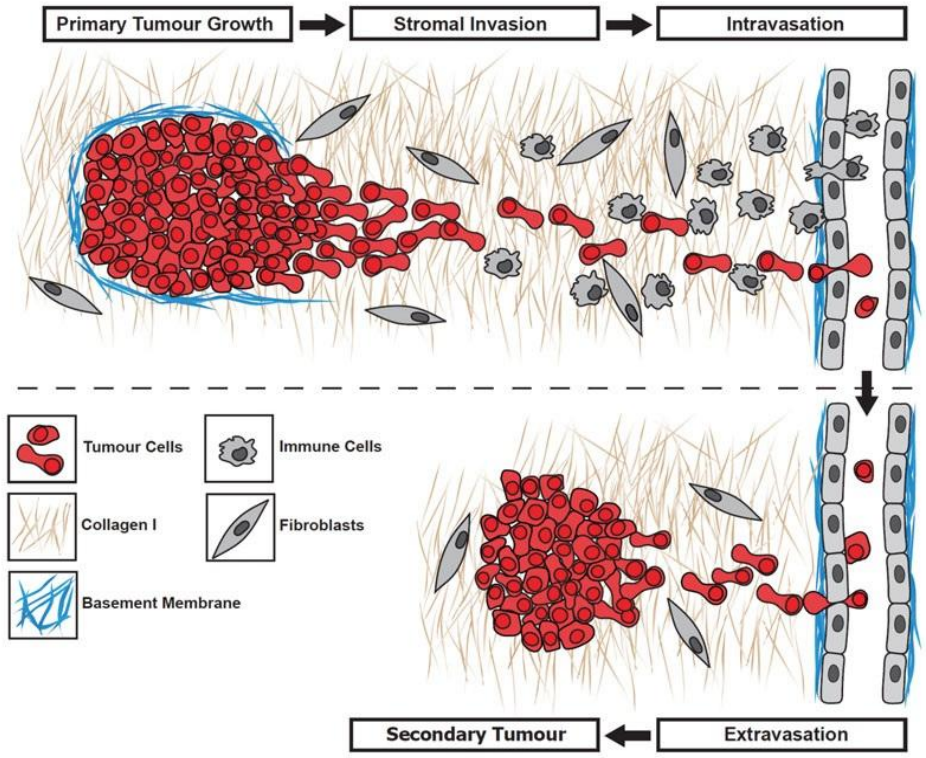

Figure 1.22 Metastasis involves the spread of cancer cells from the primary tumour to surrounding tissues and to distant organs and is the primary cause of cancer morbidity and mortality. In order to complete the metastatic cascade, cancer cells must detach from the primary tumour, intravasate into the circulatory and lymphatic systems, evade immune attack, extravasate at distant capillary beds, and invade and proliferate in distant organs. Currently, several hypotheses have been advanced to explain the origin of cancer metastasis[125].

One of the most prominent histological features of PDAC is an extensive stroma that surrounds the tumour cells and accounts for up to 90% of the tumour volume. There is a growing understanding of the contribution of the stromal microenvironment to the mechanisms responsible for malignant transformation and progression. The transition from a fixed, tissue-anchored state to a mobile state is often induced by extracellular chemokines, cytokines and growth factors released by tumour cells themselves or activated stromal cells [122]. Cancer cells can alter their adjacent stroma to form a permissive and supportive environment for tumour progression by producing stroma modulating growth factors [126]. These factors act in a paracrine manner to induce the inflammatory response and activate surrounding stromal cells, such as pancreatic stellate cells (PSCs) and

fibroblasts, smooth muscle cells and adipocytes. This activation leads to the secretion of additional growth factors, cytokines and proteases, which in turn activate both cancer cells and the surrounding stromal cells, indicating the existence of an interaction loop. This interaction results in a positive feedback effect on the growth and progression of PDAC[127].

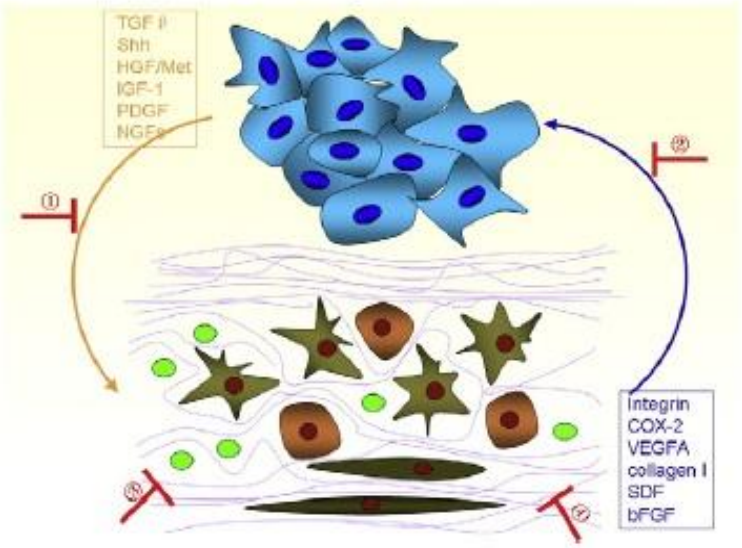

Figure 1.23 Interaction loop between PDA cells and stroma and potential therapeutic strategies. Multiple cancer cell-derived factors, including TGF-β, Shh and HGF/Met, mediate stroma production through autocrine and paracrine mechanisms. In response to the changes in the cancer cells, there is an altered gene expression profile in the cancer-associated stroma, including Integrin, COX-2, VEGFA and collagen I. Crosstalk between epithelial tumour cells and cells of the stromal compartment by means of these factors will result in the acquisition and enhancement of the pancreatic tumour abilities, such as cancer development, migration and invasiveness.

The cells responsible for producing the stromal reaction in pancreatic cancer are pancreatic stellate cells (PSCs, the key fibrogenic cells in the pancreas). PSCs are resident cells of the pancreas predominantly located in the periacinar, periductal and perivascular spaces of the pancreas. In health, PSCs comprise 4-7% of pancreatic cells and exist in their quiescent phenotype where they contain numerous cytoplasmic vitamin A containing lipid droplets and express specific markers such as desmin and glial fibrillary acidic protein (GFAP). In a normal

pancreas, PSCs may play a role in normal tissue architecture by regulating extracellular matrix turnover, given their known synthesis of ECM proteins and matrix degrading enzymes (matrix metalloproteinases [MMPs] and tissue inhibitors of metalloproteinases [TIMPs]). In response to pancreatic injury, PSCs transform into an active myofibroblast-like phenotype, under the influence of activating factors such as alcohol and oxidant stress or from products of injured cells including pro-inflammatory cytokines and growth factors. This transdifferentiation is accompanied by a loss of cytoplasmic vitamin-A lipid droplets and increased cytoskeletal protein α-SMA expression. Activated PSCs subsequently develop functional alterations including: 1) increased proliferation and migration; 2) synthesis of excessive ECM proteins (collagen, fibronectin, laminin) as well as matrix metalloproteinases and their inhibitors and 3) secretion of growth factors and cytokines which exert both paracrine and autocrine effects that enhance cell growth and migration [128].

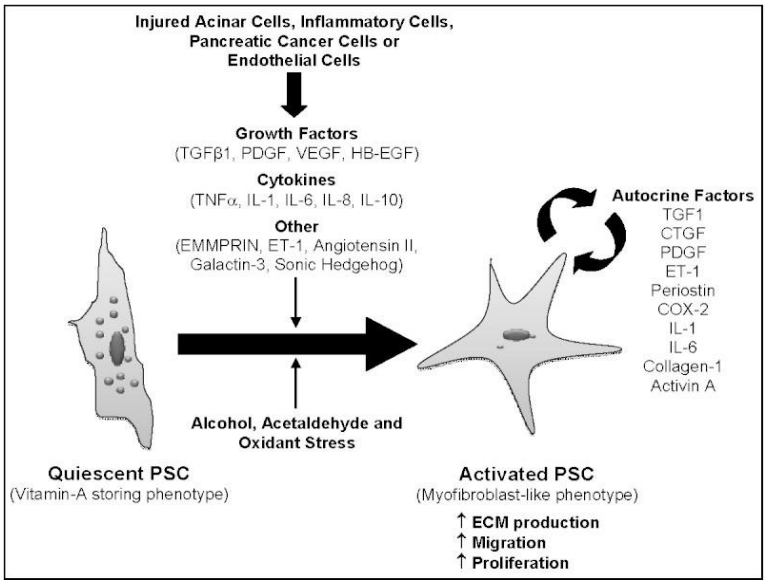

Figure 1.24 Pancreatic stellate cell activation

PSCs appear to be able to support cancer cells in achieving the key hallmarks of malignancy [129] including: self-sufficiency in growth signals, insensitivity to growth-inhibitory signals, evasion of apoptosis, limitless replicative potential, sustained angiogenesis, tissue invasion and metastasis and immune evasion. Most

recently, PSCs have been shown to increase the stem cell phenotype of pancreatic cancer cells [130].

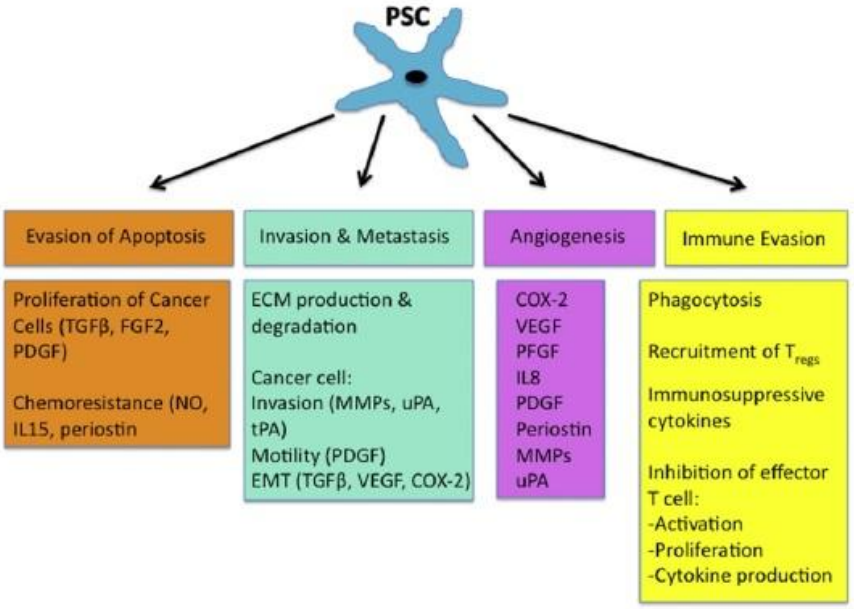

Figure 1.25 Schematic illustration of the role of PSCs in pancreatic cancer progression. Pancreatic stellate cells have been shown to promote key hallmarks of malignancy including evasion of cancer cell apoptosis, invasion and metastasis, angiogenesis, and promotion of an immunosuppressive microenvironment.

Functionally, activated PSCs perform a wide variety of roles; best recognized is the secretion of large amounts of ECM components such as collagen, laminin, and fibronectin. This can lead to fibrosis if PSC activation is perpetuated as in the setting of pancreatic cancer. Laminin and fibronectin have been shown to promote survival and prevent apoptosis of pancreatic cancer cells by stimulating reactive oxygen species (ROS) production in both pancreatic cancer cells and stellate cells. In addition to the production of ECM proteins, remodeling of the stroma by PSCs is essential for tumour cell invasion. Matrix metalloproteinases (MMPs) and tissue serine proteases are produced by both pancreatic adenocarcinoma cells and pancreatic stellate cells. Specifically, PSCs produce MMP-2, MMP-9, and MMP-13, and express their inhibitors; TIMP-1 and TIMP-2. These mediators are likely to promote cancer cell invasion and metastasis via degradation of ECM proteins. The stromal tissue of pancreatic cancer has shown up-regulation of matricellular

proteins including galectin-1, periostin, connective tissue growth factor, and tenascin-C. Matricellular proteins have been shown to stimulate both PSCs and pancreatic cancer cells and expression of these proteins correlates with poor survival in pancreatic cancer patients.

Epithelial-to-mesenchymal transition (EMT) is a dynamic process and the first step in the initiation of metastatic spread. It is required for cells to gain the migratory capabilities and dysregulation of cell-cell contacts needed to invade. PSCs also promote migration and the epithelial to mesenchymal transition in cancer cells [131]. EMT can be triggered by a variety of microenvironment stimuli in pancreatic cancer including TGF-β, HGF, EGF, IGF, VEGF, and FGF. Wnt, TGF-b, Hedgehog, Notch and NF-κB signalling pathways have been shown to be critical for EMT induction. TGF-β promotes EMT both in vitro and in vivo studies and is predominantly secreted by PSCs. In vitro, TGF-β1 promotes EMT and invasion in the Panc-1 pancreatic cancer cell line [132].

Disruption of the cell-ECM association is a major pre-requisite for tumour cell detachment and invasion. The ECM is a 3D structure which is constantly remodeled. In order to survive and invade, tumour cells need to control the extent to which the ECM is degraded as a part of the process of enabling adherence to the interstitial matrix and generating the traction necessary for migration. The tumour therefore has to remodel its microenvironment, via communication with PSCs, in order to invade. ECM degradation requires disruption of cell-cell adhesions in the basement membrane and integrins are central to this process. A variety of integrins has been implicated in different tumour types and has been demonstrated to activate MMPs and to recruit proteolytic activity, thereby facilitating degradation of the ECM. PSCs have been found to synthesize periostin which accumulates in the stroma surrounding pancreatic cancer cells and promotes invasion via α6b4 integrin. This is facilitated by MMPs and plasminogen activator, which are highly expressed at the stroma tumour border and cause degradation of the surrounding matrix components and invasion into nearby tissue [39, 132].

An implication of the extensive desmoplastic reaction in pancreatic cancer is intratumoural hypoxia, a major determinant of pancreatic cancer chemoresistance. The accumulation of ECM components distorts the normal architecture of pancreatic tissue inducing an abnormal configuration of blood and lymphatic vessels. One factor potentially contributing to therapeutic resistance in PDA may be the rigidity of the ECM that compresses blood vessels, leading to reduced perfusion that ultimately impedes the delivery of drugs to neoplastic cells [133].

In pancreatic cancer, the fibrotic and highly avascular microenvironment synergistically: 1) reduce drug delivery via the poorly perfused blood into the tumour; 2) causes the sequestering of drugs in the peritumoural stroma; and 3) leads to a decline in the effective intracellular drug concentration within pancreatic cancer cells, compromising therapeutic success [134].

It is clear that the pancreatic tumour stroma promotes pancreatic cancer development and is an important target for new therapeutics. Over the past two decades there has been a steep rise in our understanding of pancreatic fibrogenesis and the central role of PSCs in this process. It is also clear that PSCs have functions over and beyond the regulation of pathologic fibrosis in the pancreas, with the cells likely playing important roles in health as immune and/or progenitor cells. Improved understanding of PSC biology will underpin the development of novel therapies in the future for the treatment of chronic pancreatitis and pancreatic cancer [135].

1.4 TRANSLATIONAL STUDIES IN PANCREATIC CANCER

The past two decades have witnessed great advances in the fundamental understanding of the nature of pancreatic cancer, from the characterization of precursor lesions to the identification of an ever increasing compendium of molecular abnormalities and the development of relevant animal models. Unfortunately, despite these advances, PDAC remains a disease of near uniform lethality. Therefore, much attention has now focused on translational studies in PDAC, that is, those that can directly impact patient care and outcome.

1.4.1 Pancreatic Cancer Therapies

For decades, scientists, both in clinical as well as basic research areas, have worked intensively to make a major breakthrough in human pancreatic cancer treatment and to improve its clinical prognosis. Unfortunately, little progress has been achieved. Although complete surgical resection of the tumour mass is the most effective regimen in pancreatic cancer treatment, it can only be used in limited cases with localized tumours and there exists a significant rate of cancer relapse[136]. Chemotherapy, radiation therapy and adjuvant therapy together with palliative treatment are other approaches for pancreatic cancer treatment. Among these therapies, Gemcitabine has been recognized by many oncologists as the first-line drug to treat pancreatic cancer for more than a decade.

Although new combination chemotherapy regimens have recently demonstrated a significant survival benefit compared to Gemcitabine-based therapies, the search for novel treatment options still remains a huge challenge. After numerous potential targets have proven to be futile in clinical trials, recent efforts have been made to both improve drug delivery and to identify drugs targeting novel signalling pathways within the tumours including the putative stem cell compartment and the tumour stroma. Furthermore, predictive markers are needed to define tailored treatment regimens according to the molecular profile of individual tumours [137].

Gemcitabine (2´-2´-difluorodeoxycytidine, dFdC) must be taken into the cell where it is phosphorylated by deoxycytidine kinase (dCK) to its monophosphate (dFdCMP). This is regarded as the rate-limiting step. dFdCMP is phosphorylated again to its active diphosphate (by the uridine monophosphate kinase, UMK) and triphosphate metabolites (dFdCDP and dFdCTP). 5´-nucleotidase reduces them. Gemcitabine is inactivated mainly by deoxycytidine deaminase (dCDA) generating difluorodeoxyuridine (dFdU). Deamination of dFdCMP to 2´, 2´-difluorodeoxyuridine monophosphate (dFdUMP) by the action of deoxycytidine monophosphate deaminase (dCMPDA) and subsequently to dFdU represents another inactivation pathway of Gemcitabine. The drug is then excreted out of the cell [138-141].

dFdCTP, the main active metabolite of Gemcitabine, rivals with deoxycytidine triphosphate (dCTP) for incorporation into DNA (Figure 1.26). Once dFdCTP is incorporated into DNA, only one more deoxynucleoside triphosphate can be incorporated, after which DNA replication finishes. The dFdCTP is not removed from the DNA strand by proofreading enzymes ("masked-chain termination"). However, the incorporated Gemcitabine can be recognized by p53 and DNA dependent protein kinase, which might result in apoptosis [142]. However, as DNA damage system is altered in PDAC, this effect could result limited. dFdCTP inhibits the chain elongation of DNA strands which produces the block at the S-phase. In addition, Gemcitabine diphosphate (dFdCDP) inhibits ribonucleotide reductase, which produces deoxycytidine triphosphate (dCTP), an antagonist of dFdCTP. This leads to a reduction of dCTP but augmentation of dFdCTP into cells and enhances its antitumour activity. This inhibition reduces the synthesis of deoxynucleotide triphosphates, primarily dATP. This causes cells to redistribute into the early S-phase of the cell cycle [143]. dFdCTP also inhibits cytidine triphosphate synthetase (CTP-synthetase) which results in CTP pool depletion. Again, dFdCTP suppresses inactivation of dFdCMP by inhibiting deoxycytidine monophosphate deaminase (dCTD). Those are self-potentiating mechanism [144-146]. Gemcitabine is also incorporated to RNA but the significance of the incorporation into RNA is not yet clear [147]. Recent studies have shown that part of the cytotoxicity of dFdC could be explained by the poisoning of the ubiquitous topoisomerase1 enzyme due to

incorporation of the nucleoside analog into nascent DNA [141, 148-149]. Thus, Gemcitabine exerts its antineoplastic activity through an array of cellular effects on DNA synthesis [142].

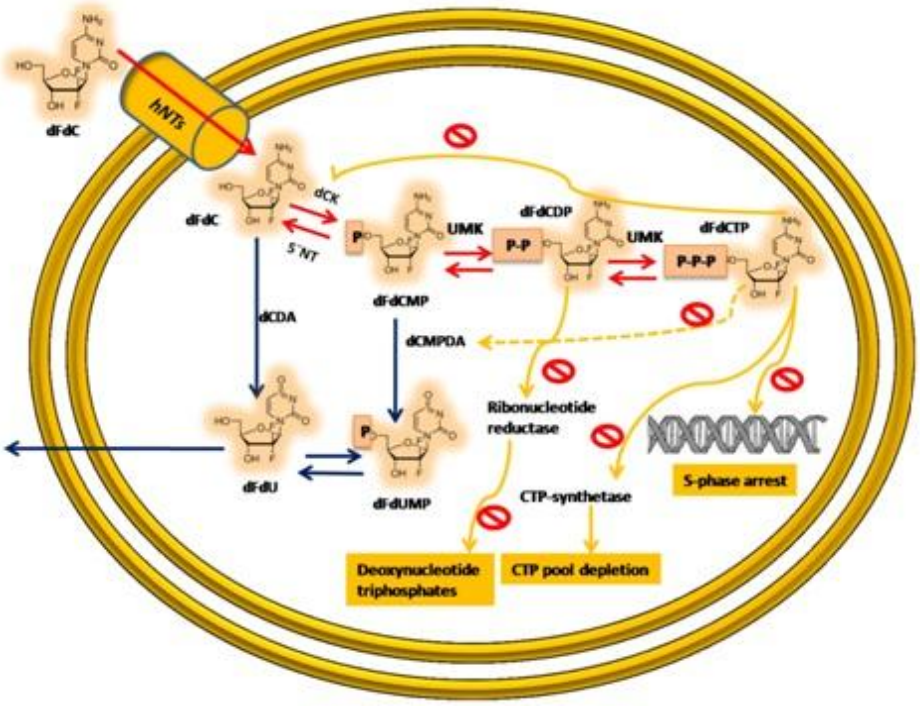

Figure 1.26 Gemcitabine biotransformation. Reactions involved in metabolic activation and inactivation. hENT, equilibrative nucleoside transporters; dFdC, Gemcitabine; dFdCMP, Gemcitabine monophosphate; dFdCDP, Gemcitabine diphosphate; dFdCTP, Gemcitabine triphosphate; dFdU, 2´,2´-difluorodeoxyuridine; dFdUMP, 2´,2´-difluorodeoxyuridine monophosphate; dCK, deoxycytidine kinase; UMP, deoxycytidylate kinase; dCDA, deoxycytidine deaminase; dCMPDA, deoxycytidine monophosphate deaminase.

With the progression of in-depth research on pancreatic cancer, several important pathologic processes related to pancreatic cancer pathobiology have been elucidated and many therapeutic strategies targeting key molecules in these processes have been developed. For example, cetuximab as well as Erlotinib have been used to target the EGFR pathway to inhibit tumour growth.

The most successful molecular targeted therapy against pancreatic cancer is the inhibition of epidermal growth factor receptor (EGFR)[150]. Erlotinib (Tarceva)

inhibits phosphorylation of the EGFR tyrosine kinase without inducing EGFR internalization or degradation. Inhibition of EGFR downstream signalling by Erlotinib exerts antitumour activity through inhibition of proliferation and tumour angiogenesis and through induction of apoptosis. It is being used in combination with Gemcitabine for the first-line treatment of advanced, unresectable, or metastatic pancreatic cancer[151]. However, discrete survival improvement in advanced pancreatic cancer patients has been obtained combining Gemcitabine with Erlotinib [152]. There has been debate about the advantages of this combination due to the lack of known specific targets for pancreatic cancer, the only 0.33-month survival advantage [153-154] and overall because *k-ras* mutations are present in a 90% of pancreatic cancers. This treatment would be only indicated for those carrying wild-type *k-ras*.

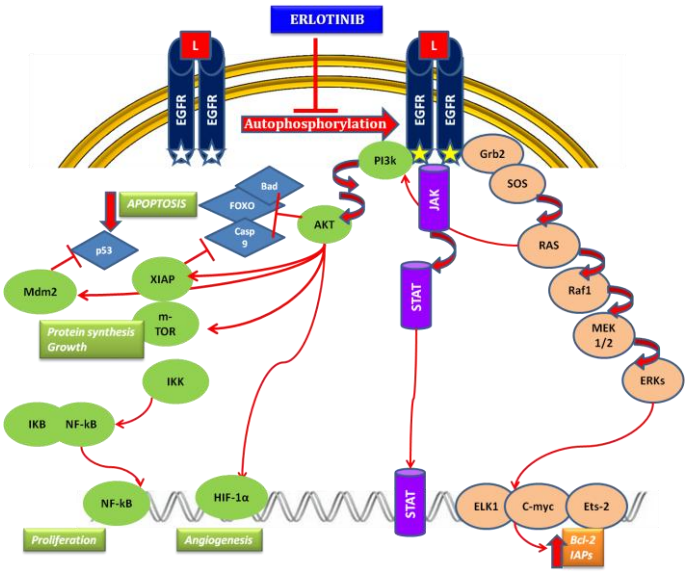

Figure 1.27 Effect of the Erlotinib on proliferative pathways.

The long list of investigative treatment methods for pancreatic cancer with low success rates indicates human pancreatic cancer is not a disease controlled by a simple pathological process. Discoveries in pathogenesis of pancreatic cancer, including abnormalities at the gene level and signal transduction pathways, revealed very valuable information. However, targeted therapies based on these discoveries have not changed the overall survival of this malignant disease clinically, despite very promising results in some pre-clinical studies.

The role of molecular targets in pancreatic cancer development need to be evaluated not only with in vitro studies or preclinical studies, but also at different stages of this disease using clinical samples. The importance of molecular targets at different stages during cancer development needs to be analyzed with integration of information collected from multiple pathways. New therapeutic approaches for pancreatic cancer need to be considered based on combined analysis of pathophysiological information obtained from multiple levels and dimensions. Successful molecular targeted and chemotherapy based regimens may be established based on this information. Gene mutation determination, proteomic analysis and integration efforts using advanced informatics may help to uncover the complicated pathological processes and expose the resistance mechanisms in pancreatic cancer patients.

1.4.2 Biomarkers

The dreadful prognosis of patients with this disease, less than 5% reaching 5 years survival after diagnosis, is due to the little impact of the available chemotherapy on the course of the disease and to tumour metastasis at presentation. Owing to the impact and the dramatic change that early diagnosis has in patient survival [155], better diagnostic tools (biomarkers) for the detection and evaluation of this disease are urgently needed.

As defined by the NIH Biomarker Working Group, a biological marker (biomarker) is a characteristic that is objectively measured and evaluated as an indicator of normal biological processes, pathogenic processes, or pharmacologic responses to a therapeutic intervention [156]. In PDAC, three types of biomarkers are desirable: those that help in the detection of the disease onset (*diagnosis biomarkers*); those that predict responses to treatments *(predictive biomarkers*) and those that forecast the likely course of the disease, including survival and recurrence pattern in the absence of therapy (*prognosis biomarkers*).
Serum is the preferred option to obtain specimens for testing malignant tumours as it can be taken by non-invasive methods and because, specifically for pancreas, the access to the organ is very difficult. For these reasons, serum-based cancer biomarkers constitute the easiest screening test [157].

Tumour marker carbohydrate antigen CA19-9 has been widely used in PDAC diagnosis and is still the current standard serum tumour marker. Nevertheless there are some limitations in the usefulness of this marker such as it is elevated in only about 65% of individuals with resectable pancreatic cancer, it has no role in screening asymptomatic populations, it is no possible to discern between pancreatic cancer patients and those with chronic pancreatitis and it appearances in other malignances. In this way, the European Group of Tumour Markers (EGTM) the National academy of Clinical Biochemistry (NACB) recommend that CA19-9 should not be the only indicator used for diagnosing PDAC [158-159]. Serum CA19-9 reaches sensitivity of 70–80% but with specificities less than 50% [160].

The poor prognosis of patients is primarily due to the fact that most patients present, and are treated, in the terminal stage of the disease [161]. Early detection biomarkers are of utmost importance to improve the dreadful outcome. Besides, finding a biomarker or a panel of biomarkers that would be able to predict the clinical impact of a chemotherapy regimen even before it is initiated is highly warranted to: 1) identify those patients more likely to benefit from aggressive therapies; 2) reduce risks of useless side effects and may help to set expectations for doctors and patients and 3) make attempt to apply new combination of therapies or individualized treatment protocols according to their expected responses. In addition, markers that display prognosis significance also offer the potential to become emergent therapeutic targets and novel strategies in the management of PDAC [162-163].

In the recent years, an extensive research has been focused on the discovery of prognosis biomarkers for PDAC using immunohistochemistry, Western Blot, PCR, miRNA, proteomics or DNA methylation based methods amongst others [164-171]. One of the most promising tools for biomarker determination is protein microarray.

1.4.3 Protein microarrays

Protein microarray technology is an emerging field that provides a versatile platform for the characterization of hundreds of thousands of proteins in a highly parallel and high-throughput manner.

Microarray technology refers to the miniaturization of thousands of assays on one small plate. This approach was developed from an earlier concept called ambient analyte immunoassay, which was first introduced by Roger Ekins in 1989 [172]. In the decade that followed, this concept was successfully transformed into the DNA microarray, a technology that determines the mRNA expression levels of thousands of genes in parallel. However, DNA microarray technology possesses some limitations because mRNA profiles do not always correlate with protein expression. More importantly, proteins are the major driving force in almost all cellular processes. Therefore, protein microarrays were developed as a high throughput tool to overcome the limitations of DNA microarrays and to provide a direct platform for protein function analyses [173].

In this thesis, we present a study in which the Human Cytokine Array from RayBiotech was used to analyze simultaneously 507 cytokines in collected sera from pancreatic cancer patients. Human cytokine arrays have shown utility in a wide number of clinical applications, most notably in biomarker discovery due to the fact that cytokines are abnormally expressed in inflammatory and infectious disease and cancers [174]. The Array includes cytokines, chemokines, growth and differentiation factors, angiogenic factors, adipokines, adhesion molecules and matrix metalloproteases, as well as binding proteins, inhibitors and soluble receptors to these proteins [175].

There is increasing evidence of a link between cancer and inflammation [176-178]. As described in section 1.3.6, PDAC is characterized by a dense desmoplastic reaction which represents a noteworthy barrier preventing the effective delivery of chemotherapeutic agents into the site of primary disease. Besides, the complex tumour microenvironment nurtures pancreatic cancer invasion and metastasis

[127, 179-180]. Recently it has been pointed out that infiltrating inflammatory cells within the tumour or tumour cells themselves produce cytokines and chemokines leading to a modulation of the microenvironment, which fosters angiogenesis, growth, invasiveness and metastasis. Due to its relation to inflammation, we speculated that altered levels of cytokines in the systemic circulation could be illustrative of their deregulation in the tumour microenvironment.

Therefore serum protein predictive patterns based on cytokines could have great meaning in predicting new PDAC patients. Besides, serum cytokines levels in treated patients compared with non-treated patients could provide profiles of responses to therapy and lastly, serum cytokines could reflect the host response to the tumour in PDAC patients and act as prognosis factors.

Recent years have seen a rapid increase in availability of high dimensional genomic and proteomic information in biomedical research that could potentially be used for risk prediction, diagnosis, prognosis and targeted therapeutic interventions. The situation is almost always characterized by a relatively small number of individuals and a large number of potential predictors, thus prohibiting the direct use of classical approaches of statistical modeling and data analysis [181]. Various diagnostic plots were used to assess the distribution and quality of the data and thereby judge whether any outliers were present in the data set. Then, a feature selection method was applied in the attempt to reduce the so-called high dimensionality small sample problem. Feature selection plays an important role in clinical data analysis for three reasons. First, using all features in forming the classification rule in general does not give the best performance. The second reason is a technical one: some classification methods require the number of objects to be larger or equal to the number of features. Since proteomics data sets usually consist of far more features than samples, a selection has to be made before constructing the classification rule. Third, one of the goals of a proteomics study is to find leads for potential markers for disease. Hence, the number of variables in the final model should be small to enhance the interpretability of the model [182]. The filter Mann-Whitney U test was applied to assess diagnosis biomarkers. In the

case of prognosis biomarkers, a wrapper method was used as feature selection method. The classification method is used to test relevance of the variables. Variables that lead to good performance are selected. The next step towards clinical utility is validation. The performance of a classifier in clinical applications is usually given in two measures. The sensitivity is the fraction of cases that are classified as cases. The specificity is the fraction of controls that is correctly identified. The sensitivity and specificity can take values between zero and 1, where zero means all samples in that class are misclassified and 1 means that they are all correctly identified. The sensitivity and specificity can be plotted together in a receiver operating characteristic (ROC) curve. Besides, the variability of the classifier should be reflected in the performance estimator. Cross validation makes efficient use of the available data, which is especially helpful in small data sets [182].

As a result of this thorough statistical assessment, the combination of cytokines FGF-10/KGF-2, I-TAC/CXCL11, OSM, GPNMB/Osteoactivin and SCF was associated with PDAC and could represent novel diagnostic biomarkers of PDAC disease. Amongst these five cytokines, we chose GPNMB/Osteoactivin to study its molecular role in pancreatic cancer first because the link of it with PDAC was original and had not been described elsewhere and also because it has been recently associated with several cancers such as melanoma [183-184], uveal melanoma [185] glioma, [186] hepatocellular carcinoma [187] and breast cancer in which it has been described also as a prognosis indicator of recurrence [188].

1.4.4 GPNMB/Osteoactivin

GPNMB, initially termed glycoprotein non-metastatic gene B (NMB), was first cloned and described in 1995 as a protein highly expressed in a melanoma cell line with low metastatic potential [189]. GPNMB, also named hematopoietic growth factor inducible neurokinin-1 type (HGFIN), dendritic cell-associated heparin sulfate proteoglycan-integrin ligand (DC-HIL) or osteoactivin, is a highly glycosylated type I transmembrane protein of 572 amino acids. The human GPNMB gene was localized to the small arm of the chromosome 7 (7p15.1) whereas the mouse GPNMB was mapped to chromosome 6 [190].

GPNMB belongs to the vertebrate Pmel17/NMB family, which encompasses GPNMB, Pmel17 (melanocyte protein 17) and their orthologues. Pmel17 is the main structural component of melanosomes, where it plays a key role in the pigment biogenesis of melanocytes. To a lesser extent, GPNMB also shares homology with lysosome-associated membrane protein (LAMP-1) family members, which are glycoproteins with potential roles in cell adhesion and metastasis.

1.4.4.1 GPNMB structure

GPNMB is a type I transmembrane protein that contains an N-terminal signal peptide, an integrin-binding (RGD) motif and a polycystic kidney disease (PKD) domain in its extracellular domain (ECD), a single pass transmembrane domain, and a 53 amino acid cytoplasmic tail [191](Figure 1.28). The cytoplasmic tail harbors a half immunoreceptor tyrosine-based activation motif (hemITAM) and a dileucine-based sorting signal (which mediates the sorting of transmembrane proteins to endosomes and lysosomes [192]). In addition to these domains and motifs, there are two known splice variants of GPNMB, comprising a short 560aa and a long 572aa isoform. The long isoform contains a 12aa insertion within a poorly conserved region downstream of the PKD-domain [186]. To date, there has been no evidence that the short and long isoforms have disparate functions.

1.4.4.1.1 RGD DOMAIN

This motif, comprised of only 3 amino acids, arginine (R), glycine (G), and aspartic acid (D), is found near the N-terminus of the GPNMB ECD and is well characterized in numerous proteins as an integrin-binding motif. Integrins are heterodimeric transmembrane proteins expressed on a wide variety of cells, which regulate cell spreading, adhesion, migration, proliferation and apoptosis. The RGD recognizing integrins are α5β1, αVβ1, αVβ3, αVβ5, αVβ6, αVβ8 and αIIbβ3 [193].

1.4.4.1.2 PKD DOMAIN

The PKD domain belongs to the immunoglobulin-(Ig) like fold superfamily (E-set), which also includes cadherins, protein families containing bacterial Ig-like domains and several fibronectin type III domain-containing protein families. While the function of the PKD domain is still unclear, based on its structure, it has been proposed to mediate protein-protein or protein-carbohydrate interactions [194] and has been shown to mediate cell-cell adhesion [195].

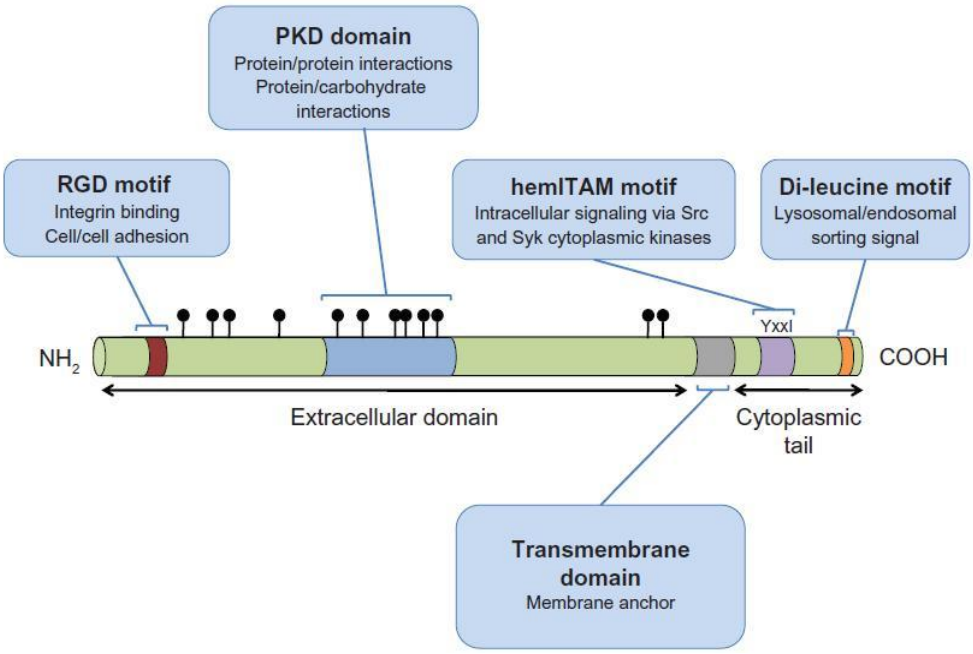

Figure 1.28 A schematic representation of GPNMB indicating the domains and motifs contributing to GPNMB function. The symbols (filled circles) located above the extracellular

domain of GPNMB represent glycosylation sites. The RGD sequence comprises an integrin binding domain, where R = Arginine, G = Glycine, D = Aspartic acid. The YxxI sequence constitutes a hemITAM motif, where Y = tyrosine, x = any amino acid, I = Isoleucine. The di-leucine motif is a lysosomal/endosomal targeting motif of the D/ExxxLL type, where D = Aspartic acid, E = Glutamic acid, x = any amino acid, L = leucine

1.4.4.1.3 HEMITAM

ITAM (immunoreceptor tyrosine-based activation motif) motifs are commonly found in the cytoplasmic domains of receptors expressed by cells of the hematopoietic systems. It consists of the sequence YxxL/I with six to twelve intervening residues before the YxxL/I sequence is repeated. ITAM motifs are found in antigen receptors, cytokine receptors and toll-like receptors. ITAM signalling usually occurs in response to ligand binding, via phosphorylation of the ITAM resident tyrosine residues, primarily by Src-family kinases (ie, Src, Hck, Fgr, Lyn)[196]. It triggers downstream processes that lead to several cellular processes including cytoskeletal changes, ROS production, differentiation, proliferation, survival and cytokine release [197].

GPNMB is one of several proteins whose cytoplasmic tail contains a highly conserved, single YxxL/I sequence, which has been referred to as a hemi-ITAM or hemITAM motif. Proteins with hemITAMs still exhibit robust ITAM signalling capacity. The current view suggests that ligand binding stimulates dimerization of hemITAM-bearing receptors; however, it remains to be seen whether GPNMB is capable of forming such homodimers.

1.4.4.1.4 DILEUCINE SORTING MOTIF

GPNMB contains a dileucine motif in its cytoplasmic tail, near the carboxy-terminus, with the sequence EKDPLL (E: glutamic acid; K: lysine; D: aspartic acid; P: proline; L: leucine). Dileucine-based motifs of this type (D/ExxxLL) are often implicated in rapid receptor internalization from the plasma membrane and

lysosomal/endosomal targeting. Indeed, when either of these leucine residues is mutated to glycine in GPNMB, it is retained at the plasma membrane of HeLa or pigmented quail cells and not routed to endosomes and lysosomes, as is the case for wild type GPNMB [198].

1.4.4.1 Post-translational modifications

1.4.4.1.1 GLYCOSYLATION

GPNMB is a heavily glycosylated protein, possessing 12 putative N-glycosylation sites within its extracellular domain, 6 of which are found in the PKD domain (Figure 1.28). Glycosidase treatments have confirmed that GPNMB can be N- and O-glycosylated in a variety of cell types. Following immunoblotting analyses, human GPNMB is detected as two broad bands that correspond to precursor (MW ~90 kDa) and mature (MW ~115 kDa) GPNMB isoforms. In addition, the unglycosylated form of GPNMB (MW~65 kDa) has been detected in cells, such as osteoclasts [199-200]. Studies using N-glycosidases suggest that GPNMB is first N-glycosylated in the endoplasmic reticulum to yield the precursor isoform, and these N-glycans are further modified during processing in the Golgi apparatus to produce the mature form. While both isoforms are susceptible to tyrosine phosphorylation, only the mature form can be proteolytically processed through shedding [198, 200]. To date, the importance of these glycosylation events for GPNMB/Osteoactivin function has not been assessed. But given that only the mature form of GPNMB is proteolytically processed and that altered glycosylation pattern promote aberrant protein-protein interactions [201], we can presume that this modifications are required for at least some of its functions.

1.4.4.1.2 PROTEOLYTIC CLEAVAGE AND ECD SHEDDING

GPNMB is also subject to proteolytic processing, which was first uncovered by the detection of two heavily glycosylated, high molecular weight forms of murine

GPNMB (97 kDa and 116 kDa) and a stable c-terminal fragment of ~20 kDa. It was postulated that GPNMB was susceptible of shedding by members of the matrix metalloproteinase (MMP) family, such as a disintegrin and metalloproteinase (ADAMs), because treatment with a broad-spectrum inhibitor of MMPs (GM6001) reduced the degree to which GPNMB was shed. Hash et all confirmed that the GPNMB detected in the cell media was not a full-length secreted form, as it was only detectable with an antibody that recognized its N-terminus but not its C-terminus [200]. Treatment with a calmodulin inhibitor (W7) or a protein kinase C activator (phorbol myristate acetate [PMA]) enhanced GPNMB shedding, further implicating the ADAMs, as these compounds have both been reported to enhance ADAM-10 and ADAM-17 activity, respectively. In agreement with an important role for ADAMs in GPNMB processing, constitutive GPNMB shedding was observed in breast cancer cells and definitively characterized ADAM10 as a sheddase responsible for this cleavage event in breast cancer cells [202].

1.4.4.2 Regulation of GPNMB/Osteoactivin expression

1.4.4.2.1 GROWTH FACTORS AND CYTOKINES

Depending on de cell type it is expressed, GPNMB/Osteoactivin expression is enhanced by numerous cytokines and growth factors such as: G-CSF [203]; M-CSF [203-204]; GM-CSF [205]; TGF-β [206]; IL-3 [205]; FGF-2 [207]; PDGF [207]; BMP-2 [208]; α-MSH [209]. Ultraviolet light (type A) has also been shown to induce GPNMB expression [209]. Moreover, while they have no effect on overall GPNMB expression, INF-γ and TNF-α have been reported to promote mobilization of GPNMB form intracellular stores to the plasma membrane [209].

1.4.4.2.2 TRANSCRIPTION FACTORS

In the promoter region of GPNMB there are two highly conserve consensus sequences for microphthalemia-associated transcription factor (Mitf) [210-211].

Mitf is a master regulator of osteoclastogenesis [212] and melanocyte differentiation [213] and enhances the expression of GPNMB/Osteoactivin in developing osteoclasts [210] or its orthologue, QNR-71, in neural retinal cells [214].

The GPNMB/Osteoactivin promoter region also contains a consensus sequence for the AP1 transcription factor, directly upstream of the Mitf site [211]. Given that a physical interaction between MITF and AP-1 has been previously demonstrated [215], the proximity of the AP-1 site to Mitf suggests a possible direct interaction between Mitf and AP-1 in regulation of GPNMB expression. AP1 is a heterodimeric transcription factor comprised of proteins of the FOS and Jun transcription factor families. This is of particular interest because AP1 transcription factors have been implicated in regulating osteoblastogenesis [216] and tumour cell invasion [217] both of which are processes that depend on GPNMB/Osteoactivin function.

Its promoter region also contains consensus sites for p53, and in T47D but not HCC70 breast cancer cells, p53 was capable of binding to these sites [203] but it has yet to be determined if GPNMB/Osteoactivin mRNA expression is indeed regulated by p53.

Finally, in osteoblasts, GPNMB/Osteoactivin protein expression is reduced when the SMAD-1 transcription factor (which is induced by bone morphogenetic protein-2, BMP-2) is knockdown [208]. So, BMP-2 regulates GPNMB/Osteoactivin expression through the Smad1 signalling pathway (refer to section 1.3.5.1.1 to further details about SMAD regulation).

1.4.4.3 Gpnmb/Osteoactivin expression in normal tissue

GPNMB mRNA has been detected in the long bones, bone marrow, adipose, thymus, skin, placenta, heart, kidney, pancreas, lung, liver and skeletal muscle [199, 203, 205, 218-219]. However, the precise expression patterns varied between these studies. These studies clearly demonstrate that GPNMB is

expressed in a wide range of tissues and suggest its involvement in a variety of physiological processes.

The molecular functions of GPNMB are just beginning to be elucidated and perhaps have been best characterized in the immune system. Expression of GPNMB has been detected in leukocytes and antigen presenting cells, including macrophages [220-221] and dendritic cells [218, 222] and has been involved in promoting various cell-cell interactions GPNMB expression on dendritic cells has been shown to mediate their adhesion to endothelial cells through its RGD domain [218]. Additionally, the extracellular domain of GPNMB can suppress T-cell activation and proliferation by binding to syndecan-4 on the surface of activated T-cells, and this interaction requires an intact PKD domain [223-224]. GPNMB binding to syndecan-4 leads to the recruitment of syntenin and the CD148 protein tyrosine phosphatase, the activation of which occurs following complex formation and is required for syndecan-4 mediated suppression of T-cell activation [225].

In contrast to these immunosuppressive roles, activation of GPNMB in dendritic cells, either by ligand binding or antibody cross-linking, can induce an innate immune response against fungal antigens. Under these conditions, the hemITAM tyrosine residue of GPNMB became phosphorylated, which induced widespread changes in gene and protein expression, including increased cytokine secretion (TNFα, IL-1β). This activation of GPNMB stimulated dendritic cell maturation and augmented their ability to potentiate the activation of naive T-cells [226]. While these findings are strongly suggestive of functional hemITAM-based signalling in GPNMB, more research is needed to definitively characterize the role of this motif when GPNMB is expressed in immune or non-immune cells.

Besides, GPNMB is expressed and contributes to the differentiation and function of both osteoblasts and osteoclasts within the bone microenvironment [227].

1.4.4.4 Gpnmb/Osteoactivin expression in disease processes

GPNMB expression is widespread and it is able to regulate a wide range of physiological and pathological processes. Its established roles during normal tissue processes, such as adhesion during transendothelial migration of dendritic cells and autophagy during tissue repair, are also important mechanisms observed during cancer progression and metastasis. Intriguingly, GPNMB expression can be upregulated in pathological conditions, such as chronic liver disease, which can lead to carcinogenesis [228]. Considering that the mechanisms of action for GPNMB in tumour progression have yet to be fully elucidated, these observations of GPNMB function in normal tissues represent compelling potential roles for GPNMB in cancer and warrant further investigation.

It has become increasingly clear that the initial designation of GPNMB as "glycoprotein non-metastatic gene B" is a misnomer. It was given this name after a partial Gpnmb/Osteoactivin cDNA was transfected into a highly invasive melanoma cell line and suppressed spontaneous metastasis in one of three transfected clones. However, further research revealed that Gpnmb/Osteoactivin was expressed in the majority of metastatic melanomas and that the frequency of Gpnmb/Osteoactivin expression in cutaneous melanomas was 80% [184] and in uveal melanomas was 85.7% [229]. The role of Gpnmb/Osteoactivin in tumour progression was next re-visited in 2003 when it was reported to promote the invasion of glioma cells [230]. They found that tumour cells expressing Gpnmb/Osteoactivin acquired a highly invasive phenotype when implanted intracranially in immunocompromised mice and in vitro and increased invasiveness and expression of MMP-9 and MMP-3. Gpnmb/Osteoactivin overexpression also increased the invasiveness and metastasis of rat hepatoma cells in vitro and in vivo [228]. Kuan et al [186] revealed that 35 of 50 glioblastoma multiforme (GBMs) patients (70%) were positive for Gpnmb/Osteoactivin mRNA and 52 of 79 GBMs patients (66%) were detected Gpnmb/Osteoactivin in a membranous and cytoplasmic pattern. Rose et al [231] identified Gpnmb/Osteoactivin as a gene that was highly and selectively expressed in

aggressive bone metastatic sub-populations of 4T1 breast cancer cells, and demonstrated that, when Gpnmb/Osteoactivin was overexpressed in an independent, weakly bone metastatic 66cl4 breast cancer cells, it promoted breast cancer metastasis to bone in vivo. Then, they employed IHC-based analysis of tissue microarrays to investigate the relevance of Gpnmb/Osteoactivin expression in human breast cancer and found that Gpnmb/Osteoactivin was expressed in the tumour epithelium of approximately 10% of human breast cancers and the stromal compartment of nearly 70% of breast tumours. Moreover, epithelial, but not stromal, Gpnmb/Osteoactivin expression was a prognostic indicator of cancer recurrence across all breast cancer subtypes, and specifically within "triple negative" breast cancers [24].

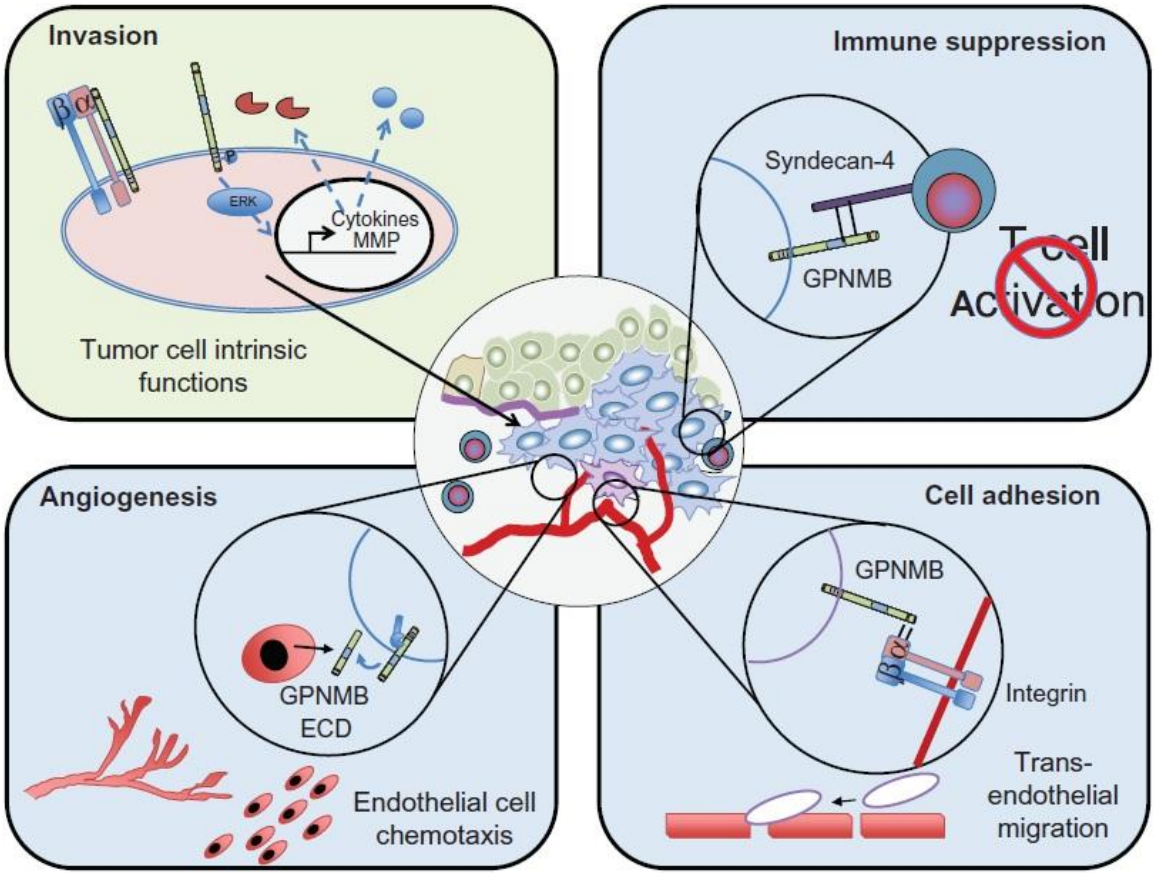

Figure 1.29 Potential mechanisms through which GPNMB promotes malignant cellular phenotypes within cancer cells. GPNMB may act cell autonomously (green panel) to induce intracellular signalling, which can influence the expression of multiple targets, including matrix metalloproteinases and cytokines and enhance the invasiveness of tumour cells.

GPNMB may also be important in regulating interactions between tumour cells and cells within the tumour microenvironment (blue panels). It can act as a cell/cell adhesion molecule by engaging integrins expressed on cells in the tumour microenvironment, such as endothelial cells. GPNMB-mediated interactions with syndecan-4 expressed on T cells can block the proliferation and activation of these cells, leading to an immunosuppressive environment favouring tumour growth. Finally, GPNMB may function in a paracrine fashion due to shedding of its extracellular domain, or through its release from cells in the form of microvesicles, leading to endothelial cell recruitment. All of these potential functions of GPNMB can promote tumour growth, invasion, and metastasis in a variety of cancer cells.

The molecular functions of Gpnmb/Osteoactivin in tumour growth, invasion and metastasis are just beginning to be elucidated [209, 218, 221, 232] and it was could be involved in cancer pathophysiology through the following ways:

1.4.4.4.1 MMP PATHWAY AND METASTASIS

Material analysis of glioma cells expressing Gpnmb/Osteoactivin with specific MMP-2, MMP-9 and MMP-3 inhibitors ablated the increase in invasion associated with Gpnmb/Osteoactivin expression relative to vector controls [230]. Ogawa et al [207] found that overexpression of Gpnmb/Osteoactivin in NIH-3T3 fibroblasts induced expression of MMP-3 [201]. Gpnmb/Osteoactivin-mediated induction of pro-invasive matrix metalloproteases, such as MMP-3 and MMP-9, may represented one mechanism by which it promoted metastasis.

1.4.4.4.2 INHIBITION OF TUMOUR-REACTIVE T CELLS ACTIVATION

Gpnmb/Osteoactivin is capable of suppressing the activation of T-cell activation, by binding to syndecan-4 and on the surface of activated T cells and inducing its auto-phosphorylation, thereby allowing melanoma to evade immunologic recognition and destruction [223-224, 226, 233].

1.4.4.4.3 INHIBITION OF APOPTOSIS AND INCREASE OF VASCULAR DENSITY

Some researchers injected 66cl4 mouse mammary carcinoma cells into the mammary fat pads of Balb/c mice. They removed the primary tumours and by quantifying the number of apoptotic cells in non-necrotic regions of mammary tumours found that, on average, fewer cells in Gpnmb/Osteoactivin expressing tumours were undergoing apoptosis when compared to control mammary tumours. They assessed the vascular density of these tumours by quantifying the degree of CD31 positivity, a routinely used endothelial cell marker. These analyse revealed that the vascular density in Gpnmb/OA expressing mammary tumours was significantly higher when compared to control tumours. They ectopically expressed Gpnmb/Osteoactivin in BT549 cells, a basal breast cancer model and revealed that matrigel plugs containing Gpnmb/OA-expressing BT549 cells displayed greater endothelial recruitment when compared to matrigel plugs composed of empty vector control cells. Primary human breast cancers characterized by high vascular density also displayed elevated levels of Gpnmb/Osteoactivin when compared to those with low vascular density. Gpnmb/Osteoactivin ectodomain was shed from the surface of breast cancer cells and the shed ECD of Gpnmb/Osteoactivin could promote endothelial migration in vitro [202]. These data suggested a role for Gpnmb/Osteoactivin in promoting endothelial recruitment during mammary tumourogenesis. Gpnmb/Osteoactivin-expressing tumours displayed elevated endothelial recruitment and reduced apoptosis when compared to vector control-derived tumours.

1.4.4.5 GPNMB as a therapeutic target

Given the increasing association between GPNMB expression and a variety of cancers, and the acquisition of aggressive cellular phenotypes in GPNMB-expressing cancer cells, there has been growing interest in the development of GPNMB-targeted therapies [234-236]. The pattern of GPNMB expression in normal and cancerous tissues makes it an intriguing target for cancer therapy. Generally speaking, GPNMB localization tends to be restricted to intracellular compartments

in normal cells, such as macrophages, melanocytes and pigmented retinal epithelial cells [190, 221, 237]. In contrast, GPNMB expression in tumour cells is enriched on the cell surface [238-239]. This pattern of sub-cellular localization makes tumour-specific GPNMB more readily available for antibody targeting, thus providing a therapeutic window and making GPNMB a uniquely attractive target for antibody based therapies [240].

CR011–vcMMAE (CR011), which is now referred to as *glembatumumab vedotin* or CDX-011, is a GPNMB-targeted therapeutic that belongs to a class of drugs known as antibody–drug conjugates (ADCs) [184]. These drugs consist of antibodies that bind to cell surface molecules, which are linked to highly potent cytotoxins. In the case of CDX-011, the cytotoxin is auristatin E, a tubulin destabilizer. ADCs bind to the extracellular domain of their target protein on the surface of cancer cells, which is then rapidly internalized. ADCs are pro-drugs that require the release of the cytotoxin for activation. Upon internalization, the drug is released and induces cell-cycle arrest and apoptosis of the cancer cell [241]. In clinical trials, CDX-011 is currently being investigated in two multicenter Phase II trials; one for patients with unresectable melanoma, and the other for patients with locally advanced or metastatic breast cancer. Preliminary results from these trials were presented at the 2009 annual meeting of the American Society for Clinical Oncology and were very promising [242-245].

2

OBJECTIVES

The main objectives in this thesis are:

1. To assess *"in vitro"* the molecular interplay between Gemcitabine and Erlotinib regarding their effects over cytotoxicity, proliferation, apoptosis and migration on pancreatic cancer cell lines.

2. To analyze *"in vivo"* the serum cytokine profile in PDAC patients using a powerful antibody array system in the attempt to find any modulation between the former and healthy volunteers. This objective would lead to the determination of an altered cytokine profile that could be useful in the diagnosis of pancreatic cancer.

3. To analyze *"in vivo"* any modulation in the serum cytokine profile in PDAC patients before and after Gemcitabine + Erlotinib combined therapy. This objective could help to analyze the response of PDAC patients to the treatment regimen and also to find novel therapeutic targets.

4. To determine *"in vivo"* if a certain cytokine profile is related to the overall survival. This objective would establish a prognosis index (PI) that significantly predicts PDAC patient outcomes.

5. To assess *"in vitro"* the role of GPNMB/Osteoactivin, highlighted as a predictive biomarker for PDAC, in the development and progression of the disease.

3

MATERIAL AND METHODS

3.1 CELL LINES

3.1.1 Phenotype and genotype of pancreatic cancer cell lines

Pancreatic cancer is characterized by a conspicuous desmoplastic stroma which makes the isolation of cells very difficult. For this reason, molecular studies in primary ductal carcinoma of the pancreas are problematic. Therefore, the use of tumour cell lines and xenografts ease the problem performing these studies. Cell lines represent a commonly used source of material and some of these have been characterized for a number of different chromosomal and gene anomalies. Deep studies have been conducted to analyze the mutational status of several pancreatic cancer cell lines [246-247].

The well-differentiated epithelial human pancreatic adenocarcinoma cell lines Panc-1, MiaPaCa-2 and BxPC-3 (moderately differentiated) were obtained from American Type Cell Culture (*ATCC*, Manassas, VA).

PANC-1 cells are used as an in vitro model of non-endocrine pancreatic cancer for tumorigenicity studies. It has been established from a pancreatic carcinoma of ductal origin from a 56-year-old Caucasian male in the head of the pancreas which invaded the duodenal wall. Metastases in one peripancreatic lymph node were discovered during a pancreaticoduodenectomy [248] (Figure 3.1). The cells possess the type B phenotype for glucose-6-phosphate dehydrogenase G6PD and overexpress heregulin/human epidermal growth-factor receptor 2 (HER2/Neu) oncogene (which is present in 60-70% of human pancreatic carcinomas) but are estrogen receptor (ER) negative. Cells are also negative for MUC4 (Sialomucin complex SMC, an intramembrane ligand for ErbB2) and positive for Smad4 (a TGF beta signalling cascade protein inactivated in human gastrointestinal cancers)[249]. Growth is inhibited by 1 unit/ml L-asparaginase [250].

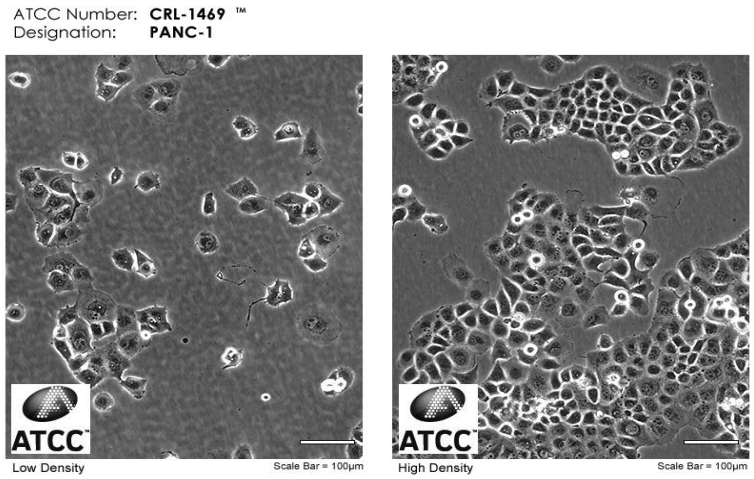

Figure 3.1 Optical microphotographs of Panc-1 pancreatic cancer cell line.

The **MiaPaca-2** cell line (Figure 3.2) was established by A. Yunis, et al. in 1975 from tumour tissue of the pancreas obtained from a 65-year-old Caucasian male [251]. The tumour involved the body and tail of the pancreas and had infiltrated the periaortic area. The tumour did not express measurable amounts of carcinoembryonic antigen and an alkaline phosphatase stain was negative [248]. The established cell line reportedly has a doubling time of about 40 hours.

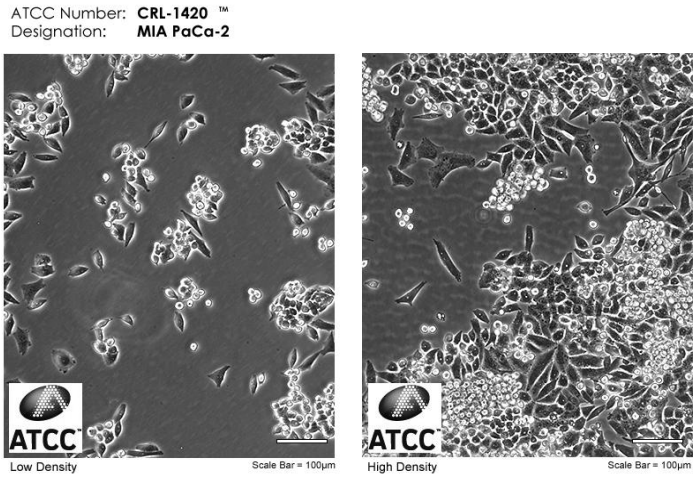

Figure 3.2 Optical microphotographs of MiaPaca-2 pancreatic cancer cell line.

BxPC-3 was cultured from a 61-year-old woman's adenocarcinoma of the body of the pancreas. The patient died 6 months later despite radiation and chemotherapy. No evidence of metastasis was found (Figure 3.3). Tumours grown in nude mice

resemble the primary tumour of the patient and produced carcinoembryonic antigen, human pancreas cancer-associated antigen, human pancreas-specific antigen, and traces of mucin [252].

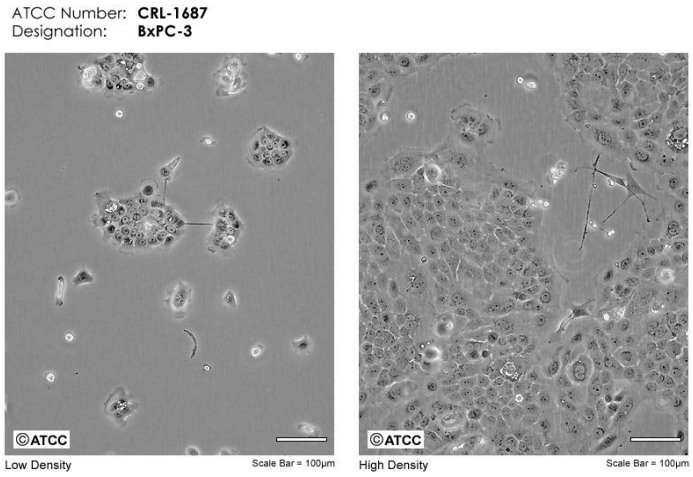

Figure 3.3 Optical microphotographs of BxPC-3 pancreatic cancer cell line.

Most PDACs are characterized by the presence of hallmark mutations in the oncogene K-Ras and in three tumour suppressor genes p16INK4/CDKN2A, TP53, and SMAD4. Information regarding the mutational status of these genes is summarized in Table 3-1.

Table 3-1: Molecular alterations of k-ras, p53, cdkn2a/p16 and dpc4 in pancreatic ductal carcinoma cell lines. HD: homozygous deletion, WT: wild type [246, 248, 253].

Gene	*K-Ras*		*p53*		*CDKN2A/p16*		*DPC4*	
	Mutation	**Predicted product**	**Mutation**	**Predicted product**	**Mutation**	**Predicted product**	**Mutation**	**Predicted product**
Panc-1	12GGT-TGT Activating	Gly to cys	273CGT-CAT Loss	Arg to his	HD	Absent	NONE	Wt
MiaPaca-2	12GGT-GAT Activating	Gly to asp	248CGG-TGG Loss	Arg to trp	HD	Absent	NONE	Wt
BxPC-3	NONE	Wt	220TAT-TGT Loss	Tyr to Cys	HD	Absent	HD	Absent

Panc-1 and MiaPaca-2 cells contain mutated ***k-ras*** while BxPC-3 is wild-type. K-Ras mutations are very common in pancreatic cancer, occurring in almost all primary

tumours and are present early in the progression of the disease. Mutations in Panc-1 and MiaPaca-2 cell lines inhibit the GTPase activity of RAS, leading to an oncogenic RAS protein that is constitutively activated in its GTP-bound state, inducing multiple signalling pathways. The entire three cell lines have **p53** mutated genes and also harbour homozygous deletion in the **p16INK4A** gene, so the product of this gene is absent.

The comprehensive data regarding the multigenic alterations in these large series of cell lines should prove valuable for studies involving drug sensitivity or resistance that may be associated with inactivation of a particular gene or molecular pathway. Information on the genotype of these cell lines provide a background for understanding how alterations in these pathways contribute to the growth characteristics, tumorigenicity and chemosensitivity.

3.2 CELL CULTURE CONDITIONS

Cells were grown in Dulbecco's Modified Eagle medium (DMEM, *Sigma-Aldrich*) supplemented with 10% FBS (*PAA Laboratories*, The cell culture company), 20mM HEPES, 100 U/ml penicillin G and 100 µg/ml streptomycin (*Sigma-Aldrich*). All of the cultured cells were maintained in a humidified 5% CO_2 atmosphere at 37°C. Every 2–3 days (depending on the growth rate), cells were sub-cultured to keep exponential growth. Trypsin-EDTA solution (*Sigma-Aldrich*) was used to detach cell from the surface of the culture incubating them at 37°C for 3 minutes. As soon as cells were detached, medium containing serum to inhibit the Trypsin, that might damage cells, was added (at least to dilute Trypsin 1:8). Then they were reseeded into secondary cultures using 1/2 or 1/3 split ratios. If cells were to be used for any experimental procedure, cell concentration was determined by using the Neubauer chamber.

All the experiments were conducted with cells in exponential growth phase. Cells were tested for mycoplasma contamination by qPCR every two weeks.

3.3 TREATMENTS

Gemcitabine: Gemzar was provided by the oncology service of the Virgen de las Nieves Hospital (Granada, Spain) and dissolved in PBS. A stock solution of 200µg/ml was prepared, filtered through a 0.22 µm filter and stored at -20°C.

Erlotinib: Erlotinib hydrochloride was purchased from *Santa Cruz* (sc-202154) and dissolved in DMSO (*Sigma-Aldrich*) with slightly heating at a concentration of 10mg/ml. The final concentration of DMSO never exceeded 1% (v/v) in the culture. No effect of DMSO was observed.

Cells were incubated 24 or 48 h for detection of any chemicals effect.

3.4 OTHERS CHEMICALS APPLIED

Ampicillin sodium salt (*Sigma-Aldrich A0166*): Ampicillin is a semi-synthetic derivative of penicillin that interferes with peptidoglycan cross-linking and thus inhibits cell wall synthesis. Ampicillin was used to select transformed DH5α bacteria incorporating the pCMV6-GPNMB-GFP plasmid. This product was dissolved in water (50 mg/ml) and sterilized by filtration through a 0.22 µm filter. Ampicillin solution was added at a concentration of 100µg/ml to LB and LB agar media which had been autoclaved and cooled to 50°C. Ampicillin stock solutions were stored at -20°C [254].

Kanamycin sulfate (*Sigma-Aldrich K1377*): Kanamycin sulfate is an antimicrobial agent effective against Gram-negative and Gram-positive bacteria and mycoplasma. It binds to the 70S ribosomal subunit, inhibits translocation and elicits miscoding. This product was also dissolved in water (50 mg/ml) and sterilized by filtration through a 0.22 µm filter. Kanamycin solution was added at a concentration of 25µg/ml to LB and LB agar media which had been autoclaved and cooled to 50°C. Kanamycin was used to select transformed DH5α bacteria incorporating the pGFP-V-RS shRNA expression plasmid. Kanamycin stock

solutions were stored at -20°C [254].

G418 (*Sigma-Aldrich A1720*): Geneticin is an aminoglycoside antibiotic similar in structure to gentamycin. It exhibits toxicity towards both eukaryotic and prokaryotic cells. The G418 powder was dissolved in PBS at 50 mg/ml. This reagent was applied to select those pancreatic cancer cells that had been transfected with pCMV6-GPNMB-GFP plasmid. Concentrations of 500 μg/ml were used for selection and 100μg/ml for maintenance of mammalian cells cultures. Geneticin stock solutions were stored at -20°C [255].

Puromycin (*Santa Cruz* sc-108071): Puromycin dihydrochloride is an antibiotic substance produced by the soil actinomycete Streptomyces alboniger which induces apoptosis in cells by interfering with RNA function, leading to inhibition of protein synthesis. It is toxic to both eukaryotic and prokaryotic cells. The puromycin powder was also dissolved in PBS at 50 mg/ml. Puromycin was used for selection (at a concentration of 2μg/ml) and maintenance (at a concentration of 1μg/ml) of cell lines transfected with the pGFP-V-RS shRNA expression plasmid. Puromycin stock solutions were stored at -20°C [255].

3.5 PLASMIDS

Both plasmids were purchased from *OriGene Technologies* (Rockville, MD).

pCMV6-GPNMB-GFP (RG207615) **plasmid:** The vector pCMV6-AC-GFP was used to clone the ORF from the gene **gpnmb/osteoactivin**. Once cloned, GPNMB is expressed in mammalian cells as a tagged protein with GFP at its carboxy terminus.

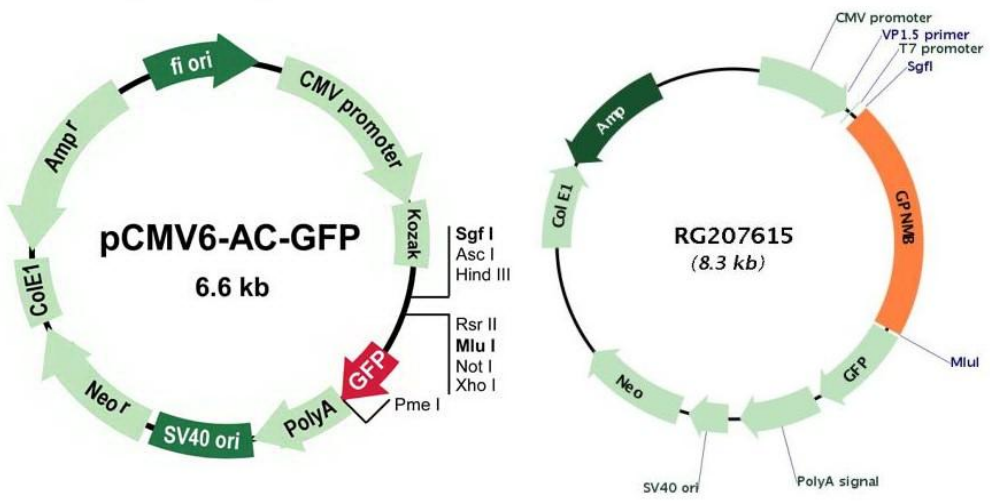

Figure 3.4 Generic plasmid map for pCMV6-AC-GFP vector showing restriction sites and sequence characteristics (left) and plasmid map for pCMV6-AC-GFP carrying the ORF from the gpnmb/osteoactivin gen.

The antibiotic selection marker for E. coli was ampicillin and geneticin (G418) for mammalian cells as the vector contains the neomycin phosphotransferase gene under the SV40 promoter. Expression of the neomycin phosphotransferase gene in mammalian cells allows stable cell selection with a neomycin analog such as G418. The green fluorescence tag allows to monitor the ORF product in live mammalian cells.

HuSH pGFP-V-RS plasmid: This is a retroviral silencing plasmid (pRS) that contains retroviral long terminal repeats (LTR) from the murine moloney leukemia virus (MMLV), the puromycin resistance gene and a U6 small nuclear RNA gene

promoter [256-257] to effectively express the inserted hairpin sequence and to achieve RNA interference upon introduction and subsequent processing by mammalian cells. The puromycin-N-acetyl transferase gene and kanamycin gene provide selection of antibiotics puromycin and kanamycin, respectively. The integrated turboGFP element is driven by one of the most used constitutive promoter, the cMV promoter [258], so the verification of the transfection efficiency is very quickly.

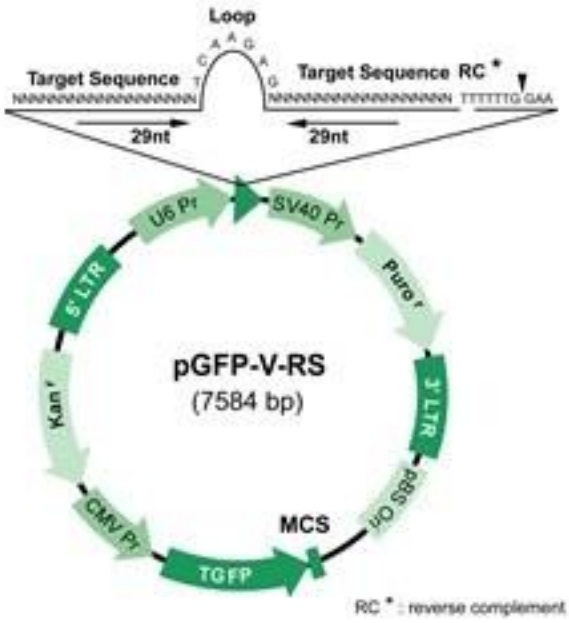

Figure 3.5: Map of Sh cloning vector pGFP-V-RS. Constructs consist of 29 bp target gene specific sequence, a 7 bp loop and another 29 bp reverse complementary sequence, all under human U6 promoter. A termination sequence (TTTTTT) is located immediately downstream of the second 29 bp reverse complementary sequence to terminate the transcription by RNA Pol III.

4 shRNA constructs (A, B, C and D) against multiple splice variants of the gpnmb/osteoactivin were used. Besides, a scrambled negative control was also performed.

3.6 DH5ATRANSFORMATION

3.6.1 Preparation of competent cells

A single colony of E. coli cells was inoculated into 5 ml of LB medium and grown overnight at 37°C with moderate shaking. That overnight culture was subcultured into 400ml of LB medium and grown again at 37° C with moderate shaking till they reached an OD_{590} of 0.375 which indicated early- or mid-log phase. The culture was left on ice for 10 min followed by a centrifugation at 1600xg for 10 min at 4° C. Cells were resuspended in 10 ml ice-cold $CaCl_2$ solution (60 mM $CaCl_2$; 15% glycerol; 10 mM PIPES, pH 7) and centrifuged 5 min at 1100xg twice. Resupended cells can be kept on ice several days or kept at -80°C for longer periods.

10ng of every plasmid were used to transform 100µl of competent E. Coli. After 10 min on ice, the mix was heated at 42°C for 2 min and immediately 1 ml LB medium was added to each tube. For 1 hr, they were kept on a roller drum at 250 rpm at 37°C.

Aliquots of 50µl of the transformation cultures were plated on LB/ampicillin (for E. Coli transformed with the pCMV6-GPNMB-GFP vector) or LB/Kanamycin (for E. Coli transformed with the A, B, C, D pGFP-V-RS plasmids and with the scrambled one) [254]. After 12-16 hrs, colonies were picked and grown to saturation into a 5 ml LB medium with the appropriate antibiotic.

3.6.2 Alkaline lysis miniprep

Bacterial colonies were pelleted by centrifugation and resuspended and kept 5 min at room temperature in 100 µl of GTE solution (50 mM glucose; 25 mM TrisCl, pH 8.0; 10 mM EDTA, autoclaved). Following 200 µl of NaOH/SDS solution (0.2 N NaOH, 1% (wt/vol) sodium dodecyl sulfate (SDS)) were added and the mix was kept 5 min on ice. Lastly, 150 µl of potassium acetate solution (29.5 ml glacial acetic acid; KOH pellets to pH 4.8; H_2O to 100 ml) were added and well mixed by

vortexing. After an incubation of 5 min on ice, a centrifugation at maximum speed allowed us to spin chromosomal DNA and cellular debris. Plasmid DNA and RNA were precipitated with 0.8 ml of 95% ethanol. After centrifugation, the pellet was washed with 1ml of 70% ethanol. Finally, the pellet was resuspended in 30µl of TE and digested with 1µl of RNAse 10mg/ml [259].

3.6.3 Quantification of DNA

DNA was quantified by measuring absorbance at 260nm and the ratio of absorbance at 260 and 280 nm was used as an indicator of nucleic acid purity. Ratios of 1.8 to 1.9 indicate highly purified preparations of DNA [260].

Equation 3-1

$$DNAconcentration(\mu g/ml) = OD_{260} \cdot 50 \cdot DilutionFactor$$

3.7 PANC-1 CELL LINE TRANSFECTION

Trans Fast Reagent from *Promega* was applied for the transfection of the pancreatic cancer cell line Panc-1. Liposomes are one of a number of chemical reagents used to deliver nucleic acids to eukaryotic cells by a nonviral process. Liposomes are lipid bilayers that form colloidal particles in an aqueous medium. Liposome reagents specifically designed for transfection applications incorporate synthetic cationic lipids [261], often formulated together with the neutral lipid L-dioleoyl phosphatidylethanolamine (DOPE), which has been demonstrated to enhance the gene transfer ability of certain synthetic cationic lipids [262-263]. Incubation of cationic lipid-containing liposomes and nucleic acids results in quick association and a compaction of the nucleic acid, presumably from electrostatic interactions between the negatively charged nucleic acid and positively charged head group of the synthetic lipid. The liposome/nucleic acid complex then is presented to the cells that are to be transfected. The liposome complex neutralizes the negative charge of the nucleic acids, allowing closer association of the complex with the negatively charged cell membrane. Entry of the liposome complex into the cell may occur by endocytosis or fusion with the plasma membrane via the lipid moieties of the liposome. Once inside the cell, the complexes often become trapped in endosomes and lysosomes. Endosomal disruption is facilitated by DOPE, which allows the complexes to escape into the cytoplasm.

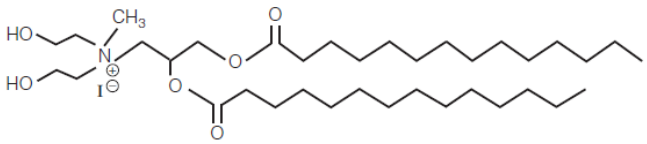

Figure 3.6 Structure of the synthetic cationic lipid component of the Trans Fast reagent.

Transfections were carried out in 24x well plates. $5 \cdot 10^4$ cells were seeded per well and adhered over night. The day before transfection, the TransFast Transfection Reagent was dissolved in 400µl of Nuclease-Free Water (1mM, final concentration of the cationic lipid component). Initially various amounts of DNA and ratios DNA/TransFast Reagent were checked. The optimal conditions for the transfection

were 1µg of DNA per well and a ratio 1:1. Cells were incubated 1hr with DNA/TransFast Reagent/Serum Free Medium mix at 37°C. After that incubation time, the cells were overlay with 1ml of complete medium. The medium was also changed the following day.

3.7.1 Stable Transfections

Capability to integrate genes into the full DNA sequence of a mammalian cell has a significant impact on biomedical research. Transfected genetic material can be expressed in the target cells either transiently or permanently depending on the methods utilized and the experimental questions being investigated. Transient transfections are used most commonly to analyze the short term impact of altered gene or protein expression. Plasmid DNA (pDNA), messenger RNA (mRNA), short interfering RNA (siRNA) and microRNA (miRNA) are introduced and gene products are expressed in the target cells, however the nucleic acids do not integrate into the host cell genome. Therefore, gene product expression is transient and typically results in high expression levels that persist for 24-72 hrs when RNA is transfected or 48-96 hrs following DNA transfection which is likely due to dilution rather than degradation of siRNAs [264].

Conversely, in order to analyze the long term impact of altered gene or protein expression stable transfection is required. The goal of stable, long-term transfection is to isolate and propagate individual clones containing transfected DNA. Therefore, it is necessary to distinguish nontransfected cells from those that have taken up the exogenous DNA. This screening can be accomplished by drug selection when an appropriate drug resistance marker is included in the transfected DNA [265-266].

3.7.2 Generation of stable Panc-1 GPNMB-transfected tumour cell lines

After 48-72h after the transfection, the medium was replaced and cells were incubated in medium DMEM containing 500µg/ml of G418 as the vector carried

the bacterial gene for aminoglycoside (e.g., neomycin) phosphotransferase. After three weeks in this selective medium, discrete colonies were obtained and kept in medium DMEM with 100µg/ml of G418.

3.7.3 Generation of stable Panc-1 shGPNMB-transfected tumour cell lines

After 48-72h after the transfection, the medium was replaced and cells were incubated in medium DMEM containing 2µg/ml of puromycin as the vector carried the bacterial gene for puromycin-N-acetyl transferase. After three weeks in this selective medium, discrete colonies were obtained and kept in medium DMEM with 1µg/ml of puromycin.

3.8 TRANSFECTION EFFICIENCY

3.8.1 Green Fluorescent Protein determination

The green fluorescent protein (GFP), the reporter protein, was measured by flow cytometry as it has a maximum excitation at 489 nm and a maximum of emission at 508 nm). This parameter was used to evaluate the transfection efficiency. Cells were washed twice with PBS, trypsinized for 3 min and resuspended in a volume of 500 µl of the same buffer for immediate flow cytometry analysis. The cells were transferred to the FACS-tube, homogenized using a vortex for guaranteeing single cells measurement and analyzed. Only viable cells were determined for the expression of GFP, considering 20000 events per measurement. A control of untransfected Panc-1 cells (negative control) was measured to eliminate fluorescent background.

3.8.2 Assessment of gene knockdown

Once the shRNA plasmid was prepared and introduced into the cells, the effective knockdown was confirmed by quantitative PCR analysis and western blot. For further details in these techniques refer to section 3.14 and 3.17.

3.9 IMMUNOCYTOCHEMISTRY AND CONFOCAL MICROSCOPY

For immunocytochemistry, both the untransfected and the transfected pancreatic cancer cell lines were seeded in multi-well chamber slides at a density of $1.5 \cdot 10^4$ cells/well. After 48h of treatment, cells were washed with PBS and fixed 30 min with 2% formaldehyde. Before blocking, cells were treated with Glycine 0.02M in PBS 10 min at room temperature to get rid of any residue of the formaldehyde that could interfere. The blocking was done 1 hr at room temperature using 5% FBS/1% BSA/0.2%Triton X-100/PBS. Primary antibody Human Osteoactivin/GPNMB Antibody from *R&DSystems* was reconstituted at 0.5mg/ml in sterile PBS and used at a concentration of 12.5µg/ml in 1% BSA/0.05% Triton X-100/PBS. 200µl/well were added to the chamber slides and incubated over night at 4°C. After incubation time, chamber slides were washed three times with PBS and incubated 1 hr in darkness and at room temperature with the secondary antibody Alexa Fluor 568 donkey antimouse from *Life Technologies* (1/250).

Subsequently, both untransfected and transfected cells were washed three times with PBS and incubated with 200µl of Hoechst Stain solution (*Sigma-Aldrich,* H6024) to label the nuclei. After another three washes with PBS and one more with ddH_20, the samples were covered with anti-fade mounting medium (60% Glicerol/PBS) and slides were sealed with nail polish.

3.10 CELL VIABILITY ASSAY

Cell viability can be defined as the number of healthy cells in a sample. Whether the cells are actively dividing or are quiescent is not distinguished. Metabolic activity can be assayed as an indication of cell viability.

The viability of cells was determined by the standard 3-(4, 5-Dimethylthiazole- 2-yl)-2, 5-diphenyltetrazolium bromide (MTT) assay. The general purpose of the MTT assay is to measure viable cells in relatively high throughput (96-well plates). Therefore the most common use is to determine cytotoxicity of several drugs at different concentrations. The principle of the MTT assay is that, for most viable cells, mitochondrial activity is constant and thereby an increase or decrease in the number of viable cells is linearly related to mitochondrial activity. The mitochondrial activity of the cells is reflected by the conversion of the tetrazolium salt MTT into formazan crystals, which can be solubilized for homogenous measurement. Thus, any increase or decrease in viable cell number can be detected by measuring formazan concentration reflected in optical density (OD) using a plate reader at 570 and 630 nm. For drug sensitivity measurements the OD values of wells with cells incubated with drugs are compared to the OD of wells with cells not exposed to drugs (Figure 3.7) [267].

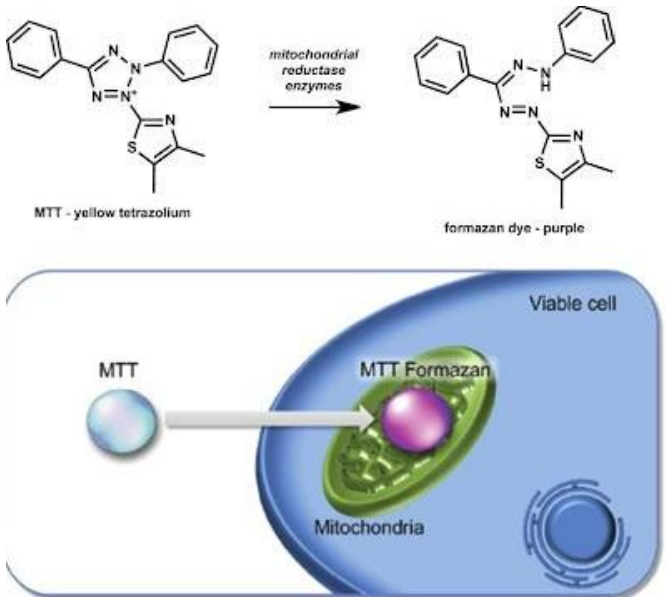

Figure 3.7 MTT assay scheme. The assay is based in the cleavage of the yellow tetrazolium salt MTT to purple formazan crystals by metabolic active cells. This cellular reduction involves de pyridine nucleotide cofactors NADH and NADPH. The formazan crystals formed are solubilized and the resulted colored solution is quantified using a scanning multiwell spectrophotometer [268].

The MTT assay is suitable for the measurement of drug sensitivity in established cell lines as well as primary cells. For dividing cells, the decrease in cell number reflects cell growth inhibition and the drug sensitivity is then usually specified as the concentration of the drug that is required to achieve 50% growth inhibition as compared to the growth of the untreated control (50% inhibitory concentration, IC_{50}). For primary (no dividing) cells, drug sensitivity is measured as enhanced cell kill of treated cells as compared to the loss of cells already commonly seen in untreated cells (50% lethal concentration, LC_{50}).

Cells were plated in 96xwell plates at a density of $1.5 \cdot 10^4$ cells/ml (Panc-1 and Miapaca-2) and $4 \cdot 10^4$cells/ml (BxPC-3) depending on their growth rate. They were left overnight to attach to the plate and then were incubated with increasing concentrations of the drugs alone. After 48h of incubation, 10µl of MTT solution (5mg/ml in PBS; *Alfa Aesar*) were added to the wells and incubated for 2 hours. Subsequently, the formazan crystals were solubilized by adding 200µL of solubilization solution (0.05 N isopropanol acidic). The absorbance was measured at a wavelength of 570 nm and with the wavelength of 630 nm as reference.

3.11 DRUG COMBINATION

The objective of any drug combination is to achieve an improved therapeutic result. Drug combinations are widely used because multiple drugs affect multiple targets and cell subpopulations. The primary aim is a mutual enhancement of the therapeutic effects, while other benefits may include decreased side effects and the delay or prevention of drug resistance. The large majority of combination regimens are being developed empirically and there are few experimental studies designed to explore thoroughly different drug combinations, using appropriate methods of analysis. However, the study of patterns of possible metabolic and biological interactions in preclinical models, as well as scheduling, should improve the development of most drug combinations [269].

Drug interaction has been classically categorized into one of three interaction types: additive, synergistic or antagonistic. The expected null interaction is called additive. Synergy occurs when the combination of two drugs has an effect greater than expected from the individual effects of the single drug. Antagonism describes a combination with less than expected effect [270].

In order to test drug combinations, a modification of the previously described MTT method was developed. Cells were seeded in the previously described conditions but doses evaluated here were based on the IC_{50} values of each individual drug. Drug combinations were assessed in duplicate in each plate and repeated at least twice.

There are various evaluation methods of drug-drug interaction [271]. Isobologram and combination index (CI) analyses are the two most popular methods for evaluating drug interactions in combination cancer chemotherapy [272].

An isobolo is a graph in cartesian coordinates in which the axes are the doses of the respective drugs. The graph consists of a line (or a curve) that represents dose pairs, used together, that give a specified effect level if the drugs act independently. Figure 3.8) [273].

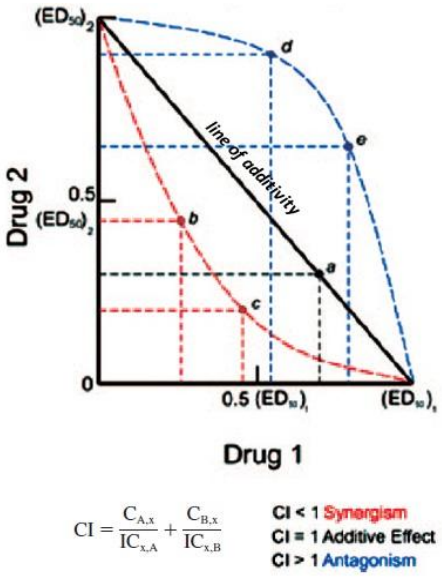

Figure 3.8: The Gemcitabine and Erlotinib combination was analyzed by MTT and evaluated by the combination index and isobologram methods. Isobologram represents doses of the single agents needed to obtain 50% inhibition. Besides, it represents doses of the two drugs used in combination to obtain the same inhibition. If that concentration lies above the line of additivity, the combination is considered as antagonist. On the contrary, if that concentration lies below the line of additivity, the combination is considered as synergic. The numerical value can be obtained applying the Combination Index (CI) of Chou and Talalay. If the result of applying the equation is above 1, the combination is regarded as antagonist. In the case of being equal to 1 is regarded as additive as finally, in the event of being less than one, it is regarded as synergic [274].

The isobologram analysis evaluates the nature of interaction of two drugs, i.e., drug A and drug B, as follows. First, the concentrations of drugs A and B required to produce a defined single-agent effect (IC_{50}), when used as single agents, are placed on the x and y axes in a two-coordinate plot, IC_A and IC_B respectively. The line connecting these two points is the line of additivity. Second, the concentrations of the two drugs used in combination to provide the same effect, denoted as (C_A, C_B), are placed in the same plot. Synergy, additivity, or antagonism are indicated when (C_A, C_B) is located below, on, or above the line, respectively [269, 275].

The CI method of Chou and Talalay was used to analyze the nature of the interaction [276]. CI analysis, similar to isobologram analysis, provides qualitative information on the nature of the drug interaction, and CI, a numerical value calculated as described in Figure 3.8 or equation 3-2, also provides a quantitative measure of the extent of the drug interaction. C_{Ax} and C_{Bx} are the concentrations of drug A and drug B used in combination to achieve x% drug effect (50% of inhibition in our case). IC_A and IC_B are the concentrations for single agents to achieve the same effect. A CI of less than, equal to and more than 1 indicates synergy, additivity and antagonism, respectively [272].

The equation to calculate the CI is the following:

Equation 3-2

$$CI = \frac{C_{A,x}}{IC_{x,A}} + \frac{C_{B,x}}{IC_{x,B}}$$

3.12 ASSESSMENT OF CELL PROLIFERATION

Cell proliferation is the measurement of the number of cells that are dividing in a culture. Cell proliferation and cell cycle distribution are important indicators of cell health and have applications in basic research as well as in discovery for anti-cancer therapeutics. We have performed direct measurement of new DNA synthesis by using the thymidine analog bromodeoxyuridine (BrdU) and also cell-cycle analysis by Propidium Iodide (PI) stain and Flow Cytometry.

3.12.1 BrdU Incorporation Assay (colorimetric)

During cell proliferation the DNA has to be replicated before the cell is divided into two daughter cells. This close association between DNA synthesis and cell doubling makes the measurement of DNA synthesis very attractive for assessing cell proliferation. If labeled DNA precursors are added to the cell culture, cells that are about to divide incorporate the labeled nucleotide into their DNA. BrdU is a sensitive mean to assess for DNA synthesis as an indication of cell proliferation. It is incorporated into newly synthesized DNA during S-phase progression. After its incorporation to DNA, BrdU is detected by immunoassay.

Cell proliferation kit from *Roche* was applied. Cells were plated in 96xwell plates at a density of $1.5 \cdot 10^4$ cells/ml (Panc-1) and $4 \cdot 10^4$cells/ml (BxPC-3) depending on their growth rate in 100 µl/well of DMEM. They were left overnight to attach to the plate. Some wells were set aside for several controls: wells with DMEM without cells (blank, provides information about the unspecific binding of BrdU and anti-BrdU-POD conjugate to the plate) and wells which contain cells but will not receive the BrdU reagent (assay background, provides information about the unspecific binding of the anti-BrdU-POD conjugate to the cells in absence of BrdU).

The next day cells were incubated with the adequate concentrations of the drugs and 10µl/well of BrdU labeling solution (final concentration 10µM) and reincubate for 2,4,6,8,10 and 12 hours at 37°C. Besides, assays at 24 and 48h were performed.

For these later, the BrdU labeling solution was added 2 hours before the end of the incubation time. After incubation time, the labeling medium was aspirated and cells were fixed for 30 min. Following, cells were incubated 90 min with the anti-BrdU-POD. After washing three times with PBS, color was developed by adding 100µl/well of substrate solution. The peroxidase reaction was stopped with 25µl of 1M H_2SO_4 and plates were measured at 450nm with the 690nm reference.

3.12.2 Propidium Iodide Stain

Fluorescent molecules such as propidium iodide (PI) and 7-amino-actinomycin D (7-AAD) were found to provide suitable chemical characteristics for univariate analysis of cellular DNA content by flow cytometry. This approach reveals distribution of cells in three clustered phases of the cycle (G0/G1, S and G2/M) and makes it possible to detect apoptotic cells by fractional DNA content (sub-G1 populations) (Figure 3.9). Cells in G0/G1 exhibit roughly one-half the fluorescence as cells in G2/M and cells in the S-phase exhibit a range of fluorescence, as they synthesize DNA [277-279].

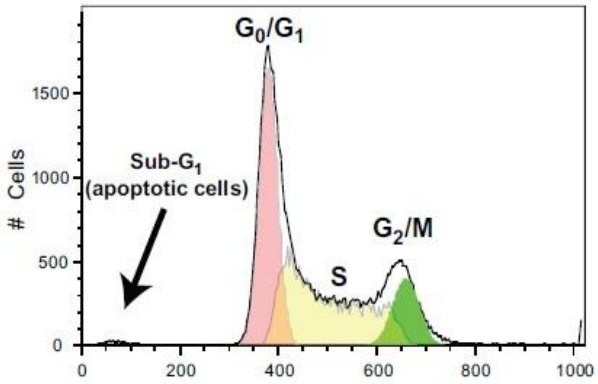

Figure 3.9 Representation of the three clustered phases of the cell cycle that can be detected by flow cytometry using PI.

Pancreatic cancer cells ($5 \cdot 10^5$ cells/ml) were seeded and incubated in 6xwell plates for 48 h with the different drug treatments. At harvest, cells were washed with PBS prior to and following trypsinization. Cell pellets were resuspended in

200 µl PBS followed by 200 µl PBS containing 2% paraformaldehyde. After an incubation period of 15 minutes at 4°C, cells were washed, resuspended in 1 ml of ice cold 70% ethanol and incubated overnight at –20°C. Fixed cells were resuspended in PBS containing 200 µg/ml ribonuclease A and 5 µg/ml PI and then incubated for 30 minutes at room temperature. Cells were then analyzed by flow cytometry [280].

3.13 ASSESSMENT OF APOPTOSIS

The process of programmed cell death, or apoptosis, is generally characterized by distinct morphological characteristics and energy-dependent biochemical mechanisms. Apoptosis is considered a vital component of various processes including normal cell turnover, proper development and functioning of the immune system, hormone-dependent atrophy, embryonic development and chemical-induced cell death. Inappropriate apoptosis (either too little or too much) is a factor in many human conditions including neurodegenerative diseases, ischemic damage, autoimmune disorders and many types of cancer [281].

Plasma membrane of a living cell is a highly organized three-dimensional system composed of lipids, proteins and glycans, so that the two leaflets forming it are of quite different composition. The major part of the electrically neutral phosphatidylcholine (PC) is located in its outer leaflet, whereas most sphyngomielin (SM), phosphatidylethanolamine (PE) and practically all anionic lipids such as phosphatidylserine (PS) and phosphatidic acid (PA) face the cytosolic milieu [282]. The appearance of anionic PS at the cell surface is the most remarkable feature in apoptosis [283]. Surface exposed PS can be detected by its affinity for Annexin V, a Ca^{2+} dependent phospholipid-binding protein [284]. Since necrotic cells also expose PS according to the loss of membrane integrity, apoptotic cells have to be differentiated from these necrotic cells. With this purpose, a simultaneous stain of DNA with PI was carried out.

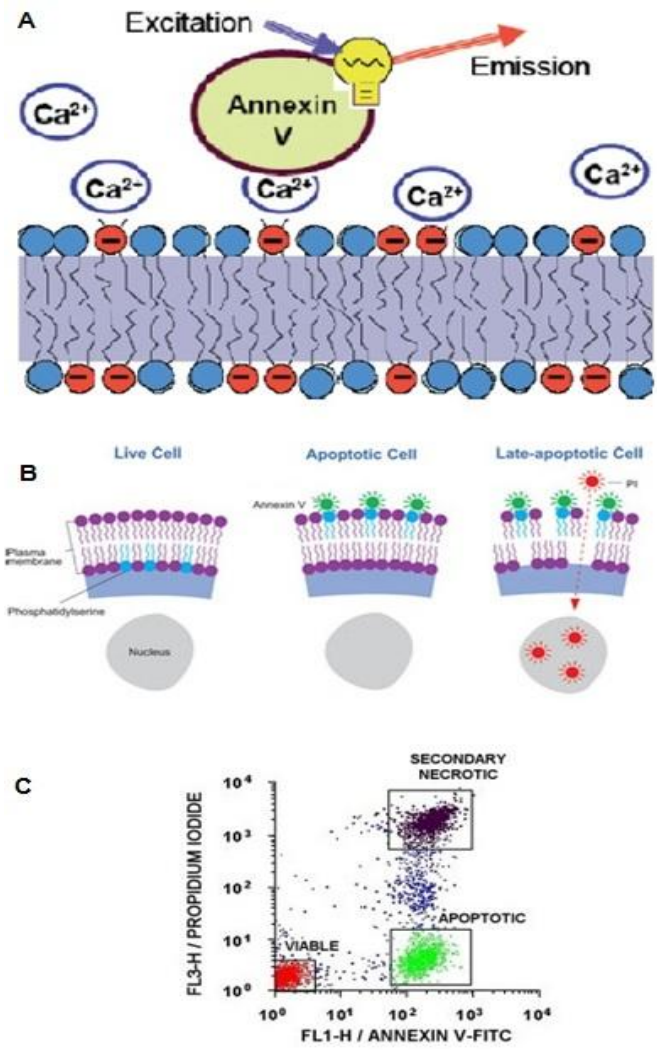

Figure 3.10 A) The principle of apoptosis detection method based on Annexin V. With the aid of Ca2+ ions, this protein interacts with high affinity with PS heads exposed on the membrane surface. Annexin V can be labeled with fluorescent dye that allows visualization of cell with exposed PS. B) Membrane modifications and schematic process of detection of apoptotic and necrotic cells C) Dot-plot showing cells staining with Annexin V-FITC versus Propidium Iodide resulting in three distinct populations.

Viable cells with intact membranes exclude PI, whereas the membranes of dead and damaged cells are permeable to PI. Therefore, cells that are considered viable are both Annexin V and PI negative, while cells that are in early apoptosis are Annexin V positive and PI negative, and cells that are in late apoptosis or already dead are both Annexin V and PI positive.

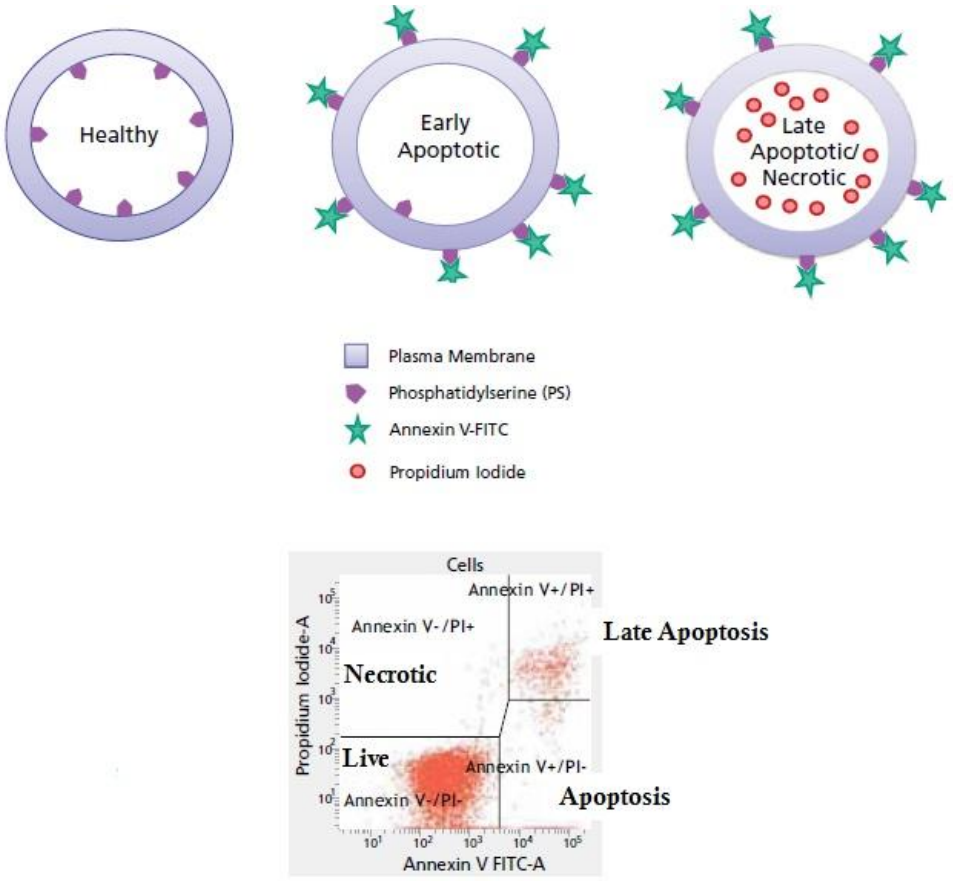

Figure 3.11 Diagram showing healthy and apoptotic cells with markers for detection of apoptosis. Different populations according to the markers they incorpore.

Pancreatic cancer cells ($5 \cdot 10^5$ cells/ml) were seeded and incubated in 6xwell plates for 48h with the different drug treatments. After that period, the culture medium of each plate (containing cells detached during the cell death process) together with trypsinized cells were centrifugated at 200 × g for 5 min after which pellets were resuspended in 100 µl of Annexin-V FLUOS labelling solution (PI and Annexin V-FITC) and incubated 30 min at room temperature in the dark. The percentage of cells undergoing early-stage apoptosis (Annexin V-FITC positive) or late-stage apoptosis/necrosis (Annexin V-FITC and PI positive) was measured with a Becton FC500 flow cytometer. Data were collected using BD FACS scan software and 10.000 cells were analyzed per sample.

3.14 REAL TIME PCR

By PCR essentially any nucleic acid sequence present in a complex sample can be amplified in a cyclic process to generate a large number of identical copies that can readily be analyzed. In real-time PCR the amount of product formed is monitored during the course of the reaction by monitoring the fluorescence of dyes or probes introduced into the reaction that is proportional to the amount of product formed, and the number of amplification cycles required to obtain a particular amount of DNA molecules is registered. Assuming a certain amplification efficiency, which typically is close to a doubling of the number of molecules per amplification cycle, it is possible to calculate the number of DNA molecules of the amplified sequence that were initially present in the sample. With the highly efficient detection chemistries, sensitive instrumentation and optimized assays that are available today the number of DNA molecules of a particular sequence in a complex sample can be determined with unprecedented accuracy and sensitivity sufficient to detect a single molecule [285].

The silence of the GPNMB/Osteoactivin was checked by analyzing the gene expression through real time PCR. This technique was also applied to analyze the expression of particular genes.

3.14.1 RNA isolation

Pancreatic cancer cells lines were seeded in 6xwell plates. Total RNA was isolated with Tri-Reagent (*Sigma-Aldrich,* T9424). 1ml of Tri-Reagent was used per 10 cm^2 of glass culture plate surface area. The cell lysate was passed several times through a pipette till a homogenous lysate was obtained. To separate the phases, 0.2ml of chloroform were added and vigorously mixed. After 15 min at room temperature, samples were centrifuged at top speed for 10 min at 4°C. The colorless upper aqueous phase (containing RNA) was recovered and the same volume of 2-propanol was added. To facilitate the RNA precipitation, samples were kept 10 min at -20°C. Then, samples were centrifuged and the pelleted RNA was washed with

70% ethanol. Finally, samples were resuspended in 30µl of nucleases free water.

3.14.2 DNAse digestion

In order to eliminate any genomic contamination, RNA samples were treated with DNAse I (*Thermo Scientific*) that digests single- and double-stranded DNA. 100µl of reaction were prepared as follows: 10µl of 10xBuffer; 2µl of DNAse I stock solution; 88µl of RNA.

The mixture was incubated 10 min at room temperature, 10 min at 37ºC, 10 min at 65ºC and 2 min at 70ºC.

To get rid of DNAse, RNA samples were cleaned using *Qiagen* Rneasy Protocol. Briefly, 350 µl of Buffer RLT (containing β-mercaptoethanol) and 250µl of absolute ethanol were added to the samples and mix thoroughly. Samples were applied to RNeasy mini spin columns and incubated 5 min. After centrifugation, columns were washed twice with 500µl of Buffer RPE. Columns were finally incubated with 50µl of Nuclease-Free water and RNA was eluted by centrifugation.

3.14.3 Determination of RNA concentration and quality

RNA was quantified by measuring absorbance at 260nm and the ratio of absorbance at 260 and 280 nm was used as an indicator of nucleic acid purity. Ratios of 1.8 to 1.9 indicate highly purified preparations of RNA [260].

Equation 3-3

$$RNAconcentration(\mu g/ml) = OD_{260} \cdot 40 \cdot Df$$

Ribosomal RNA band integrity was analyze on Agilent BioAnalyzer using an RNA 6000 Nano LabChip® and verifying that there was a sharp distinction at the small side of both the 18s and 28s ribosomal RNA (rRNA) bands (Figure 3.12) .

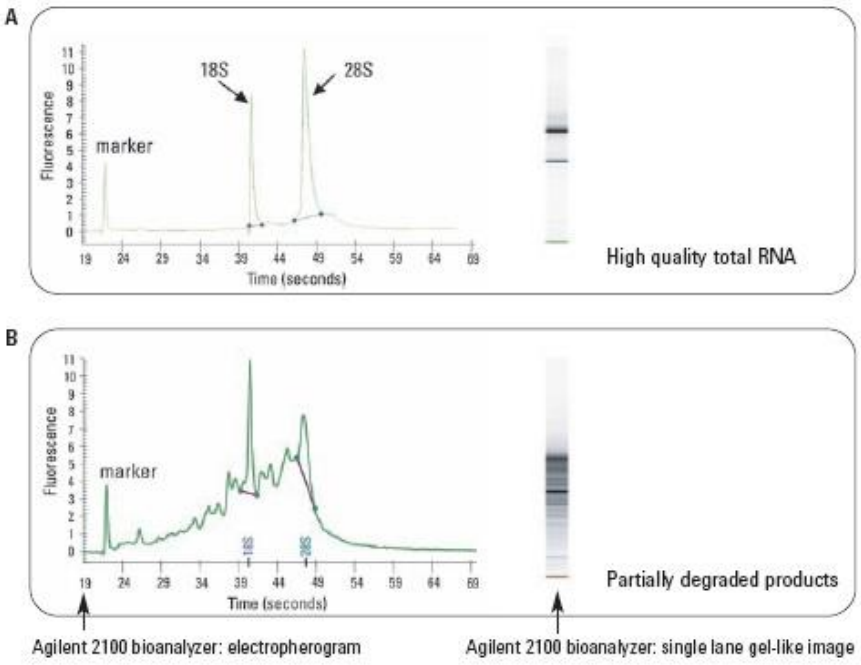

Figure 3.12 Analysis of RNA quality using the Agilent Bioanalyzer, in which 1 µL of total RNA was run, enabling the 18S and 28 bands to be visualized as an electropherogram. A. The 28S/18S ratio should be around 2 for high-quality RNA, with a flat baseline. B. RNA degradation is visible as a decrease in the two ribosomal RNA peaks with a corresponding increase in smaller RNA degradation products, resulting in a noisier baseline.

3.14.4 cDNA synthesis

qScript™ cDNA SuperMix from *Quanta Biosciences* was applied to the cDNA synthesis. The qScript reverse transcriptase is RNase H+ MMLV-derived reverse transcriptase. It uses oligo (dT) and random primers for the reaction and besides the mix is composed by buffer, dNTPs, $MgCl_2$, RNase inhibitor, qScript reverse transcriptase and stabilizers. 1µg of RNA was converted to cDNA in a final volume of 20µl with the following protocol: 5 min at 25°C, 30 min at 45°C and 5 min at 85°C. Samples were kept at 4°C.

3.14.5 Efficiency of PCR reactions

PCR amplification efficiency is the rate at which a PCR amplicon is generated, commonly expressed as a percentage value. If a particular PCR amplicon doubles in quantity during the geometric phase of its PCR amplification then the PCR assay has 100% efficiency.

The slope of a standard curve is commonly used to estimate the PCR amplification efficiency of a real-time PCR reaction. A real-time PCR standard curve is graphically represented as a semi-log regression line plot of Ct value vs. log of input nucleic acid. A standard curve slope of –3.32 indicates a PCR reaction with 100% efficiency. Slopes more negative than –3.32 (ex. –3.9) indicate reactions that are less than 100% efficient. Slopes more positive than –3.32 (ex. –2.5) may indicate sample quality or pipetting problems.

The next figure shows the amplification and efficiencies for various value of slope.

Slope	Amplification	Efficiency
-3.60	1.8957	0.8957
-3.55	1.9129	0.9129
-3.50	1.9307	0.9307
-3.45	1.9492	0.9492
-3.40	1.9684	0.9684
-3.35	1.9884	0.9884
-3.30	**2.0092**	**1.0092**
-3.25	2.0309	1.0309
-3.20	2.0535	1.0535
-3.15	2.0771	1.0771
-3.10	2.1017	1.1017

Figure 3.13 Amplification and efficiencies for various value of slope

A 100% efficient reaction will yield a 10-fold increase in PCR amplicon every 3.32 cycles during the exponential phase of amplification (log2 10 = 3.3219). A calculation for estimating the efficiency (E) of a real-time PCR assay is:

Equation 3-4

$$E = \left[10^{-1/slope} - 1\right] \cdot 100$$

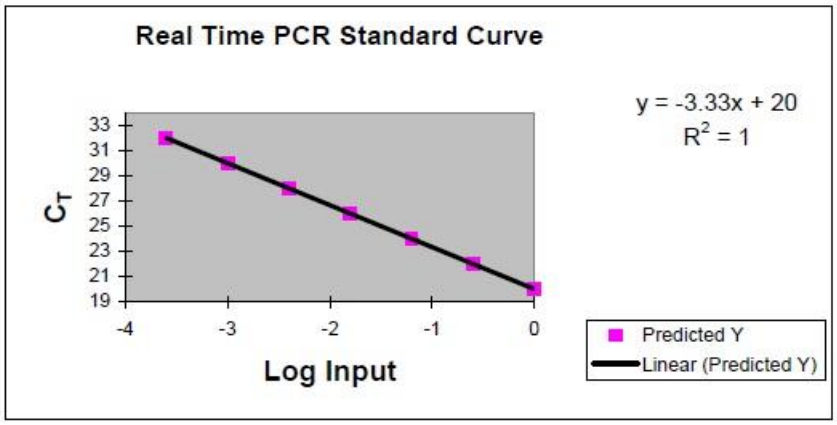

Figure 3.14 Real-Time PCR Standard Curve representing 100% PCR Efficiency.

As relative quantification was to be performed, the efficiency of the target amplification and the efficiency of the active reference (housekeeping gene) amplification needed to be approximately equal.

For the standard curve to be constructed the following amounts of cDNA were used as input: 1; 0.1; 0.01µg. The GAPDH was used as housekeeping gen.

The efficiency of the knockdown of the gpnmb/osteoactivin was assessed using the primers detailed in Table 3-2.

Table 3-2: Characteristics of primers used for real time PCR.

Gene	Forward	Reverse	Product length	Annealing T (ºC)
GPNMB	TTCACTGTGACCTGCAAAGG	CAGTAGGTGCCAGACCCATT	161	55
GAPDH	ACCCAGAAGACTGTGGATGG	TTCAGCTCTGGGATGACCTT	125	55

3.14.6 Data analysis: The Comparative CT Method (ΔΔCT Method)

The amount of target, normalized to an endogenous reference and relative to a calibrator, is given by [286]:

Equation 3-5

$$Ratio = 2^{-\Delta\Delta Ct}$$

Housekeeping genes are present in all nucleated cell types since they are necessary for basis cell survival. The mRNA synthesis of these genes is considered to be stable and secure in various tissues, even under experimental treatments. So, as indicated in section 3.14.5 our reference gen was GAPDH and the target gene expression was calculated compared with it.

For the mathematical model it is necessary to determine the crossing points (CP) or cycle threshold (Ct) for each transcript. Ct is defined as the point at which the fluorescence rises appreciably above the background fluorescence. These Ct values are directly proporcional to the amount of starting template and are the basis for calculating mRNA expression levels.

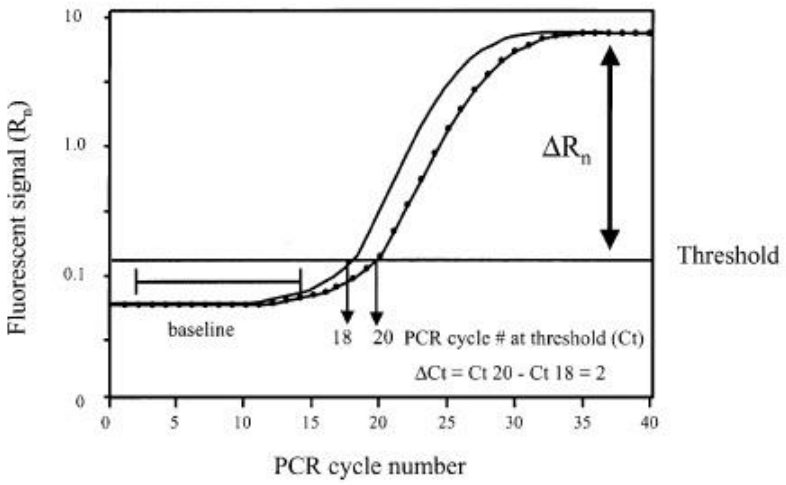

Figure 3.15 A hypothetical amplification plot illustrating the nomenclature typically used in real-time Q-PCR experiments. The amplification plot is the plot of fluorescence signal vs. PCR cycle number. The baseline is defined as the PCR cycles in which a signal is accumulating but is beneath the limits of detection of the instrument. The threshold is calculated as 10 times the standard deviation of the average signal of the baseline fluorescent signal. A fluorescent signal that is detected above the threshold is considered a real signal that can be used to define the threshold cycle (Ct) for a sample. The Ct is defined as the fractional PCR cycle number at which the fluorescent signal is greater than the minimal detection level. The Ct

values of different samples are then used to calculate the relative abundance of template for each sample [287].

The Paff mathematical model [288] was applied to determine the relative quantification of targets genes in comparison to the reference gene. The relative expression ratio (R) of a target gene is calculated based on the PCR efficiency (E) and the Ct deviation of the unknown sample versus the control, expressed in comparison to a reference gene.

Equation 3-6

$$= \frac{\left(E_{target}\right)^{\Delta Ct(Control-sample)}}{\left(E_{gapdh}\right)^{\Delta Ct(Control-sample)}}$$

where:

E_{target} is the real-time PCR efficiency of target gene transcript;

E_{gapdh} is the real-time PCR efficiency of the reference gene transcript;

ΔCt_{target} is the Ct deviation of control – sample of the target gene transcript;

ΔCt_{gapdh} is the Ct deviation of control – sample of reference gene transcript.

3.14.7 Product specificity analysis: Melting curves

Melting analysis with SYBR Green I is commonly used to characterize PCR products. Primer–dimer formation interferes with the formation of specific products because of competition of the two reactions for reagents and may lead to erroneous readouts. It is therefore good practice to control primer–dimer formation. This can be done by melting curve analysis after completing the PCR. The temperature is then gradually increased and the fluorescence is measured as function of temperature. The fluorescence decreases gradually with increasing temperature because of increased thermal motion which allows for more internal rotation in the bound dye. However, when the temperature is reached at which the double stranded DNA strand separates the dye comes off and the fluorescence

drops abruptly. This temperature, referred to as the melting temperature, Tm, is easiest determined as the maximum of the negative first derivative of the melting curve. Since primer–dimer products typically are shorter than the targeted product, they melt at a lower temperature and their presence is easily recognized by melting curve analysis [285, 289].

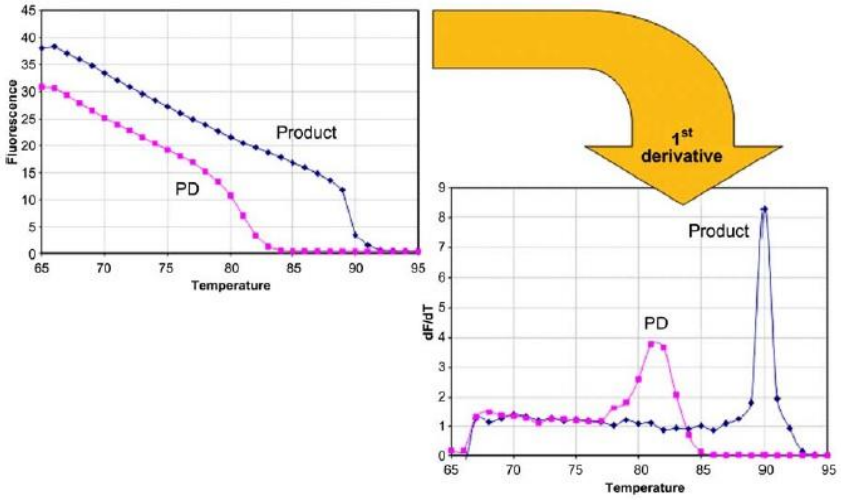

Figure 3.16 Melting curve analysis. Dye fluorescence drops rapidly when the DNA melts. The melting point is defined as the inflection point of the melting curve, which is easiest determined as the maximum in the negative 1st derivative of the melting curve. The amplicon produced from the targeted product is typically longer and melts at higher temperature than the primer–dimers.

These analyses confirmed the specificity of the primers as well as revealed the absence of primer-dimers.

3.15 HUMAN CANCER PATHWAY FINDER PCR ARRAY

To monitor the expression of a panel of cancer pathways specific genes, we performed the RT² Profiler PCR Array System from *SABiosciences* (PAHS-033Z). The Human Cancer Pathway Finder RT² Profiler PCR Array profiles the expression of 84 genes representative of the six biological pathways involved in transformation and tumorigenesis (cell cycle control and DNA damage repair, apoptosis and cell senescence, signal transduction molecules and transcription factors, adhesion, angiogenesis, invasion and metastasis). A detailed list of the genes that encompasses the array is given in the Figure 3.17. In the Annexe 9.3 there is also a complete table comprising all the genes, abbreviations and a short description.

Cell Cycle Control & DNA Damage Repair:

ATM, BRCA1, CCNE1 (cyclin E1), CDC25A, CDK2, CDK4, CDKN1A (p21Waf1), CDKN2A (p16Ink4), CHEK2 (chk2 / Rad53), E2F1, MDM2, RB1, S100A4, TP53 (p53).

Apoptosis and Cell Senescence:

APAF1, BAD, BAX, BCL2, BCL2L1 (bcl-X), CASP8, CFLAR (CASPER), FAS, GZMA, HTATIP2, TERT (telomerase), TNFRSF1A (TNF-a receptor), TNFRSF10B (DR5), TNFRSF25 (DR3).

Signal Transduction Molecules and Transcription Factors:

AKT1, ERBB2, ETS2, FOS, JUN, MAP2K1 (MEK), MYC, NFKB1 (NFκB), NFKBIA (IκBα), PIK3R1 (PI3K p85α), RAF1, SNCG.

Adhesion:

ITGA1 (integrin α1), ITGA2 (integrin α2), ITGA3 (integrin α3), ITGA4 (integrin α4), ITGAV (integrin αV), ITGB1 (integrin β1), ITGB3 (integrin β3), ITGB5 (integrin β5), MCAM, MTSS1, PNN, SYK, EPDR1.

Angiogenesis:

ANGPT1 (angiopoietin-1), ANGPT2 (angiopoietin-2), COL18A1 (endostatin), FGFR2, IFNA1 (IFNα), IFNB1 (IFNβ), IGF1, IL8, PDGFA, PDGFB, TEK (tie-2), TGFB1, TGFBR1 (ALK-5), THBS1 (thrombospondin-1), TNF, VEGFA.

Invasion and Metastasis:

MET, MMP1 (collagenase-1), MMP2 (gelatinase A), MMP9 (gelatinase B), MTA1, MTA2, NME1, NME4, PLAU, PLAUR, S100A4, SERPINB5 (maspin), SERPINE1 (PAI1), TIMP1, TIMP3, TWIST1.

Figure 3.17: List of genes analyzed using the Cancer Pathway finder PCR array. Genes are classified in six biological pathways related to cancer.

3.15.1 RNA isolation

This step was carried out as explained in section 3.14.1.

3.15.2 Determination of RNA concentration and quality

This step was carried out as explained in section 3.14.3.

3.15.3 cDNA synthesis

For this analysis, 5µg of all RNA specimens were treated with RT² First-Strand Kit (*SABiosciences*, 330401) and converted to cDNAs. The RT² First Strand Kit contains all the reagents needed not only to convert RNA into first strand cDNA, but also for the removal of genomic DNA from the RNA. The DNA elimination was performed with incubation at 42°C for 5 min with the adequate buffer. The resulting product for the genomic elimination was added to the reverse transcription mix and incubated 15 min at 42°C and 5 min at 95°C.

3.15.4 PCR amplification

Then, cDNA was mixed with the specific and ready-to use RT² Real-Time SYBR Green PCR Master Mix. 25µl/well were added and the amplification protocol applied is detailed in the Table 3-3. The reactions were conducted in the MyiQ2 Real Time PCD detector form *Bio-Rad*.

Table 3-3: PCR Amplification Protocol

Cycle	*Duration*	*Temperature*	*Comments*
1	10 min	95°C	HotStart DNA Taq polymerase activation
40	15 sec	95°C	
	1 min	60°C	Perform fluorescence data collection
1	1min	95°C	
1	1min	55°C	
81	10 sec	55°C	Melting curve protocol

Assays for 5 housekeeping genes included in the arrays enable normalization of data. The genomic DNA control (GDC) is an assay that specifically detects nontranscribed genomic DNA contamination with a high level of sensitivity. The reverse-transcription control (RTC) is an assay that tests the efficiency of the reverse-transcription reaction. The positive PCR control (PPC) consists of a predispensed artificial DNA sequence and the assay that detects it. This control tests the efficiency of the polymerase chain reaction itself. Controls provided in replicates can be used to test for interwell, intra-plate consistency.

Fold change calculations in gene expression and p-values were calculated using the web-based software package based on the ΔΔCt method using the five housekeeping genes.

3.16 CHROMATIN IMMUNOPRECIPITATION ASSAY (CHIP ASSAY)

Association between proteins and DNA is crucial for many vital cellular functions such as gene transcription, DNA replication and recombination, repair, segregation, chromosomal stability, cell cycle progression and epigenetic silencing. It is important to know the genomic targets of DNA-binding proteins and the mechanisms by which they control and guide gene regulation pathways and cellular proliferation. Chromatin immunoprecipitation (ChIP) is an important technique in the study of protein-gene interactions. Using ChIP, DNA-protein interactions are studied within the context of the cell [290].

Expression of almost every gene is regulated at the transcription level. Therefore, transcriptional factors, consequently, have marked effects on the fate of a cell by establishing the gene expression patterns that determine biological processes. In Chip Assay, intact cells are fixed with formaldehyde to cross-link proteins with their associated DNA. Then, the cells are lysed and chromatin is isolated from the nuclei. After fragmentation by sonication, chromatin fragments, containing the protein of interest and their associated DNA, are selectively precipitated using a specific antibody. Eventually, the sequence identities of the precipitated DNA fragments are determined by RT-PCR [291].

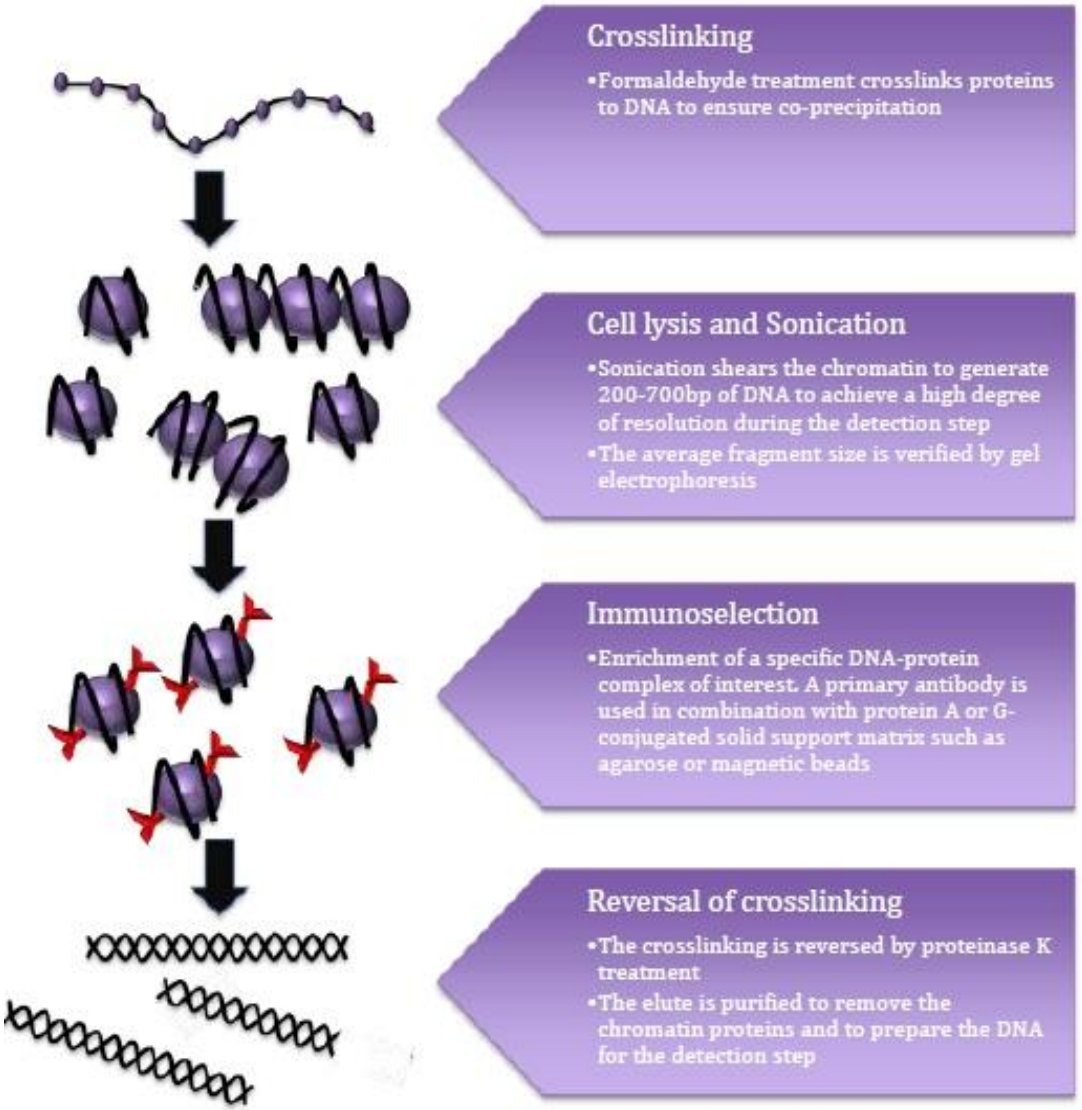

Figure 3.18 Summary of the Chromatin Immunoprecipitation (ChIP) assay.

Chromatin Immunoprecipitation (ChIP) assay was performed as follows: formaldehyde was added directly to the cell culture medium to a final concentration of 1% to cross-link DNA and its associated proteins. After incubating in formaldehyde for 10 min at room temperature, glycine was added to a final concentration of 0.125 M. Cells were washed twice with cold phosphate-buffered saline containing protease inhibitors (PMSF 10mg/ml and sodium orthovanadate 18.34mg/ml) before scraping. Cells were first resuspended in 1ml of swelling buffer (5 mM PIPES pH 8.0, 85mM KCl, 1% NP40) containing protease inhibitors

(PMSF 10mg/ml, sodium orthovanadate 18.34 mg/ml and aprotinin 0.04 mg/ml). Following, they were centrifuged and resuspended in 0.5ml of Nuclei lysis buffer (1% SDS, 10 mM EDTA, and 50 mM Tris-HCl, pH 8) containing protease inhibitors. After 10 min ice incubation, they were subjected to 15 sonication 30 seconds' pulses, with at least 30 seconds of cooling on ice between each pulse. A BioruptorTM XL sonicator was used to shear the chromatin. The resulting supernatant contained 200–1000-base pairs sheared chromatin. 5 µl of the supernatant were saved to check effectiveness of the sonication. The clarified extracts were diluted 1:10 in ChIP dilution buffer (0.01% SDS, 1.1% Triton X-100, 1.2 mM EDTA, 167 mM NaCl and 16.7 mM Tris-HCl) containing protease inhibitors. The chromatin solution was precleared 1hour with 50µl of protein G- Agarose beads (*Santa Cruz Biotechnology*, sc-2002) at 4°C on a rocking platform. At this step, after centrifugation, the 10% INPUTs (used as positive controls) were collected and stored for further use. Samples were then incubated over night at 4°C on a rocking platform with either 10µl of anti-NFκB antibody (*Santa Cruz Biotechnology*, sc-372) or 10µl of anti-IgG antibody (negative control). After incubation, 50 µl of protein G-Agarose Beads were added and incubation continued for 2 hours. The chromatin-antibody/protein G-agarose complexes were washed twice for ten minutes sequentially with low salt (0.1% SDS, 1% Triton X-100, 2 mM EDTA, 20mM Tris, pH 8.1, 150 mM NaCl), high salt (0.1% SDS, 1% Triton X-100, 2 mM EDTA, 20mM Tris, pH 8.1, 500 mM NaCl), lithium chloride (0.25 M LiCl, 1% NP40, 1% deoxycholate, 1 mM EDTA, 10 mM Tris, pH 8.0), and Tris/EDTA (1M Tris, 0.5M EDTA pH.8) buffers. DNA and protein were eluted from the pellets by incubating with freshly made elution buffer (1% SDS and 50 mM NaHCO3). 1%INPUT and immunoprecipitated samples (IPs) were incubated with 5M NaCl at 65°C overnight to reverse the crosslinking. The samples were digested first with RNAse A for 30 min and besides with proteinase K for 1 h at 45 °C. DNA from the samples was obtained by phenol/chloroform extraction and ethanol precipitation. DNA pellets were then resuspended in 50µl of sterile water and 1µl was loaded for the real time PCRs to quantitate co-immunoprecipitated promoter fragments. The immunoprecipitation was done in three independent experiments and triplicates from each one were subjected to real time.

3.16.1 Real-time PCR quantification of Co-immunoprecipitated Promoter Fragments

Promoter-specific primer pairs for the NF-κB binding site of MMP-9, Bcl-2, Bcl-X_L and NFκBIA (IκB-α) promoters were designed with Primer3 designing tool. The length (pb) amplified of each gen promoter surrounding the NF-κB site and the designed primers are summarized in Table 3-4. Ct values were determined by choosing threshold values in the linear range of each PCR reaction. PCR cycling conditions consisted of 95ºC for 10 min followed by 40 cycles of 1 min at 94ºC, 1 min at 55-60ºC (depending on the specific pair of primers), 1 min at 72ºC with a final extension at 72ºC for 10 min. Each reaction produced a single specific product as indicated by a single dissociation curve peak at a melting temperature (Tm) greater than 75°C.

Table 3-4: Characteristics of primers used for Chromatin Immunoprecipitation.

Gene	Forward	Reverse	Product length	Annealing T (ºC)	Site sequence
MMP-9	GCCATGTCTGCTGTTTTCTAGAGG	CACACTCCAGGCTCTGTCCTCTTT	207	54	*GGGGGTTGCCCC*
Bcl-2	CCTTTCAGCATCACAGAGGA	TGTGCTTTGCATTCTTGGAC	187	60	*GGGAAACACC*
Bcl-X_L	GGCGGATTTGAATGTAGGTG	GGACTCTGAATCTCCCACCA	130	54	*GGGACTGCCC*
NFKBIA	CTCATCGCAGGGAGTTTCTC	CTGGCTGGGGATTTCTCTG	151	57	*GGAAATTCCCC*

3.16.2 ChIP-qPCR Analysis Calculations

The relative proportions of co-immunoprecipitated promoter fragments were determined based on the threshold cycle (Ct) value for each PCR reaction evaluating the fold difference between experimental sample and normalized input (sample prior to immunoprecipitation) using the ΔΔCt [292] .

Chip-qPCR results were reported as "Differential Occupancy Fold Change" as multiple experimental samples were compared (Non-treated sample vs. Gemcitabine, Erlotinib and Gemcitabine + Erlotinib treated samples). They could

have also been reported either as "% Input" or "Assay Site IP Fold Enrichment if characterization of individual experimental samples was to be done. For these calculations:

1. Each ChIP DNA fractions' Ct value was normalized to the Input DNA fraction Ct value for the same qPCR Assay (ΔCt) to account for chromatin sample preparation differences.

Equation 3-7

$$\Delta Ct_{[NormalizedChIP]} = Ct_{ChIP} - \left(\left(Ct_{INPUT} - Log_2 100\right)\right)$$

The Input fraction was 1% which corresponded with a dilution factor (DF) of 100 or 6.644 cycles (i.e. log2 of 100).

2. The % Input for each ChIP fraction (linear conversion of the normalized ChIP ΔCt) was calculated.

Equation 3-8

$$\%Input = 2^{-\Delta CtNormalized}$$

3. The difference between the normalized experimental sample (S2) and the control sample (S1) ChIP fraction Ct values (second ΔΔCt) were determined.

Equation 3-9

$$\Delta\Delta Ct_{S2-S1} = \Delta Ct_{S2Normalized} - \Delta Ct_{S1Normalized}$$

4. Differential Occupancy Fold Change (linear conversion of the second ΔΔCt to yield a fold change in site occupancy) was finally calculated.

Equation 3-10

$$FoldChangeinOcupancy = 2^{-\Delta\Delta Ct_{[S2-S1]}}$$

3.16.3 ChIP-qPCR Analysis Quality Assessment

a. All the Input DNA Fraction Ct value was less than 30.
b. The % Input for the Negative/mock IP DNA fraction was less than 0.01%.
c. The Target TF ChIP DNA fraction Ct value was at least one cycle less than the Negative/mock IP DNA fraction Ct value so the sample could be considered quantitatively above the background signal (noise).

3.17 WESTERN BLOT ANALYSIS

3.17.1 Total protein extraction

Cell monolayers with an 80% confluence were washed twice with cold PBS, scraped and pelleted at 400x g and then disrupted by incubation with RIPA buffer (1x PBS, 1% NP40, 0.5% sodium deoxycholate, 0.1% SDS, 0.1 mg/ml PMSF, 0.04 mg/ml aprotinin and 0.18 mg/ml sodium orthovanadate). Cell lysates were incubated 30 min at 4ºC. The lysates were then passed through a 21g syringe to guarantee the total disruption of the sample. Cellular debris was pelleted by centrifugation at 12.000 g for 15 min at 4°C. Supernatants were used to determined protein concentration and kept at -80°C. Protein concentration was determined by the micro-BCA procedure (*Pierce*) using bovine serum albumin (BSA) as standard.

3.17.2 Electrophoretic Separation of Proteins and transference to membranes

Proteins were denatured in Sample Buffer with 5% β-mercaptoethanol at 95° for 10 min. Equal amounts of total protein were loaded and separated by SDS–PAGE (10-12%) for 45 min at 200V using the Mini-Protean tetra cell system from *Bio-Rad*.

Once finished, gels, PVDF membranes (*GE Healthcare*), fiber pads and filters were equilibrated 15 min with transfer buffer (25mM Tris HCl, pH 8.3; 192mM Glycine and 20% Methanol). Transfers were carried out over night at 30V at 4°C or 1 hour at 100V (depending on the molecular weight of the protein of interest). The pre-stained molecular marker (*Bio-Rad*) served as indicator of the transfer process.

3.17.3 Immunoblotting

Once the protein transfer was finished, the membranes were separated from the sandwich and were blocked for 1 h at room temperature in 5% non-fat dry milk in TBST (10 mM Tris–HCl (pH 7.6), 150 mM NaCl, 0.05% Tween-20) under continuous shaking. The membranes were incubated overnight at 4°C with the following primary antibodies: BAD (Santa Cruz, sc-943); Bak (Santa Cruz, sc- 832); BAX (*Santa Cruz*, sc-6236); BCL-2 (*Santa Cruz*, sc-492); BCL-$X_{S/L}$ (*Santa Cruz*, sc-1690); Cytochrome C (*Abcam*, ab13575); CAII (*Santa Cruz*, sc-133110); Cytokeratin 7 (*Santa Cruz*, sc-25721); p27 (*Santa Cruz*, sc-528), p-IKKα (*Abcam*, ab17943), IKKα (*Abcam*, ab54628), p-IKBα (*Abcam*, ab12135), IKBα (*Abcam*, ab12134), p-NF-κB (*Abcam*, ab28856) and NF-κB (*Abcam*, ab95020). The reference protein was β-Actin (*Sigma Aldrich*, A5316). Primary antibodies were detected using a horseradish peroxidase (HRP)-conjugated secondary antibody, also provided by Santa Cruz. The immunocomplex was detected by using the ECL Plus kit (Amersham, Buckinghamshire, UK) and the band density was analyzed with ImageJ software.

3.18 INVASION ASSAYS

The migration of cells from one tissue compartment to another is closely associated with extracellular matrix (ECM) remodeling, with breakdown of matrix barriers and eventual replacement, and represents a fundamental step both in physiological and pathological cell movement. The multi-step carcinogenesis theory placed the metastatic cell at the center of the metastatic process, as a cell able to complete the decathlon: (1) uncontrolled growth; (2) loss of cell–cell adhesion; (3) acquisition of migratory potential; (4) acquisition of invasive capacity, (5) exit from the primary tumour mass; (6) breaching the vascular basement membrane; (7) intravasation into the vessel; (8) survival in the circulatory system (resisting turbulence and immune surveillance); (9) extravasation at the site of the distant organ and (10) invasion into the local tissue to create a new tumour and restart the cycle [293].

In order to assay the invasive properties of tumour cells lines with or without treatments, the CHEMICON Cell Invasion Assay Kit from *Millipore* was applied. The CHEMICON Cell Invasion Assay Kit contains polycarbonate membrane inserts (8 µm pore size) in a 24-well plate. The inserts contain an 8µm pore size polycarbonate membrane over which a thin layer of ECMatrix™ is dried. The ECM layer occludes the membrane pores, blocking non-invasive cells from migrating through. Invasive cells, on the other hand, migrate through the ECM layer and cling to the bottom of the polycarbonate membrane. Finally, the cells are removed from the top of the membrane and the invaded cells are stained and quantified. The schematic representation of the assay can be observed in Figure 3.19.

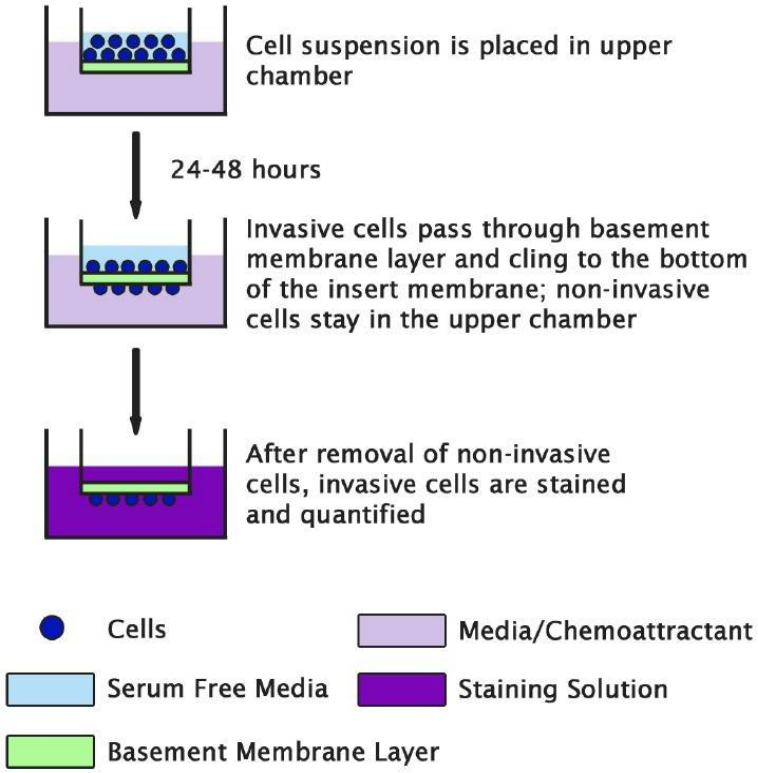

Figure 3.19 CytoSelect™ Cell Invasion Assay principle.

The basement membrane layer of the cell culture inserts was rehydrated by adding 300µl of warm, serum-free media to the inner compartment and incubated at room temperature for 1 hour. Meantime, cell suspensions containing $1 \cdot 10^6$cells/ml in serum-free media incorporating the drugs were prepared. The rehydratation medium was carefully removed and substituted with 300µl of the cell suspensions. 500µL of media containing 10% fetal bovine serum (acting as a chemo attractant) were also added to the lower well of the invasion plate. Cells were incubated for 48h. After the incubation period, non-invasive cells were removed using cotton-tipped swabs with water, pressing them against the interior of the inserts. The inserts (carrying only migratory cells) were transferred to a clean well containing 400 µL of Cell Stain Solution and incubated for 10 minutes at room temperature. After washing the stained inserts several times with water, migratory cells were extracted from the inserts by incubating the inserts with 200µL of 10% acetic acid per well for 10 minutes on an orbital shaker. 100µL from each sample were transferred to a 96-well microtiter plate and measure the OD 560nm in a plate reader.

3.19 PATIENTS

All patients were diagnosed with PDAC at *Hospital Virgen de las Nieves* (Granada, Spain) from 2008 to 2011. Thirty nine samples were enrolled in this study. Three different groups were established: 1) twelve healthy volunteers were included as control group; 2) fourteen PDAC patients who had not received any treatment (denoted as pre-treated) and 3) thirteen PDAC patients under two weeks of Gemcitabine + Erlotinib combined therapy (denoted as post-treated). All information from patients, including gender, age, disease grade and symptom was recorded. The median age of the patients was 66 years (range, 41-79 years) with a male to female ratio of 50:50. Clinical staging for patients with pancreatic adenocarcinoma was as follows: stage III (28 %) and stage IV (72%). There was not any history of pancreatitis but 36% had type II diabetes mellitus and 36% were smokers. All information regarding PDAC patients is summarized in Table 3-5.

3.20 SAMPLE COLLECTION

Blood samples were collected after obtaining the approval of relevant ethics committees and informed consents of donors. In total, 39 serum samples were collected from 2009 to 2011, using standard procedures at the Oncology Service of *Virgen de las Nieves Hospital* (Granada, Spain). Blood samples were obtained from patients diagnosed with PDAC at baseline and at two weeks after initiation of therapy (Gemcitabine + Erlotinib) and also from healthy individuals. Serum was obtained after blood centrifugation at 1500 rpm for 10 min at 4°C. Samples were aliquoted and stored at -80°C.

Table 3-5: Clinicopathologic characteristics of the study population (n=14)	
Age at diagnosis, years (mean ± StD)	66±10.5
Gender	Male: 50% Female: 50%
Disease Stage	III (28%) IV (72%)
Type of chemotherapy	Gemcitabine + Erlotinib
Clinical Response	PR (14.29%) SD (21.43%) PD (64.29%)
Survival Time, months (mean ± StD)	12.6±12.6
CEA level [µg/l] (mean ± StD)	2219±5017 Healthy: 0-37
CA 19-9 level [U/l] (mean ± StD)	899±3185 Healthy: 0-5
PR: partial response; SD: stable disease; PD: progressive disease; StD: standard deviation	

3.21 CYTOKINE ANTIBODY ARRAY

The *Human Cytokine Array* from *RayBiotech* was used to analyze simultaneously 507 cytokines in collected sera from pancreatic cancer patients. The Array includes cytokines, chemokines, growth and differentiation factors, angiogenic factors, adipokines, adhesion molecules and matrix metalloproteases, as well as binding proteins, inhibitors and soluble receptors to these proteins [175]. Antibody-based arrays represent a useful tool for cancer biomarker discovery enabling the generation of highly robust assays that can be easily standardized and automated [294] . Not only does this methodology stand out for its capacity to straightly and quickly offer insights into early cancer biomarkers detection but it also could shed light into progression, assisting clinicians in novel personalized cancer therapies approaches [295].

Soluble proteins in the sera of PDAC patients were measured using a biotin label-based human antibody array, according to the recommended protocols (Figure 3.20). The first step was to biotinylate the primary amine of the proteins in serum. The glass slide arrays were then blocked, just like in a western blot and the biotin-labelled sample was added onto the glass slide, which was pre-printed with capture antibodies, and incubated to allow for interaction of target proteins. Streptavidin conjugated fluorescent dye (Cy3 equivalent) was then applied to the array. Finally, the glass slide was dried and laser fluorescence scanning was used to visualize the signals.

Final spot intensities were measured as the original intensities subtracting the background. Data were normalized to the positive controls in the individual slide. Positive control spots are standardized amounts of biotinylated IgGs printed directly onto the array. This allows for normalization based upon the relative fluorescence signal responses to a known control.

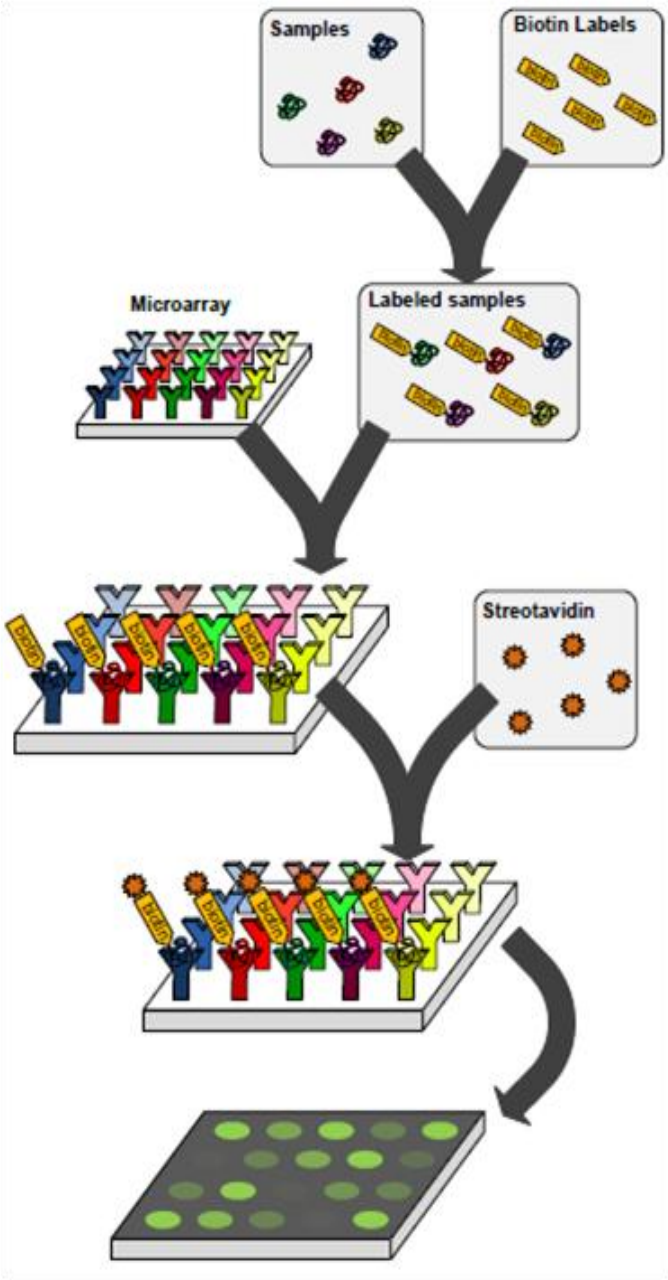

Figure 3.20 RayBio® L-Series Human Antibody Array L-507 procedure.

3.22 STATISTICAL ANALYSIS

3.22.1 In vitro assays

For all the methods, at least three different experiments and triplicates were performed. Results from the assays are expressed as mean ± standard deviation (s.d). Values of $p<0.05$ were considered statistically significant. For all measurements, statistical analyses were performed using both one-way analysis of variance (ANOVA) and two-way ANOVA.

Whereas one-way analysis of variance (ANOVA) tests measure significant effects of one factor only, two-way analysis of variance (ANOVA) tests (also called two-factor analysis of variance) measure the effects of two factors simultaneously. For example, an experiment might be defined by two parameters, such as treatment and time point. One-way ANOVA tests would be able to assess only the treatment effect or the time effect. Two-way ANOVA on the other hand would not only be able to assess both time and treatment in the same test, but also whether there is an interaction between the parameters.

3.22.2 In vivo assays

All statistics and data analysis were performed using *IBM SPSS statistic 20 software* or the statistical language R. Quality analysis was performed using the "*ArrayQualityMetrics*" package in R [296] to eliminate any feasible outlier.

3.22.2.1 Predictive biomarkers statistics

Normally, in proteomics studies, there are far more variables than samples. Due to this, a feature selection is mandatory before constructing the classification [182]. In our case, as cytokines within all groups failed to show a normal distribution, the *Mann-Whitney U* test was used to highlight differences between groups ($p<0.05$).

This test is considered as a suitable filter method for feature selection in proteomics [297]. In addition, fold change (FC) was calculated. Fold-change values of cytokines are given to indicate their relative expression levels. Any *≥1.5-FC or ≤1/1.5-FC* in signal intensity between groups was considered relevant.

To assess the performance of our cytokine panel in terms of sensitivity and specificity the receiver operating characteristic curve (ROC) and the area under the curve (AUC) were applied.

The sensitivity of a diagnostic test is the proportion of patients for whom the outcome is positive that are correctly identified by the test. The specificity is the proportion of patients for whom the outcome is negative that are correctly identified by the test. Generally, both the sensitivity and specificity of a test need to be known in order to assess its usefulness for a diagnosis. A discriminating test would have sensitivity and specificity close to 100%. However, a test with high sensitivity may have low specificity and vice versa [298] so a balance between sensitivity and specificity has to be struck .

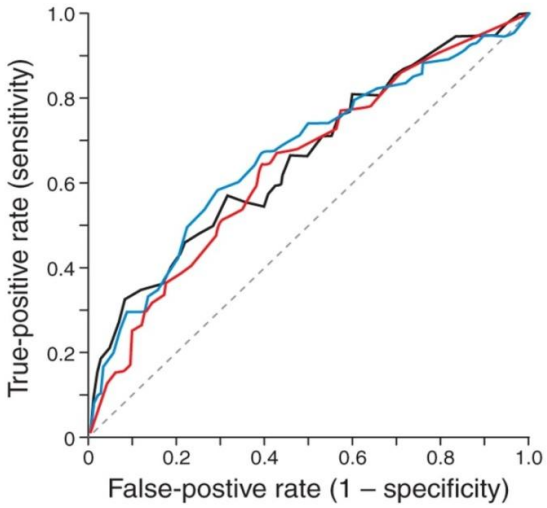

Figure 3.21 ROC curves provide a comprehensive and visually attractive way to summarize the accuracy of predictions. Each point on the curve represents the true-positive rate and false-positive rate associated with a particular test value. The AUC provides a useful metric to compare different tests (indicator variables). Whereas an AUC value close to 1 indicates an excellent diagnostic test, a curve that lies close to the diagonal (AUC = 0.5) has no information content and therefore no diagnostic utility [299].

To help decide the presence or absence of disease, a cut-off point for "normal" or "disease" is chosen. The ROC curve (Figure 3.21) is a graphical technique for assessing the ability of a test to discriminate between those individuals with disease and those without it. ROC curves allow visual analyses of the trade-offs between the sensitivity and the specificity of a test with regard to the various cut-offs that may be used. The curve is obtained by calculating the sensitivity and specificity of the test at every possible cut-off point and plotting sensitivity against 1-specificity.

The area under the curve (AUC) of the receiver-operating characteristic (ROC) was calculated for each marker to evaluate its diagnostic significance plotting the true-positive rate (sensitivity) against the false-positive rate (1-specificity) [300].

Besides, a weighted linear combination of biomarkers (weighted using each independent cytokine´s sensitivity) was generated and its ROC curve was also plotted. Cut-off values were selected to provide both the highest sensitivity and the highest specificity.

A leave-one-out cross-validation (LOOCV) was assessed as the simplest and most widely used method for estimating prediction error [301-303]. LOOCV analysis for this combination was used on the total patient dataset to evaluate the model-based cytokines set for hypothetical prediction of suffering from PDAC for each patient. Here, one sample was removed from the initial 25 sample dataset (healthy and pre-treated patients), leaving a temporary 24 sample training set and one left out-sample. On the training set, the cytokine combination obtained from the best cut-off provided by their corresponding ROC curve was then used to classify the previously left out-test sample.

3.22.2.2 Prognosis biomarkers statistics

Median survival after administration of Gemcitabine and Erlotinib was calculated from the start of treatment to death, in months. For overall survival (OS) analyses,

the Kaplan-Meier curve was used as a method that estimates the probability of survival to a given time using proportion of patients who have survived to that time [304-305]. For each time interval, survival probability is calculated as the number of subjects surviving divided by the number of patients at risk. The log-rank test was used to determine survival differences between groups. The log-rank test is used to test the null hypothesis that there is no difference between the populations in the probability of an event (here a death) at any time point [306]. Kaplan-Meier survival curves for individual markers were obtained after dichotomization. The cut-off values for each marker were those which displayed the most significant survival discrimination between the two groups.

In order to determine the most significant variables contributing to the OS, univariate and multivariate analyses were done with the Cox's proportional hazard regression model [307] to determine associations between serum cytokines and cancer-related mortality. First, we analyzed associations between death and levels of cytokines, considering one factor at a time. Second, a multivariate Cox's proportional hazard model was applied. Wrapper was used as feature selection method using conditional forward stepwise algorithm based on likelihood rate, as applied in other works [308-309]. Wrapper methods attempt to jointly select sets of variables with good predictive power for a predictor [310]. Forward selection starts with an empty set and selects the variable that gives the best classification result. Given this first variable, another variable is added that realizes the largest improvement of performance. Variables are added until the performance does not improve [182].

The overall model fit was considered significant based on chi-squared statistic test ($p<0.05$). Besides, Wald index was shown to determine the weight of each variable in the global model, both uni and multivariate. The cytokine levels were introduced in the models as continuous parameters and results were expressed as the hazard ratio (HR) or relative risk ratio for one unit change. By analysis of these variables, a prognosis index (PI), that considers the regression coefficients derived by Cox's model of all significant factors, was obtained. Differences were considered significant when $p<0.05$.

The Cox's regression model for the study of the PDAC patients' survival was defined by the following equation:

Equation 3-11

$$h(t) = h_0(t)e^{\Sigma_j^N=1^{\beta_{ij}X_{ij}}}$$

where h (t) is the hazard rate at time t, h_0 (t) is the baseline hazard rate and the exponent, which does not depend on time, is known as prognosis index (PI). The prognosis index for a specific patient i is defined as:

Equation 3-12

$$PI_i = \sum_{j=1}^{N} \beta_{ij} x_{ij}$$

where βij defines the coefficient provided by the Cox's regression model for a particular patient i and cytokine j; xij determines the expression level measured for the patient i and the cytokine j; and N represents the number of cytokines included in the model.

4

RESULTS

In this section, the results of our work are summarized. This section will be in turn structured in three subsections to ease its following:

i. Interplay between Gemcitabine and Erlotinib over pancreatic ductal adenocarcinoma cells (corresponding to objective 1, see section 2).
ii. Biomarkers identification in pancreatic ductal adenocarcinoma patients (corresponding to objectives 2-4, see section 2).
iii. The role of GPNMB/Osteoactivin (highlighted in the former section as predictive biomarker of PDAC) in the carcinogenesis of PDAC (corresponding to objective 5, see section 2).

4.1 INTERPLAY BETWEEN GEMCITABINE AND ERLOTINIB OVER PANCREATIC DUCTAL ADENOCARCINOMA CELLS

In the present subsection we have investigated the molecular interplay between Gemcitabine and Erlotinib in vitro regarding their effects over cytotoxicity, proliferation, apoptosis and chemoresistance in the pancreatic cancer cell lines Panc-1, Miapaca-2 and BxPC-3.

4.1.1 Gemcitabine and Erlotinib treatments suppressed pancreatic cancer cell lines proliferation in vitro

The effect of both drugs on pancreatic cancer cultures viability was evaluated by incubating these cell lines 48 h in culture media with Gemcitabine or Erlotinib at increasing concentrations ranging from 0 to 200 μM (except for BxPC-3 for which this range resulted excessive and the concentrations of Gemcitabine treatment varied from 0 to 2000nM) using the MTT assay, as described in section 3.10.

Data depicted in Figure 4.1 shows dose and time-dependent effects of these drugs on cell cultures. The percentage of cell growth for Gemcitabine and Erlotinib was calculated dividing the absorbance in treated cultures by the absorbance in the culture not exposed to any of the drugs. At least three independent experiments with triplicate samples were performed. The IC_{50} value for Gemcitabine was 50 μM for Miapaca-2 and Panc-1 cell lines and 0.02μM for BxPC-3 cell line. The IC_{50} value for Erlotinib was 12.5μM for all cell lines. Gemcitabine showed an inhibitory effect 50% higher for BxPC-3 than for the other two cell lines. The concentration needed to achieve 50% inhibition in Panc-1 was near 50 times the needed for the others.

Panc-1 and Miapaca-2 cell lines were considered as a Gemcitabine chemoresistant cell lines whereas BxPC-3 was considered as a Gemcitabine sensitive cell line. Indeed, the response of Panc-1 and Miapaca-2 were so similar that we decided to continue the experiments just with Panc-1 and BxPC-3.

The concentrations obtained through this assay were applied in the subsequent analysis. The MTT assay provides no useful information regarding the cell death pathway activated by these drugs so apoptosis assays were coupled to fulfil this task.

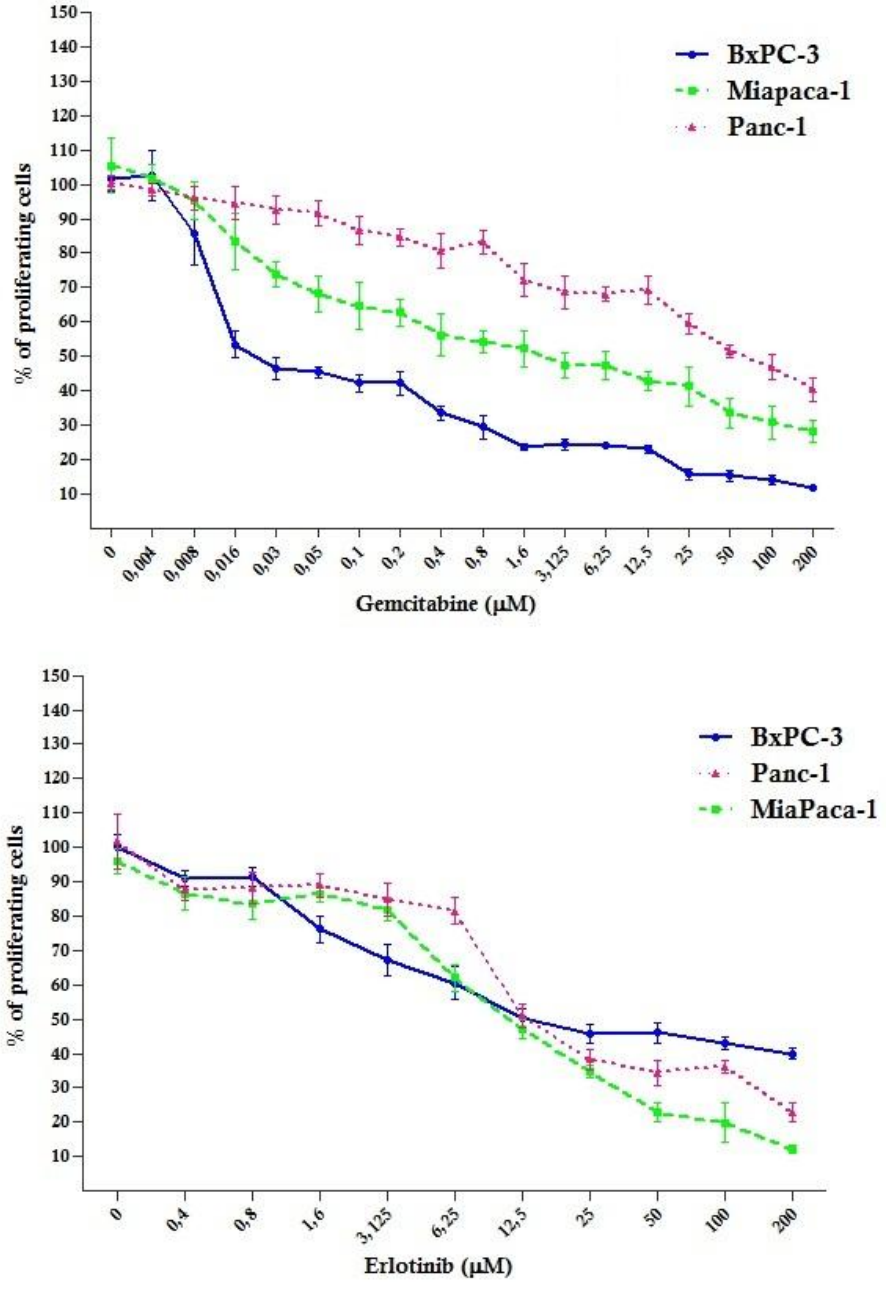

Figure 4.1 Dose and time-dependent effects of Gemcitabine and Erlotinib, as single agents, on pancreatic cancer cell cultures.

4.1.2 Gemcitabine and Erlotinib combination resulted to be additive or slightly synergistic for the pancreatic cancer cell line Panc-1 whereas the same combination resulted to be slightly antagonistic in BxPC-3

To evaluate the combination effect of Erlotinib and Gemcitabine, a combination index (CI) was determined using the Chou-Talalay method [276]. The isobolograms were constructed using the IC_{50} doses of Gemcitabine and Erlotinib as single agents obtained by the MTT assay. The obtained doses were plotted on the *x* (Gemcitabine) and *y* (Erlotinib) axes and the line of additivity was created by joining both data points. Then we analyzed also by MTT assay the dose combination needed of the two agents to get a 50% of growth inhibition. In Table 4-2 and Table 4-7 the averaged results for three independent assays with their corresponding triplicates are shown.

As it is shown in Figure 4.2, CI, a numerical value calculated as described before, provided a quantitative measure of the extent of drug interaction. The CI value was nearly equal to 1 in the Panc-1 cell line suggesting that the combination effects of Erlotinib and Gemcitabine were additive or slightly synergistic. On the other hand, the CI value for BxPC-3 was over 1 suggesting that the combination effects of Erlotinib and Gemcitabine were slightly antagonistic. Thus, the effects of Erlotinib in combination with Gemcitabine were considered additive in KRAS-mutated pancreatic cancer cells (Panc-1) whereas the effects of Erlotinib in combination with Gemcitabine were considered antagonistic in KRAS-wild type pancreatic cancer cells (BxPC-3).

Table 4-1 MTT assay results for the pancreatic cancer cell line Panc-1. Cells were incubated with increasing concentration of both agents. Combined concentration needed to obtain a 50% of growth inhibition is highlighted in bold. Results are shown together with S.D and are representative of three independent assays and triplicates.

PANC-1		GEMCITABINE (μM)					
		0	**0.5**	**1**	**5**	**10**	**20**
ERLOTINIB (μM)	**0**	100±7.85	81.80±4.30	74.84±2.57	68.26±2.09	65.53±3.68	59.57±1.60
	5	85.42±2.98	71.60±4.34	**48.36±1.26**	46.84±3.54	47.68±1.68	30.70±2.19
	10	59.74±5.29	44.32±2.05	36.64±2.30	39.96±1.78	38.41±2.75	30.56±1.80
	20	47.71±2.64	43.11±1.13	30.92±1.97	39.02±2.61	38.53±2.5	26.71±2.75

Table 4-2 MTT assay results for the pancreatic cancer cell line BxPC-3. Cells were incubated with increasing concentration of both agents. Combined concentration needed to obtain a 50% of growth inhibition is highlighted in bold. Results are shown together with S.D and are representative of three independent assays and triplicates.

BxPC-3		GEMCITABINE (μM)					
		0	**0.0125**	**0.025**	**0.05**	**0.1**	**0.2**
ERLOTINIB (μM)	**0**	100±5.17	74.51±4.34	49.16±5.86	46.14±5.36	42.55±0.6	41.51±0.8
	0.5	86.31±5.80	72.89±3.58	68.89±3.37	63.79±2.39	41.13±3.77	35.05±2.6
	1	84.13±4.21	66.98±1.87	66.82±2.24	71.59±2.78	44.01±1.86	39.97±2.01
	5	68.96±4.73	69.81±1.76	**56.32±4.36**	48.02±1.63	44.98±3.52	34.89±1.22

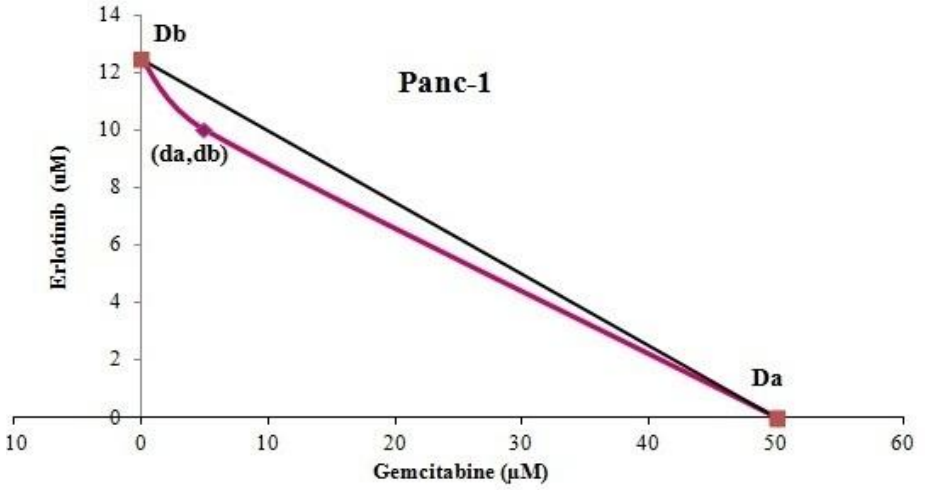

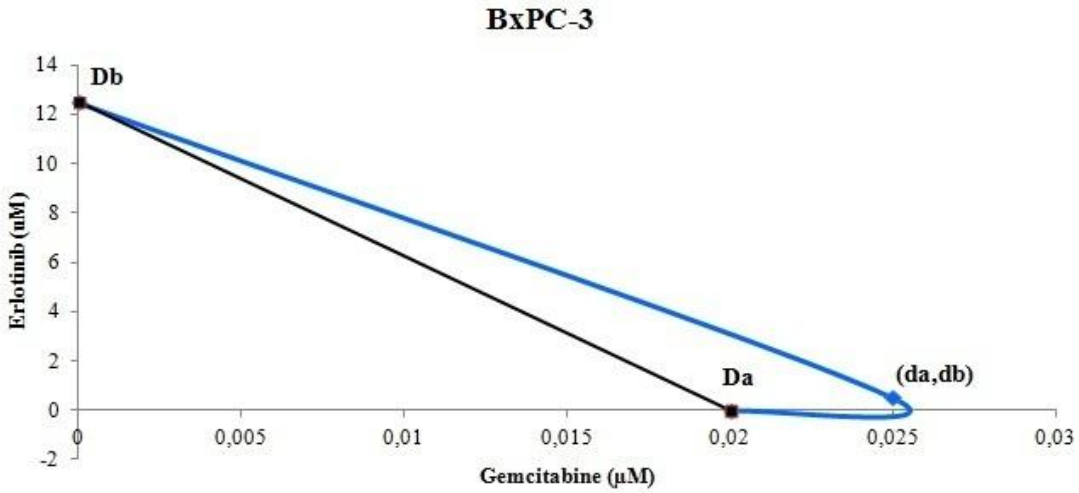

Gem+Erl	*Cell Line*	*CI values at ED_{50}*	*Influence*
	Panc-1	0.9	Slightly Synergistic
	BxPC-3	1.29	Slightly Antagonistic

Figure 4.2 Isobolograms describing the interaction of Gemcitabine and Erlotinib. The isobolograms were constructed by connecting the IC_{50} values of Gemcitabine and Erlotinib. The black lines indicate the theoretical additivity line. Results below the additivity line indicate synergism and those above it antagonism. Da: Concentration of Gemcitabine alone; Db: Concentration of Erlotinib alone; da,db: dose combination of the two agent.

4.1.4 Gemcitabine and Erlotinib treatment induced cell apoptosis in the Panc-1 cell line whereas the combined treatment failed to exert similar effects on the BxPC-3 cell line

4.1.4.1 Analysis of translocation of phosphatidyl serine (PS) to the outer membrane of the cells

To determine whether the suppression in the proliferation shown with the MTT analyses was accompanied by an induction of cell death, we analyzed if Gemcitabine and Erlotinib were able to trigger apoptosis in the pancreatic cancer cell lines Panc-1 and BxPC-3. For this purpose, we first evaluated the presence of PS on the cell surface using FITC-conjugated Annexin-V. Cells were harvested after 48 h of treatment with Gemcitabine, Erlotinib or the combination and used for Annexin V/PI double staining followed by FACS analyses.

Dot plot results of the Gemcitabine treated Panc-1 and BxPC-3 cell lines showed the presence of both early and late apoptotic cells as can be observed in Figure 4.3 and Figure 4.6. The effect was more pronounced when the experiment was performed on Panc-1 cells (45.44 % vs. 17.89%, Panc-1 and BxPC-3 respectively).

Dot plot results of the Erlotinib treated Panc-1 and BxPC-3 cell lines showed the presence of both early and late apoptotic cells as can be observed in Figure 4.3 and Figure 4.6. Despite what described before, here the effect was more pronounced when the experiment was performed on BxPC-3 cells (81.58 % vs. 21.12%, BxPC-3 and Panc-1 respectively).

Dot plot results of the Gemcitabine and Erlotinib combined treated Panc-1 and BxPC-3 cell lines showed the presence of both early and late apoptotic cells as can be observed in Figure 4.3 and Figure 4.6. For the Panc-1 cell line, the combined treatment greatly outperformed the single therapy reaching almost a 60% of apoptotic cell death. Surprisingly for BxPC-3, combined therapy did not even reach 20% of cell death. This could be a consequence of the

synergism/antagonism previously described for Gemcitabine and Erlotinib in the Panc-1/BxPC-3 cell lines respectively.

When untreated cells were subjected to similar analysis, most of the control cells were negative for both Annexin V and PI, indicating that there was not much cell damage.

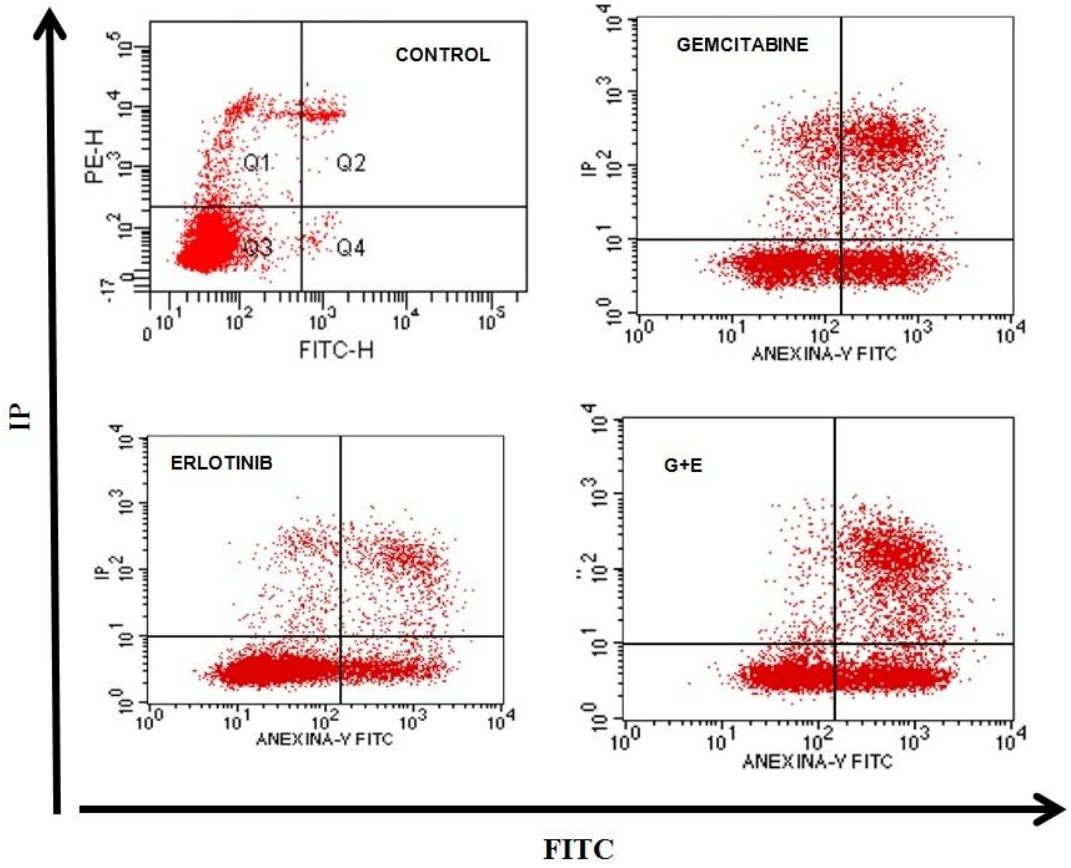

Figure 4.3 Bivariate PI/Annexin V analysis. Apoptotic effect of Gemcitabine, Erlotinib and G+E combined treatment on the Panc-1 cell line. Using the Annexin V-affinity assay, the number of apoptotic cells in suspension was determined.

Detailed results for the Panc-1 cell line are below summarized in Figure 4.4 and Table 4-3. Figure 4.4 depicts percentages of live, apoptotic and necrotic cells after Gemcitabine, Erlotinib and Gemcitabine+Erlotinib combined treatment. Their corresponding percentages are included in Table 4-3.

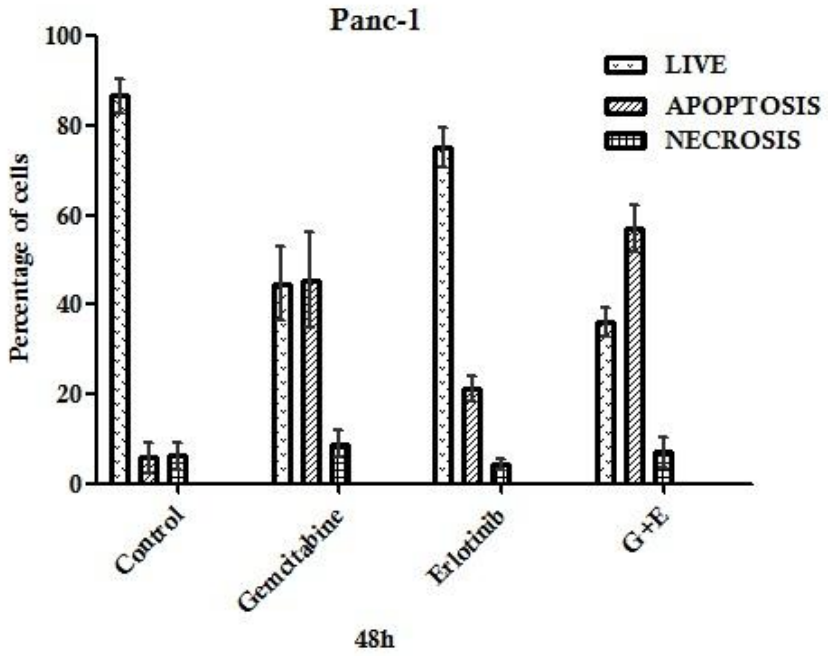

Figure 4.4 Effects of Gemcitabine, Erlotinib and combined treatment on the Panc-1 cell line. Cells were incubated for 48h in the presence/absence of 50μM of Gemcitabine, 12.5μM of Gemcitabine and/or 1+5μM of Gemcitabine + Erlotinib. Apoptosis was evaluated by cytometric analysis (See Section 3.13 for further details). Data is expressed as mean ± S.D of at least 4 experiments. Statistical analyses are detailed in Figure 4.5.

Table 4-3 Percentages of Panc-1 living, apoptotic and necrotic cells after 48h of treatments. Data is expressed as mean ± S.D of at least 4 experiments.

PANC-1	Live	Apoptosis	Necrosis
Control	86.74±1.057	5.868±0.94	6.213±0.83
Gemcitabine	44.71±2.26	45.44±2.95	8.78±0.85
Erlotinib	75.16±1.22	21.12±0.81	4.238±0.37
Gem+Erl	36.08±1.09	57.00±1.88	6.928±1.19

Statistically significant changes between treatments are shown in Figure 4.5 for the Panc-1 cell line.

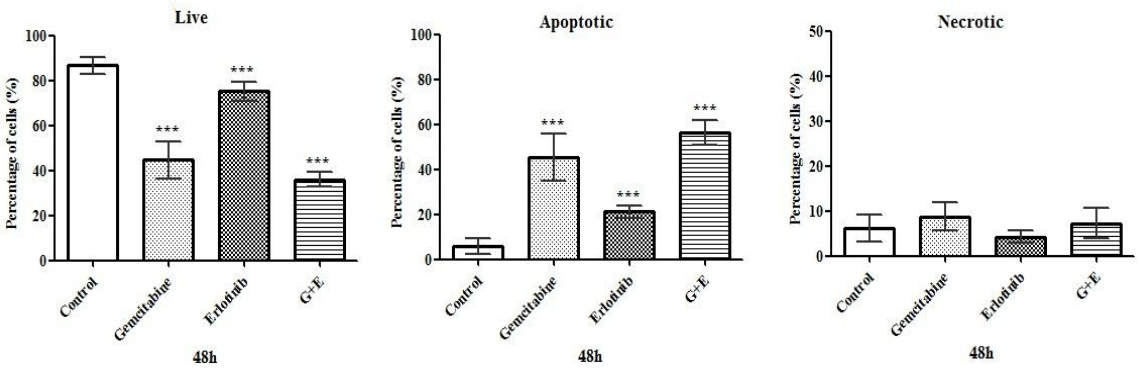

Figure 4.5 Panc-1 cell line GraphPath Prism 5 plots representing the differences living, apoptotic and necrotic cell percentages between treatments. ***: P< 0.0001; **: P<0.01; *: P<0.05 (one-way ANOVA).

Our results demonstrated a high induction of apoptosis in the Panc-1 cell line after treatment with Gemcitabine as a single agent. The addition of Erlotinib did not achieve Gemcitabine levels, obtaining only half of the induction of apoptosis. The highest level of apoptosis was obtained after the Gemcitabine and Erlotinib combined therapy, proving that Gemcitabine and Erlotinib have synergic effect on the Panc-1 cell line.

Detailed results for the BxPC-3 cell line are below summarized in Figure 4.7 and Table 4-4. Figure 4.7 depicts percentages of live, apoptotic and necrotic cells after the Gemcitabine, Erlotinib and Gemcitabine+Erlotinib combined treatments. Their corresponding percentages are included in Table 4-4.

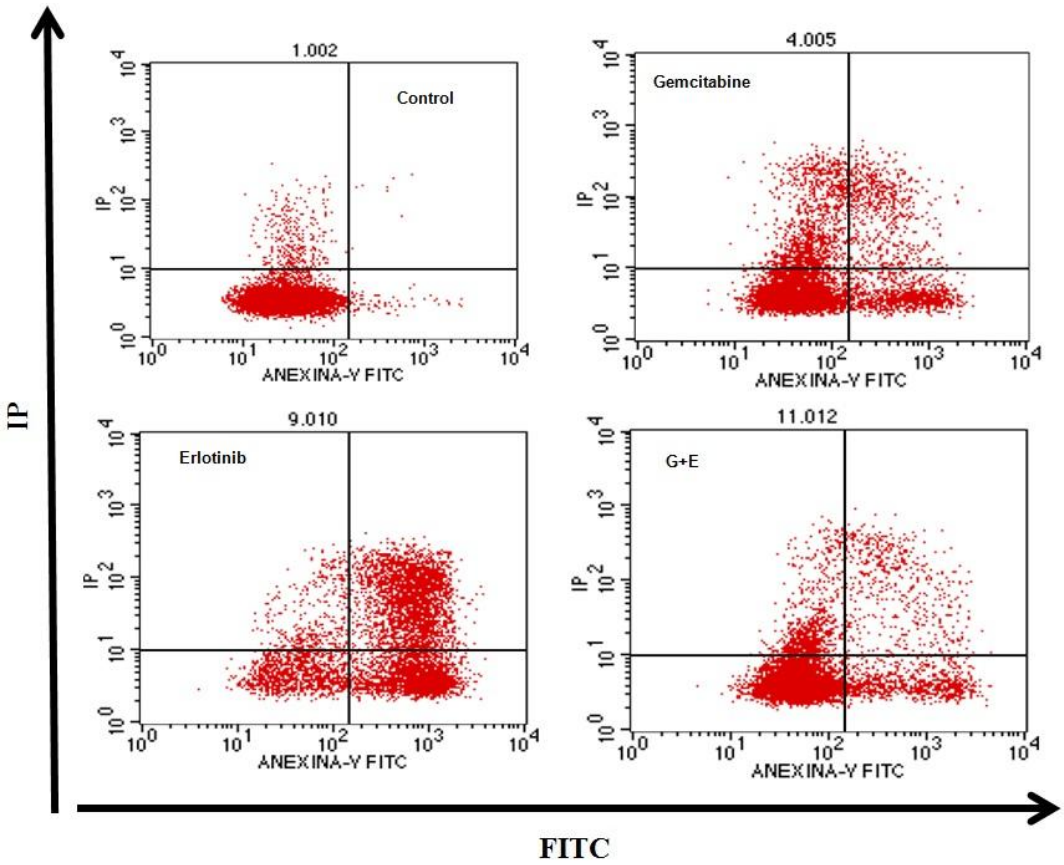

Figure 4.6 Bivariate PI/Annexin V analyses. Apoptotic effect of the Gemcitabine, Erlotinib and G+E combined treatments on the BxPC-3 cell line. Using the Annexin V-affinity assay, the number of apoptotic cells in suspension was determined.

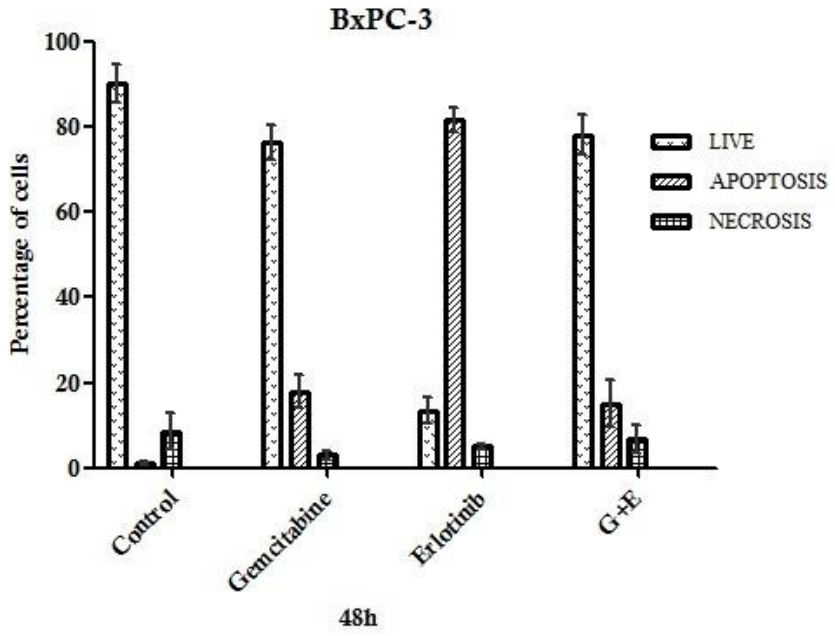

Figure 4.7 Effects of the Gemcitabine, Erlotinib and combined treatments on the BxPC-3 cell line. Cells were incubated for 48h in the presence/absence of 0.02µM of Gemcitabine,

12.5µM of Erlotinib and 0.025+5µM of Gemcitabine + Erlotinib respectively. Apoptosis was evaluated by cytometric analysis (See Section 3.13 for further details). Data is expressed as mean ± S.D of at least 4 experiments. Statistical analyses are detailed in Figure 4.8.

Table 4-4 Percentages of BxPC-3 living, apoptotic and necrotic cells after 48h of treatments. Data is expressed as mean ± S.D of at least 4 experiments.

BxPC-3	Live	Apoptosis	Necrosis
Control	90.37±2.02	1.08±0.1	8.54±1.96
Gemcitabine	76.48±1.80	17.89±1.73	2.92±0.38
Erlotinib	13.45±1.32	81.58±1.28	4.97±0.32
Gem+Erl	78.11±2.11	15.10±2.40	6.79±1.54

Statistically significant changes between treatments are shown in Figure 4.8 for BxPC-3.

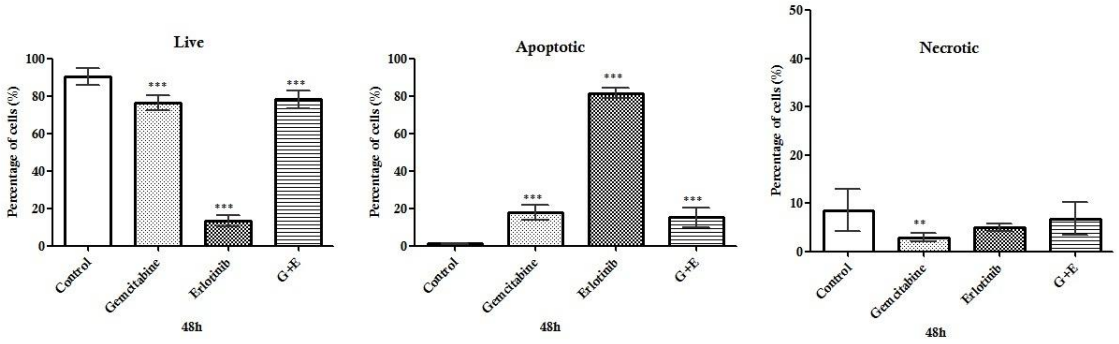

Figure 4.8 BxPC-3 cell line GraphPath Prism 5 plots representing the differences living, apoptotic and necrotic cell percentages between treatments. ***: P< 0.0001; **: P<0.01; *: P<0.05 (one-way ANOVA).

Our results demonstrated a high induction of apoptosis in the BxPC-3 cell line after treatment with Erlotinib as a single agent. The addition of Gemcitabine only achieved a 20% of apoptosis. The same percentage of apoptosis was obtained after the Gemcitabine and Erlotinib combined therapy, proving that Gemcitabine and Erlotinib have antagonist effect on the BxPC-3 cell line.

4.1.4.2 Analysis of proteins involved in apoptosis

To investigate the underlying mechanisms by which the Gemcitabine, Erlotinib and Gemcitabine plus Erlotinib combined treatments induced apoptosis in pancreatic cancer cell lines, we studied the changes in the levels of proteins involved in apoptosis. Since Bcl-2 family proteins play important roles in apoptosis by functioning as promoters (e.g., Bax, Bak and Bad) or inhibitors (e.g., Bcl-2 or Bcl-X_L) of cell death process, we next studied the changes in the levels of some of these proteins in pancreatic cancer cells.

The Bcl-2 family of proteins plays a major role in both sensing different types of cellular stresses and regulating mitochondrial outer membrane permeabilization (MOMP). To accomplish these tasks, different members of the Bcl-2 family are located in multiple parts of the cell and function as both cytoplasmic and membrane proteins by adopting distinct conformations that dictate their function [311].

Cell lysates were prepared from the Panc-1 cell line treated with Gemcitabine (50μM), Erlotinib (12.5μM) and Gemcitabine plus Erlotinib (1+5μM) for 48 h and used for western blot studies. Figure 4.9 depicts representative western blot images for the Bcl-2 family proteins studied.

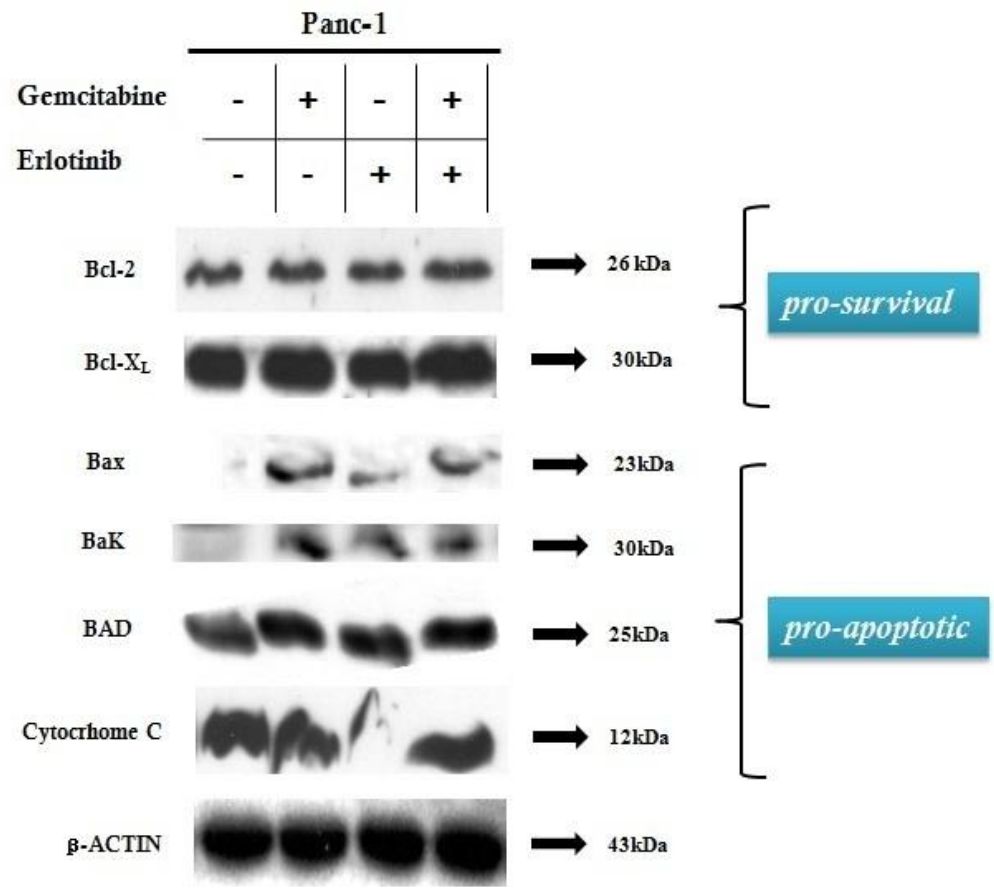

Figure 4.9 Effects of the Gemcitabine, Erlotinib and Gemcitabine plus Erlotinib combined treatments on the expression of BCL-2 family proteins in the pancreatic cancer cell line Panc-1 were analyzed by western blot. Cells were incubated 48h with the IC_{50} concentrations for every treatment. For further detailed see section 3.17. Beta-actin was used as a loading control.

Cell lysates were prepared from the BxPC-3 cell line treated with Gemcitabine (0.02 μM), Erlotinib (12.5μM) and Gemcitabine plus Erlotinib (0.025+5μM) for 48 h and used for western blot studies. Figure 4.10 depicts representative western blot images for the Bcl-2 family proteins studied.

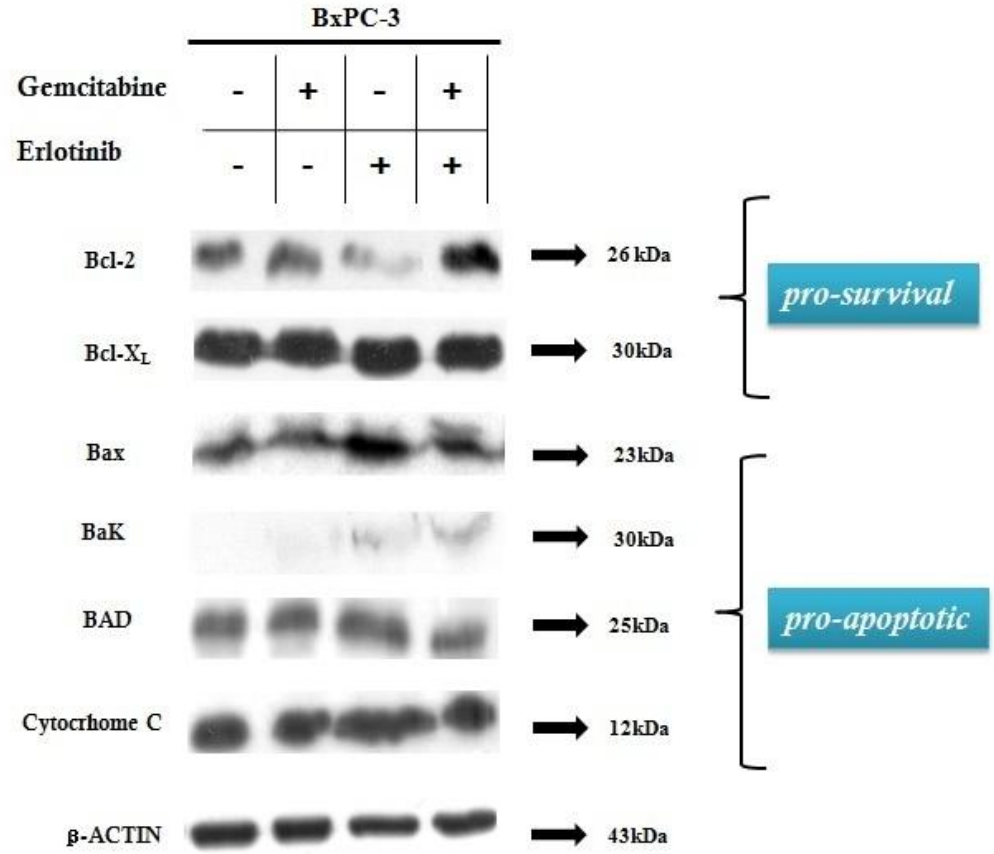

Figure 4.10 Effects of Gemcitabine, Erlotinib and Gemcitabine plus Erlotinib combined treatments on the expression of the BCL-2 family proteins in the pancreatic cancer cell line BxPC-3 were analyzed by western blot. Cells were incubated 48h with the IC_{50} concentrations for every treatment. For further detailed see section 3.17. Beta-actin was used as a loading control.

Bcl-2: Bcl-2 plays a role in cell survival and also inhibits cell death induced by various stimuli such as chemotherapeutic agents, ethanol and heat shock, indicating that Bcl-2 is a negative regulator of cell death [107]. Regarding this protein, in the Panc-1 cell line, Gemcitabine exerted an induction of its expression of 10% ($p<0.01$, Figure 4.12). The same treatment, in the BxPC-3 cell line, exerted the same effect, though a bit more intense, a 30%. Erlotinib failed to produce any significant effect on the Bcl-2 expression in the Panc-1 cell line. On the contrary, it achieved an inhibition of 50% in the expression of the Bcl-2 protein in the BxPC-3 cell line. When the combined therapy was applied, the obtained results resembled those obtained using the Gemcitabine as a single agent, a highly significant induction of the Bcl-2 protein in both cell lines ($p<0.001$).

BCL-X_L: The BCL-2 homolog BCL-X_L, one of the two protein products of BCL2L1, has originally been characterized for its prominent prosurvival functions. Similar to BCL-2, BCL-X_L binds to its multidomain proapoptotic counterparts BAX and BAK, hence preventing the formation of lethal pores in the mitochondrial outer membrane, as well as to multiple BH3-only proteins, thus interrupting apical proapoptotic signals [312]. Regarding this protein, in the Panc-1 cell line, Gemcitabine exerted a significant induction of its expression of 20% ($p<0.001$, Figure 4.12). The same treatment in the BxPC-3 cell line exerted the same effect, inducing the expression of Bcl-X_L in a 25% ($p<0.001$, Figure 4.13). Erlotinib produced the attenuation on Bcl-X_L expression in the Panc-1 cell line. On the contrary, it achieved an augment of 30% in the expression of Bcl-X_L in the BxPC-3 cell line. When the combined therapy was applied, again the obtained results resembled those obtained using Gemcitabine as a single agent, a significant induction of Bcl- X_L in both cell lines ($p<0.001$).

Bax and Bak: They are considered to be downstream mediators of the mitochondrial apoptotic pathway because their combined absence abolishes most apoptotic responses. When activated, these proteins translocate to the outer mitochondrial membrane, oligomerize and permeabilize the outer mitochondrial membrane, freeing proapoptogenic factors such as cytochrome c (Cyt C), which promotes activation of caspases. The activation of Bax/Bak family and thereby the mitochondrial apoptotic process is a function of the relative abundance of the antiapoptotic Bcl-2 family members and the BH3-only proteins [313].

It is noteworthy that there was loss of expression of Bax in the Panc-1 cell line together with an absence of Bak in both pancreatic cancer cell lines, at baseline, before any treatment (Figure 4.9 and Figure 4.10). For the Panc-1 cell line, Bax achieved 18 times the expression of the untreated control after incubation with Gemcitabine. More modest but still significant effect had Erlotinib over the Panc-1 cell line. The combination of Gemcitabine and Erlotinib in the Panc-1 cell line achieved 12 times the expression of the untreated control. For the BxPC-3 cell line, Gemcitabine failed to yield any significant modulation when compared against the control. The Bax expression in the BxPC-3 treated with Gemcitabine

reached twice the expression of the control and these results were similar or slightly lesser in the combined therapy.

Regarding Bak expression, although in the BxPC-3 there was no expression neither in untreated control nor in Gemcitabine treated samples, Erlotinib and overall the combined therapy resulted in an induction of this proapoptotic protein. In the case of the Panc-1 cell line, Gemcitabine did affect the expression of this protein, what was also found in Erlotinib and in the combined therapy.

BAD: In the absence of various survival factors, Bad binds, through its BH3 domain and inactivates Bcl-2 and/or Bcl-X_L at the outer mitochondrial membrane, thereby promoting cell death. As it is shown in Figure 4.9, all the treatment regimens achieved similar induction of this protein, in the Panc-1 cell line. As it is shown in Figure 4.10, the greatest induction of this protein in the BxPC-3 was obtained after the Erlotinib treatment.

Cytochrome C: In healthy cells, cytochrome c (Cyt C) is located in the mitochondrial intermembrane space, where it functions as an electron shuttle in the respiratory chain and interacts with cardiolipin. Several proapoptotic stimuli induce the permeabilization of the outer membrane, releasing it form the cardiolipin. Once unleashed from its usual context, Cyt C can be recruited in the cytoplasm into the death squad and contributes to the apoptotic dismantling of the cell [314]. There is a striking contrast between results obtained with the Erlotinib treatment between the two cell lines. While a remarkable increase of released Cyt C protein was monitored after the Erlotinib treatment in the BxPC-3 cell line, the expression was almost vanished in the Panc-1 cell line.

In order to ease the comparison between the two cell lines and to numerically determined induction/repression of BCL-2 protein family members, results were summarized in Table 4-5.

Table 4-5 BCL-2 protein family member expression after Gemcitabine, Erlotinib and Gemcitabine plus Erlotinib combined therapy in the pancreatic cancer cell lines Panc-1 and BxPC-3.						
	PANC-1			BxPC-3		
	Gemcitabine	Erlotinib	Gem+Erl	Gemcitabine	Erlotinib	Gem+Erl
BCL-2	1.11±0.01	0.97±0.001	1.15±0.025	1.19±0.013	0.48±0.014	1.96±0.017
BCL-X_L	1.263±0.02	0.73±0.01	1.35±0.02	1.25±0.008	1.33±0.009	1.15±0.002
BAX	18.57±0.37	7.68±0.11	15.71±0.41	0.96±0.08	1.95±0.04	1.45±0.01
BAK	15.62±0.24	15.25±0.11	12.24±0.23	5.9±0.16	50.09±0.20	58.94±0.29
BAD	1.23±0.017	1.19±0.018	1.27±0.025	0.97±0.008	1.2±0.005	0.97±0.022
Cit.C	0.95±0.02	0.13±0.007	0.99±0.02	1.03±0.002	1.44±0.009	1.05±0.035

4.1.4.3 Comparison between Panc-1 and BxPC-3´s Bcl-2, Bcl-X_L and Bax basal levels

In order to determine whether any differences between the two cell lines regarding the starting concentrations of the Bcl-2, Bcl-X_L and Bax proteins could contribute to the sensibility of these cell lines to the chemotherapy, we compared the expression of these proteins in cell cultures without any treatment. In Figure 4.11 the comparison between the two cell lines is depicted. Each protein was normalized against its β-actin and the ratio of Panc-1 value (for Bcl-2, Bcl-X_L and Bax) to BxPC-3 value (for Bcl-2, Bcl-X_L and Bax) was calculated as Panc-1/BxPC-3.

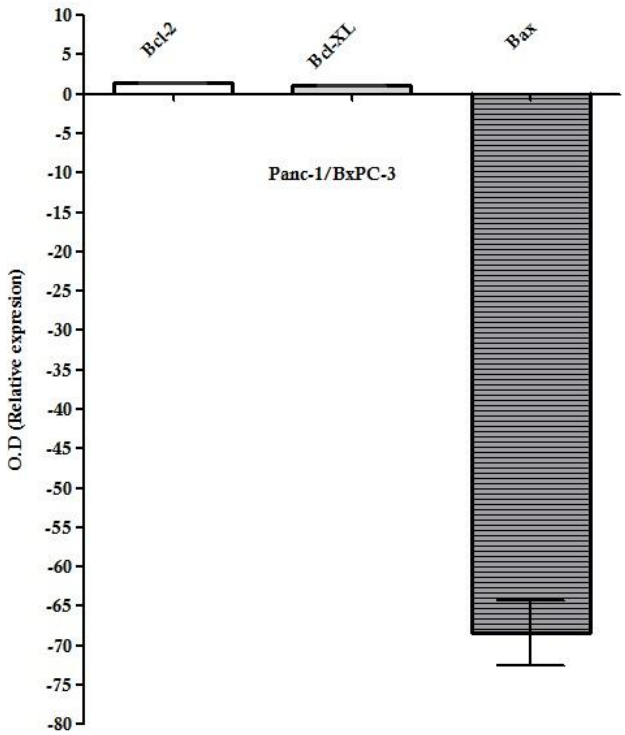

Figure 4.11 Bcl-2, Bcl-X_L and Bax ratios for Panc-1/BxPC-3 in control samples.

The Bcl-2 expression in the Panc-1 cell line without any treatment exceeded the BxPC-3 cell line expression in almost a 40%. The higher initial expression of this antiapoptotic protein in the Panc-1 cell line could be related to the higher resistance of this cell line to the chemotherapy applied. The Bcl-X_L expression in both cell lines did not show any significant difference. The Bax expression in the BxPC-3 cell line was 60 times the expression of the Panc-1 cell line.

Taking all these results into account, the sensibility of the BxPC-3 cell line to the treatments could be related to the lower expression of antiapoptotic proteins and to the higher expression of proapoptotic proteins. On the other hand, the resistance of the Panc-1 cell line to the treatments could be related to the higher expression of antiapoptotic proteins and to the lower expression of proapoptotic proteins.

4.1.4.4 Analysis of the Bcl-2/Bax and Bcl-X_L/Bax Ratios

The ratio of Bcl-2/Bax genes and/or proteins is one the most important indicators of whether a cell will survive or undergo apoptosis [315-316], regulating the release of Cyt C from the mitochondria [317]. On the other hand, Bcl-X_L inhibits and maintains Bax in the cytosol by constant retrotranslocation of mitochondrial Bax [318]. Bcl-X_L retrotranslocation activity prevents the commitment to apoptosis and protects cells from Bax dependent cell death [319]. To determine whether the increase in apoptosis was due to any alteration in these ratios, we quantified the Bcl-2/Bax and BCL-X_L ratios.

After western blotting, quantitative analysis of the Bcl-2, Bcl-X_L and Bax protein expression was performed using scanning densitometer and *ImageJ software* (National Institutes of Health). Relative expression of the Bcl-2, Bcl-X_L and Bax proteins against β-actin for the Panc-1 cell line is shown in Figure 4.12. Relative expression of the Bcl-2, Bcl-X_L and Bax proteins against β-actin for the BxPC-3 cell line is shown in Figure 4.13.

The disruption of this balance sensitizes cells to the apoptotic effects of chemotherapy. A Bcl-2/Bax ratio >1 implies resistance to apoptosis. A Bcl-2/Bax ratio <1 implies sensitivity to apoptosis. In the same way, a Bcl-X_L/Bax ratio >1 implies resistance to apoptosis and a Bcl-X_L /Bax ratio <1 implies sensitivity to apoptosis.

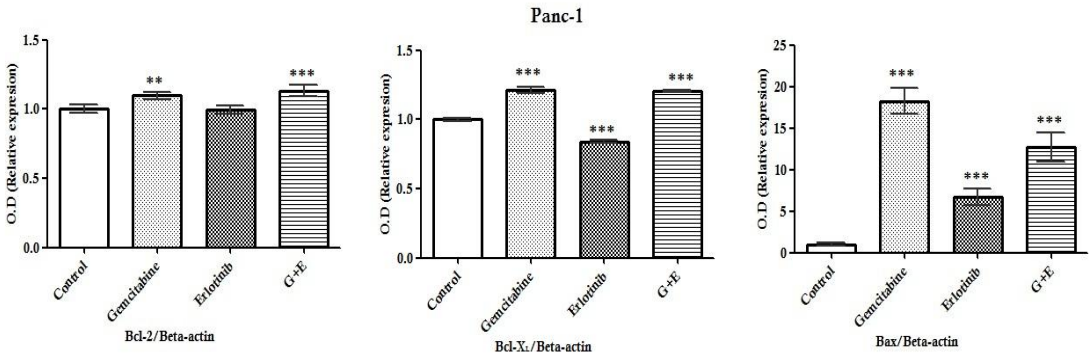

Figure 4.12 Quantitative analysis of the immunoreactive Bcl-2, Bcl-X_L and Bax proteins in

the Panc-1 cell line after 48h of Gemcitabine, Erlotinib and the Gemcitabine plus Erlotinib combined therapy. The autoradiographs were scanned and the level of each protein expression was quantified by densitometry. Results are expressed as optical density relative to the beta-actin. Each value is represented as mean ± S.D of 3 independent determinations. Asterisks indicate significant differences from control values (*: P< 0.0001; **: P<0.01; *: P<0.05).**

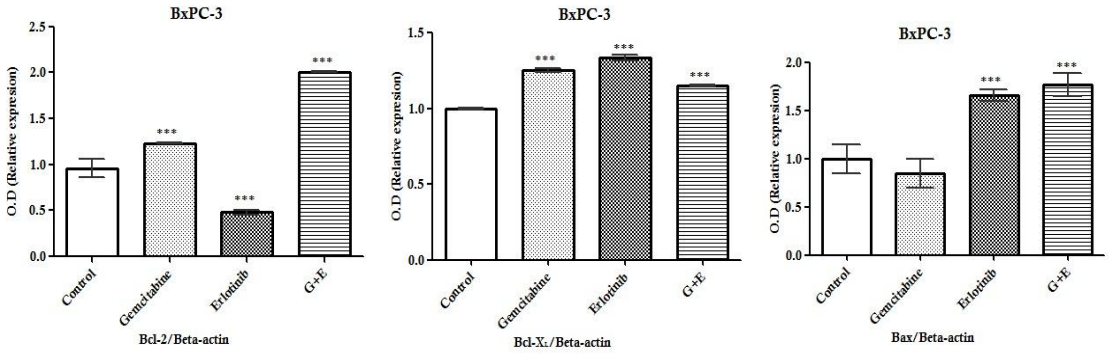

Figure 4.13 Quantitative analysis of the immunoreactive Bcl-2, Bcl-X_L and Bax proteins in the BxPC-3 cell line after 48h of Gemcitabine, Erlotinib and Gemcitabine plus Erlotinib combined therapy. The autoradiographs were scanned and the level of each protein expression was quantified by densitometry. Results are expressed as optical density relative to the beta-actin. Each value is represented as mean ± S.D of 3 independent determinations. Asterisks indicate significant differences from control values (*: P< 0.0001; **: P<0.01; *: P<0.05).**

Results obtained from the Bcl-2/Bax ratio for both cell lines are depicted in Figure 4.14.

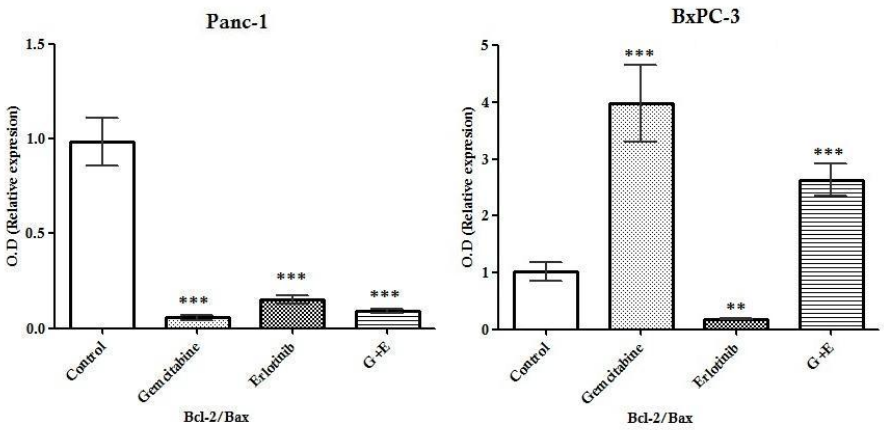

Figure 4.14 Determination of the Bcl-2/Bax protein expression ratio in pancreatic cancer cell lines after 48h of treatment with Gemcitabine and Erlotinib as single agents or in combination. Each value is represented as mean ± S.D of 3 independent determinations. Asterisks indicate significant differences from control values (*: P< 0.0001; **: P<0.01; *: P<0.05).**

Results obtained from the Bcl-X_L/Bax ratio for both cell lines are depicted in Figure 4.15.

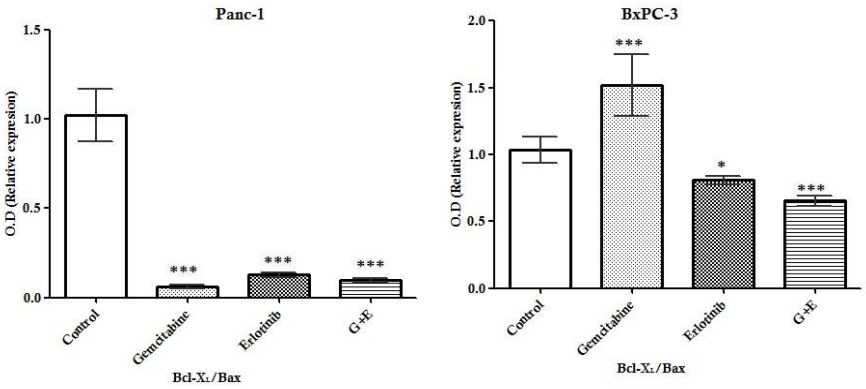

Figure 4.15 Determination of the Bcl-X_L/Bax protein expression ratio in pancreatic cancer cell lines after 48h of treatment with Gemcitabine and Erlotinib as single agents or in combination. Each value is represented as mean ± S.D of 3 independent determinations. Asterisks indicate significant differences from control values (*: P< 0.0001; **: P<0.01; *: P<0.05).**

Table 4-6 details the Bcl-2/Bax and Bcl-X_L/Bax ratios in the Panc-1 and BxPC-3 cell lines after the different treatment regimens.

Table 4-6 Disruption of Bcl-2/Bax and Bcl-X_L/Bax balances			
Panc-1	**Bcl-2 /Bax ratio**	**Bcl-X_L/Bax ratio**	**Sensitivity to apoptotic stimuli**
Control	0.98±0.12	1.024±0.14	
Gemcitabine	0.05±0.01	0.06±0.007	***
Erlotinib	0.2±0.02	0.13±0.019	**
Gem+Erl	0.08±0.01	0.09±0.006	***
BxPC-3	**Bcl-2 /Bax ratio**	**Bcl-XL/Bax ratio**	**Sensitivity to apoptotic stimuli**
Control	1.018±0.17	1.017±0.13	
Gemcitabine	3.97±0.68	1.51±0.20	
Erlotinib	0.18±0.01	0.81±0.02	**
Gem+Erl	2.63±0.27	0.65±0.04	

For the Panc-1 cell line, although there was an induction of prosurvival proteins, the global balance between pro and anti apoptotic proteins showed susceptibility to apoptosis when treated with Gemcitabine. These results matched those obtained with the Annexin-V that showed nearly a 50% of Annexin-V positive cells (Table 4-3). Regarding Erlotinib, although both ratios were below 1, so it implied sensitivity to apoptosis, the values for the Erlotinib ratios were nearly 4 times bigger than those for Gemcitabine and it was reflected in the percentage of Annexin-V positive cells, only a 20%. The combined therapy equaled the results obtained for Gemcitabine used as a single agent.

For the BxPC-3 cell line, Erlotinib showed the lowest ratios, increasing the susceptibility to apoptosis. Results from Annexin-V depicted an 80% of Annexin-V positive cells when treated with Erlotinib as a single agent (Table 4-4). Annexin-V positive cells barely achieved a 20% in the two other treatments what can be associated with pro and antiapoptotic ratios above 1.

4.1.5 Gemcitabine and Erlotinib inhibited cell cycle progression in the G0/G1 phase

Somatic cells proliferate to support tissue and organism growth and to replace damaged cells. Proliferation is also a fundamental response that underlies cellular mechanisms involved in immunity, inflammation, hematopoiesis, neoplasia and other biological responses. Cell growth, replication and division in eukaryotic cells occur according to a highly controlled series of events called the cell cycle.

Cell proliferation was quantified by end-point 5-bromo-2'-deoxyuridine (BrdU) labeling, as a marker of synthesis of DNA, and by analyzing the distribution of cells among the different phases of their growth cycles using PI staining and flow cytometry. Besides, the effect of the chemotherapy on proteins related to cell cycle control and differentiation were analyzed by western blot.

We speculated that, although inhibition of cell proliferation in the BxPC-3 cell line was not accompanied by an induction of apoptosis, it could be due to a block in the cell cycle progression.

4.1.5.1 PI staining and flow cytometry

To analyze cell proliferation, measurement of DNA synthesis as a marker for proliferation was carried out. The rate of cell division is a tightly regulated process that is intimately associated with growth, differentiation and tissue turnover.

DNA content is the most frequently measured entity of the cell. Analysis of DNA content reveals cell ploidy, provides information on cell position in the cell cycle and also allows one to estimate frequency of apoptotic cells that are characterized by fractional DNA content.

Distribution of cells within the major phases of the cell cycle is based on differences in DNA content between the cells in prereplicative phase (the G0/G1) versus the cells that actually replicate DNA (the S-phase) versus the postreplicative plus mitotic (the G2/M) phase cells.

It is generally accepted that DNA content measured by cytometry (DNA ploidy) is defined as DNA index (DI) and for normal (non tumour, euploid) cells in the G0/G1 phase of the cell cycle DI = 1.0. Cells in the G2/M phase of the cell cycle have DI = 2.0 and the S-phase normal cells are characterized by 1.0 < DI < 2.0. Due to extensive internucleosomal DNA fragmentation that takes place during apoptosis, the low molecular (mono- and oligo- nucleosomal) DNA fragments are extracted during cell preparation for staining and such apoptotic cells can be identified as the cells with fractional DNA content (DI < 1.0). They are often being defined as "sub-G1" or "sub-diploid" cell population [320].

The effects of Gemcitabine and Erlotinib on cell growth were examined using flow cytometry, as single agents or in combination. In normal tissues and most low-grade or slowly proliferating neoplasms, approximately 85% of the cell population forms the G0/G1 peak and 15% of the cells are in the remaining S and G2M phases [321]. As shown in Figure 4.16 the cell cycle profile of pancreatic untreated cancer cells line Panc-1 revealed a typical distribution of proliferating cells, having a higher percentage of cells in the S-phase of the cell cycle. BxPC-3 (Figure 4.18) has a lower percentage of cells in the S-phase although they have higher G2/M phase (S and G2/M phases can be considered as proliferating phases).

As shown in Figure 4.16, flow cytometry studies demonstrated that Gemcitabine and Erlotinib inhibited cell proliferation by arresting cells into the G0/G1 phase in the Panc-1 cell line. Gemcitabine, when used as a single agent, increased the amount of cells in the G0/G1 phase in a 30%. Erlotinib, when used as a single agent, obtained similar results to Gemcitabine. The effect obtained with the combined therapy was very similar to those obtained with the single agents, with 70% of cells stopped in the G0/G1 phase (See Table 4-7 for detailed information

of percentages in each phase of the cell cycle.).

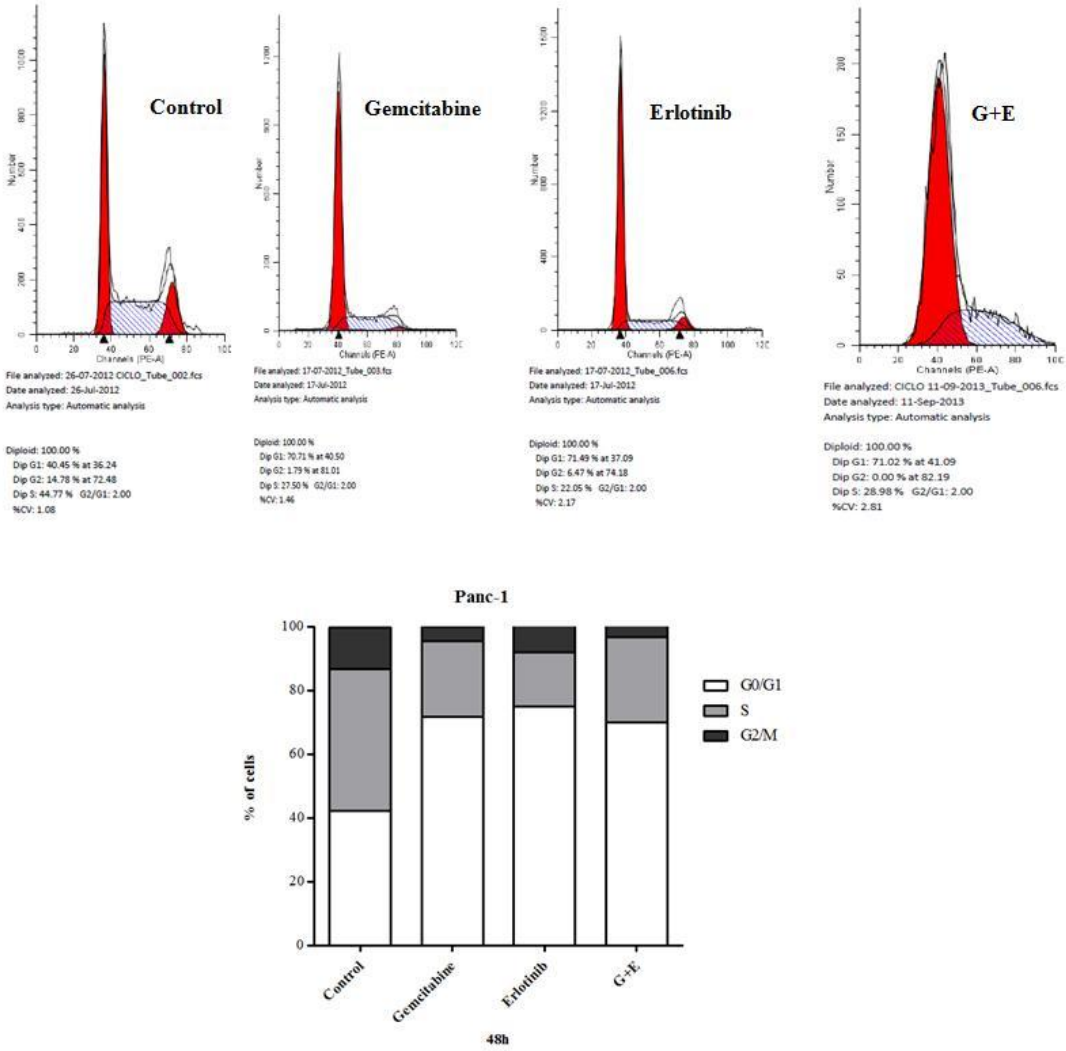

Figure 4.16 Representative histograms of flow cytometry performed in the Panc-1 cell lines. Cells were treated with 50μM of Gemcitabine, 12.5μM of Erlotinib and 1+5μM of Gemcitabine + Erlotinib respectively. After treatment, cells were harvested, fixed, stained with propidium iodide and analyzed for DNA content by flow cytometry.

Table 4-7 shows detailed information of percentages in each phase of the cell cycle.

Table 4-7 Percentages of Panc-1 in the three cell cycle phases after 48h of treatments. Data is expressed as mean ± S.D of at least 4 experiments.			
PANC-1	**G0/G1**	**S**	**G2/M**
Control	42.23±1.19	44.64±1.05	13.13±0.77
Gemcitabine	71.86±0.63	23.68±0.70	4.46±0.83
Erlotinib	74.25±1.31	16.44±1.04	8.68±1.00
Gem+Erl	70.07±1.12	26.72±0.72	3.59±0.98

Figure 4.17 shows detailed information about the significantly differences in cell percentages in every cell cycle phase, compared against the untreated samples.

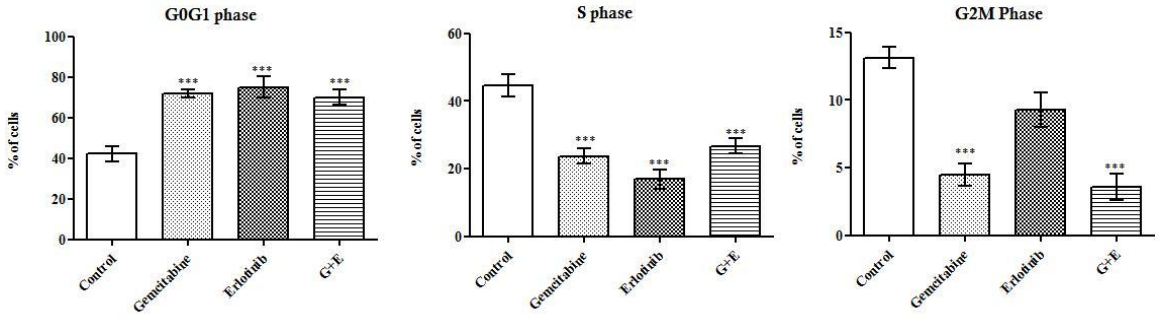

Figure 4.17 GraphPath Prism 5 plots representing the differences in Panc-1 cell populations in the G0/G1, S and G2/M phases between treatments. ***: P< 0.0001; **: P<0.01; *: P<0.05 (one-way ANOVA).

Results showed that in the Panc-1 cell line, the Gemcitabine, Erlotinib and combined treatments induced a halt in the cell cycle progression, lowering proliferative fractions (S and G2/M phases) and inducing cells to accumulate in the G0/G1 phase.

As shown in Figure 4.18, flow cytometry studies demonstrated that Gemcitabine and Erlotinib also inhibited cell proliferation by arresting cells into the G0/G1 phase in the BxPC-3 cell line. Gemcitabine, when used as a single agent, reached an 87% of cells in the G0/G1 phase. However, in this cell line the greatest effect

was obtained with Erlotinib used as a single agent. The amount of cells in the G0/G1 phase reached 92%. The amount of cells arrested in the G0/G1 phase after the Gemcitabine and Erlotinib combined treatment did not significantly differ from those obtained with single agents.

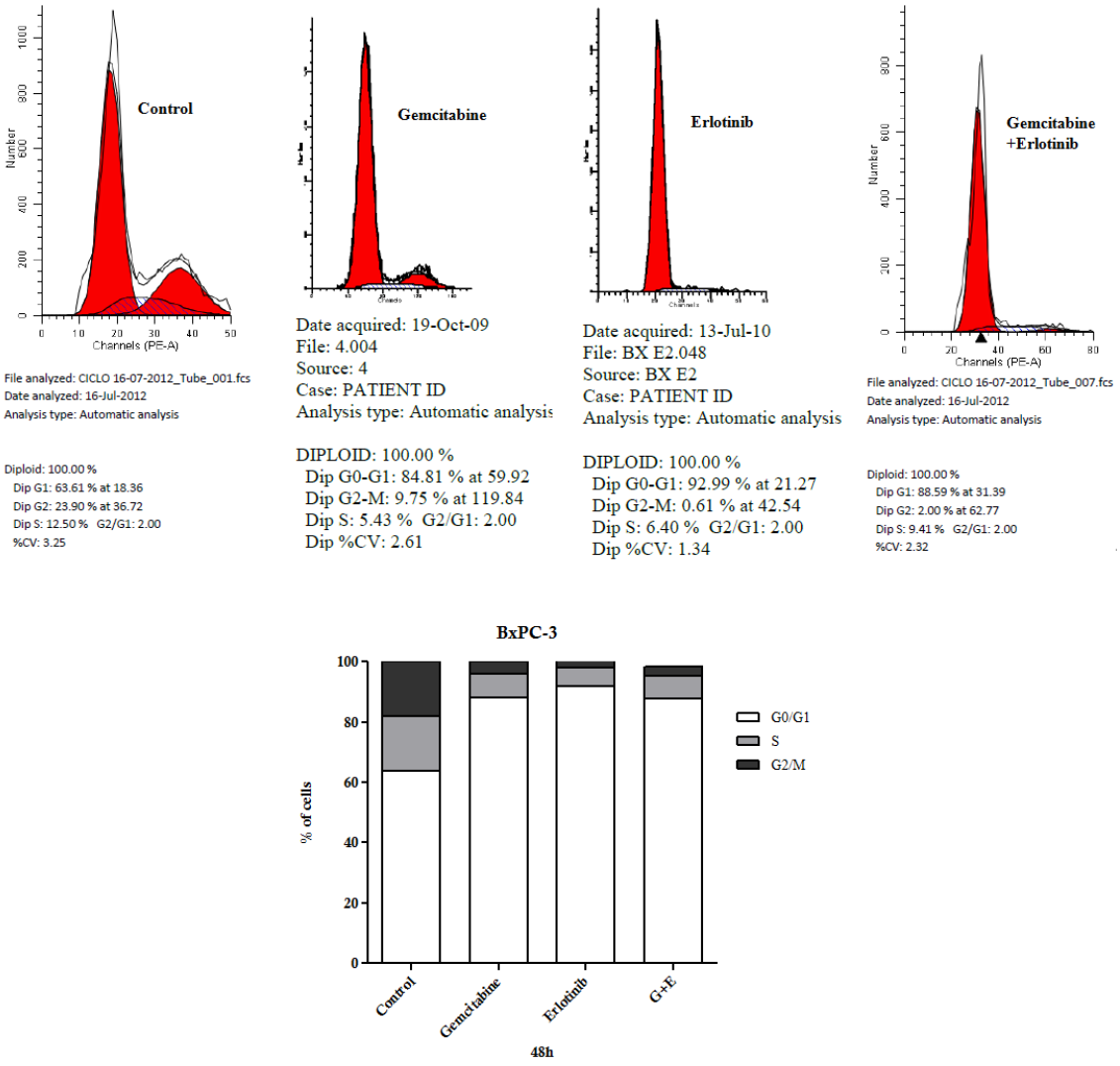

Figure 4.18 Representative histograms of flow cytometry performed in the BxPC-3 cell lines. Cells were treated with 0.02µM of Gemcitabine, 12.5µM of Erlotinib and 0.025+5µM of Gemcitabine + Erlotinib respectively. After the treatment, cells were harvested, fixed, stained with propidium iodide and analyzed for DNA content by flow cytometry.

Table 4-8 shows detailed information of percentages in each phase of the cell cycle.

Table 4-8 Percentages of BxPc-3cells in the three cell cycle phases after 48h of treatments. Data is expressed as mean ± S.D of at least 4 experiments.			
BxPC-3	**G0/G1**	**S**	**G2/M**
Control	63.87±1.66	18.17±1.72	17.97±1.61
Gemcitabine	87.93±1.92	7.97±1.30	4.10±1.46
Erlotinib	91.98±0.27	5.91±0.35	2.12±0.55
Gem+Erl	87.71±1.79	7.53±2.01	3.14±0.76

Figure 4.19 shows detailed information about the significantly differences in cell percentages in every cell cycle phase, compared against the untreated samples.

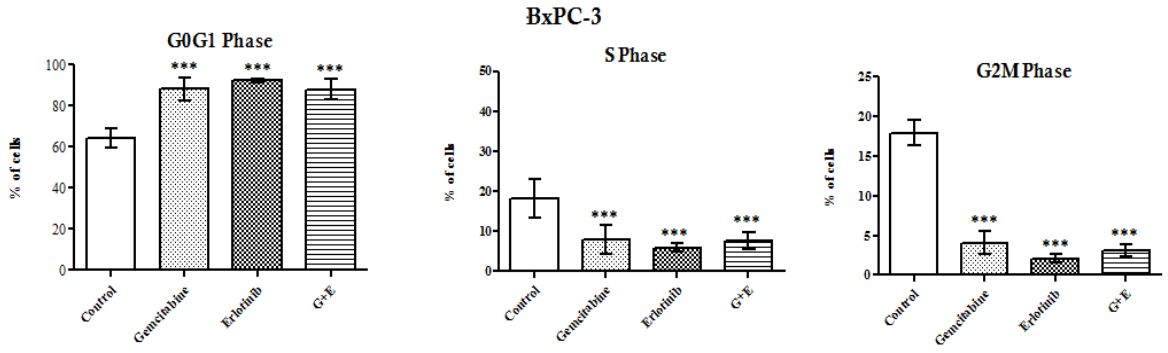

Figure 4.19 GraphPath Prism 5 plots representing the differences in BxPC-3 cell populations in the G0/G1, S and G2/M phases between treatments. ***: P< 0.0001; **: P<0.01; *: P<0.05 (one-way ANOVA).

Results showed that in the BxPC-3 cell line, the Gemcitabine, Erlotinib and combined treatments induced a halt in the cell cycle progression, almost erasing proliferative fractions (S and G2/M) and inducing cells to accumulate in the G0/G1 phase.

4.1.5.2 BrdU incorporation

Flow cytometric analyses of cell DNA content are widely used for the estimation of the cell cycle phase distributions as described before. However, this analysis does not provide cytodynamic information such as cycle traverse rates and phase transit times. The cell cycle frequency histograms provides a static image of the cell population showing only the position of all cells at a given moment, but the proportions of cycling and non-cycling cells within the various phases are not known [322]. These parameters can be obtained determining the fraction of labeled mitosis [323].

The duplication of the entire complement of genetic information in an organism is essential for cell division in living organisms. Initiation of DNA synthesis for cell division is highly regulated in eukaryotic cells where it is confined to the S-phase of the cell cycle. A method to measure de novo DNA synthesis is the analysis of cellular incorporation of bromodeoxyuridine (BrdU), an analog of the DNA precursor thymidine, during S-phase. The incorporated BrdU can be readily detected by anti-BrdU-specific antibodies (that do not recognize thymidine)[324].

In order to complement the cell cycle analyses obtained by flow cytometry, BrdU staining procedures were carried out. Cell proliferation was measured for 24 and 48 h after addition of Gemcitabine and Erlotinib by BrdU incorporation assay.

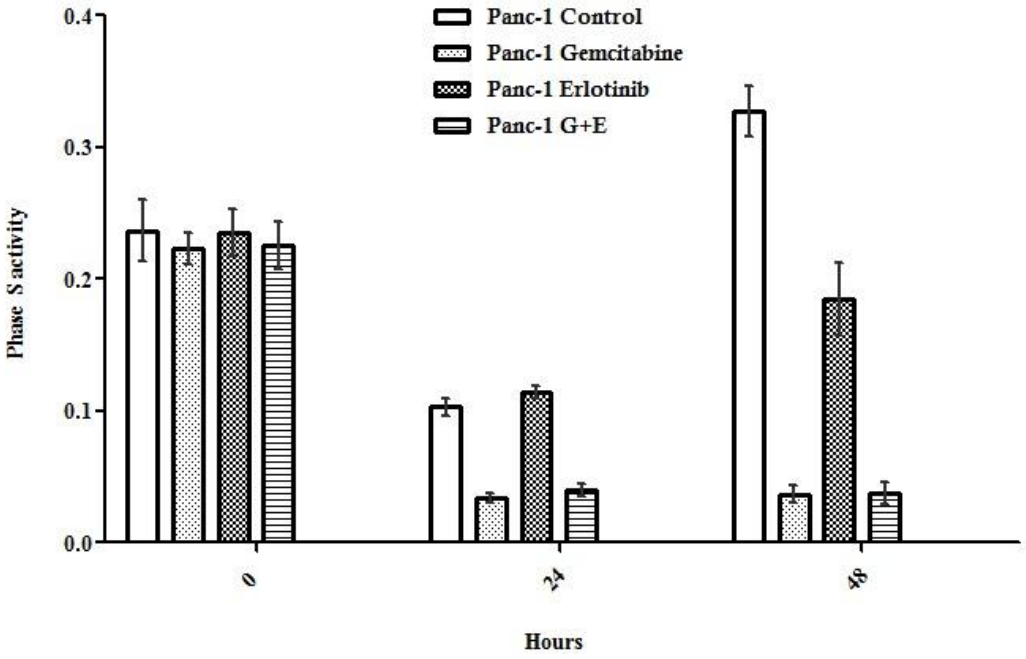

Figure 4.20 The detection of bromodeoxyuridine (BrdU) incorporated into DNA in the Panc-1 cell line. In vitro or in vivo labelling of tumour cells with the thymidine analogue BrdU and the subsequent detection of incorporated BrdU with specific anti-BrdU monoclonal antibodies is an accurate and comprehensive method to quantitate the degree of DNA-synthesis. BrdU is incorporated into the newly synthesized DNA of S-phase cells may provide an estimate for the fraction of cells in S-phase.

As shown in Figure 4.20, after 24h of treatment, the amount of cells in the S-phase was reduced. However, as this reduction was also found in the control samples, this effect should be considered as the normal cycling behavior of the cell cycle. After 48h of treatment, Gemcitabine significantly inhibited Panc-1 cell proliferation, as revealed by inhibition of BrdU incorporation. Similar results were obtained with the combined therapy. After 48h, Erlotinib decreased BrdU incorporation but in a slightly way, resulting in a phase S activity bigger than other treatments but lower than control. Statistically significant changes are shown in Figure 4.21.

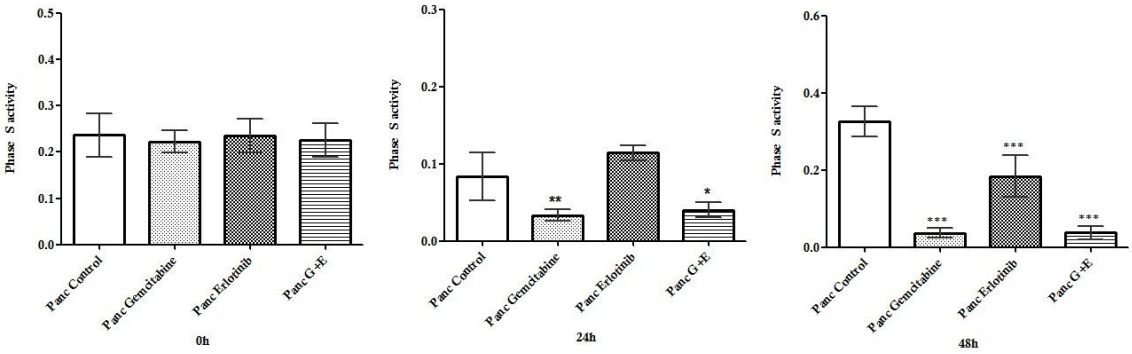

Figure 4.21 Panc-1 cell line GraphPath Prism 5 plots representing the differences in phase S activity between treatments. ***: P< 0.0001; **: P<0.01; *: P<0.05 (one-way ANOVA).

As shown in Figure 4.22, the tendency in BxPC-3 after 24h of treatment to reduce the amount of cells in the S-phase was the same as Panc-1. In the same way, this reduction should be granted as the normal cycling behavior of the cell cycle. After 48h of treatment, cells treated with Gemcitabine, although did not achieve control sample levels of BrdU incorporation, did increase showing that the effect of Gemcitabine on the BxPC-3 cell line proliferation is limited. A bigger effect was obtained with the treatment of Erlotinib and the greatest effect was obtained with the combined therapy, as revealed by the inhibition of BrdU incorporation. Statistically significant changes are shown in Figure 4.23.

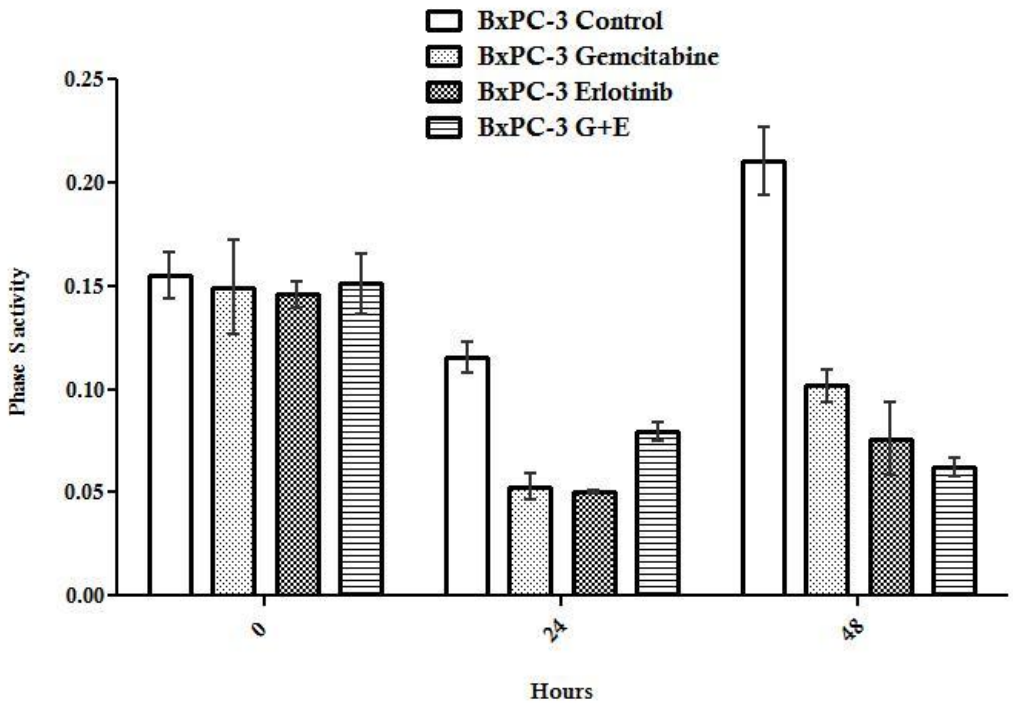

Figure 4.22 The detection of bromodeoxyuridine (BrdU) incorporated into DNA in the BxPC-3 cell line.

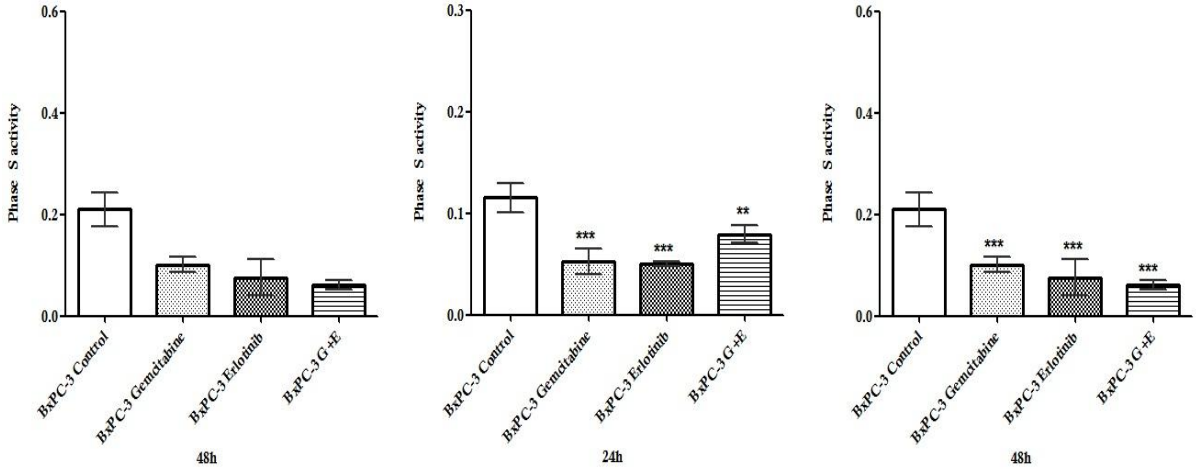

Figure 4.23 Figure 4.8 BxPC-3 cell line GraphPath Prism 5 plots representing the differences in phase S activity between treatments. ***: P< 0.0001; **: P<0.01; *: P<0.05 (one-way ANOVA).

4.1.5.3 Effect of Gemcitabine and Erlotinib on the expression of the p27Kip1 protein as a G0/G1 transition regulator

To determine whether the induced growth inhibition of pancreatic cancer cells was due to the regulation of regulatory molecules, the p27 (*Santa Cruz*, sc-528) protein was examined. p27 negatively regulates the cell cycle. While the p27 protein level is high in early- and mid-G1 to prevent untimed activation of cyclin E/cyclin A-CDK2 to progress into the S-phase, the p27 protein is targeted for degradation at the late G1 or in S-phase through its phosphorylation at threonine 187 (T187) by kinases such as cyclin E/CDK2 or cyclin A/CDK2.

Panc-1 and BxPC-3 cells treated with Gemcitabine (50μM and 20nM), Erlotinib (12.5 μM) or the combination of both agents for 48 h were used to evaluate the effects of the treatments on the p27Kip1 (p27) expression.

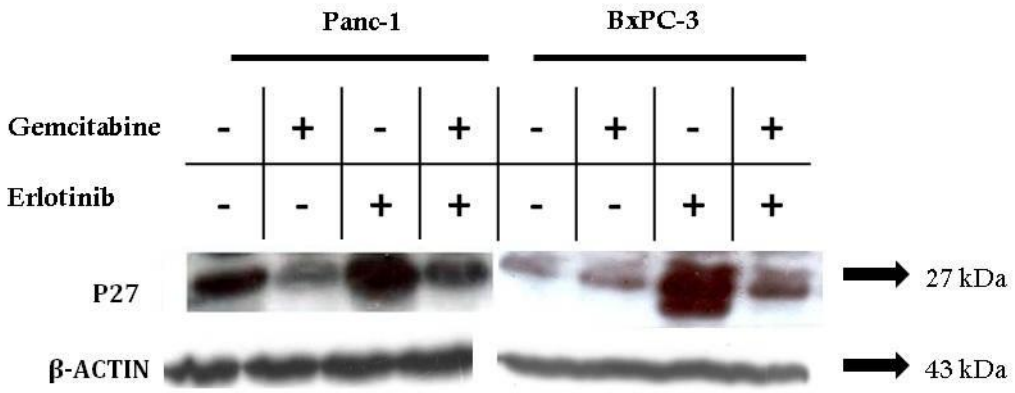

Figure 4.24 Western blots of the p27 expression in the Panc-1 and BxPC-3 cell lines. As detailed in Materials and Methods (section 3.17), the Panc-1 cell line was treated with 50μM of Gemcitabine, 12.5μM of Gemcitabine and/or 1+5μM of Gemcitabine + Erlotinib. The BxPC-3 cell line was incubated in the presence/absence of 0.02μM of Gemcitabine, 12.5μM of Erlotinib and 0.025+5μM of Gemcitabine + Erlotinib respectively. Total cell lysates were prepared and subjected to SDS-PAGE followed by western blot analysis for the protein level of P27Kip1. B-actin was detected as protein loading control. The immunoblots shown here are representative of at least three independent experiments with similar results.

Western blot revealed that the negative regulator of the cell cycle, p27Kip1, is highly induced after the Erlotinib treatment both in the Panc-1 and BxPC-3 cell lines. However the mayor induction was obtained in the BxPC-3 cell line. This result matched those obtained by flow cytometry where we detected a block in the cell cycle in the G0/G1 phase after the Erlotinib treatment. This block was of almost a 92% of the cells in the BxPC-3 cell line treated with Erlotinib whereas it achieved a 74% of the cells in the Panc-1 cell line after that treatment. These halts could be directed by the inhibitory effect of the p27Kip1 protein over the cell cycle progression.

The Gemcitabine treatment as a single agent did not show any significant effect over the p27Kip1 expression in the BxPC-3 cell line. The Gemcitabine and Erlotinib combined therapy slightly induced the p27Kip expression, although it did not reach Erlotinib levels. On the contrary, in the Panc-1 cell line after the Gemcitabine treatment as a single agent, the expression of the p27Kip1 protein was reduced. Note that Gemcitabine acts inhibiting DNA synthesis and potentiates the accumulation of cells in the S-phase. Once again, in the Panc-1 cell line, the Gemcitabine and Erlotinib treatment enhanced the p27Kip1 expression but it did not reach Erlotinib levels.

4.1.5.4 Effect of Gemcitabine and Erlotinib on cell differentiation

The differentiation state of epithelial cells can be characterized by their expression of cytokeratins. Epithelial cells can be characterized by expression of discrete epithelial cell-specific markers, cytokeratins [325-327]. Cytokeratins are intermediate cytoskeleton filaments which serve to provide physical support for the cells.

Panc-1 and BxPC-3 cells treated with Gemcitabine (50μM and 20nM), Erlotinib (12.5 μM) or the combination of both agents for 48 h were used to evaluate the effects of the treatments on cytokeratin 7 (*Santa Cruz*, sc-25721). Besides, we

evaluated the expression pattern of CAII (carbonic anhydrase II, *Santa Cruz*, sc-133110) as a marker for pancreatic ductal differentiation [328].

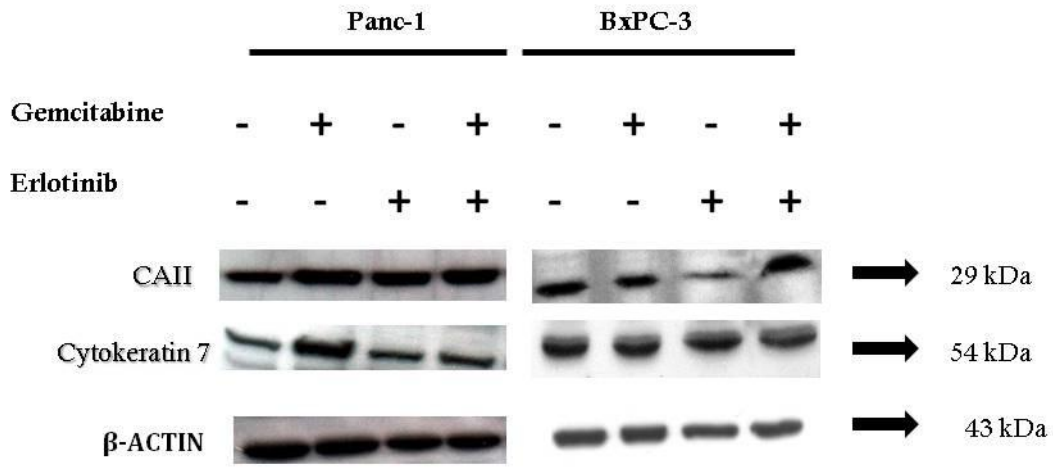

Figure 4.25 Western blots of CAII and Cytokeratin 7 in the Panc-1 and BxPC-3 cell lines. As detailed in Materials and Methods (section 3.17), the Panc-1 cell line was treated with 50μM of Gemcitabine, 12.5μM of Gemcitabine and/or 1+5μM of Gemcitabine + Erlotinib. The BxPC-3 cell line was incubated in the presence/absence of 0.02μM of Gemcitabine, 12.5μM of Erlotinib and 0.025+5μM of Gemcitabine + Erlotinib respectively. Total cell lysates were prepared and subjected to SDS-PAGE followed by western blot analysis for the protein level of CAII and Cytokeratin7. B-actin was detected as protein loading control. The immunoblots shown here are representative of at least three independent experiments with similar results.

Western blot revealed that in the Panc-1 cell line, Gemcitabine as a single agent treatment enhanced the expression of both CAII and Cytokeratin 7. All the other drug combinations failed to show any significant modulation. On the other hand, for the BxPC-3 cell line, the Gemcitabine plus Erlotinib combined therapy significantly enhanced expression of CAII. On the contrary, Erlotinib alone reduced the expression of this marker in BxPC-3. In the case of Cytokeratin 7, no one of the treatments seemed to exert any significant modulation.

4.1.6 RT² Profiler PCR Array

To gain insight into the molecular basis of the Gemcitabine and Erlotinib combined treatment on pancreatic cancer cells we conducted a PCR array of representative genes of the six biological pathways involved in transformation and tumorigenesis. Refer to section 3.15 for further detailed.

The results of the RT² Profiler PCR Array System for the Panc-1 cell line were analyzed according to the six studied biological pathways and results are depicted in figures from Figure 4.26 to Figure 4.31.

Figure 4.26 shows genes related to the apoptosis and cell senescence in the pancreatic cancer cell line Panc-1. As previously shown in Figure 4.3, the Gemcitabine and Erlotinib combined treatment exerted an induction of the apoptosis in the Panc-1 cell line. PCR array results of genes related to apoptosis and cell senescence demonstrated that the Gemcitabine and Erlotinib combined therapy enhanced expression of pro-apoptotic genes such as *Apaf-1*, *Bax*, *Caspase 8*, *Fas*, *DR3* and *DR5*. It is noteworthy that there were also enhanced expression of anti-apoptotic genes such as *Bcl-2* and *Bcl-X_L*. In the same sense as in western analysis, overexpression of Bax tipped the balance in favour of apoptotic procedure.

Tert expression was found to be remarkably upregulated. A correlation between short telomere length and increased mortality was revealed in many studies. *C-Flip*, a key anti-apoptotic regulator that inhibits cell death mediated by the death receptors Fas, DR4, DR5 and TNF-R1, was also found to be enhanced after the Gemcitabine and Erlotinib treatment. Both genes could be relevant in tumour chemoresistance and could represent novel molecular targets to enhance apoptosis in pancreatic cancer cells.

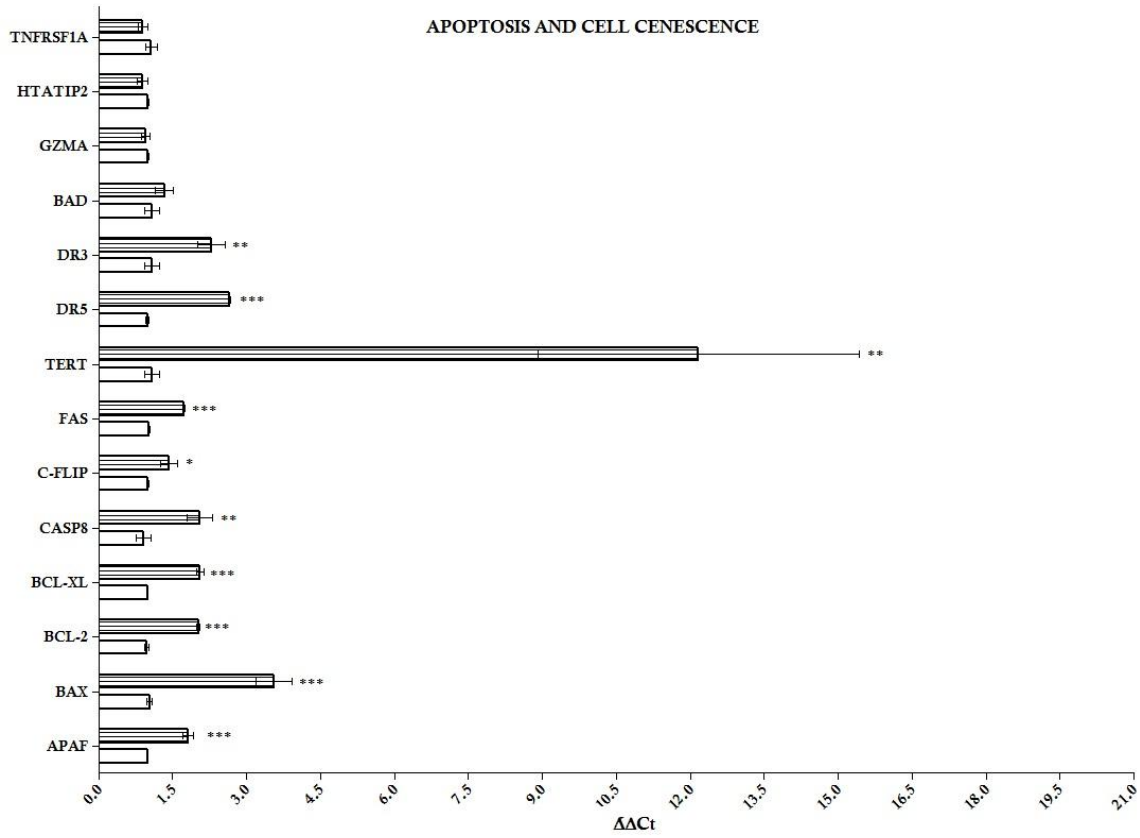

Figure 4.26 Apoptosis and cell senescence related genes whose expression is regulated by the Gemcitabine and Erlotinib treatment in the Panc-1 cell line. Histograms represent mean values for each gene ±SD. Asterisks indicate significant differences from control values (*: P< 0.0001; **: P<0.01; *: P<0.05).**

Regarding genes related to the cell cycle control and DNA damage control, PCR array results of the Panc-1 cell line are depicted in Figure 4.27. It is noteworthy that *E2F1* was overexpressed 60 times. Accordingly, overexpression of genes influenced by *E2F1* was also found (*atm*, *Chk2* and *Rb1*). As the Gemcitabine and Erlotinib combined therapy exerted a block in the G0/G1 phase in the cell cycle, the overexpression of G1/S transition genes must be related to the E2F1-induced apoptosis.

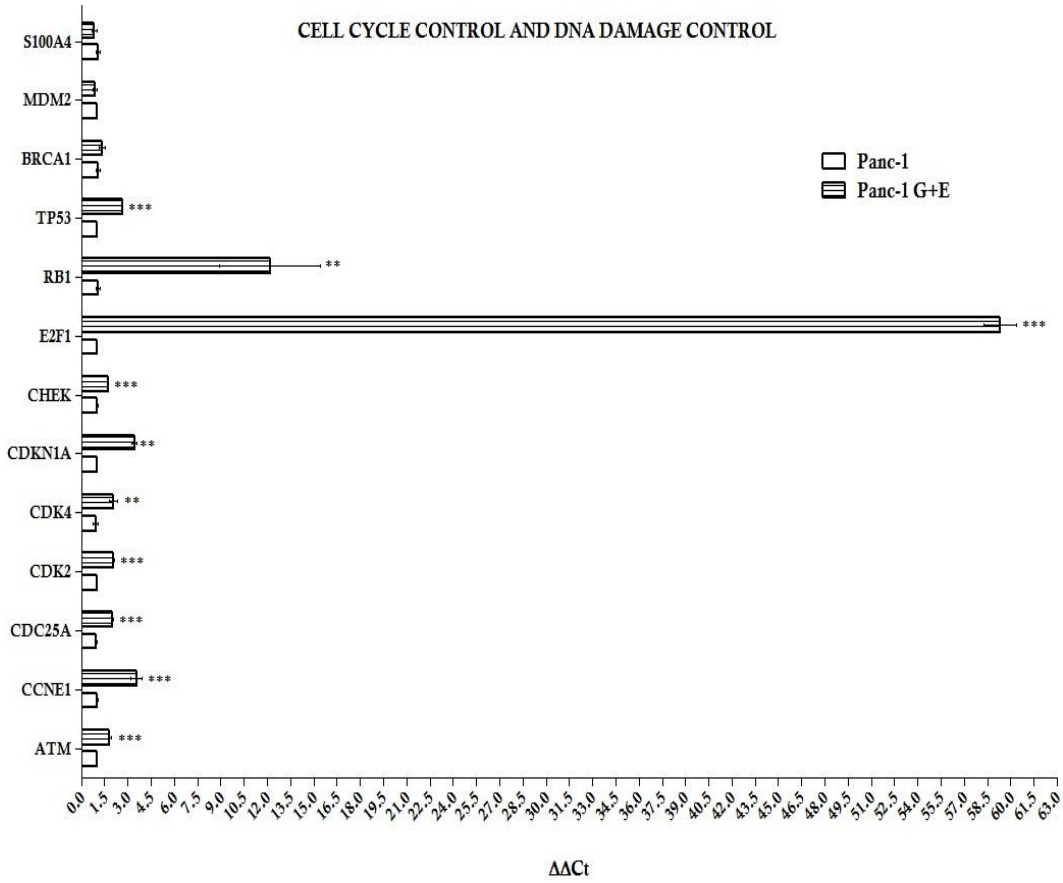

Figure 4.27 Cell cycle control and DNA damage repair related genes whose expression is regulated by the Gemcitabine and Erlotinib treatment in the Panc-1 cell line. Histograms represent mean values for each gene ±SD. Asterisks indicate significant differences from control values (*: P< 0.0001; **: P<0.01; *: P<0.05).**

Regarding genes related to signal transduction and transcription factors, PCR array results of the Panc-1 cell line are depicted in Figure 4.28.

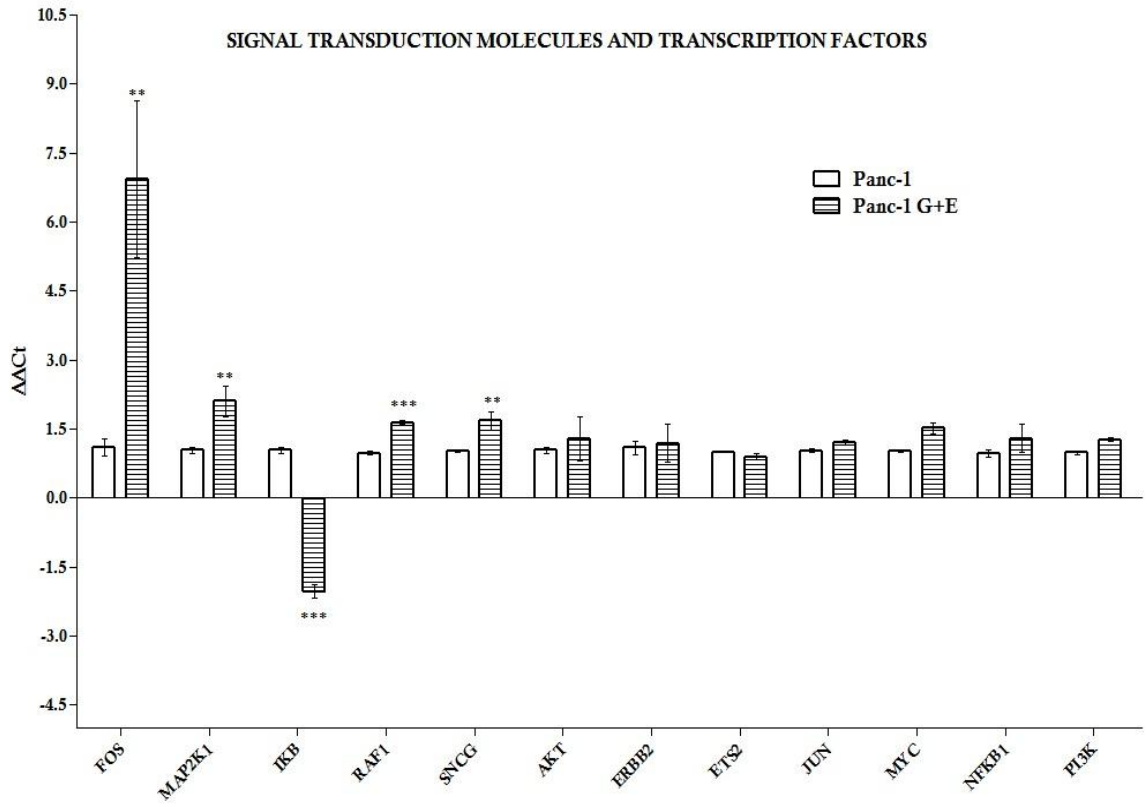

Figure 4.28 Signal transduction molecules and transcription factors related genes whose expression is regulated by the Gemcitabine and Erlotinib treatment in the Panc-1 cell line. Histograms represent mean values for each gene ±SD. Asterisks indicate significant differences from control values (*: P< 0.0001; **: P<0.01; *: P<0.05).**

After the Gemcitabine plus Erlotinib combined treatment, an induction in the expression of *Fos*, *Map2k1*, *Raf1* and *sncg* were determined. Abnormal activation of Raf pathway occurs in human cancer due to mutations at Ras which serves to regulate Raf activity. SNCG has been shown to be involved in tumorigenesis and metastasis of a wide range of malignancies. Besides, the Gemcitabine and Erlotinib combined treatment induced the expression of the genes *c-fos* and *Map2K1* (*MEK1*), both components of signalling pathways leading to proliferation and induction of metastasis.

IκB-α expression was found to be repressed after the combined treatment in the Panc-1 cell line although the NF-κB failed to show any significant modulation.

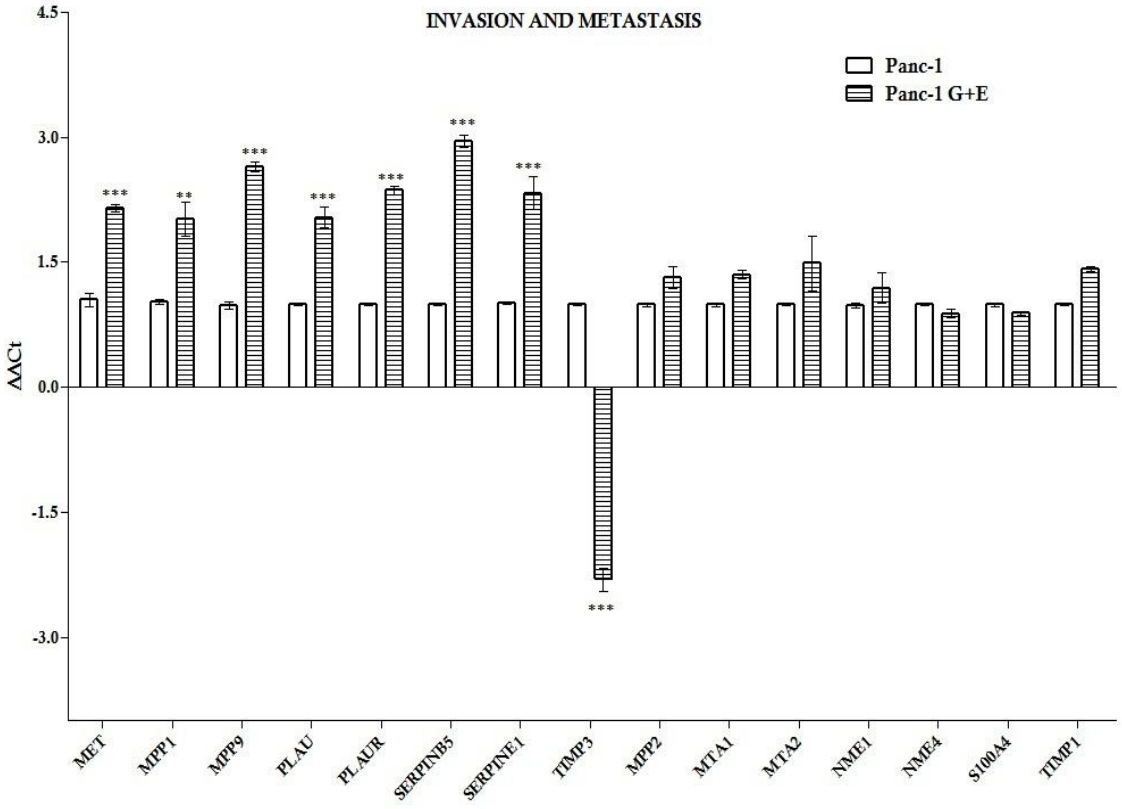

Figure 4.29 Invasion and metastasis related genes whose expression is regulated by the Gemcitabine and Erlotinib treatment in the Panc-1 cell line. Histograms represent mean values for each gene ±SD. Asterisks indicate significant differences from control values (*: P< 0.0001; **: P<0.01; *: P<0.05).**

Regarding genes related to invasion and metastasis, PCR array results of the Panc-1 cell line are depicted in Figure 4.29. After the Gemcitabine and Erlotinib combined therapy, there was a general induction of the genes related to invasion and metastasis as matrix metalloproteases or the Plau/PlauR system. Concomitantly, there was a significant repression of *Timp3*, tissue inhibitor of metalloproteinases-3, which inhibits MMPs.

Regarding genes related to adhesion molecules, PCR array results of the Panc-1 cell line are depicted in Figure 4.30.

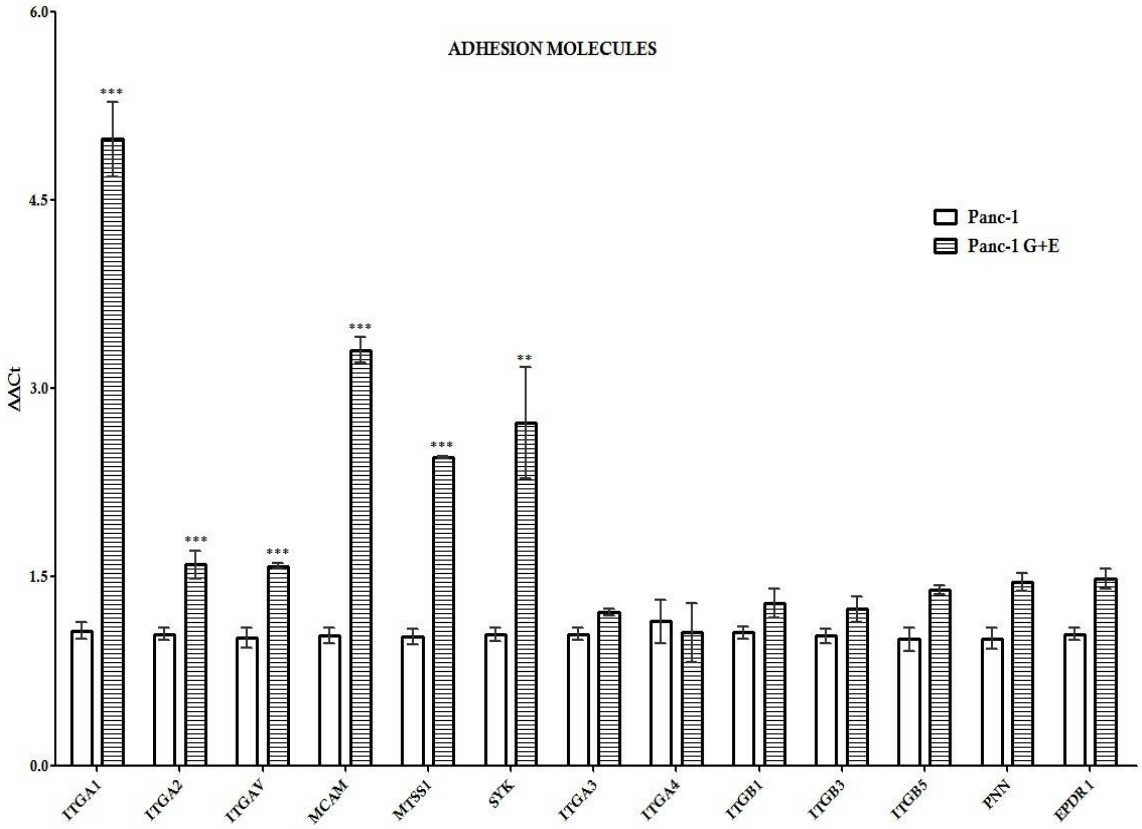

Figure 4.30 Adhesion related genes whose expression is regulated by the Gemcitabine and Erlotinib treatment in the Panc-1 cell line. Histograms represent mean values for each gene ±SD. Asterisks indicate significant differences from control values (*: P< 0.0001; **: P<0.01; *: P<0.05).**

Several molecules that are crucial for cell adhesion, cell signalling, cell viability and motility were found to be enhanced after the combined treatment in the Panc-1 cell line.

Lastly, those genes related to angiogenesis are depicted in Figure 4.31. Once again, it seemed that the Gemcitabine plus Erlotinib treatment enhanced genes related to the angiogenesis in the Panc-1 cell line.

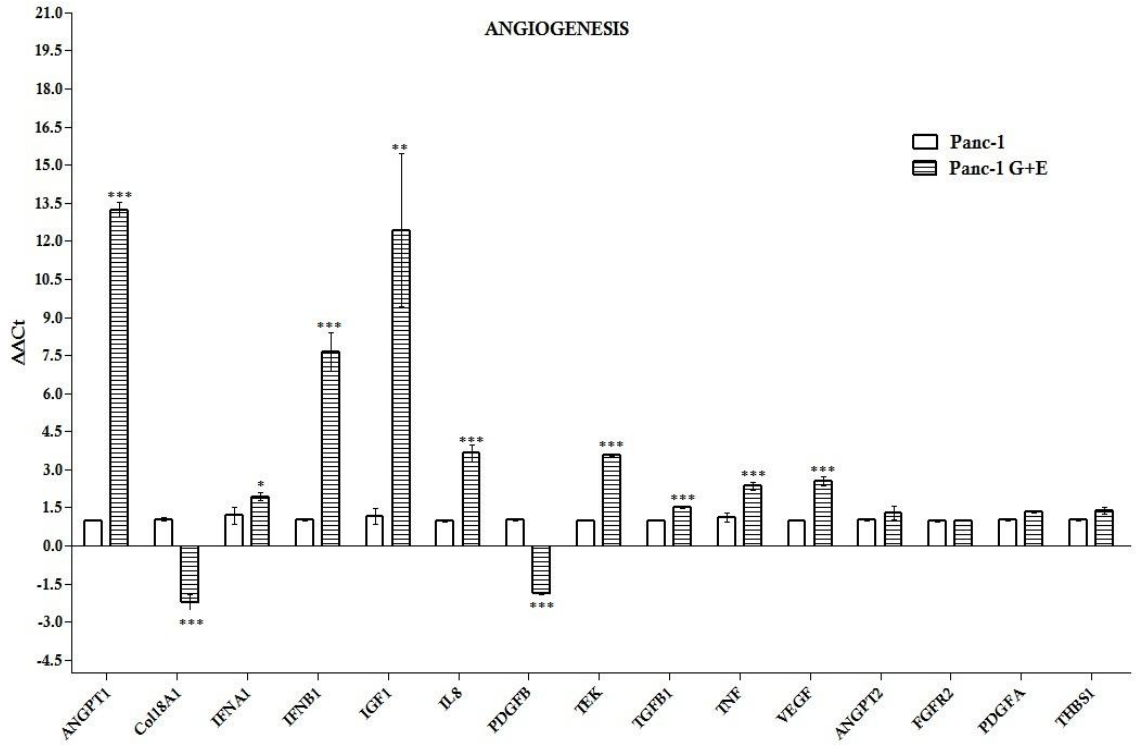

Figure 4.31 Angiogenesis related genes whose expression is regulated by the Gemcitabine and Erlotinib treatment in the Panc-1 cell line. Histograms represent mean values for each gene ±SD. Asterisks indicate significant differences from control values (*: P< 0.0001; **: P<0.01; *: P<0.05).**

In essence, Gemcitabine plus Erlotinib in the pancreatic cancer cell line Panc-1 induced the genetic expression of genes related to apoptosis (which were also observed by Annexin-V and western blot analysis) and also induced E2F1 and related molecules expression. These effects resulted, in turn, also in the apoptotic process as we have previously reported a block in the G0/G1 phase after incubation with the combined treatment. However, our results showed that independently of this induction of apoptosis, the Gemcitabine plus Erlotinib treatment enhanced transcription factors and signalling pathways that finally led to induction of invasion and metastasis. This could be related to the scarce effect of this therapy and to the observed chemoresistance.

The results of the RT^2 Profiler PCR Array System for the BxPC-3 cell line were analyzed according to the six studied biological pathways and results are depicted in figures from Figure 4.32 to Figure 4.37.

Figure 4.32 shows genes related to the apoptosis and cell senescence in the pancreatic cancer cell line BxPC-3. As previously shown in Figure 4.6, the Gemcitabine and Erlotinib combined treatment exerted an induction of the apoptosis in the BxPC-3 cell line, although this effect was only slightly moderate. In this sense, PCR arrays of genes related to apoptosis only exhibited effect over 6 genes, compared with the 10 genes previously described in the Panc-1 cell line. *Bax*, *BCL-2* and *DR5* showed similar tendency in both cell lines although *Bax* expression did not achieve the same levels as in the Panc-1 cell line. The *htatip2* gene was found enhanced after the Gemcitabine and Erlotinib treatment. *Htatip2* is a putative tumour suppressor gene that promotes apoptosis and inhibits angiogenesis.

On the contrary of what was found in the Panc-1 cell line, *Tert* gene was down regulated in the BxPC-3 cell line.

PCR array results demonstrated that for the BxPC-3 cell line, although there was an induction of apoptosis, it did not achieve the Panc-1 cell line levels, as it shown by the limited effect of the treatment over apoptotic genes.

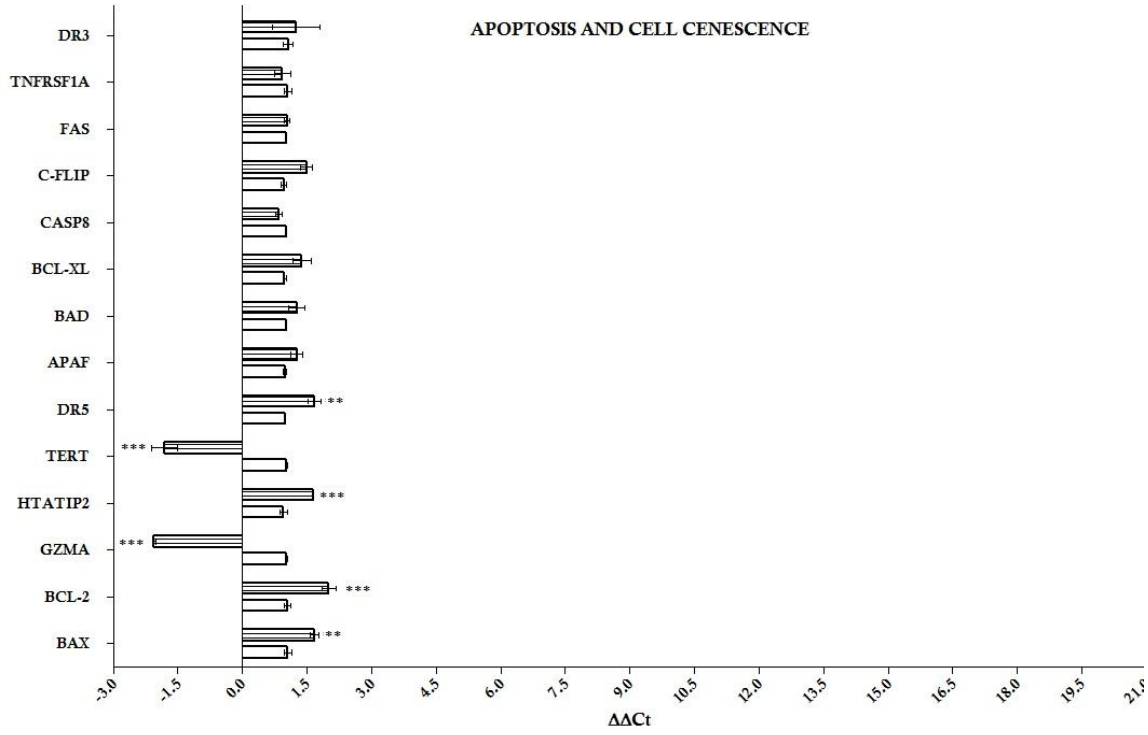

Figure 4.32 Apoptosis and cell senescence related genes whose expression is regulated by the Gemcitabine and Erlotinib treatment in the BxPC-3 cell line. Histograms represent mean values for each gene ±SD. Asterisks indicate significant differences from control values (*: P< 0.0001; **: P<0.01; *: P<0.05).**

Figure 4.33 shows genes related to the apoptosis and cell senescence in the pancreatic cancer cell line BxPC-3. On the contrary of what we obtained in the Panc-1 cell line, genes related to G1/S transition were found to be repressed in the BxPC-3 cell line after the Gemcitabine and Erlotinib combined treatment. Once again, Gemcitabine and Erlotinib seemed to exert its antiproliferative effects by inhibiting the cell cycle progression rather than inducing apoptosis.

Anti-apoptotic protein S100A4, which has multiple functions in the S-phase progression, was significantly down regulated after the Gemcitabine and Erlotinib combined treatment in the BxPC-3 cell line. It has also been linked to migratory and invasive properties in several solid tumours, including prostate cancer, breast cancer and gastric cancer. This role will be discussed below.

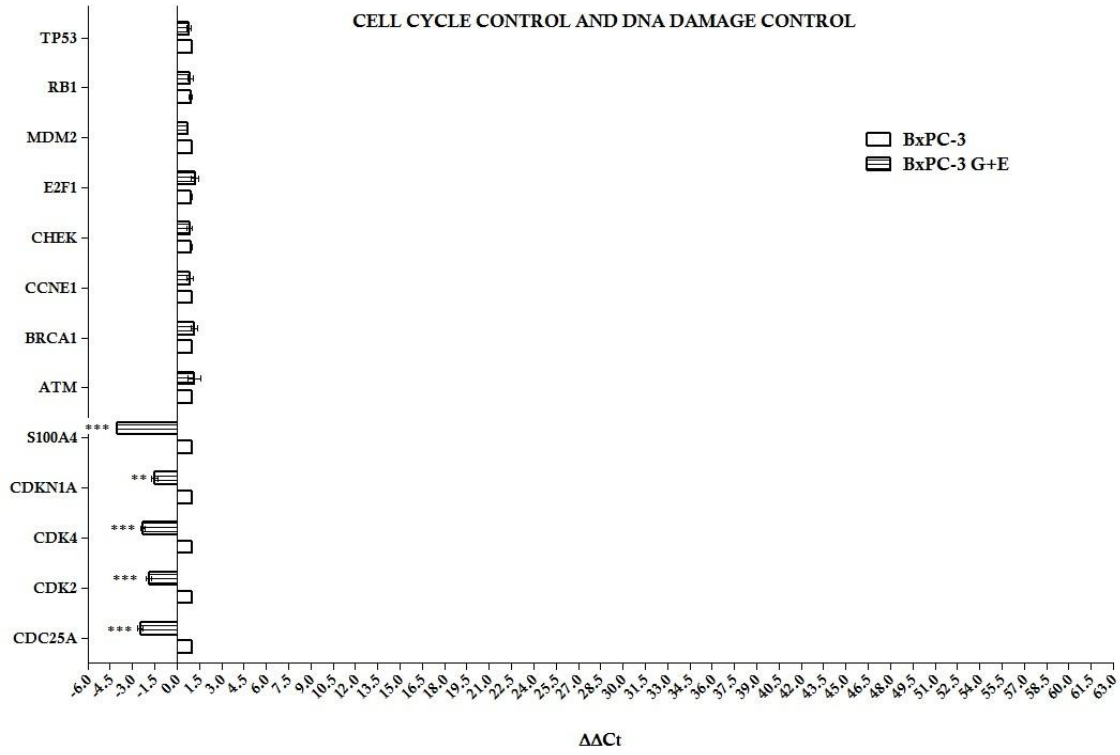

Figure 4.33 Cell cycle control and DNA damage repair related genes whose expression is regulated by the Gemcitabine and Erlotinib treatment in the BxPC-3 cell line. Histograms represent mean values for each gene ±SD. Asterisks indicate significant differences from control values (*: P< 0.0001; **: P<0.01; *: P<0.05).**

Regarding genes related to signal transduction and transcription factors, PCR array results of the BxPC-3 cell line are depicted in Figure 4.34. On the contrary of what was obtained in the Panc-1 cell line, a remarkable repression was obtained in the genes *Fos*, *Map2K1* and also in *PI3K*. This could be related to the *k-ras* wild type genotype of the BxPC-3 cell line which would imply that Erlotinib was indeed blocking downstream signalling pathways of Ras.

IκB-α expression was found to be overexpressed after the combined treatment in the BxPC-3 cell line although NF-κB, in the same way as in the Panc-1 cell line, failed to show any significant modulation.

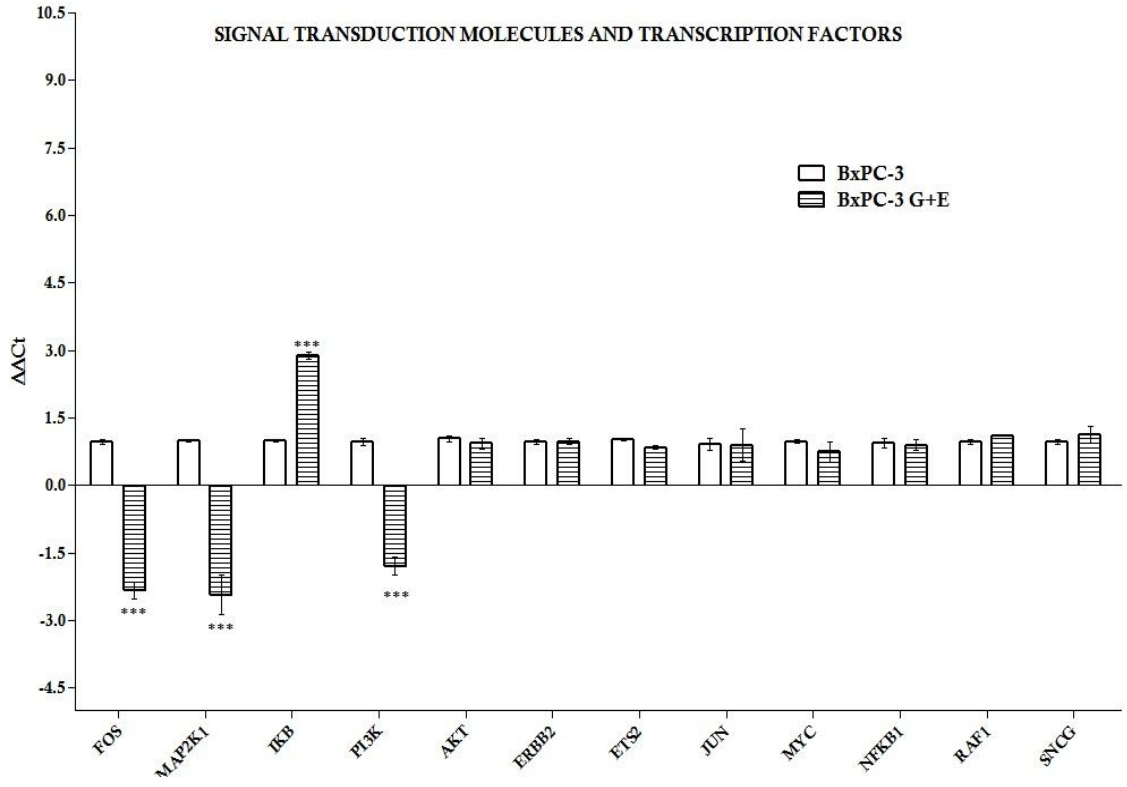

Figure 4.34 Signal transduction molecules and transcription factors related genes whose expression is regulated by the Gemcitabine and Erlotinib treatment in the BxPC-3 cell line. Histograms represent mean values for each gene ±SD. Asterisks indicate significant differences from control values (*: P< 0.0001; **: P<0.01; *: P<0.05).**

Regarding genes related to invasion and metastasis, PCR array results of the BxPC-3 cell line are depicted in Figure 4.35. After Gemcitabine plus Erlotinib combined therapy, there was a general remarkable repression of genes related to invasion and metastasis as matrix metalloproteases or the Plau/PlauR system. Here is again represented S100A4 as it has a role in invasion. Concomitantly, there was a significant enhancement of *Timp1 and Timp3* which inhibit MMPs.

Serpine1 or plasminogen activator inhibitor-1 (PAI-1), which is important for tumour growth, invasion and metastasis, was also found to be repressed.

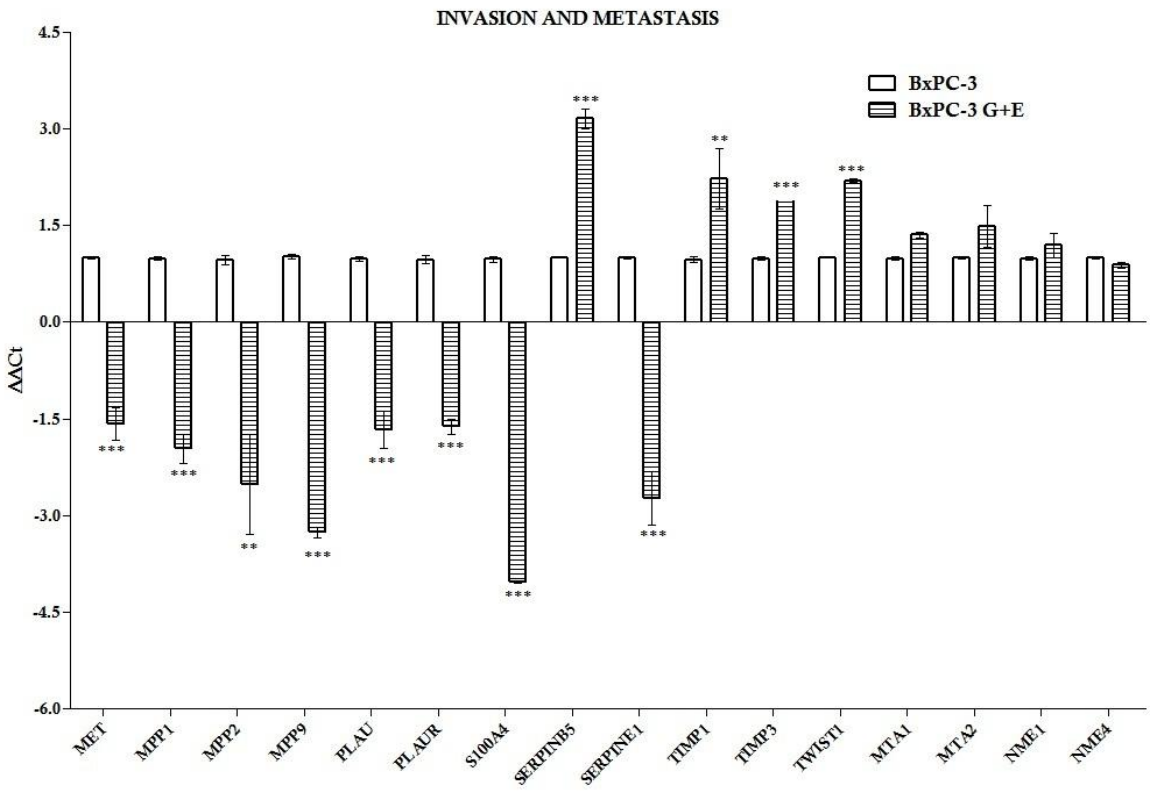

Figure 4.35 Invasion and metastasis related genes whose expression is regulated by the Gemcitabine and Erlotinib treatment in the BxPC-3 cell line. Histograms represent mean values for each gene ±SD. Asterisks indicate significant differences from control values (*: P< 0.0001; **: P<0.01; *: P<0.05).**

Regarding genes related to adhesion molecules, PCR array results of the Panc-1 cell line are depicted in Figure 4.36. Our results failed to show any significant modulation in any of these genes. This could be explained as invasion and metastasis is in general repressed in the BxPC-3 cell line after the Gemcitabine and Erlotinib treatment.

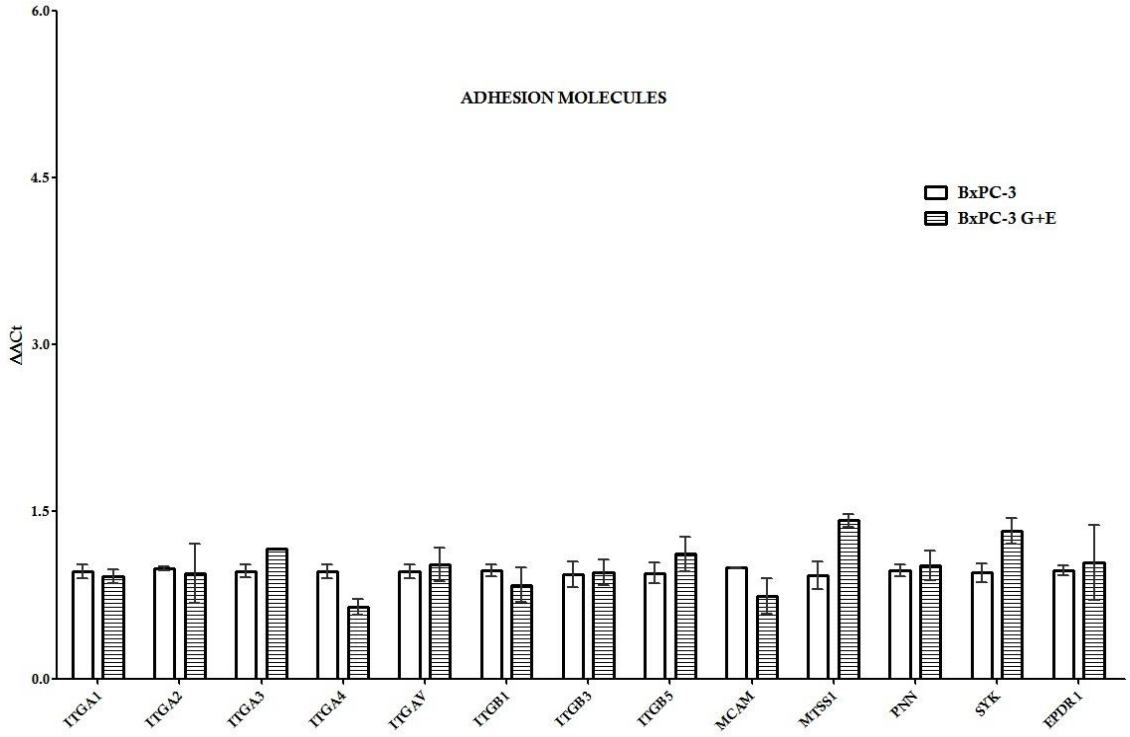

Figure 4.36 Adhesion related genes whose expression is regulated by the Gemcitabine and Erlotinib treatment in the BxPC-3 cell line. Histograms represent mean values for each gene ±SD. Asterisks indicate significant differences from control values (*: P< 0.0001; **: P<0.01; *: P<0.05).**

Those genes related to angiogenesis are depicted in Figure 4.37. The majority of the genes did not show any significant modulation after the Gemcitabine plus Erlotinib treatment and those which did, resulted in a downregulation of their expression. Only IFNA1 appeared overexpressed in BxPC-3 after the combined treatment.

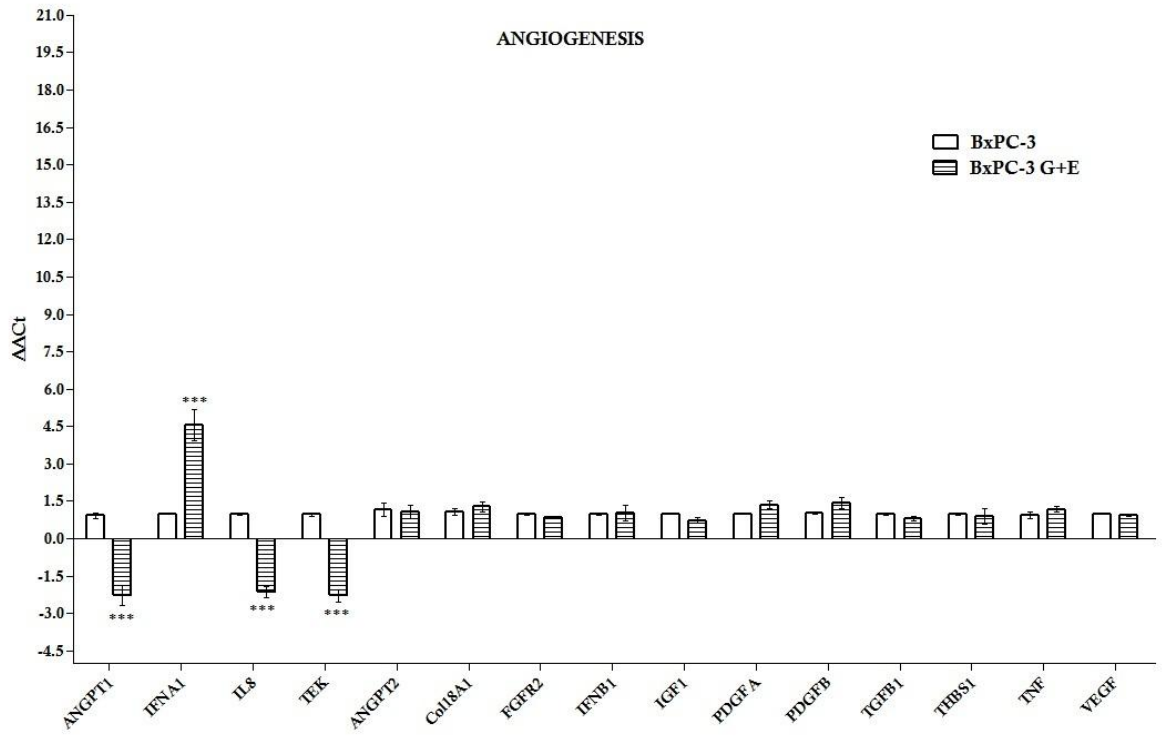

Figure 4.37 Angiogenesis related genes whose expression is regulated by the Gemcitabine and Erlotinib treatment in the BxPC-3 cell line. Histograms represent mean values for each gene ±SD. Asterisks indicate significant differences from control values (*: P< 0.0001; **: P<0.01; *: P<0.05).**

In essence, Gemcitabine plus Erlotinib in the pancreatic cancer cell line BxPC-3 induced the genetic expression of some genes related to apoptosis although the major effect described was the block in the G0/G1 phase after incubation with the combined treatment. Our results showed that the most important effect of Gemcitabine and Erlotinib on the BxPC-3 cell line was the inhibition of transcription factors and signalling pathways that finally lead to induction of invasion and metastasis. The combination of drugs would be effective blocking invasion and metastasis in *k-ras* wild type genotype as these effects were only obtained in the BxPC-3 cell line but not in the Panc-1 cell line.

In order to highlight the similarities and differences of responses between the two cell lines, all genes of the six studied biological pathways were compared. Table 4-9 to Table 4-14 summarized them.

Table 4-9 ***Comparison between apoptosis related genes in the Panc-1 and BxPC-3 cell lines after treatment with G+E.***

Gene	*Panc-1*		*BxPC-3*	
	Fold change	*p-value*	*Fold change*	*p-value*
APAF1	1.813	0.0002	1.26	ns
BAD	1.339	ns	1.26	ns
BAX	3.555	0.0003	1.67	0.0013
BCL2	2.021	< 0.0001	2.00	0.0007
BCL-X_L	2.057	< 0.0001	1.38	ns
CASP8	2.048	0.0029	0.85	ns
C-Flip	1.431	0.013	1.49	ns
FAS	1.729	< 0.0001	1.04	ns
GZMA	0.953	ns	-2.06	< 0.0001
HTATIP2	0.881	ns	1.64	0.0002
TERT	12.167	0.0042	-1.82	< 0.0001
TNFRSF1A	0.831	ns	0.93	ns
DR5	2.657	< 0.0001	1.67	0.0014
DR3	2.290	0.0029	1.25	ns

Table 4-10 ***Comparison between cell cycle and DNA damage repair related genes in the Panc-1 and BxPC-3 cell lines after treatment with G+E.***

Gene	*Panc-1*		*BxPC-3*	
	Fold change	*p-value*	*Fold change*	*p-value*
ATM	1.813	0.0002	1.16	ns
BRCA1	1.34	ns	1.16	ns
Cyclin E1	3.553	0.0003	0.8567	ns
CDC25A	2.023	< 0.0001	-2.475	< 0.0001
CDK2	2.06	< 0.0001	-1.892	< 0.0001
CDK4	2.05	0.0029	-2.292	< 0.0001
P21	3.43	0.0018	-1.519	0.002
CHEK2	1.73	< 0.0001	0.8567	ns
E2F1	59.31	< 0.0001	1.223	ns
MDM2	0.8833	ns	0.7133	ns
RB1	12.17	0.0042	0.8967	ns
S100A4	0.83	ns	-4.042	< 0.0001
TP53 (p53)	2.66	< 0.0001	0.7733	ns

Table 4-11 ***Comparison between transcription factor and signal transduction related genes in the Panc-1 and BxPC-3 cell lines after treatment with G+E.***

Gene	*Panc-1*		*BxPC-3*	
	Fold change	*p-value*	*Fold change*	*p-value*
AKT1	1.29	ns	0.93	ns
ERBB2	1.187	ns	0.9767	ns
ETS2	0.89	ns	0.84	ns
FOS	6.927	0.0041	-2.326	< 0.0001
JUN	1.2	ns	0.8967	ns
MAP2K1 (MEK)	2.097	0.0051	-2.435	0.0002
MYC	1.51	ns	0.74	ns
NFκB	1.29	ns	0.8967	ns
IκBα	-2,027164	0.0003	2.88	< 0.0001
PI3K p85α	1.26	ns	-1.796	< 0.0001
RAF1	1.64	< 0.0001	1.103	ns
SNCG	1.68	0.0049	1.12	ns

Table 4-12 ***Comparison between invasion related genes in the Panc-1 and BxPC-3 cell lines after treatment with G+E.***

Gene	*Panc-1*		*BxPC-3*	
	Fold change	*p-value*	*Fold change*	*p-value*
MET	2.15	< 0.0001	-1.578	< 0.0001
MMP1	2.02	0.0011	-1.968	< 0.0001
MMP2	1.317	ns	-2,52	0.0015
MMP9	2.647	< 0.0001	-3.261	< 0.0001
MTA1	1.35	ns	0.9133	ns
MTA2	1.483	ns	0.93	ns
NME1	1.19	ns	0.7267	ns
NME4	0.8833	ns	1.19	ns
PLAU	2.037	0.0001	-1.676	< 0.0001
PLAUR	2.36	< 0.0001	-1.622	< 0.0001
S100A4	0.8867	ns	-4.042	< 0.0001
SERPINB5	2.95	< 0.0001	3.153	< 0.0001
SERPINE1 (PAI1)	2.327	0,0003	-2.734	0.0001
TIMP1	1.447	ns	2.23	0.0096
TIMP3	-2.313	< 0.0001	1.94	< 0.0001
TWIST1	0.97	ns	2.197	< 0.0001

Table 4-13 ***Comparison between adhesion related genes in the Panc-1 and BxPC-3 cell lines after treatment with G+E.***

Gene	*Panc-1*		*BxPC-3*	
	Fold change	*p-value*	*Fold change*	*p-value*
ITGA1	4.983	< 0.0001	0.92	ns
ITGA2	1.6	0.0008	0.9433	ns
ITGA3	1.22	ns	1.17	ns
ITGA4	1.057	ns	0.6467	ns
ITGAV	1.587	< 0.0001	1.027	ns
ITGB1	1.293	ns	0.84	ns
ITGB3	1.243	ns	0.9533	ns
ITGB5	1.393	ns	1.12	ns
MCAM	3.307	< 0.0001	0.7433	ns
MTSS1	2.453	< 0.0001	1.42	ns
PNN	1.46	ns	1.017	ns
SYK	2.727	0.0026	1.327	ns

Table 4-14 ***Comparison between angiogenesis related genes in the Panc-1 and BxPC-3 cell lines after treatment with G+E.***

Gene	*Panc-1*		*BxPC-3*	
	Fold change	*p-value*	*Fold change*	*p-value*
ANGPT1	13.24	< 0.0001	-2.268	0.0002
ANGPT2	1.313	ns	1.057	ns
COL18A1	-2.231	< 0.0001	1.283	ns
FGFR2	1	ns	0.85	ns
IFNA1 (IFNα)	1.943	0.0222	4.547	0.0006
IFNB1 (IFNβ)	7.643	0.0001	1.043	ns
IGF1	12.44	0.003	0.7233	ns
IL8	3.653	0.0002	-2.152	< 0.0001
PDGFA	1.34	ns	1.363	ns
PDGFB	-1.876	< 0.0001	1.433	ns
TEK (tie-2).	3.57	< 0.0001	-2.294	< 0.0001
TGFB1	1.527	< 0.0001	0.8033	ns
THBS1 (thrombospondin)	1.393	ns	0.9	ns
TNF	2.353	0,0009	1.183	ns
VEGFA	2.55	< 0.0001	0.94	ns

4.1.7 Effect of the Gemcitabine/Erlotinib treatment over NF-κB activation

NF-κB is a family of transcription factors with well known roles in immunity and inflammation[329]. Abnormal constitutive NF-κB activation has been linked to oncogenic growth/survival of many cancer types [330] including pancreatic ductal adenocarcinoma [84-85, 331]. Here we studied the role of NF-κB in pancreatic cancer cells response to chemotherapy with a double approach. First, we analyzed the protein expression of some of the NF-κB family members. Secondly, to analyze the mechanisms regulating transcription of NF-κB–responsive genes in Panc-1 and BxPC-3 cells, we used chromatin immunoprecipitation (ChIP) assay to measure the *"in vivo"* recruitment of the NF-κB p65 subunit to promoters of the Bcl-2, Bcl-X_L, MMP-9 and IκB-α genes.

4.1.7.1 Gemcitabine and Gemcitabine plus Erlotinib combined therapy abrogated IκB-α expression; Erlotinib induced IκB-α expression and the inactivation of NF-κB.

The basic scheme of the NF-κB signalling consists of a series of positive and negative regulatory elements. Inducing stimuli trigger IKK activation leading to phosphorylation, ubiquitination and degradation of the IκB-α protein. Released NF-κB dimers are further activated through various posttranslational modifications and translocate to the nucleus where they bind to specific DNA sequences and promote transcription of target genes. In its most basic form, therefore, the pathway consists of receptor and receptor proximal signalling adaptor molecules; the IKK complex; IκB-α proteins and NF-κB dimmers [92].

To evaluate whether Gemcitabine and/or Erlotinib could modulate NF-κB signalling components, NF-κB, IκB-α, p-IκB-α, IKK and p-IKK were determined by western blot analysis after each treatment for 48 h in vitro in the Panc-1(Figure 4.38) and BxPC-3 (Figure 4.39) cell lines.

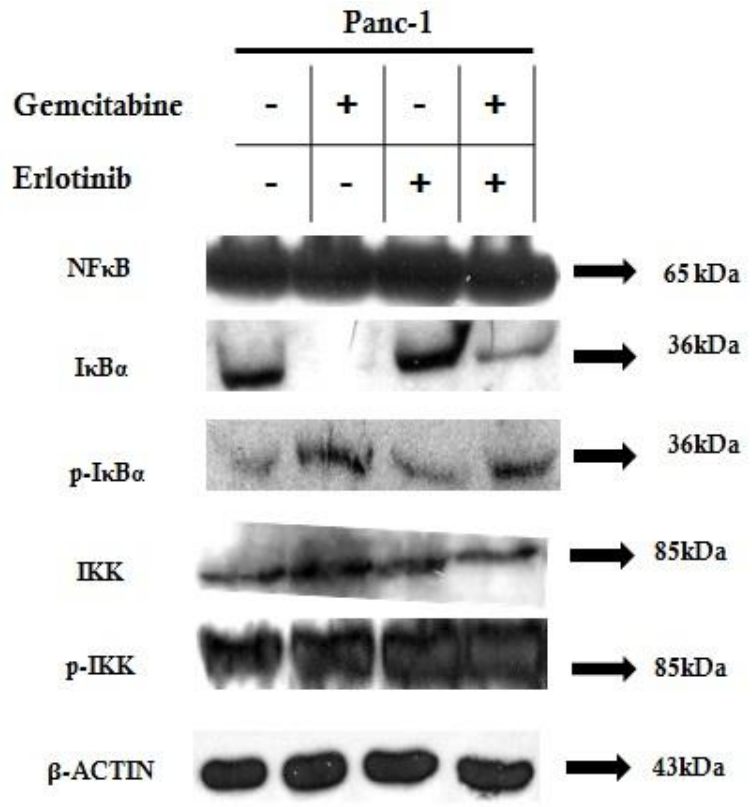

Figure 4.38 Effect of Gemcitabine, Erlotinib and Gemcitabine plus Erlotinib combined therapy on NF-κB signalling components in the Panc-1 cell line. As detailed in Materials and Methods (section 3.17), the Panc-1 cell line was incubated 48h in the presence/absence of 50μM of Gemcitabine, 12.5μM of Gemcitabine and/or 1+5μM of Gemcitabine + Erlotinib. Total cell lysates were prepared and subjected to SDS-PAGE followed by western blot analysis for the protein level of NF-κB, IκB-α, p-IκB-α, IKK and p-IKK. B-actin was detected as protein loading control. The immunoblots shown here are representative of at least three independent experiments with similar results.

Our results demonstrated that in the Panc-1 cell line the mayor modulation in NF-κB signalling components affected IκB-α. As described in section 1.3.5.2, NF-κB is anchored in the cytoplasm by IκB-α. In this state, NF-κB is inhibited and it cannot translocate to the nucleus to induce the expression of its target genes. Our results showed that, although p65 seemed to be equally expressed regardless the treatment, the expression of the inhibitor was markedly altered. Not only Gemcitabine as a single agent did abrogate IκB-α expression but it also induced its phosphorylation. In consequence, the minimal amount of inhibitor that was

present in the Panc-1 cell line after the Gemcitabine treatment was phosphorylated and so, marked to be proteolytically degraded. This implied that NF-κB was free and active to induce the expression of its target genes. Similar results but in a lesser level were obtained by the Gemcitabine and Erlotinib combined therapy. In Panc-1 cells treated with Erlotinib as a single agent, an induction in the IκB-α expression was detected. This was followed by a limited augmentation of its phosphorylation when compared with the Gemcitabine treatment so NF-κB is retained in the cytoplasm by IκB-α and, as a consequence, there would be lower expression of its target genes.

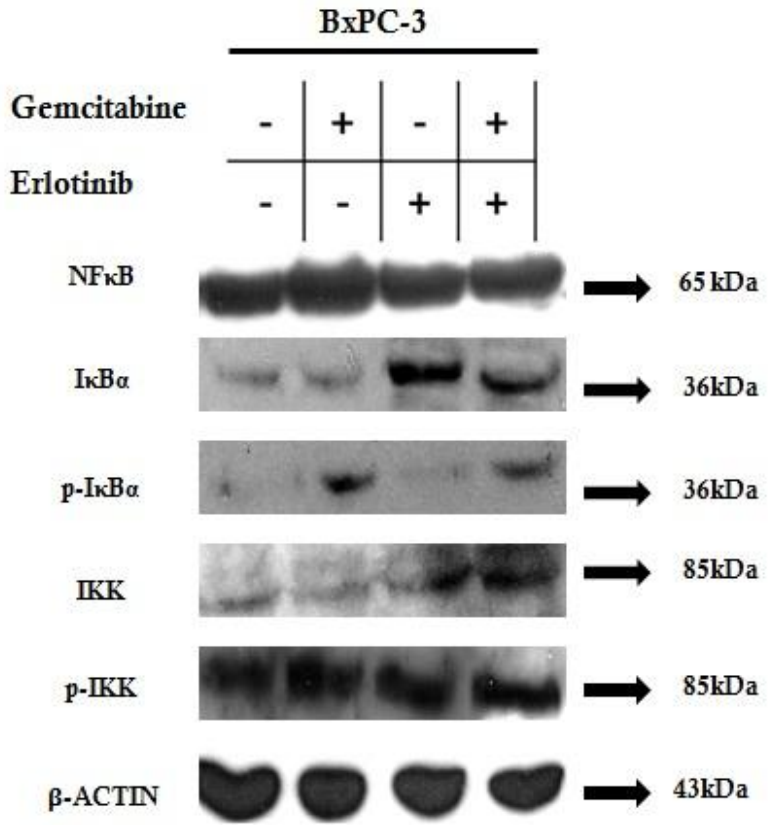

Figure 4.39 Effect of Gemcitabine, Erlotinib and Gemcitabine plus Erlotinib combined therapy on NF-κB signalling components in the BxPC-3 cell line. As detailed in Materials and Methods (section 3.17), the BxPC-3 cell line was incubated in the presence/absence of 0.02μM of Gemcitabine, 12.5μM of Erlotinib and 0.025+5μM of Gemcitabine+Erlotinib respectively. Total cell lysates were prepared and subjected to SDS-PAGE followed by western blot analysis for the protein level of NF-κB, IκBα, p-IκBα, IKK and p-IKK. B-actin was detected as protein loading control. The immunoblots shown here are representative of at least three independent experiments with similar results.

For the BxPC-3 cell line, Erlotinib as a single agent provoked an induction in IκB-α expression. This was not followed by an increase in IκB-α phosphorylation. In BxPC-3, all IκB-α present was active and joined to NF-κB. In this sense, an inhibition of the translocation of NF-κB to the nucleus was obtained and, as a consequence, there would be lower expression of its target genes. Erlotinib as a single agent induced apoptosis in the BxPC-3 cell line with a reduction of Bcl-2 expression. Bcl-2 is a NF-κB target gene and the effect of Erlotinib over NF-κB signalling pathway could be responsible of the apoptotic induction.

A comparison of relative expression of proteins implicated in NFκB signalling pathway is shown in Table 4-15.

Table 4-15 NF-κB protein family member expression after Gemcitabine, Erlotinib and Gemcitabine plus Erlotinib combined therapy in the pancreatic cancer cell lines Panc-1 and BxPC-3.

	PANC-1			BxPC-3		
	Gemcitabine	Erlotinib	Gem+Erl	Gemcitabine	Erlotinib	Gem+Erl
NF-κB	0.95±0.02	0.98±0.001	0.99±0.04	1.27±0.002	0.94±0.015	1.01±0.002
IκBα	0.2±0.001	3.02±0.008	0.47±0.002	0.84±0.01	3.1±0.05	2.87±0.01
p-IκBα	3.2±0.03	0.78±0.01	2.19±0.07	5.35±0.08	0.74±0.04	4.32±0.01
IKK	1.6±0.05	1.22±0.005	0.83±0.005	1.07±0.05	3.45±0.15	4.12±0.007
p-IKK	0.91±0.006	1.1±0.008	1.002±0.003	1.07±0.01	0.97±0.03	1.38±0.029

4.1.7.2 Chromatin immunoprecipitation (ChIP) assay: Gemcitabine and Gemcitabine plus erlotinib augmentation of NF-κB translocation to the nucleus was followed by an induction of the binding activity of NF-κB to BCL-2, BCL-X_L and MMP-9 promoters in the k-ras mutated cell line and by an induction of the binding activity of NF-κB to BCL-2 and IκB-α in the wild type cell line. Erlotinib induced the binding activity of NF-κB to IκB-α in pancreatic cancer cell lines and also repressed the the binding activity of NF-κB to BCL-2 and MMP-9 in the wild type k-ras cell line

In order to elucidate the interaction between the NF-κB transcription factor and its native chromatin sites to provide insights into physiological transcription, we performed a powerful approach: the chromatin immunoprecipitation (ChIP) assay.

The ChIP assay is a very powerful technique used to identify regions of a genome associated with specific proteins including, but not limited to, transcription factors within their native chromatin context. In this technique, intact cells are fixed with formaldehyde to cross-link proteins with their associated DNA. Then, the cells are lysed and chromatin is isolated from the nuclei. After fragmentation by sonication, chromatin fragments, containing the protein of interest and their associated DNA, are selectively precipitated using a specific antibody. Eventually, the sequence identities of the precipitated DNA fragments are determined. ChIP has been coupled with many commonly used molecular biology techniques such as PCR and real-time PCR, gene cloning and DNA microarray to elucidate DNA-protein interactions. In a standard ChIP procedure, specific DNA sequences are examined by PCR using gene specific primers [291].

We have analyzed the binding of NF-κB to the promoter of the genes Bcl-2, Bcl-X_L, MMP-9 and the inhibitor of NF-κB (IκB-α) as they have been reported to be direct transcriptional targets of NF-κB [332-335].

There are plenty of critical parameters in the ChIP assay procedure[290]. One of them is the sonication procedure. It is critical to break the DNA to 100–1000 bp fragments to pinpoint the location of the DNA sequence of interest (Figure 4.40).

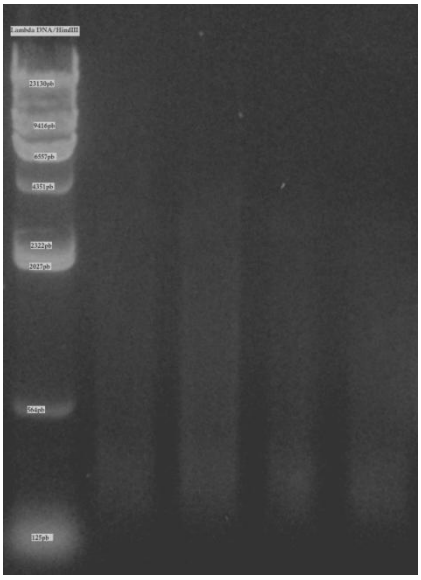

Figure 4.40 Agarose gel electrophoresis analysis of purified DNA fragments that have undergone sonication, proteinase digestion, crosslink reversal, extraction and precipitation.

All samples were then subjected to immunoprecipitation using either NF-κB antiserum or normal rabbit serum (negative). Immunoprecipitated samples were subjected to quantitative real-time PCR using specific primers against NF-κB binding sites (see Table 3-4). Data for ChIP-qPCR assays were reported as the site IP fold enrichment for the normalized background fraction. For further details refer to section 3.16. To ensure the reliability of the ChIP results, 3 control samples, particular to the ChIP experiments, were included to normalize for the source of variability with every primer set applied: precleared chromatin (Input) as a positive control, the "no-antibody" as a first negative control and chromatin without crosslinking as a second negative control. Raw data values and melting curve analyses were consistent throughout the experiments.

A particular interest has been professed in the role of the transcription factor NF-κB in human pancreatic cancer. To determine whether the NF-κB transcription factor contribute to the regulation of Bcl-2, Bcl-X_L, MMP-9 and its own inhibitor we performed chromatin immunoprecipitation (ChIP) experiments on pancreatic cancer cells Panc-1 and BxPC-3.

As a negative control, an antibody against IgG was used in the ChIP assays. As expected no one of the target genes could be detected above background by real time PCR in any NF-κB ChIP assays performed. Untreated cells without crosslinking were also used as negative control. Due to the absence of any linked transcription factor to the chromatin, no signal should be obtained in these samples after immunoprecipitation with anti-NF-κB. Once again, no one of the target genes was detected above background by real time PCR. The analysis of immunoprecipitated samples and controls by agarose electrophoresis is shown in Figure 4.43, Figure 4.46, Figure 4.49 and Figure 4.52.

Bcl-2, Bcl-X_L, MMP9 and IκB-α primers were design against the region of the promoters containing the NF-κB response element.

Regarding the Bcl-2 gene, in the Panc-1 cell line, amplification of the region of the Bcl-2 promoter containing the NF-κB response element was observed in the Gemcitabine, Erlotinib and Gemcitabine plus Erlotinib combined treatment samples. The fold change above 1.0 signified that a greater amount of the Bcl-2 promoter was isolated by anti-NF-κB compared to control samples. These results indicated that NF-κB transcription factor was bound to the Bcl-2 promoter region containing the NF-κB regulatory element in the Panc-1 cell line incubated with the different treatments. Gemcitabine exerted an induction of the binding of NF-κB to the Bcl-2 promoter of 8.7 times (8.7±1.24); Erlotinib exerted an induction of the binding of NF-κB to the Bcl-2 promoter of 5.66 times (5.66±1.8) and Gemcitabine +Erlotinib exerted the greatest induction of the binding of NF-κB to the Bcl-2 promoter, 11.77 times (11.77±1.9). These results are shown in Figure 4.41.

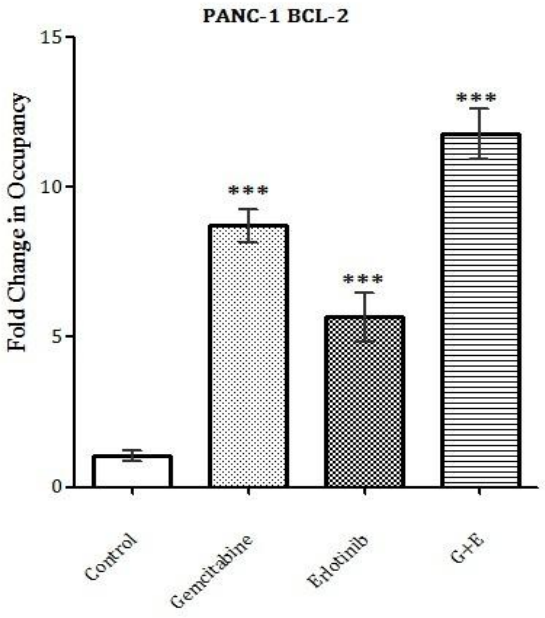

Figure 4.41 ChIP of NF-κB binding to the human Bcl-2 promoter in the Panc-1 cell line after treatment with 50μM of Gemcitabine, 12.5μM of Gemcitabine and/or 1+5μM of Gemcitabine + Erlotinib. Differential Occupancy Fold Change (linear conversion of the second ΔΔCt) was used as multiple experimental samples were compared. Each value is represented as mean ± S.D of triplicates from three independent Chip assays. Asterisks indicate significant differences from control values (*: P< 0.0001; **: P<0.01; *: P<0.05).**

In the BxPC-3 cell line, a significant amplification of the region of the Bcl-2 promoter containing the NF-κB response element was only observed after the Gemcitabine plus Erlotinib combined treatment. Gemcitabine + Erlotinib exerted an induction of the binding of NF-κB to the Bcl-2 promoter of 6.9 times (6.9±2.43). It is noteworthy that in the case of the Erlotinib treatment, the recruitment of NF-κB p65 protein to the Bcl-2 promoter was only marginal and a repression in the amplification of the region of the Bcl-2 promoter containing the NF-κB response element was significantly determined. This could mean that Erlotinib is lowering the NF-κB binding to the Bcl-2 promoter in the BxPC-3 cell line. These results are shown in Figure 4.42. Gemcitabine, as a single agent, did not significantly modify the binding of NF-κB to drive the Bcl-2 gene expression when compared against the control sample.

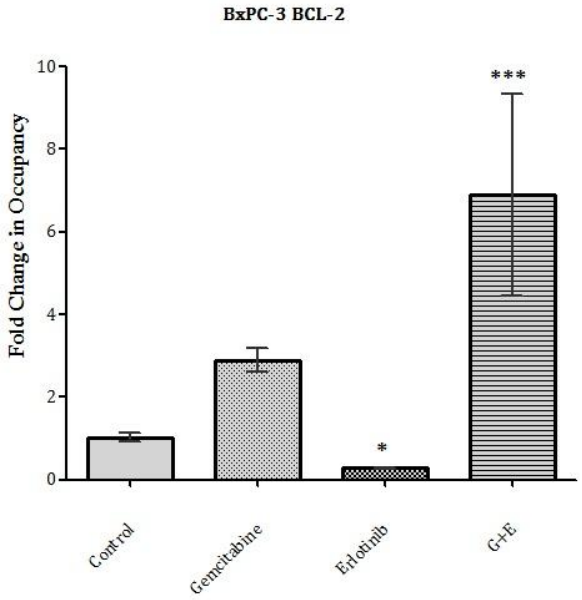

Figure 4.42 ChIP of NF-κB binding to the human Bcl-2 promoter in the BxPC-3 cell line after treatment with 0.02μM of Gemcitabine, 12.5μM of Erlotinib and 0.025+5μM of Gemcitabine + Erlotinib respectively. Differential Occupancy Fold Change (linear conversion of the second ΔΔCt) was used as multiple experimental samples were compared. Each value is represented as mean ± S.D of triplicates from three independent Chip assays. Asterisks indicate significant differences from control values (*: P< 0.0001; **: P<0.01; *: P<0.05).**

A comparison of the amplification of the region of the Bcl-2 promoter containing the NF-κB response element between Panc-1 and BxPC-3 is depicted in Figure 4.43. The products of the PCR were resolved by electrophoresis (Figure 4.43, right).

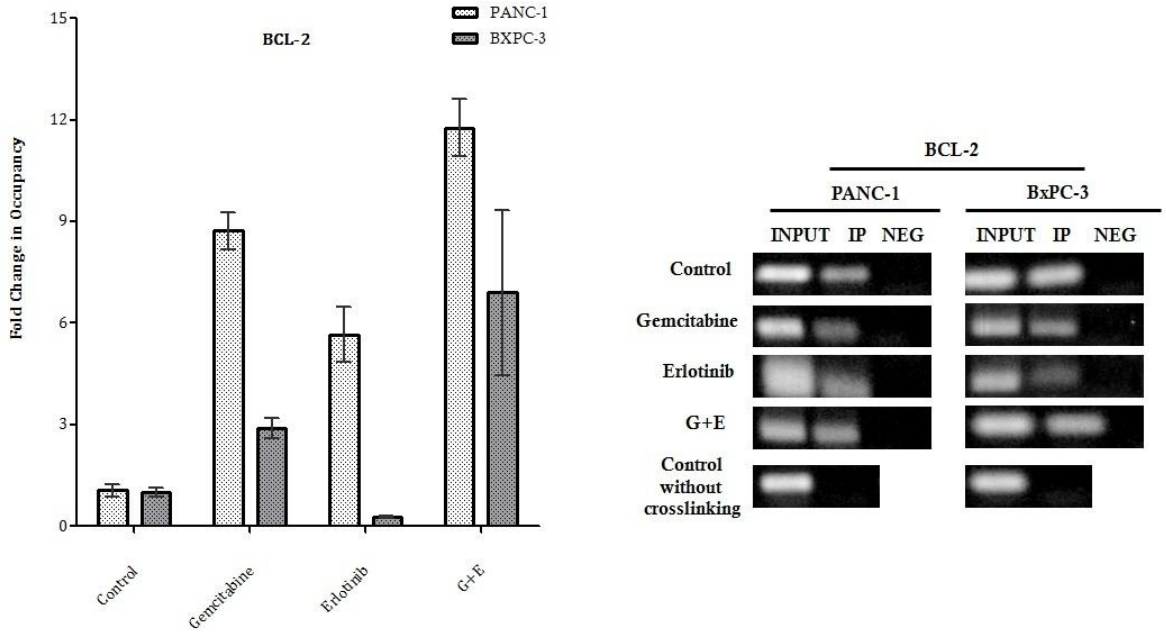

Figure 4.43 ChIP analyses of the association of NF-κB transcription factor with the Bcl-2 promoter region in the Panc-1 and BxPC-3 cell lines. Pancreatic cancer cells were treated 48h with their IC_{50} of Gemcitabine, Erlotinib and/or Gemcitabine+Erlotinib combined therapy. Cells were cross-linked with formaldehyde, lysed, chromatin was sheared by sonication and NF-κB p65 protein was immunoprecipitated. The binding of NF-κB p65 to promoter regions of Bcl-2 was measured by quantitative real-time PCR. Agarose gel electrophoresis of polymerase chain reaction products from each CHIP assay are shown in the right. Input lanes show the positive control; IP lanes show amplification of the immunoprecipitated promoter; Neg lanes show normal rabbit immunoglobulin G (IgG) immunoprecipitated samples.

Following, we measured the in vivo recruitment of NF-κB p65 subunit to promoters of Bcl-X_L gene. In the Panc-1 cell line, amplification of the region of the Bcl-X_L promoter containing the NF-κB response element was observed in the Gemcitabine and the Gemcitabine plus Erlotinib combined treatment samples. The fold change above 1.0 signified that a greater amount of the Bcl-X_L promoter was isolated by the anti-NF-κB compared to control samples. These results indicated that NF-κB transcription factor was bound to the Bcl-X_L promoter region containing the NF-κB regulatory element in the Panc-1 cell line incubated with the Gemcitabine and the Gemcitabine plus Erlotinib treatment. Gemcitabine exerted the greatest induction in the binding of NF-κB to the Bcl-X_L promoter, 4.55 times (4.55±0.73) and Gemcitabine + Erlotinib exerted a more modest but

still significant induction of the binding of the NF-κB to the Bcl-X_L promoter of 2.6 times (2.6±0.41). Erlotinib, as a single agent, did not significantly modify the binding of the NF-κB to drive the Bcl-X_L gene expression when compared against the control sample. These results are shown in Figure 4.44.

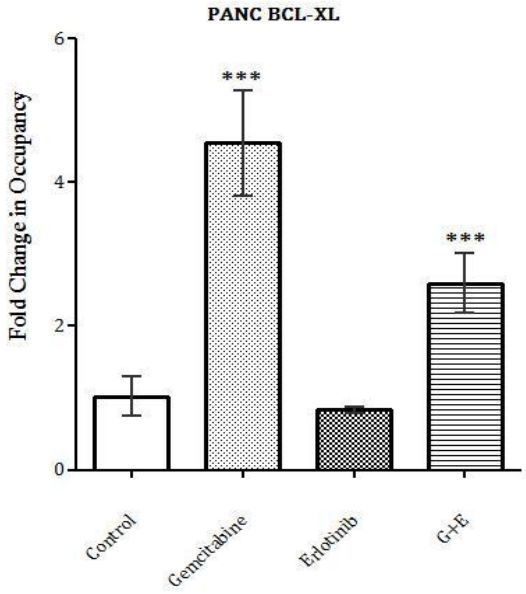

Figure 4.44 ChIP of NF-κB binding to the human Bcl-X_L promoter in the Panc-1 cell line after treatment with 50μM of Gemcitabine, 12.5μM of Gemcitabine and/or 1+5μM of Gemcitabine + Erlotinib. Differential Occupancy Fold Change (linear conversion of the second ΔΔCt) was used as multiple experimental samples were compared. Each value is represented as mean ± S.D of triplicates from three independent Chip assays. Asterisks indicate significant differences from control values (*: P< 0.0001; **: P<0.01; *: P<0.05).**

In the BxPC-3 cell line, no significant amplification of the region of the Bcl-X_L promoter containing the NF-κB response element was observed after any of the treatments when compared against control samples. These results are shown in Figure 4.45.

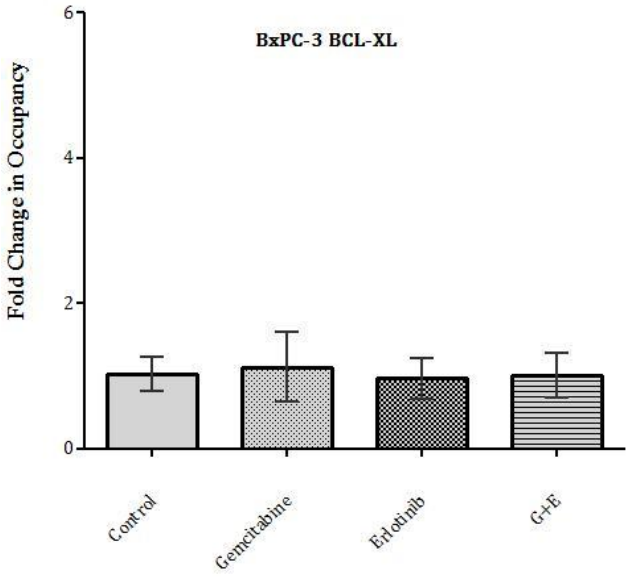

Figure 4.45 ChIP of NF-κB binding to the human Bcl-X_L promoter in the BxPC-3 cell line after treatment with 0.02μM of Gemcitabine, 12.5μM of Erlotinib and 0.025+5μM of Gemcitabine + Erlotinib respectively. Differential Occupancy Fold Change (linear conversion of the second ΔΔCt) was used as multiple experimental samples were compared. Each value is represented as mean ± S.D of triplicates from three independent Chip assays. Asterisks indicate significant differences from control values (*: P< 0.0001; **: P<0.01; *: P<0.05).**

A comparison of the amplification of the region of the Bcl-X_L promoter containing the NF-κB response element between Panc-1 and BxPC-3 is depicted in Figure 4.46. The products of the PCR were resolved by electrophoresis (Figure 4.46, right).

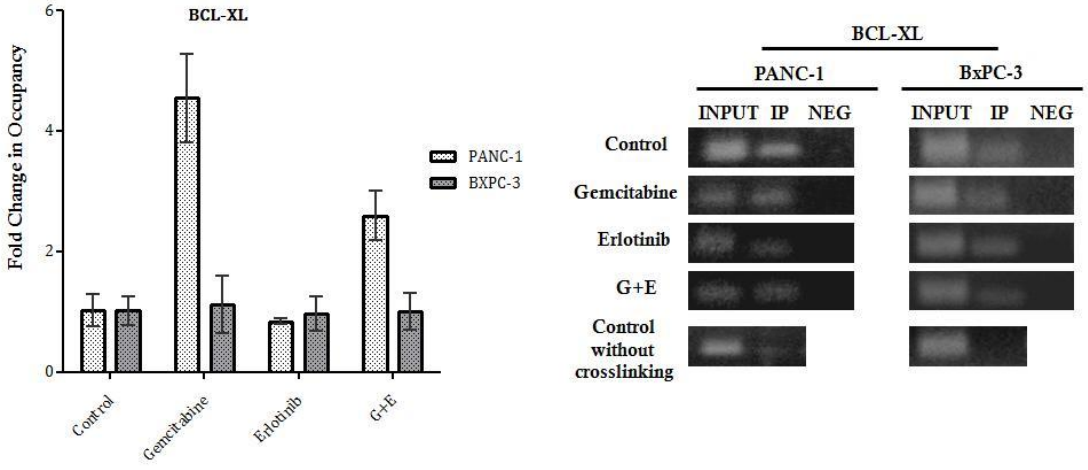

Figure 4.46 ChIP analyses of the association of NF-κB transcription factor with the Bcl-X_L

promoter region in the Panc-1 and BxPC-3 cell lines. Pancreatic cancer cells were treated 48h with their IC_{50} of Gemcitabine, Erlotinib and/or Gemcitabine+Erlotinib combined therapy. Cells were cross-linked with formaldehyde, lysed, chromatin was sheared by sonication and NF-κB p65 protein was immunoprecipitated. The binding of NF-κB p65 to promoter regions of Bcl-X_L was measured by quantitative real-time PCR. Agarose gel electrophoresis of polymerase chain reaction products from each CHIP assay are shown in the right. Input lanes show the positive control; IP lanes show amplification of the immunoprecipitated promoter; Neg lanes show normal rabbit immunoglobulin G (IgG) immunoprecipitated samples.

Subsequently, the in vivo recruitment of the NF-κB p65 subunit to the promoter of the MMP-9 gene was studied. In the Panc-1 cell line, amplification of the region of the MMP-9 promoter containing the NF-κB response element was observed in the Gemcitabine and in the Gemcitabine plus Erlotinib combined treatment samples. The fold change above 1.0 signified that a greater amount of the MMP-9 promoter was isolated by the anti-NF-κB compared to control samples. These results indicated that the NF-κB transcription factor was bound to the MMP-9 promoter region containing the NF-κB regulatory element in the Panc-1 cell line incubated with the Gemcitabine and the Gemcitabine plus Erlotinib treatments. Gemcitabine exerted an induction in the binding of the NF-κB to the MMP-9 promoter of 2.77 times (2.77±0.51) and Gemcitabine + Erlotinib exerted a very similar induction in the binding of NF-κB to the MMP-9 promoter, 2.13 (2.13±0.41). Erlotinib, as a single agent, did not significantly modify the binding of the NF-κB to drive the MMP-9 gene expression when compared against the control sample. These results are shown in Figure 4.47.

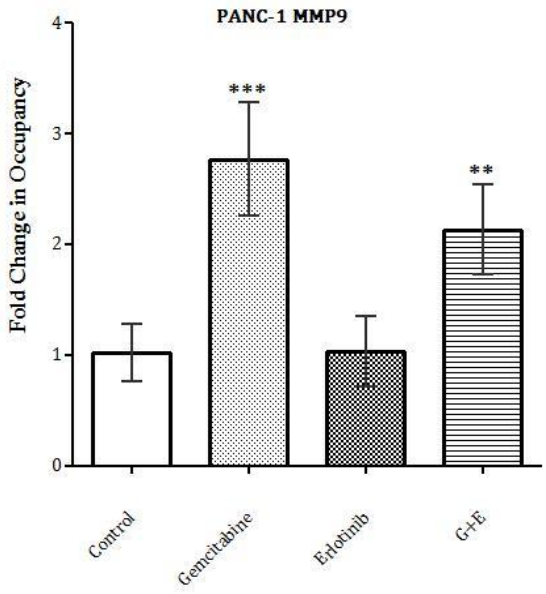

Figure 4.47 ChIP of NF-κB binding to the human MMP9 promoter in the Panc-1 cell line after treatment with 50μM of Gemcitabine, 12.5μM of Gemcitabine and/or 1+5μM of Gemcitabine + Erlotinib. Differential Occupancy Fold Change (linear conversion of the second ΔΔCt) was used as multiple experimental samples were compared. Each value is represented as mean ± S.D of triplicates from three independent Chip assays. Asterisks indicate significant differences from control values (*: P< 0.0001; **: P<0.01; *: P<0.05).**

In the BxPC-3 cell line, no significant amplification of the region of the MMP-9 promoter containing the NF-κB response element was observed after the Gemcitabine treatment when compared against control samples. However, the recruitment of the NF-κB p65 protein to the MMP-9 promoter was only marginal in the Erlotinib and in the Gemcitabine + Erlotinib combined treatments and a repression in the amplification of the region of the MMP-9 promoter containing the NF-κB response element was significantly determined. This could mean that Erlotinib and the combination are lowering the NF-κB binding to the MMP-9 promoter in the BxPC-3 cell line. These results are shown in Figure 4.48.

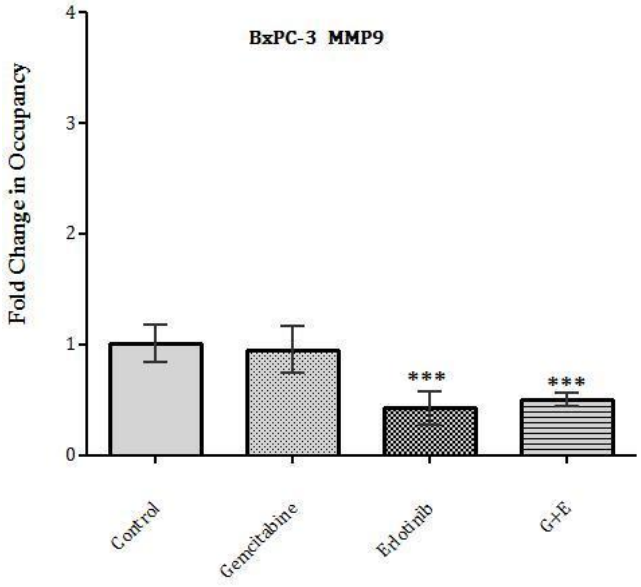

Figure 4.48 ChIP of NF-κB binding to the human MMP9 promoter in the BxPC-3 cell line after treatment with 0.02μM of Gemcitabine, 12.5μM of Erlotinib and 0.025+5μM of Gemcitabine + Erlotinib respectively. Differential Occupancy Fold Change (linear conversion of the second ΔΔCt) was used as multiple experimental samples were compared. Each value is represented as mean ± S.D of triplicates from three independent Chip assays. Asterisks indicate significant differences from control values (*: P< 0.0001; **: P<0.01; *: P<0.05).**

A comparison of the amplification of the region of the MMP9 promoter containing the NF-κB response element between Panc-1 and BxPC-3 is depicted in Figure 4.49. The products of the PCR were resolved by electrophoresis (Figure 4.49, right).

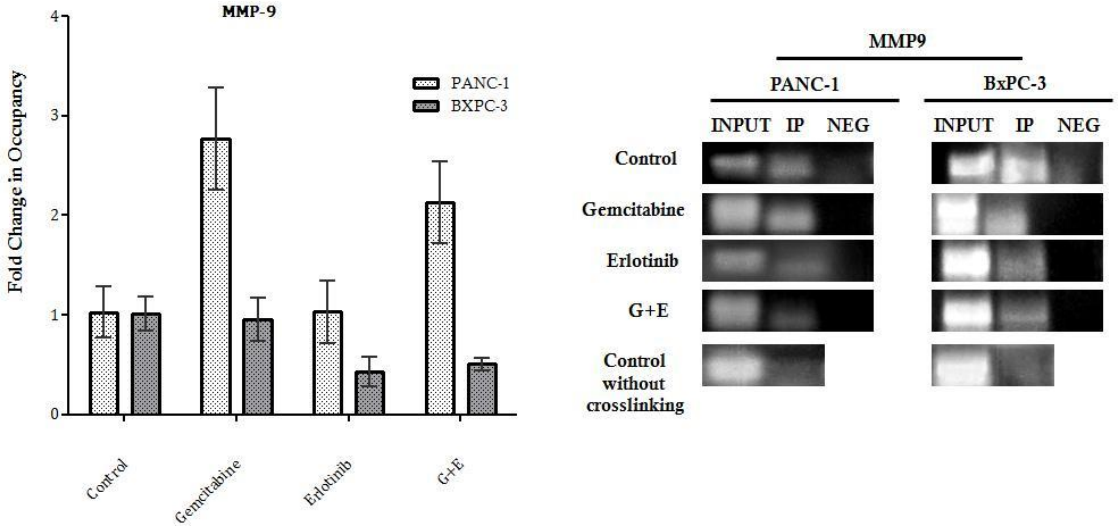

Figure 4.49 ChIP analyses of the association of NF-κB transcription factor with the MMP9 promoter region in the Panc-1 and BxPC-3 cell lines. Pancreatic cancer cells were treated 48h with their IC50 of Gemcitabine, Erlotinib and/or Gemcitabine+Erlotinib combined therapy. Cells were cross-linked with formaldehyde, lysed, chromatin was sheared by sonication and NF-κB p65 protein was immunoprecipitated. The binding of NF-κB p65 to promoter regions of MMP9 was measured by quantitative real-time PCR. Agarose gel electrophoresis of polymerase chain reaction products from each CHIP assay are shown in the right. Input lanes show the positive control; IP lanes show amplification of the immunoprecipitated promoter; Neg lanes show normal rabbit immunoglobulin G (IgG) immunoprecipitated samples.

Finally, the in vivo recruitment of the NF-κB p65 subunit to the promoter of the IκB-α gene was studied. In the Panc-1 cell line, amplification of the region of the IκB-α promoter containing the NF-κB response element was observed in the Erlotinib treated samples. The fold change above 1.0 signified that a greater amount of the IκB-α promoter was isolated by the anti-NF-κB compared to the control samples. These results indicated that the NF-κB transcription factor was bound to the IκB-α promoter region containing the NF-κB regulatory element in the Panc-1 cell line incubated with Erlotinib treatment. Erlotinib exerted an induction in the binding of NF-κB to the IκB-α promoter of 2.6 times (2.6±0.89). Gemcitabine, as a single agent, inhibited the recruitment of the NF-κB p65 protein to the IκB-α promoter and a repression in the amplification of the region of the IκB-α promoter containing the NF-κB response element was significantly determined. This could mean that Gemcitabine is lowering the NF-κB binding to the IκB-α promoter in the Panc-1 cell line.

Although an inhibition in the transcription of the IκB-α gene was found in PCR arrays (Figure 4.28) for the Panc-1 cell line incubated with the combined treatment, and despite that this regimen appeared to inhibit the recruitment of the NF-κB p65 protein to the IκB-α promoter, results did not reach a sufficient level of significance. These results are shown in Figure 4.50.

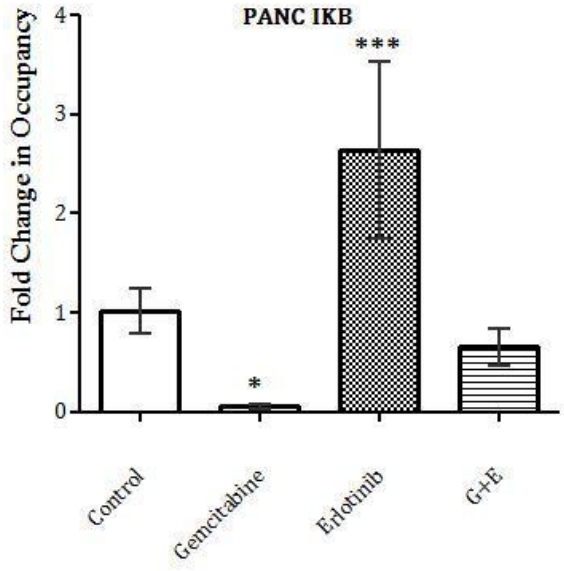

Figure 4.50 ChIP of NF-κB binding to the human IκBα promoter in the Panc-1 cell line after treatment with 50μM of Gemcitabine, 12.5μM of Gemcitabine and/or 1+5μM of Gemcitabine + Erlotinib. Differential Occupancy Fold Change (linear conversion of the second ΔΔCt) was used as multiple experimental samples were compared. Each value is represented as mean ± S.D of triplicates from three independent Chip assays. Asterisks indicate significant differences from control values (*: P< 0.0001; **: P<0.01; *: P<0.05).**

In the BxPC-3 cell line, no significant amplification of the region of the IκB-α promoter containing the NF-κB response element was observed after the Gemcitabine treatment when compared against control samples. However, the recruitment of the NF-κB p65 protein to the IκB-α promoter seemed to be induced in the Erlotinib and in the Gemcitabine + Erlotinib combined treatments. Erlotinib exerted an induction in the binding of the NF-κB to the IκB-α promoter of 9 times (8.9±0.43) and Gemcitabine + Erlotinib exerted an induction in the binding of the NF-κB to the IκB-α promoter of 3 times (3.07±0.39). These results are shown in Figure 4.51.

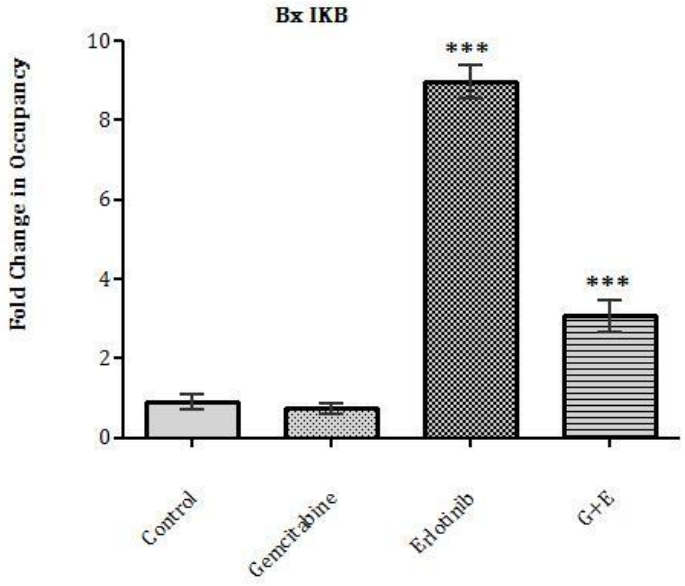

Figure 4.51 ChIP of NF-κB binding to the human IκBα promoter in the BxPC-3 cell line after treatment with 0.02μM of Gemcitabine, 12.5μM of Erlotinib and 0.025+5μM of Gemcitabine + Erlotinib respectively. Differential Occupancy Fold Change (linear conversion of the second ΔΔCt) was used as multiple experimental samples were compared. Each value is represented as mean ± S.D of triplicates from three independent Chip assays. Asterisks indicate significant differences from control values (*: P< 0.0001; **: P<0.01; *: P<0.05).**

A comparison of the amplification of the region of the IκB-α promoter containing the NF-κB response element between Panc-1 and BxPC-3 is depicted in Figure 4.52. The products of the PCR were resolved by electrophoresis (Figure 4.52, right).

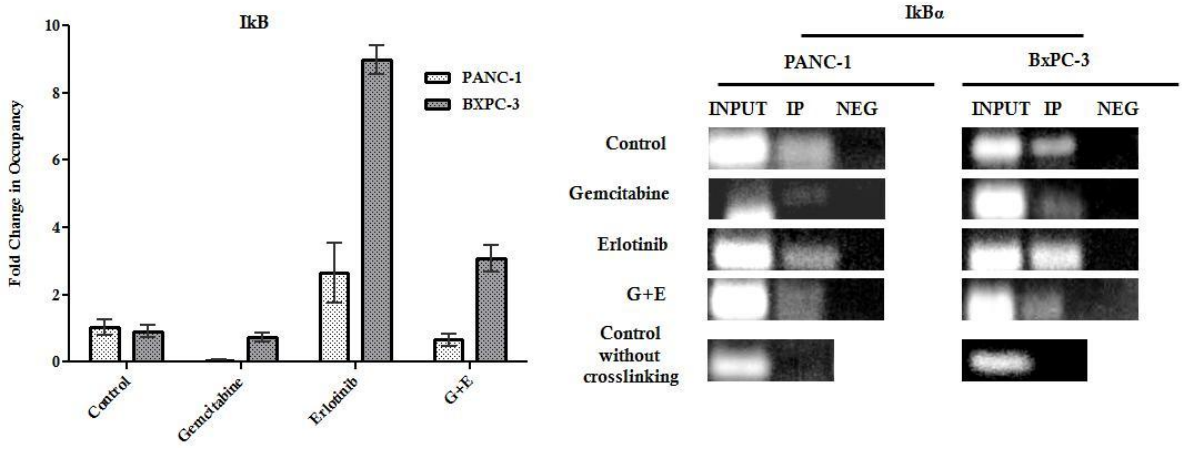

Figure 4.52 ChIP analyses of the association of NF-κB transcription factor with the IκBα

promoter region in the Panc-1 and BxPC-3 cell lines. Pancreatic cancer cells were treated 48h with their IC50 of Gemcitabine, Erlotinib and/or Gemcitabine+Erlotinib combined therapy. Cells were cross-linked with formaldehyde, lysed, chromatin was sheared by sonication and NF-κB p65 protein was immunoprecipitated. The binding of NF-κB p65 to promoter regions of IκBα was measured by quantitative real-time PCR. Agarose gel electrophoresis of polymerase chain reaction products from each CHIP assay are shown in the right. Input lanes show the positive control; IP lanes show amplification of the immunoprecipitated promoter; Neg lanes show normal rabbit immunoglobulin G (IgG) immunoprecipitated samples.

4.2 BIOMARKERS IDENTIFICATION IN PANCREATIC DUCTAL ADENOCARCINOMA PATIENTS

Here we present a study in which the Human Cytokine Array from *RayBiotech* was used to analyze simultaneously 507 cytokines in collected sera from pancreatic cancer patients. The array includes cytokines, chemokines, growth and differentiation factors, angiogenic factors, adipokines, adhesion molecules and matrix metalloproteases, as well as binding proteins, inhibitors and soluble receptors to these proteins [175]. Antibody-based arrays represent a useful tool for cancer biomarker discovery enabling the generation of highly robust assays that can be easily standardized and automated [294]. Not only does this methodology stand out for its capacity to straightly and quickly offer insights into early cancer biomarkers detection but it also could shed light into progression, assisting clinicians in novel personalized cancer therapies approaches [295]. However, potential features easily outnumber samples and an overfitting problem can arise. Development of an appropriate feature selection model such filters and validation methods such as leave-one-out cross validation (LOOCV) ensures the smallest bias for model building [336].

This study had three main objectives: identification and validation of individual biomarkers or sets of biomarkers for the detection of PDAC (***diagnostic biomarkers***), the treated-patient monitoring to determine ***predictive biomarkers*** that would forecast the likely course of disease in a defined clinical population under the Gemcitabine and Erlotinib treatment conditions and forecast the likely course of the disease, including survival and recurrence pattern in the absence of therapy (***prognosis biomarkers***).

4.2.1 Diagnosis biomarkers

4.2.1.1 Analysis of serum diagnostic biomarkers in PDAC patients and healthy controls

To find markers for the detection of PDAC, an extensive screening with a 507 human cytokine antibody array was carried out to identify those differentially expressed cytokines among healthy individuals and PDAC patients. Clinicopathologic characteristics of PDAC patients are summarized in Table 3-5. As shown in Table 4-16, we have found five cytokines that were overexpressed in PDAC non-treated patients when compared to healthy volunteers ($p<0.05$). FGF-10/KGF-2, I-TAC/CXCL11, OSM, Osteoactivin/GPNMB and SCF cytokines could represent an altered serum cytokine profile in PDAC patients.

Table 4-16: Differentially overexpressed cytokines in PDAC patients

ID	*P-Value*	*Log FC*	*FC*
FGF-10 / KGF-2	0.040	1.10	2.15
I-TAC / CXCL11	0.046	0.93	1.91
OSM	0.040	0.96	1.95
Osteoactivin / GPNMB	0.019	1.36	2.56
SCF	0.022	1.51	2.85

Table 4-16 Five significantly overexpressed cytokines. Differences were obtained by the Mann-Whitney U test ($p<0.05$). Their relative expression levels are given by their corresponding fold changes (FC). Every ≥1.5-FC or ≤1/1.5-FC in signal intensity between groups was considered relevant.

4.2.1.2 Analysis of sensitivity and specificity of individual serum diagnostic biomarkers for PDAC

In order to determine whether these five cytokines could be used as markers for the detection of PDAC, we evaluated diagnostic value (the ability to differentiate between health and illness) of each biomarker separately and in combination. Sensitivity and specificity for each biomarker were analyzed employing the area under the receiver operator characteristics (ROC) curve method. The curves are based on cytokine levels in healthy donors and patients before and after treatment. Each independent candidate biomarker was investigated as depicted in Figure 4.53 (A-E). All possible new biomarkers showed AUC values between 0.74-0.78 for the discrimination of healthy and PDAC patients. Areas under the ROC curve for FGF-10/KGF-2, I-TAC/CXCL11, OSM, Osteoactivin/GPNMB and SCF cytokines were 0.744, 0.737, 0.744, 0.776 and 0.772 respectively. Osteoactivin stood out with the highest sensibility to predict PDAC alone. To determine sensitivity and specificity of each biomarker, we established those cut-off points providing the best trade off point between both the highest sensitivity and the highest specificity (Figure 4.53). All of them showed a specificity of 75% and sensitivities ranging between 69-77%.

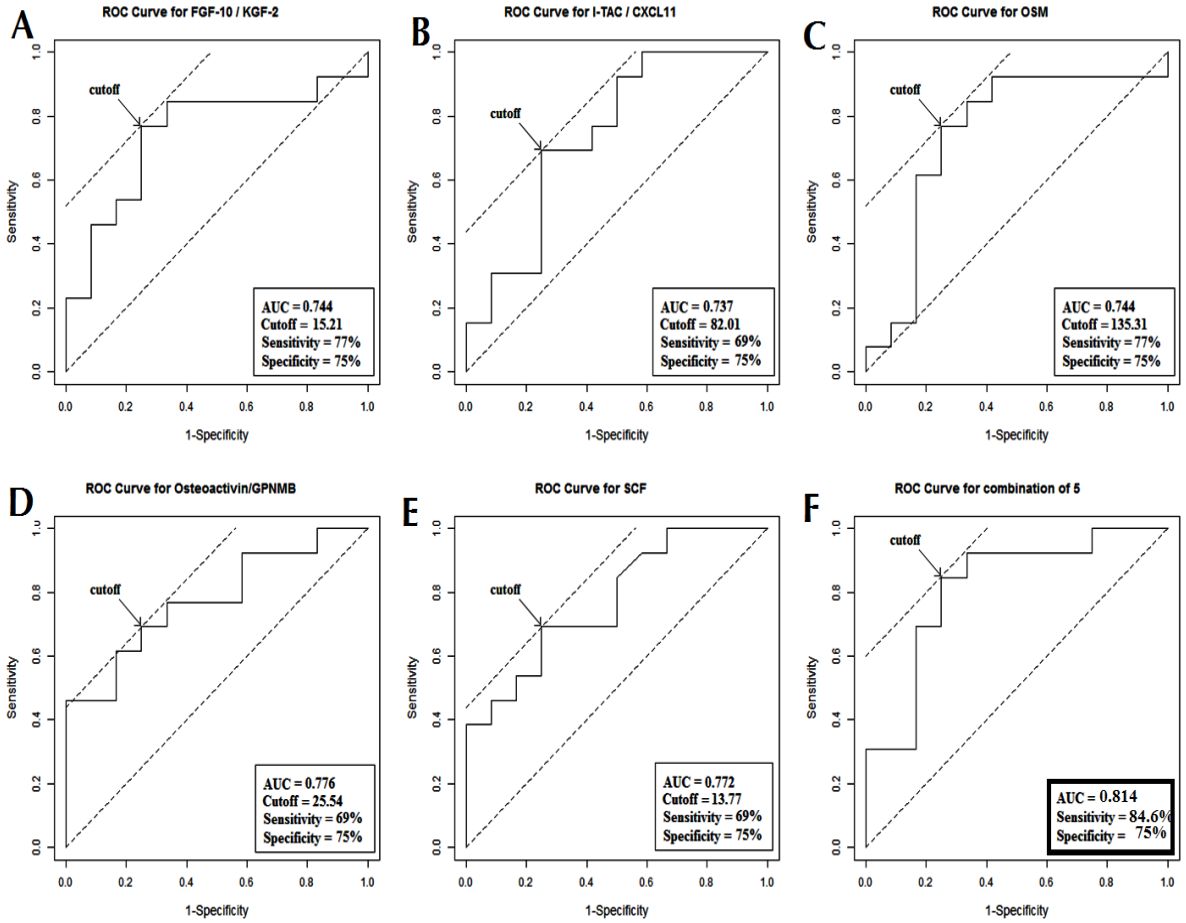

Figure 4.53 Receiver operating characteristics (ROC) curve analysis for each of the five serum cytokines found to be differentially expressed amongst PDAC patients. ROC curves summarize the accuracy of cytokines in predicting PDAC patients. The area under the ROC curve (AUC) is the average sensitivity of the biomarker. A biomarker with no predictive value would have an AUC of 0.5 while a biomarker with perfect ability to predict disease would have an AUC of 1. A shows AUC, cut-off, sensitivity and specificity values for FGF-10/KGF-2; B shows AUC, cut-off, sensitivity and specificity values for values for I-TAC/CXCL11; C shows AUC, cut-off, sensitivity and specificity values for values for OSM; D shows AUC, cut-off, sensitivity and specificity values for values for Osteoactivin; E shows AUC, cut-off, sensitivity and specificity values for values for SCF; F shows AUC, sensitivity and specificity values for values for the five cytokines combined. Cut-offs (values of signal intensities) selected were those with both the highest sensitivities and specificities.

4.2.1.3 Analysis of sensitivity and specificity of combined serum diagnostic biomarkers for PDAC

Following, in order to determine whether these five cytokines, taken together, could be used as a panel of biomarkers for detection of PDAC, a combination of these five markers was analyzed to obtain an integrated ROC curve using a weighted linear combination sum (weighted using each independent cytokine´s sensitivity).

Leave-one-out cross-validation analyses (LOOCV) for this combination were used on the whole patient dataset to evaluate the model-based cytokines set for hypothetical prediction of suffering from PDAC for each patient. Here, one sample was removed from the initial 25 sample dataset (healthy and pre-treated patients), leaving a temporary 24 sample training set and one left out-sample. On the training set, the cytokine combination obtained from the best cut-off provided by their corresponding ROC curve was then used to classify the previously left out-test sample. Performing LOOCV using the weighted sum cytokines combination with the cut-off provided by each training set, a specificity of 84.9% and a sensitivity of 75% were estimated for the former and a specificity of 84.6% and a sensitivity of 67% were estimated for the test set.

Once the merged model was validated, the specificity and the sensitivity of the whole final model gathering the twenty-six samples were 75% and 84.6% respectively. The 5-cytokine panel displaying the best performance for detecting PDAC in sera samples reflected similar specificity but significantly higher sensitivity when compared with the individual cytokines. Therefore, the combined panel of cytokines indeed improved the ability of all biomarkers in isolation to distinguish patients with pancreatic cancer from healthy controls. This can be also proven by the improved AUC value. It reached 0.814 (Figure 4.53, F).

4.2.2 Predictive biomarkers

4.2.2.1 Analysis of serum markers in pre- and post-treated PDAC patients as predictive biomarker of Gemcitabine and Erlotinib response

The second goal of this study was also to assess predictive biomarkers to forecast the likely response to the Gemcitabine and Erlotinib treatment. To address whether this regimen modulates immune contexture, we compared serum cytokine profile between non-treated and PDAC patients under two weeks of the Gemcitabine and Erlotinib combination treatment. Given that the treatment itself can have an impact on cytokines expression due to inflammation side effects of the drugs, we developed two types of comparisons. In addition to the pre-treated against healthy controls comparisons, we analyzed pre- against post-treated PDAC patients. Only those common proteins in both analyses were chosen since they can be linked to tumour behavior outcomes after the treatment, regardless any side effect.

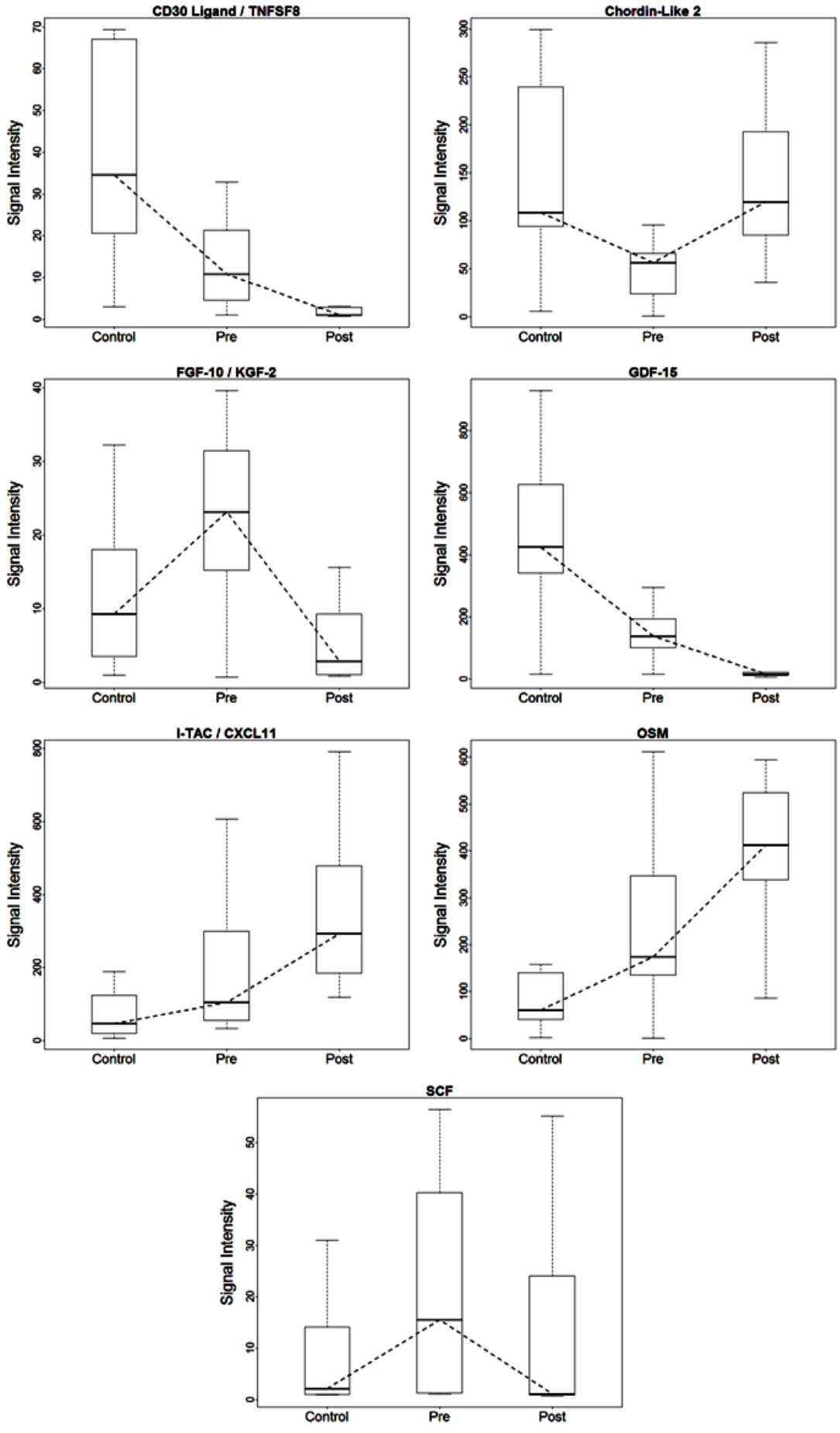
CD30 Ligand / TNFSF8
Chordin-Like 2
FGF-10 / KGF-2
GDF-15
I-TAC / CXCL11
OSM
SCF
Signal Intensity
Control
Pre
Post

Figure 4.54 Boxplots displaying differences between the seven common significantly modified serum cytokines comparing healthy, pre and post PDAC patients. Center line indicates the median for each data set. Differences between groups were statistically significant (p<0.05; for detailed p-values and further detail see Table 4-17). Dotted lines show the direction of the modulation provoked by chemotherapy.

CD30 Ligand/TNFSF8, Chordin-Like 2, GDF-15 and so those that were previously described as diagnostic biomarkers (except Osteoactivin) resulted significantly altered (p<0.05) (Table 4-17 and Figure 4.54 summarize the statistically significant common cytokines that may represent predictive biomarkers for the Gemcitabine and Erlotinib treatment regimen). Then, these cytokines could have been altered by the chemotherapy and/or the cancer itself.

Table 4-17: Predicted biomarkers for the Gemcitabine and Erlotinib treatment

MATCHED PROTEINS	Pre vs Control			Pre vs Post			Signal	Post vs Control	Balanced (1/1.5<FC<1.5)	
	P-value	Log2(FC)	FC	P-value	Log2(FC)	FC		FC		
CD30 Ligand/ TNFSF8	0.0188	-1.514	0.350	0.007	-1.610	0.328	**-/-**	0.115	×	◎
Chordin-Like 2	0.0066	-1.407	0.377	0.004	1.504	2.836	**-/+**	1.070	✓	
FGF-10/ KGF-2	0.0398	1.104	2.149	0.002	-2.238	0.212	**+/-**	0.455	×	◎
GDF-15	0.0045	-1.624	0.324	0.001	-1.208	0.433	**-/-**	0.140	×	◎
I-TAC/ CXCL11	0.0457	0.933	1.909	0.019	1.020	2.028	**+/+**	3.871	×	◎
OSM	0.0398	0.964	1.951	0.030	0.799	1.739	**+/-**	3.394	×	◎
SCF	0.0223	1.512	2.851	0.047	-0.890	0.540	**+/-**	1.539	✓	

Table 4-17 Predictive biomarkers for the PDAC patients' response to Gemcitabine and Erlotinib. The column Matched Proteins makes reference to those common cytokines found significantly modified between healthy, pre and post PDAC patients. Columns under the heading Pre vs. Control and Pre vs. Post display statistical results for their respective

Mann-Whitney U tests. Beside, fold change (FC) indicating cytokine relative expression levels is shown. In the signal column, the first sign indicates induction (+) or repression (-) in the cytokine expression levels in pre-treated patients compared with the control. The second sign indicates induction (+) or repression (-) in the cytokine expression levels in post-treated patients compared with pre-treated. The FC for Post vs. Control makes reference to the global FC. The last two columns show whether the cytokine expression is balanced after the treatment or if this cytokines could represent a novel target in the attempt to overcome chemoresistance. A balance in cytokine level was set as long as the global FC for Post vs. Control was not significant (for those cytokines that had previously shown a significant FC between Pre and Control).

The pivotal results shown in Table 4-17 and Figure 4.54 are the differences in cytokines levels before and after the treatment. The last four columns of Table 4-17 show the cytokine expression modulation between healthy, pre and post-treated PDAC patients. Dotted lines in Figure 4.54 and signal column in Table 4-17 depict these modulations amongst groups. In the signal column, the first sign indicates induction (+) or repression (-) in the cytokine expression levels in pre-treated patients compared with the control. The second sign indicates induction (+) or repression (-) in the cytokine expression levels in post- compared with pre-treated patients. Whether the global FC for post-treated vs. control was lower than 1.5 or higher than 1/1.5, a balance in cytokine expression levels was set. Only in the Chordin-Like 2 and SCF a balance in the cytokine expression was obtained after the treatment. In the specific case of FGF10/KGF-2, the treatment balanced the expression of the cytokine but reaching levels even lower than controls. In the remaining four cytokines, the treatment could be heightening the modulation prompted by the cancer. Amongst them, we have found an overexpression in I-TAC/CXCL11 and OSM cytokine levels of 3.8 and 3.4 times respectively in post-treated patients when compared with control group. On the contrary, CD30 Ligand/TNFSF8 and GDF-15 levels were more repressed. All these unbalanced cytokines appear to be promising prime targets for novel therapies or chemoresistance. Interestingly, although Osteoactivin is not significantly modified in post- vs. pre-treated comparisons, this fact does not exclude it from being another potential target for treatment improvements. We have reported higher levels of this cytokine in PDAC

patients and its absence in post-treated patients just indicates that the treatment is neither affecting, nor balancing it.

4.2.3 Prognostic biomarkers

4.2.3.1 Survival analysis of patients with PDAC

For the whole study population, the overall survival (OS) rates were 46.15% at 6 months, 23.08% at 12 months and 7.69% at 24 months. Median duration of follow-up for the entire study group was 12 months (range: 1–40 months) and during that time the 100% of the PDAC patients died due to the disease. Survival probabilities were calculated using the Kaplan-Meier method. The survival curve for the whole cohort of patients is shown in Figure 4.55 A.

4.2.3.2 Univariate analysis between serum cytokines and survival

First, a univariate approach was used in this study to identify relevant and independent measurable factors at diagnosis that could be associated to a higher risk of PDAC death. Serum levels of cytokines and clinicopathologic parameters such as age, gender, stage and clinical response were analyzed.

Amongst the clinicopathologic parameters, age and the clinical response (progressive or non-progressive disease, according to the RECIST criteria [337]) were associated with poor prognosis on univariate analysis (p=0.030 and p=0.013, respectively*)*.

Concerning cytokines, at univariate analysis after feature selection, expression levels of **BDNF** (p=0.034, HR 1.005, 95% CI (1.000 - 1.009)); **HVEM/TNFRSF14** (p= 0.039, HR 0.924, 95% (CI 0.858- 0.996)); **IL-24** (p=0.023, HR 1.041, 95% CI (1.006- 1.078)); **IL-29** (p=0.021, HR 1.012, 95% CI (1.002- 1.023)); **Leptin R** (p=0.018, HR 1.008, 95% CI (1.001- 1.015)); **LRP-6** (p=0.022 HR 1.027, 95% CI (1.004- 1.051)) and **ROBO4** (p=0.045 HR 1.002, 95% CI (1.000- 1.004)) showed a significant influence on prognosis.

Results of the univariate analysis of each cytokine as independent prognosis factors and its beta-coefficients (β), hazard ratios (representing the factor by which the hazard changes for each one-unit increase of the cytokine expression), 95% CI (upper and lower limits of the confidence interval with a significance level of 0.05) and p-values are shown in Table 4-18. In order to determine survival differences of these individual markers in PDAC patients, Kaplan-Meier survival curves were generated using the cut-off points providing the most significant discrimination in terms of survival between groups. Figure 4.55 (B-J) depicts Kaplan-Meier survival plots of individual markers showing significant prognosis differences.

Table 4-18: Prognosis factors in univariate analysis.

Variable	*Overall survival*				
	β	*HR*	*95% CI*		*p -value*
BDNF	0.005	1.005	1.000	1.009	0.034
HVEM / TNFRSF14	-0.079	0.924	0.858	0.996	0.038
IL-24	0.040	1.041	1.006	1.078	0.023
IL-29	0.012	1.012	1.002	1.023	0.021
Leptin R	0.008	1.008	1.001	1.015	0.018
LRP-6	0.027	1.027	1.004	1.051	0.022
ROBO4	0.002	1.002	1.000	1.004	0.045
Age	0.086	1.089	1.008	1.177	0.030
Clinical response	2.064	8.706	1.057	71.692	0.013
Cytokines	***Overall Model Fit (p= 0.0023)***				
	β	*HR*	*95% CI*		*p -value*
Il-24 (1)	0.042	1.042	1.003	1.023	0.026
Il-29 (2)	0.014	1.014	1.005	1.081	0.017

β: coefficient provided by the Cox's regression model for a particular patient and cytokine; HR: hazard ratio (represents the factor by which the hazard changes for each one-unit increase of the cytokine expression); 95% CI: upper and lower limits of the confidence interval with a significance level of 0.05.

Table 4-18 Prognosis factors in the univariate analyses. Variables significantly associated

with survival in PDAC patients at univariate analysis. Beta-coefficients (β), hazard ratio (HR), 95%CI and p-values for the selected variables are shown. Positive beta-coefficients for an explanatory variable represent a higher hazard and therefore the prognosis is worse. Conversely, a negative regression coefficient implies a better prognosis for patients with higher values of that variable. The hazard ratio is a descriptive measure used to compare the survival times of two different groups of patients. The hazard ratio indicates the change in the risk of death if the variable rises by one unit (one unit of expression for cytokines, 1 year for the age variable and disease progression in clinical response). CI: 95% confidence interval for hazard ratio. The p-values in the upper part of the table reflect the significance of each individual variable explaining survival. The lower part of the table shows the stepwise model using only those significant cytokines obtained in the univariate analysis. The p-values indicated there reflect the significance of the cytokines in the whole model.

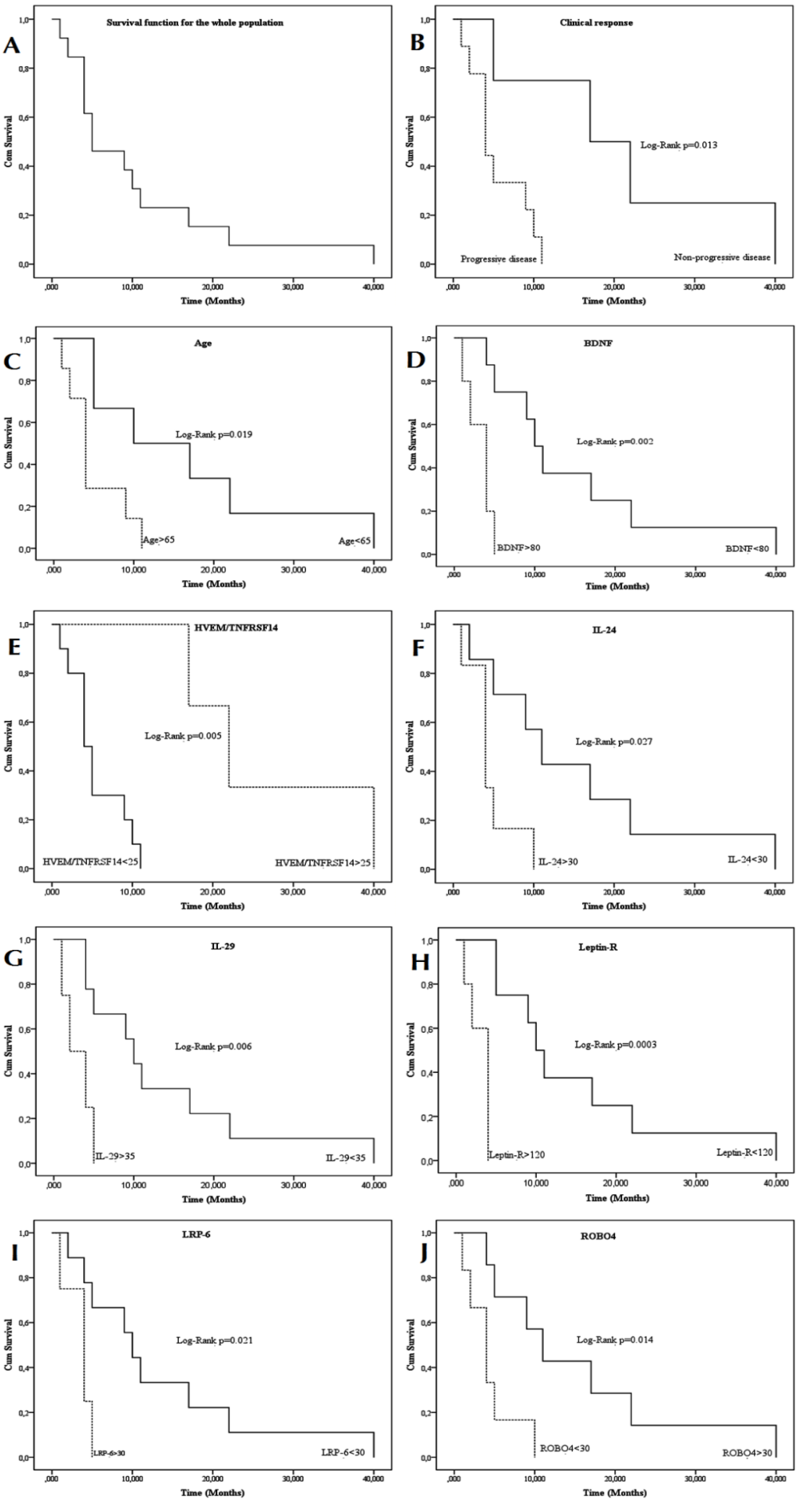
A
Survival function for the whole population
Cum Survival
Time (Months)
B
Clinical response
Log-Rank p=0.013
Progressive disease
Non-progressive disease
C
Age
Log-Rank p=0.019
Age>65
Age<65
D
BDNF
Log-Rank p=0.002
BDNF>80
BDNF<80
E
HVEM/TNFRSF14
Log-Rank p=0.005
HVEM/TNFRSF14<25
HVEM/TNFRSF14>25
F
IL-24
Log-Rank p=0.027
IL-24>30
IL-24<30
G
IL-29
Log-Rank p=0.006
IL-29>35
IL-29<35
H
Leptin-R
Log-Rank p=0.0003
Leptin-R>120
Leptin-R<120
I
LRP-6
Log-Rank p=0.021
LRP-6>30
LRP-6<30
J
ROBO4
Log-Rank p=0.014
ROBO4<30
ROBO4>30

Figure 4.55 (A) shows Kaplan-Meier disease-specific survival curve for the whole population in the study. The Kaplan-Meier survival curve is defined as the probability of surviving in a given period of time. Each period of time is the interval between two non-simultaneous terminal events. There were no survival data censored as no information was lost about the survival time of any individual. (B-H) plots depict Kaplan-Meier survival curves of individual biomarkers tagged as significant prognosis markers: (B), clinical response; (C), Age; (D), BDNF; (E), HVEM/TNFRSF14; (F), IL-24; (G), IL-29; (H), Leptin-R; (I), LRP-6 and (J), ROBO4. Most significant cut-off values in terms of survival were used to dichotomization. The p-values for the Log-Rank tests are shown for every variable.

4.2.3.3 Multivariate analysis between serum cytokines and survival

Despite the fact that often only those statistically significant variables in univariate analysis are included in multivariate analysis, some variables not being significant in univariate analysis may appear jointly significant in a multivariate analysis. Thus, in addition to the statistically significant variables related to poor prognosis on the univariate analysis, those also selected by the feature selection procedure were also included in the multivariate model. In proteomics studies, the number of samples is usually low compared to the number of variables, due to the limited availability or the cost of measurements. Taking this into account and in order not to introduce bias due to the high dimensionality of the small sample problem, a wrapper was used as a feature selection method using conditional forward stepwise algorithm based on likelihood rate to reduce the dimensionality of the data [182]. To assess the performance of the multivariate survival model, a leave-one-out cross-validation (LOOCV) analysis was performed. All estimated models using the different training sets in the LOOCV displayed an average goodness of fit (R-squared measurement) of 0.914. These results can be translated into that a 91.4% of the variability in the survival time was accounted for by the statistical model. In the test set, this validation showed an accuracy of 92.3%, sensitivity of 85.57% (true-poor prognosis rate) and specificity of 100% (true-fair prognosis rate) for all the left out samples (test samples). All estimated models are depicted in Figure 4.56.

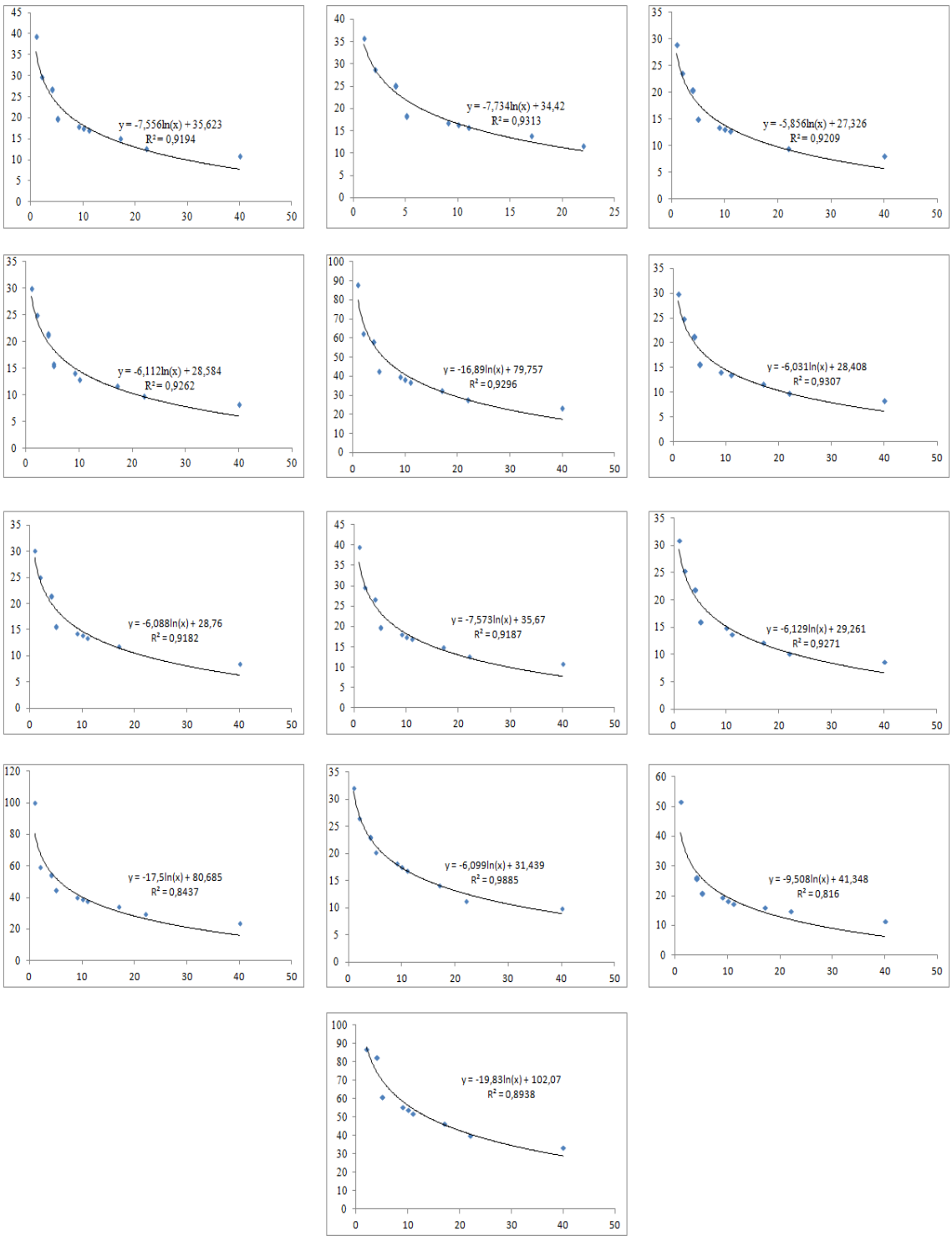

Figure 4.56 Estimated models using the different training sets in the LOOCV

The best combination of cytokines selected by the multivariate Cox's proportional hazard analysis is shown in Table 4-19. No one of the clinicopathologic parameters demonstrated a significant trend towards shortened overall survival ($p>0.05$) and were not considered in the global

model. Concerning cytokines, at multivariate analysis, expression levels of **B7-1/CD80** (p=0.043, HR 77.574, 95% CI (1.138-5289.4)); **EG-VEGF/PK1** (p= 0.049, HR 1.003, 95% CI (1.000-1.005)) and **IL-29** (p= 0.026, HR 1.084, 95% CI (1.010-1.164)) showed a significant influence on prognosis. The significant influence on survival observed in univariate analyses for IL-29 was confirmed in multivariate analyses. Beta-coefficients (β), hazard ratio (HR), 95% CI and p-values for the selected cytokines are shown in Table 4-19. Although **NRG1-beta1/HRG1-beta1** ((p= 0.129), HR 1.020, 95% CI 0.994-1.047)) and **PD-ECGF** ((p= 0.108) HR 1.302, 95% CI 0.944-1.797)) failed to significantly influence the prognosis as independent factor, the Cox's proportional hazard analyses using conditional forward stepwise algorithm based on likelihood rate did select them as variables of significant influence on the overall survival model (see below).

Table 4-19: Prognosis factors in multivariate analysis.

Cytokines	*Overall survival*					*Overall Model Fit*
	β	*HR*	*95% CI*		*p-value*	*p-value*
IL-29	0.081	1.084	1.010	1.164	0.026	0.004212
B7-1/CD80	4.351	77.574	1.138	5289.453	0.043	0.002494
PD-ECGF	0.264	1.302	0.944	1.797	0.108	0.001350
EG-VEGF/PK1	0.003	1.003	1.000	1.005	0.049	0.000134
NRG1-beta1 / HRG1-beta1	0.020	1.020	0.994	1.047	0.129	0.000286

β: coefficient provided by the Cox's regression model for a particular patient and cytokine; HR: hazard ratio (represents the factor by which the hazard changes for each one-unit increase of the cytokine expression); 95% CI: upper and lower limits of the confidence interval with a significance level of 0.05.

Table 4-19 Prognosis factors in the multivariate analyses. Cytokines significantly associated with survival in PDAC patients at multivariate analysis. Beta-coefficients (β), hazard ratio (HR), 95% CI and p-values for the selected cytokines are shown. The p-value last column represents the significance of the cytokines in the whole model as they are being introduced in the stepwise analysis.

4.2.3.4 Prognosis indexes (PI) of serum cytokines in PDAC patients

As combinations of biomarkers are likely to provide more accurate prognosis information, the most accurate subset of variables was sought using the conditional forward stepwise regression approach based on likelihood rate. To illustrate the interrelated effect on OS of the seven markers highlighted by the univariate analysis, the Cox's proportional hazard analysis was employed to select those variables jointly correlated with the survival. As a result of this analysis, a model containing only **IL-24** (p= 0.026, HR 1.042, 95% CI (1.003-1.023)) and **IL-29** (p=0.017, HR 1.014, 95% CI (1.005- 1.081)) was returned. The overall model fit was shown to be significant by the chi-squared statistic test (*p=0.0023*). So as to establish a prognosis index to determine PDAC patients OS, these cytokines β-coefficients were entered in the Equation 2 and the following PI model was generated:

Equation 4-1

$$PI_{univariate} = 0.042 \cdot (IL-24) + 0.014 \cdot (IL-29)$$

$PI_{univariate}$ represents the multivariate model derived from the combination of the underlined markers in the univariate analysis.

Regarding filtered cytokines obtained by multivariate analysis, a second statistically significant *(p=0.0003)* survival model was built and the following PI model was generated:

Equation 4-2

$$PI_{multivariate} = 4.351 \cdot (\text{B7-1/CD80}) + 0.03 \cdot (EG-VEGF\ /\ PK1) + 0.081 \cdot (IL-29) + 0.020 \cdot (\text{NGR1-beta1/HRG1-beta1}) + 0.264 \cdot (\text{PD-ECGF})$$

$PI_{multivariate}$ represents the multivariate model derived from the best of all

possible combinations using the cytokines in the multivariate analysis having being previously selected by the wrapper feature selection method.

Whether these PIs contributed to accurately model survival for this patient cohort was assessed by regression analyses. R-squared measurement was given as a proof of goodness of fit. Applying the equations for both PIs, scores of the proposed $PI_{univariate}$ and $PI_{multivariate}$ were calculated, ranked and correlated to OS. As expected, both survival models showed a logarithmic tendency when plotted against time.

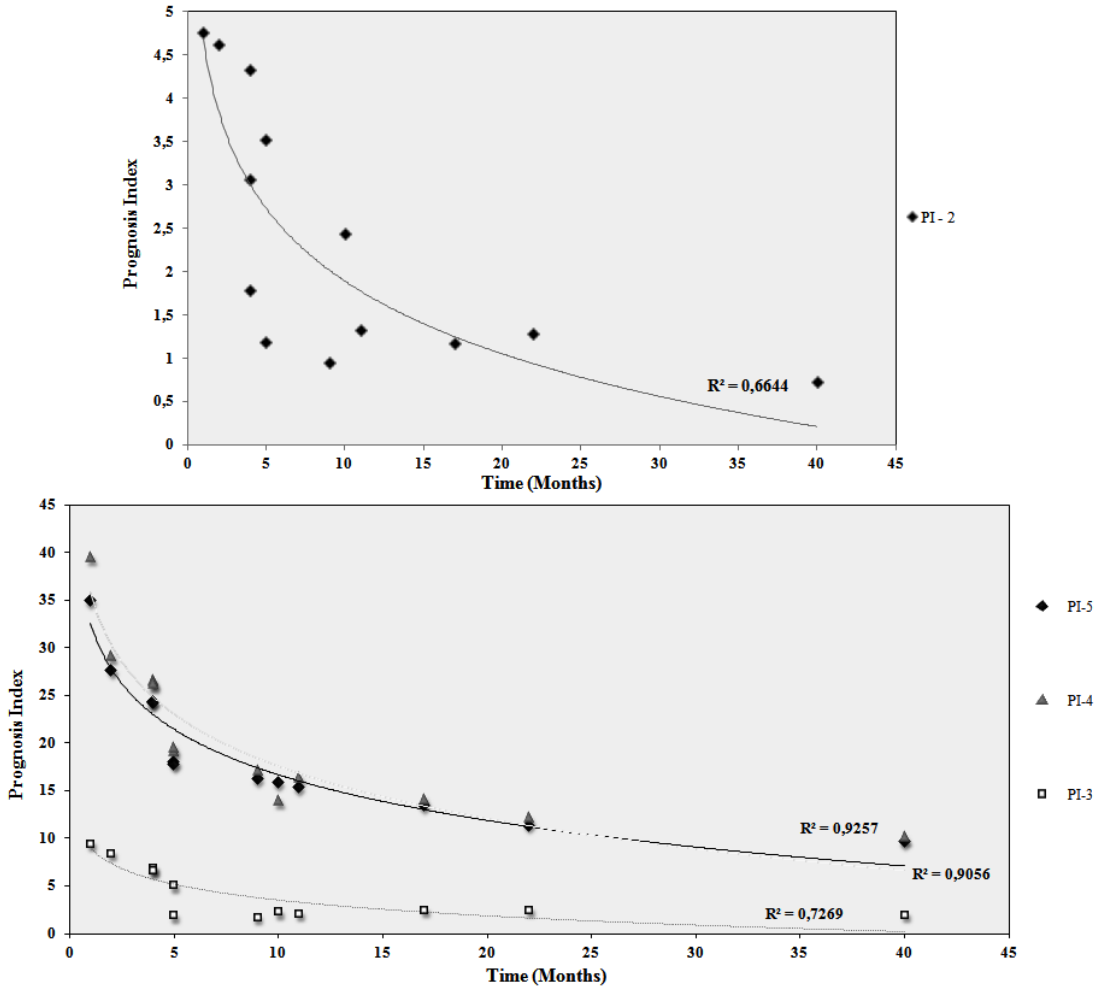

Figure 4.57 The Cox's regression model. Observed (denoted by square, diamonds and triangles points) and predicted (denoted by solid line) prognosis curves for the PDAC patients according to (A): univariate o (B): multivariate Cox's proportional hazard model analysis. As explained in the text, the stepwise procedure based on the likelihood ratio was used to select a model containing a statistically significant subset of prognosis factors. The three predicted prognosis curves in (B) are derived from the step 3 (where three cytokines

are included), step 4 (four cytokines included) and step 5 (five cytokines included) of this stepwise procedure. The predict survival curves are adjusted to a logarithmic distribution function, as expected. The coefficient of determination R2 is illustrative of the model goodness of fit. As coefficient attested, these models would yield useful predictions being the five cytokines multivariate model the most accurate, reaching a 92.6%. This means that our PI properly models approximately 93% of the survival variation.

Figure 4.57 depicts observed PI scores and predicted logarithmic adjustments for these models. For the multivariate model, although the overall model with five cytokines was probed to be statistically significant, regression analyses for models containing 3 and 4 cytokines were also evaluated. R-squared values obtained were 0.664, 0.727, 0.906 and 0.926 for $PI_{univariate}$ and 3, 4 and 5 cytokines $PI_{multivariate}$ respectively. These results can be translated into that a 66.4%, 72.7%, 90.6% and 92.6% respectively of the variability in the survival time was accounted for by the statistical model. All models yielded satisfactory results but multivariate model embracing B7-1/CD80, EG-VEGF/PK1, IL-29, NRG1-beta1/HRG1-beta1 and PD-ECGF stood out from the rest.

Prognosis index for multivariate model with these five cytokines ranged from 0 to 40 in our cohort. Patients were categorized into two groups according to their prognosis index: poor prognosis (PI>17) and fair prognosis (PI<17). Survival curves were then compared among these two prognosis groups (Figure 4.58, A). The proposed groups were shown to properly difference overall survival time: low (<5months) and high (>5months). Overall survival in these groups was highly statistically significant ($p<0.00056$). Prognosis index for univariate model was also depicted and it ranged from 0 to 5. According to this PI, patients were again categorized into two groups: poor prognosis (PI>1.5) and fair prognosis (PI<1.5). Furthermore, survival curves were compared among these two prognosis groups (Figure 4.58, B) and a significant correlation with the overall survival was also obtained as low (<5months) and high (>5months) survival. Overall survival in these groups was less but still significant ($p<0.004$) compared with the PI multivariate.

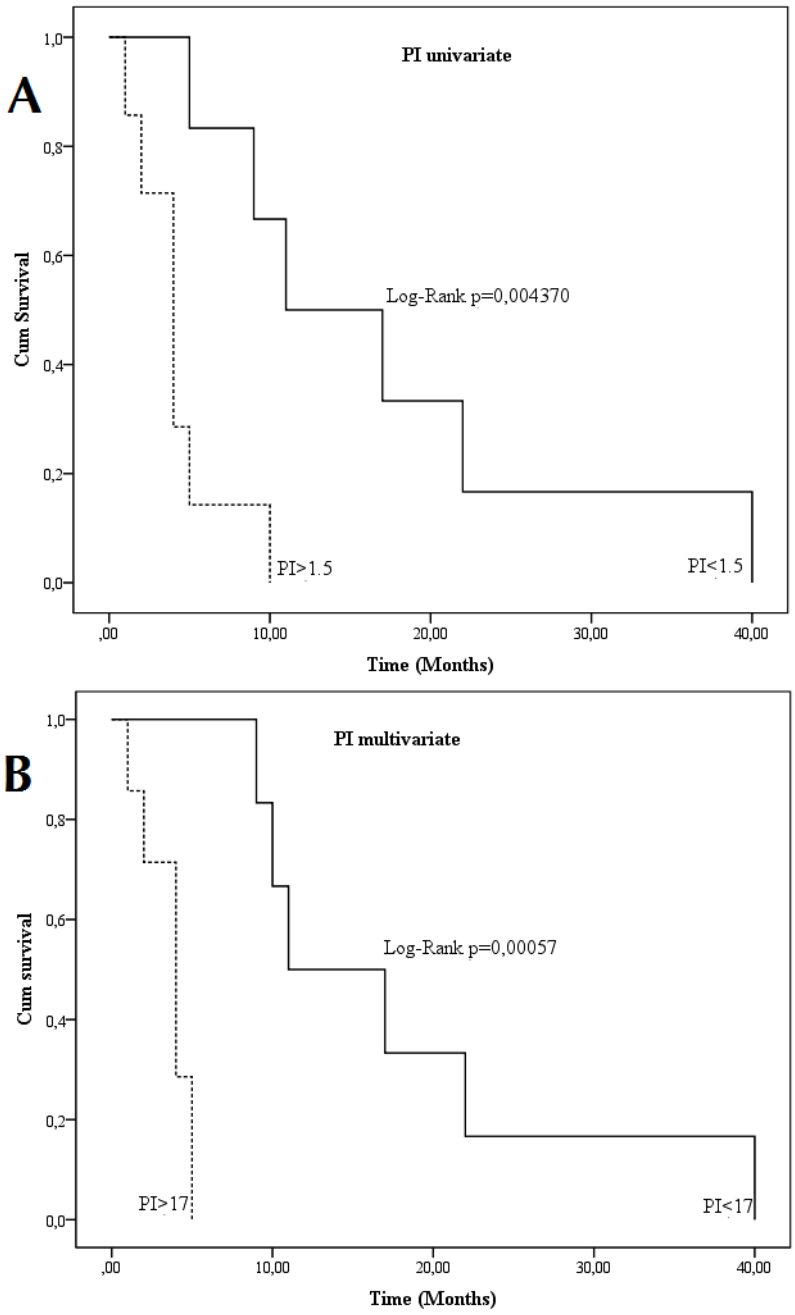

Figure 4.58 Kaplan-Meier PI survival curves. (A) shows survival plot for PI derived from univariate model, embracing 2 cytokines. A cut-off of 1.5 was chosen to divide cohort of patients in short (<5months) and long (>5 months) survival times. (B) shows survival plot for PI derived from multivariate model, embracing 5 cytokines. A cut-off of 17 was chosen to divide cohort of patients in short (<5months) and long (>5 months) survival times. The p-values for the Log-Rank tests are shown for both comparisons.

4.3 THE ROLE OF GPNMB/OSTEOACTIVIN (HIGHLIGHTED IN SECTION 4.2.1 AS PREDICTIVE BIOMARKER OF PDAC) IN THE CARCINOGENESIS OF PDAC

Using an extensive screening with a 507 human cytokine antibody array we previously described a significantly different expression of the cytokine GPNMB/Osteoactivin between PDAC patients and healthy volunteers.

Glycoprotein non-metastatic melanoma protein B (GPNMB), also known as Osteoactivin (OA), Dendritic Cell–Heparin Integrin Ligand (DC-HIL) or Hematopoietic Growth Factor Inducible Neurokinin-1 type (HGFIN) is a type I transmembrane protein which was first described as low to undetectable in malignant cells [189]. However, more recently studies have described GPNMB/Osteoactivin as a promoter of metastasis and invasion [202] in several cancers such as melanoma [183-184], uveal melanoma [185] glioma, [186] hepatocellular carcinoma [187] and breast cancer in which it has been described also as a prognosis indicator of recurrence [188]. It has been recently described an induction of GPNMB in the spinal cords of amyotrophic lateral sclerosis patients as an inductor of motor neuron degeneration [338].

Due to the potential role of this protein in PDAC development and progression, we assessed "*in vitro*" its involvement in the disease using both GPNMB-overexpressed transfected pancreatic cancer cell line Panc-1 (transfected Panc-1 cell cultures with the pCMV6-GPNMB-GFP plasmid; refered as the GPNMB+ cell line onwards) and GPNMB-silenced transfected pancreatic cancer cell line Panc-1 (transfected Panc-1 cell cultures with the HuSH pGFP-V-RS plasmid; refered as the GPNMB- cell line onwards).

4.3.1 Determination of transfection efficiencies

Thank to the presence of GFP in the plasmids (refer to section 3.5 for further details about them), transfection efficiency was examined by fluorescence-activated cell sorting (FACS) system and the efficiency of transfection was estimated from the percentage of cells expressing GFP.

For GPNMB+ all replicates showed high transfection efficiency when compared against untransfected cells.

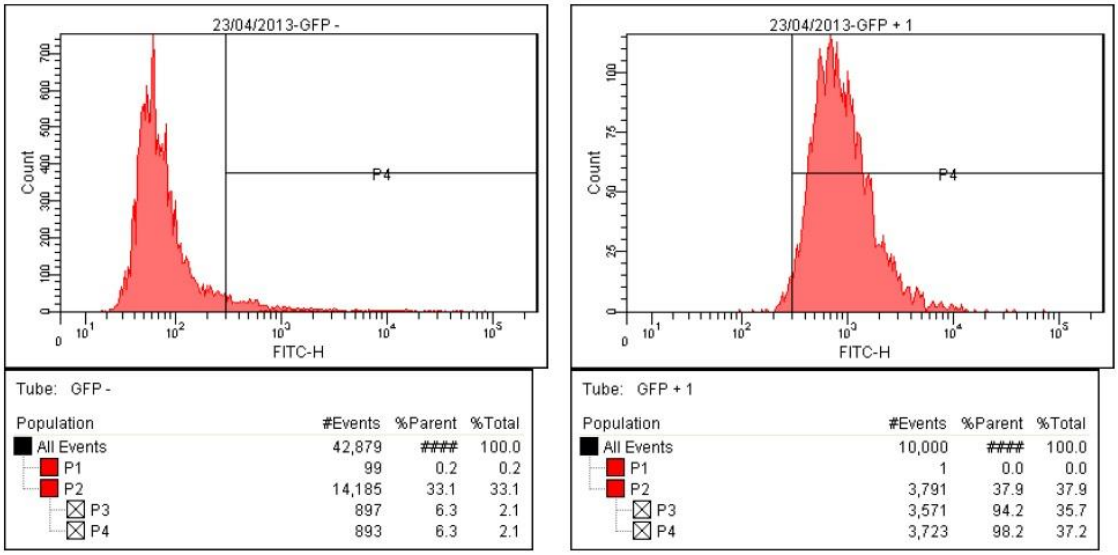

Figure 4.59 Transfection efficiencies measured by FACS. Transfection was carried out with the TransFast Transfection Reagent from *Promega* using an optimal ratio Transfection Reagent: DNA 1:1. Cells were incubated 1hr with DNA/TransFast Reagent/Serum Free Medium mix at 37°C. After that incubation time, the cells were overlay with 1ml of complete medium. After 72 hr, transfected cells were selected using G418 and maintained for three weeks. After that time, efficiency was measured.

For GPNMB-, 4 shRNA constructs (A, B, C and D) against multiple splice variants of the *gpnmb/osteoactivin* gen and a scrambled negative control were assessed. As shown in Figure 4.60, high efficiencies were also obtained ranging from 66 to 97% of GFP+ cells.

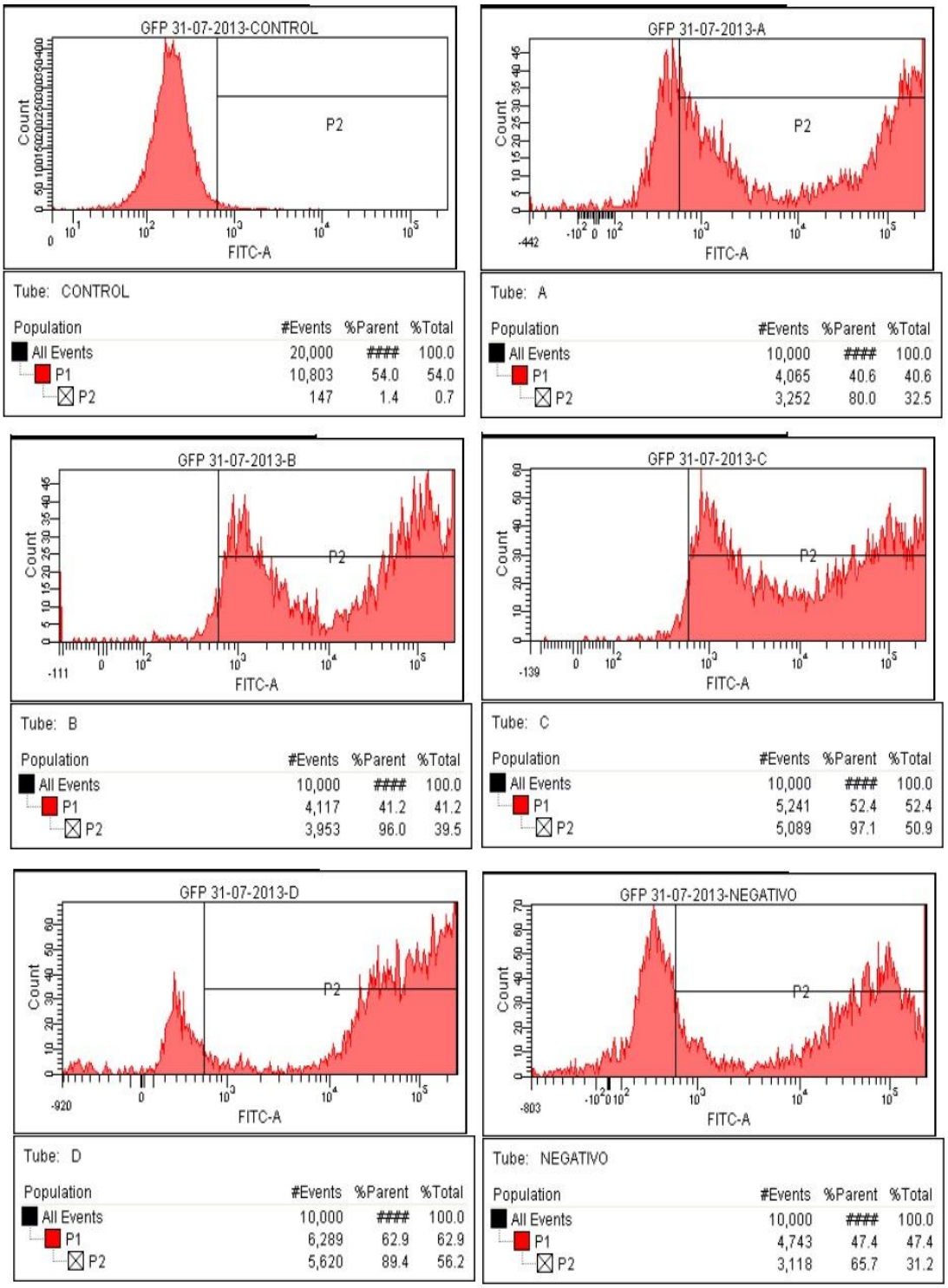

Figure 4.60 Transfection efficiencies measured by FACS. Transfection was carried out with the TransFast Transfection Reagent from *Promega* using an optimal ratio Transfection Reagent: DNA 1:1. Cells were incubated 1hr with DNA/TransFast Reagent/Serum Free Medium mix at 37°C. After that incubation time, the cells were overlay with 1ml of complete medium. After 72 hr, transfected cells were selected using puromycin and maintained for three weeks. After that time, efficiency was measured.

Although all samples showed high efficiencies of transfection, to verify the knockdown of the *gpnmb/osteoactivin* gene by the Sh RNA, we performed real time-PCR and immunoblotting.

First, we analyzed gene expression using real time PCR. The assay efficiency was calculated from the slope of the plot of Ct vs. log dilution series. The corresponding efficiencies for *gpnmb* and *gapdh* after applying Equation 3.4 (section 3.14.5) were 99.25% and 97.11% respectively. As amplification efficiencies were very close, the relative quantification could be performed and the efficiency of the gpnmb gene knockdown was calculated.

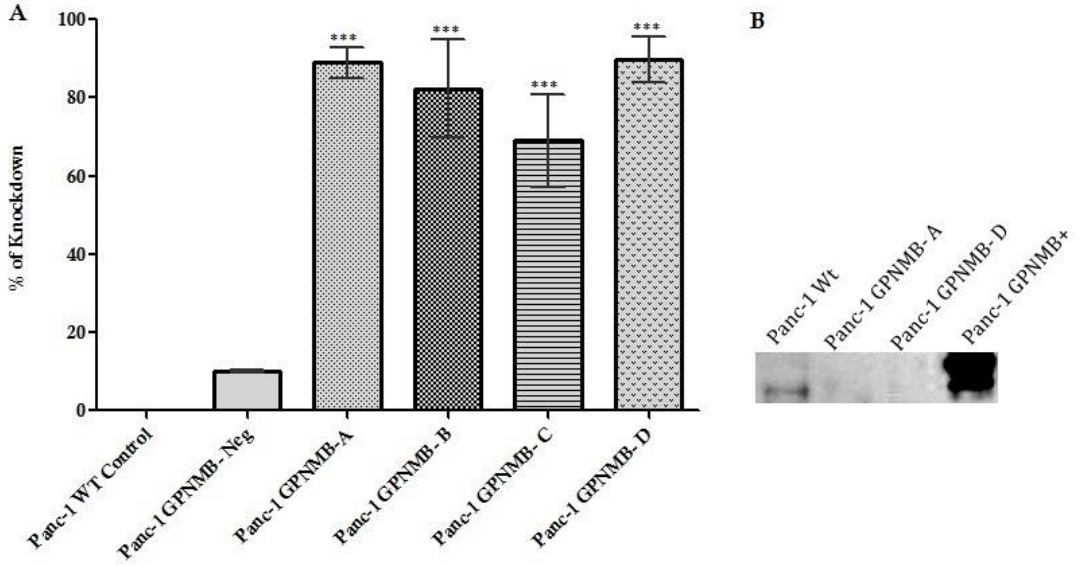

Figure 4.61 A. Comparison of the percentage of knockdown achieved by the 4 shRNA constructs (A, B, C and D) against and the scrambled negative. B. The efficiency of the knockdown was also assessed by western blot. The expression of the GPNMB/Osteoactivin protein was undetectable in cells transfected with the shRNA construct (results shown only for two of the 4 shRNA constructs). The induction of the protein expression in GPNMB+ is highly notorious. Each value is represented as mean ± S.D of triplicates from three independent qPCR assays. Asterisks indicate significant differences from control values (*: P< 0.0001; **: P<0.01; *: P<0.05).**

As shown in Figure 4.61, the efficiency of the knockdown was assessed both by real time-PCR and western blot. Real time-PCR determined percentages of inhibition in GPNMB expression ranged from 70% (Sh-C) to 90% (Sh-A or Sh-D). As expected, differences in inhibition between the wild type Panc-1 cell line and the transfected with the scramble Sh were no significant.

In the same way, we checked by western blot the GPNMB protein expression in the cell cultures. Silence pancreatic cancer cell showed no expression of this protein while GPNMB+ showed a remarkably enhancement of GPNMB expression (Figure 4.61, B).

4.3.2 Sub-cellular localization of GPNMB

Once again, the recombinant fusion construct with the GFP allowed us to detect the expression and sub-cellular localization of the GFP fusion protein in the Panc-1 cell line. It has been described that GPNMB/Osteoactivin is highly expressed at the surface of cancer cells but predominantly intracellularly in normal cells [184, 209, 339]. To further visually confirm the intracellular localization of GPNMB/Osteoactivin, confocal laser scanning microscopy was applied (Refer to section 3.9 for further details). Figure 4.62 shows representative results for Panc-1 (Wild type, non-transfected, A and B), Panc-1 GPNMB+ (transfected with the pCMV6-GPNMB-GFP plasmid, C and D) and Panc-1 GPNMB- (transfected with the HuSH pGFP-V-RS plasmid, E and F).

GPNMB/Osteoactivin expression pattern followed membranous and cytoplasmic pattern in the wild type Panc-1 cell line (Figure 4.62, A). When GPNMB/Osteoactivin was overexpressed, the main localization was at the membrane (Figure 4.62, C) what demonstrated that synthesis and processing were correct. The Gemcitabine plus Erlotinib combined therapy resulted in no change of the previously described pattern (Figure 4.62, B for thewild type Panc-1 cell line and D for the Panc-1 GPNMB+ cell line). No expression pattern was found in the Panc-1 GPNMB- cell line (Figure 4.62, E and F).

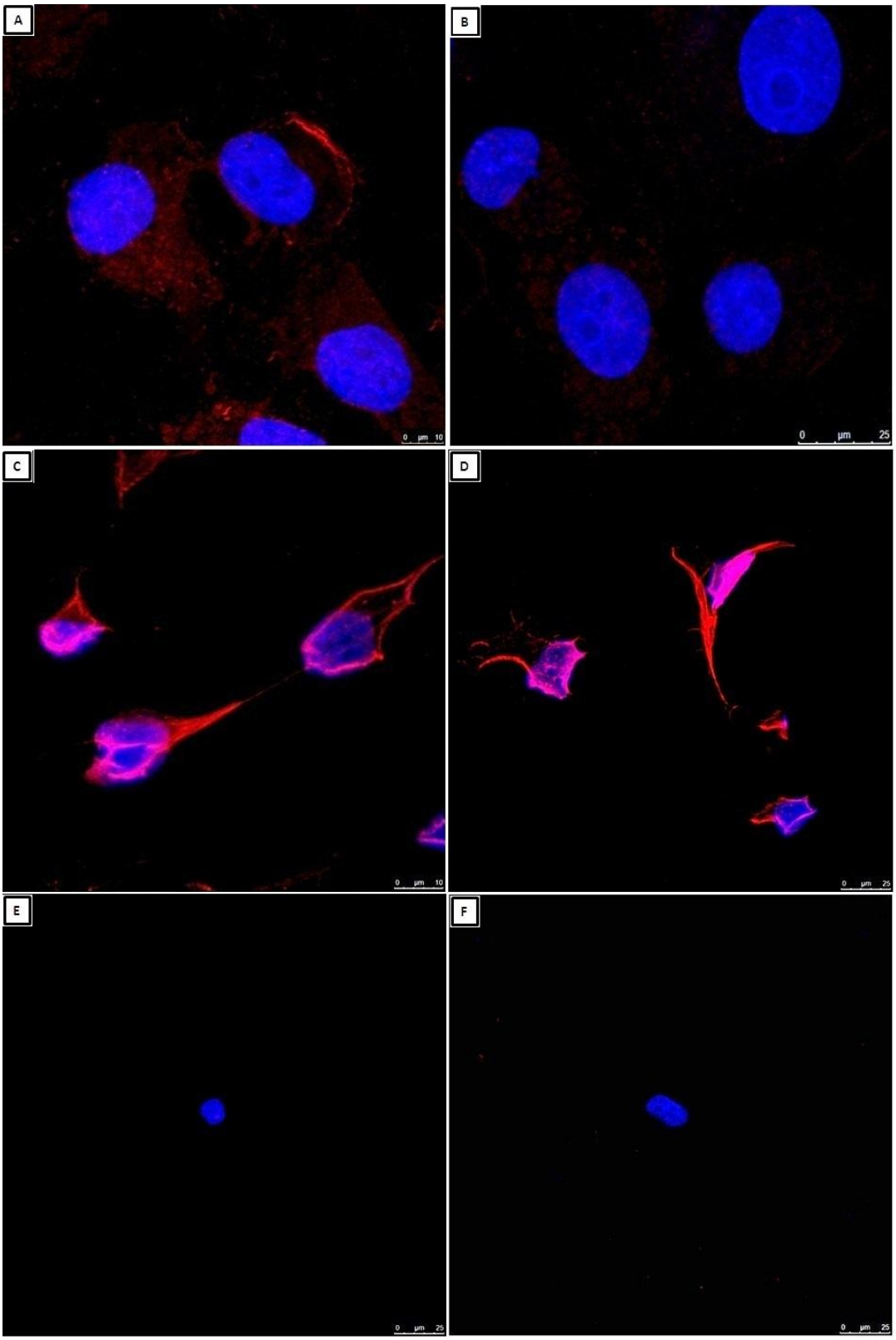

Figure 4.62 Localization of osteoactivin into pancreatic cancer cells Panc-1. The Panc-1 wild type cell line (A and B) was transfected with pCMV6-GPNMB-GFP (C and D) or with HuSH pGFP-V-RS (E and F) plasmids. Slides were examined using confocal laser scanning microscope.

4.3.3 Ectopic GPNMB/OA expression enhanced proliferation in pancreatic cancer cells.

4.3.3.1 PI staining and flow cytometry

The role of GPNMB/Osteoactivin on cell growth was examined by DNA synthesis as a marker for proliferation using flow cytometry (Refer to section 3.12 for further details about the methodology).

As shown in Figure 4.63, Figure 4.64 and Table 4-20, ectopic GPNMB/Osteoactivin expression enhanced the S-phase of the cell cycle which implied that GPNMB+ cells were more proliferative. Indeed, a higher percentage of GPNMB+ cells in the S-phase was observed when compared against the wild type Panc-1 cell line and this change was remarkably significant (Figure 4.65). It is noteworthy that the increase in the S-phase of GPNMB+ cells was also assessed after 48h of the Gemcitabine and Erlotinib combined treatment.

The GPNMB- cell line showed an augmented percentage of cells in the G0/G1 phase when compared against the wild type Panc-1 cell line and a reduced percentage of cells in the G2/M phase. This could represent that absence of the GPNMB protein could prevent cells to complete the cell cycle and accumulate in the G0/G1 phase. These effects were even more significant when the GPNMB- cell line was treated with Gemcitabine + Erlotinib combined therapy. However, the treatment combination was less effective blocking the cell cycle progression in the GPNMB- cell line as starting proliferating fractions (S and G2M) were already lower.

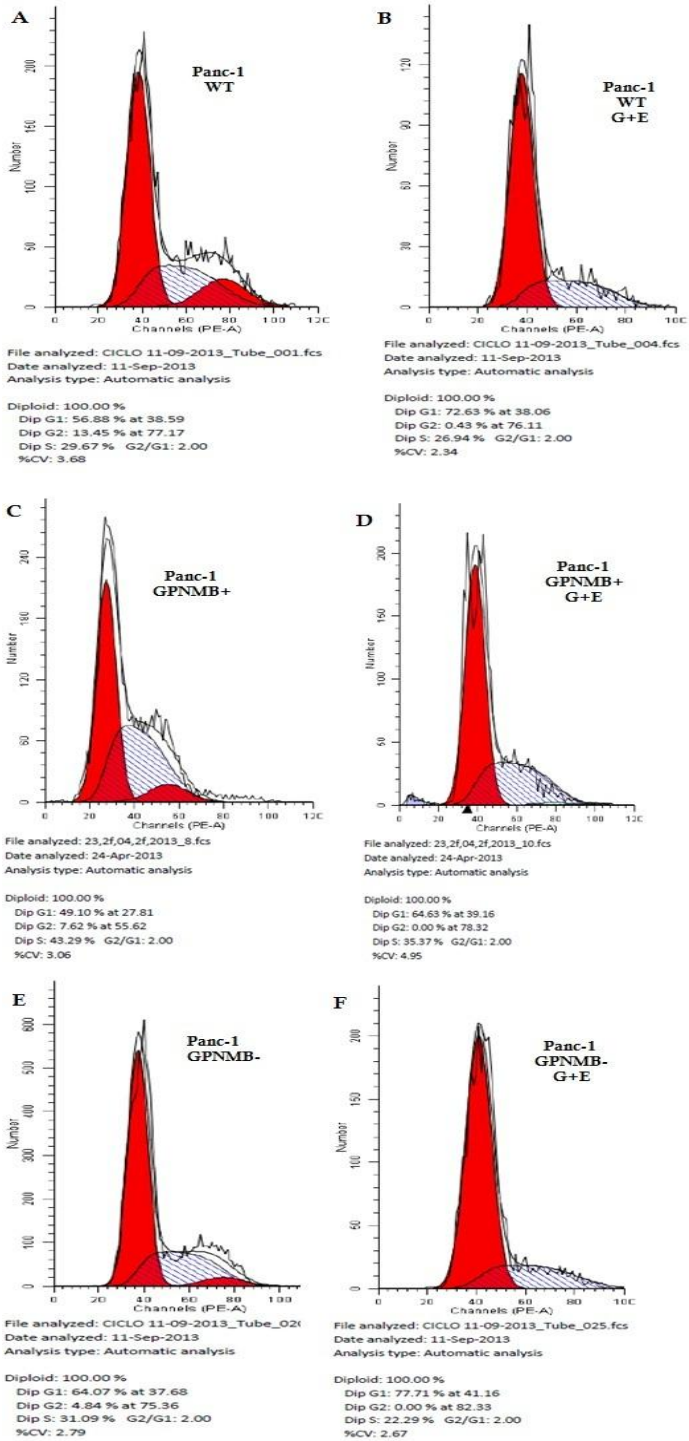

Figure 4.63 Representative histograms of flow cytometry performed in the wild type Panc-1 cell lines (A and B), in the GPNMB+ Panc-1 cell line (C and D) and in the GPNMB- Panc-1 cell line (E and F). Cells were also treated with 1+5μM of Gemcitabine+ Erlotinib (B, D and F). After the treatment, cells were harvested, fixed, stained with propidium iodide and analyzed for DNA content by flow cytometry.

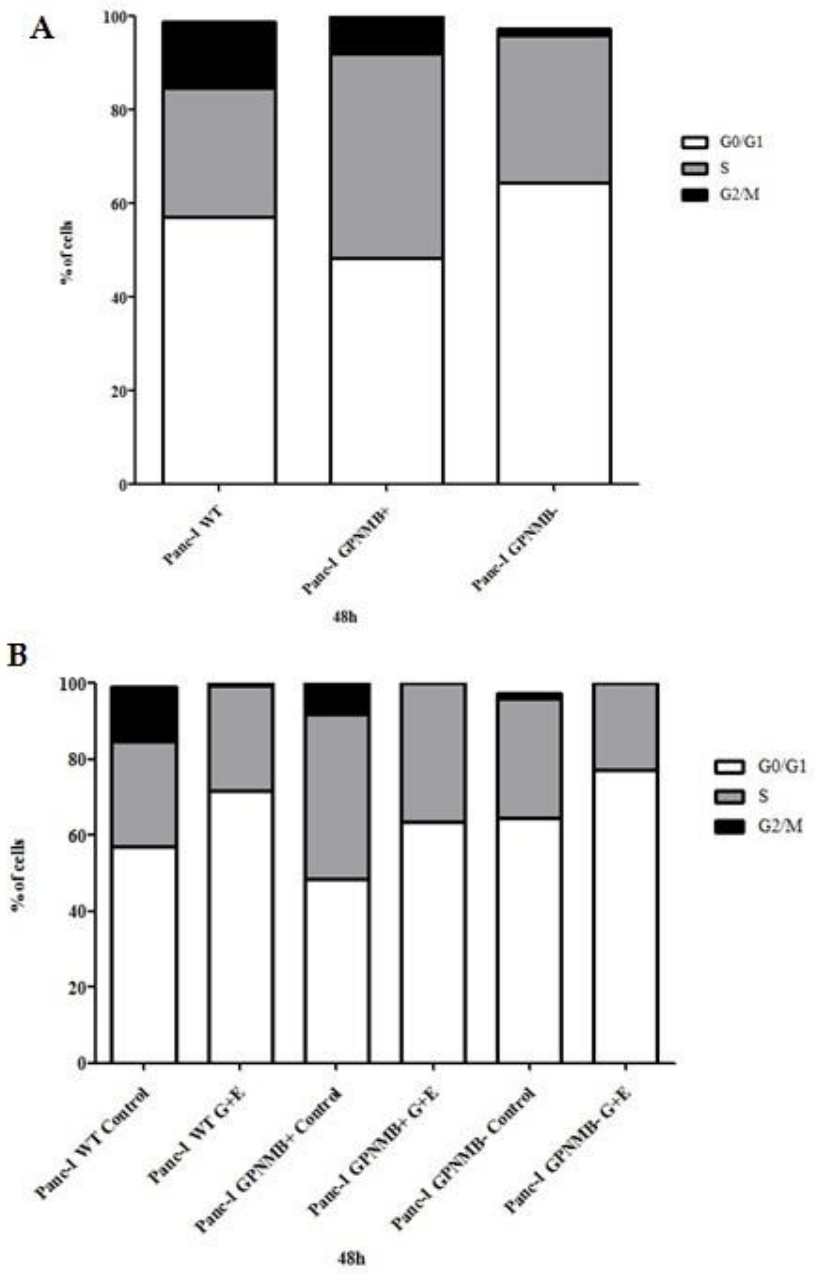

Figure 4.64 A, Percentages of cells in each phase of the cell cycle corresponding to thewild type, GPNMB+ and GPNMB- Panc-1 cell lines without any treatment. B, Percentages of cells in each phase of the cell cycle corresponding to the wild type, GPNMB+ and GPNMB- Panc-1 cell lines without and with the Gemcitabine and Erlotinib combined treatment.

Table 4-20 shows detailed information of percentages in each phase of the cell cycle.

Table 4-20 Percentages of cells in the three cell cycle phases after 48h of treatments. Data is expressed as mean ± S.D of at least 4 experiments.			
	G0/G1	**S**	**G2/M**
Panc-1 WT	57.02±2.66	27.72±3.11	14.20±1.67
Panc-1 WT G+E	71.73±2.71	27.62±2.7	3.85±2.1
Panc-1GPNMB+	48.40±2.71	43.51±1.34	9.74±3.74
Panc-1GPNMB+ G+E	63.46±3.09	36.54±1.38	0.0±0.0
Panc-1GPNMB-	64.34±0.92	31.56±0.6	1.49±0.24
Panc-1GPNMB- G+E	77.19±1.89	22.81±4.24	0.0±0.0

Figure 4.65 shows detailed information about the significantly differences in percentages of cells in every cell cycle phase.

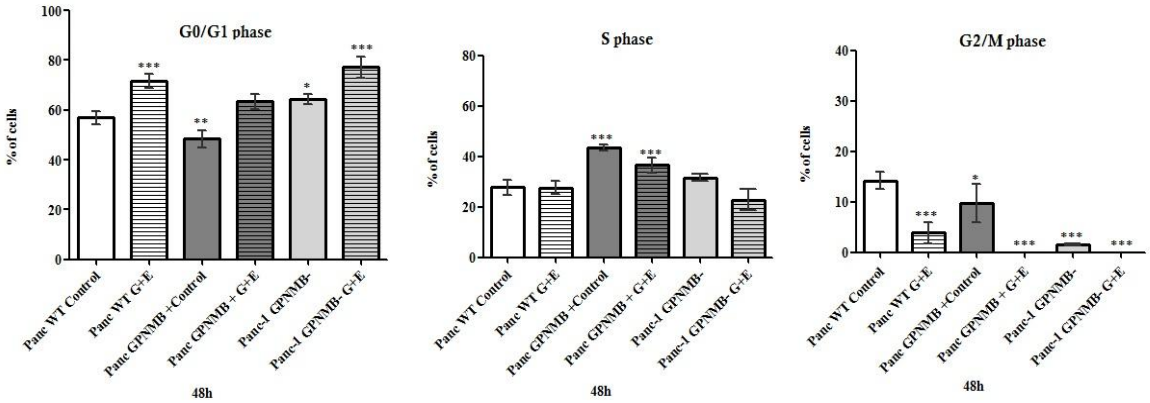

Figure 4.65 GraphPath Prism 5 plots representing the differences in Panc-1 WT, Panc-1 GPNMB+ and Panc-1 GPNMB- cell populations in G0/G1, S and G2/M phases. ***: P< 0.0001; **: P<0.01; *: P<0.05 (one-way ANOVA).

4.3.3.1 BrdU incorporation

In order to complement the cell cycle analysis obtained by flow cytometry, BrdU staining procedures were carried out. Cell proliferation was followed for 12 h at regular intervals of two hours by BrdU incorporation assay. Besides cell

proliferation was measured for 24 and 48 h after addition of Gemcitabine and Erlotinib.

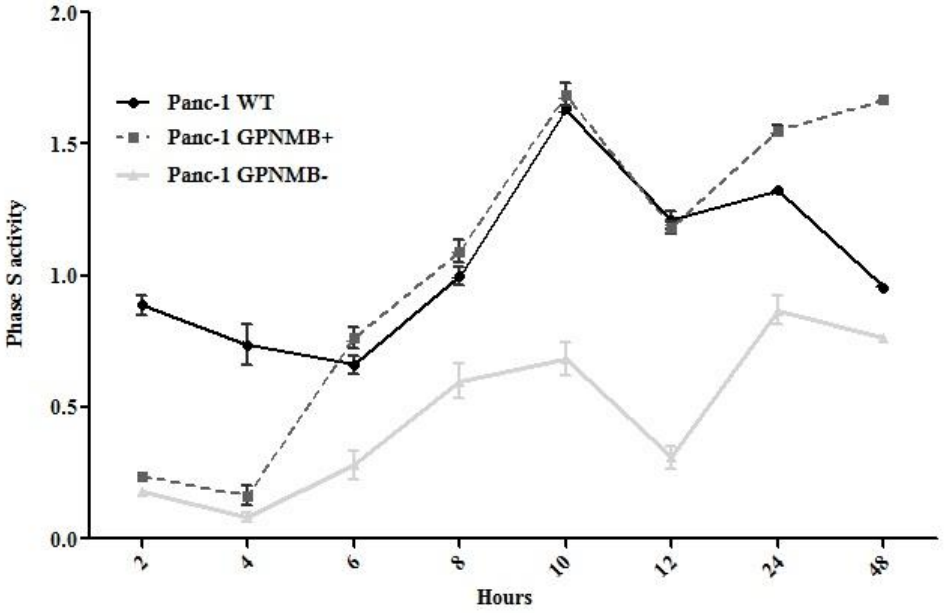

Figure 4.66 Detection of bromodeoxyuridine (BrdU) incorporated into DNA in the wild type Panc-1 cell line, the GPNMB+ Panc-1 cell line and the GPNMB- Panc-1 cell line every two hours.

As shown in Figure 4.66, the GPNMB+ cell line, especially between 6 and 10h, incorporated higher amount of BrdU which could be translated in an increased phase S activity and proliferation. For the GPNMB- cell line, the phase S activity and the proliferation were diminished when compared against the wild type Panc-1 cell line and also against the GPNMB+ cell line.

Next, the effects of the treatment were analyzed at 24 and 48h. Results are depicted in Figure 4.67. A shows the mean ± SD of at least three independent experiments of the Panc-1 wild type, the GPNMB+ and the GPNMB- cell lines without any treatments. These results were consistent with previous one. The GPNMB+ cell line resulted in an increased phase S activity and proliferation both at 24 and 48h. For the GPNMB- cell line, the proliferation was inhibited, being half as high as the GPNMB+ cell line at 48h.

In Figure 4.67 B, the proliferation inhibition after 24 and 48h of the treatment is depicted. After 24h of the treatment, the most important inhibitory effect was obtained in the GPNMB- cell line with 80% of inhibition of BrdU incorporation compared against the GPNMB- control samples.

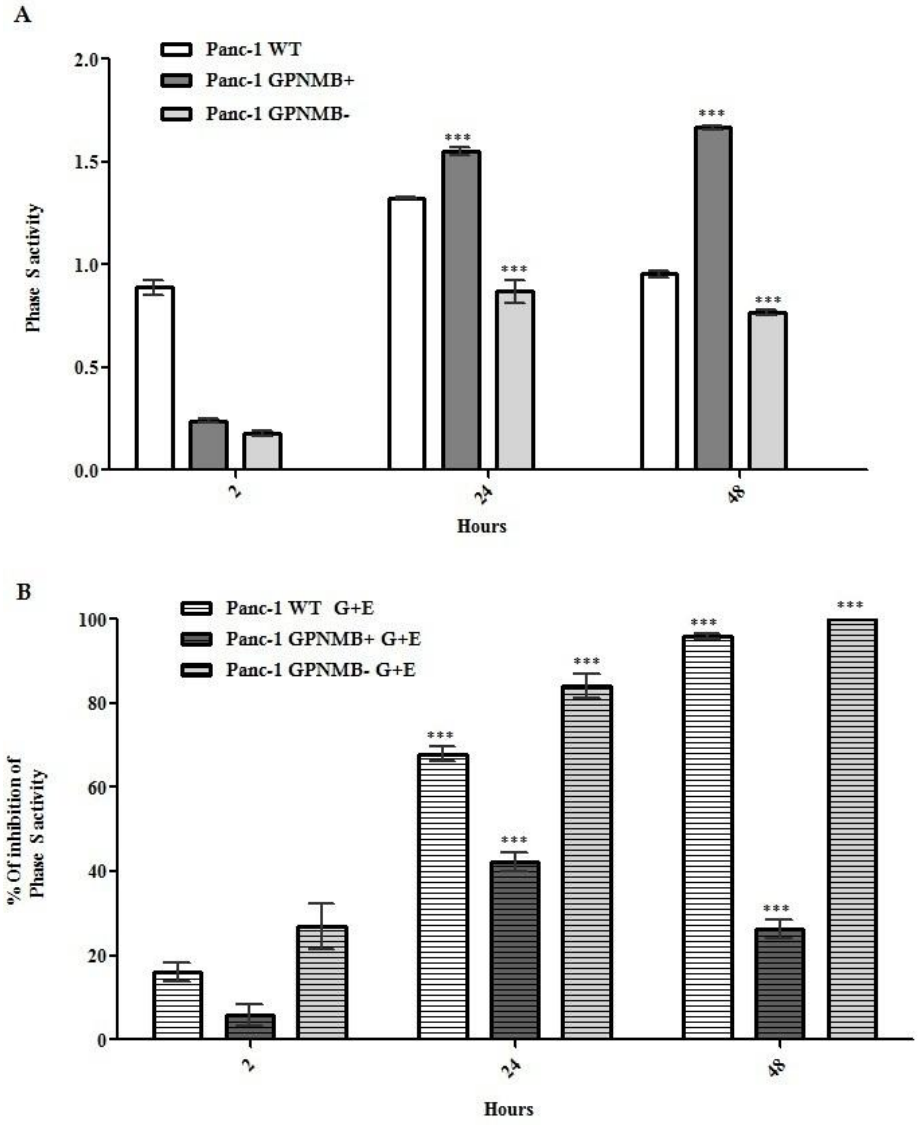

Figure 4.67 A shows phase S activity of the wild type Panc-1, GPNMB+ and GPNMB- cell lines without being treated. B shows the inhibition achieved by the Gemcitabine and Erlotinib treatment after 24 and 48h of incubation compared with their corresponding controls.

After 48h of the treatment, the GPNMB- cell line tendency was the same, reaching a 100% of inhibition. The Gemcitabine and Erlotinib combined treatment on the Panc-1 wild type cell line exerted an arrest of the cell cycle in the G0/G1 phase

(see section 4.1.5.1) and a 90% inhibition in phase S activity. In consistency with our previous results, treatment in the GPNMB+ cell line seemed to exert no effect over proliferation especially at 48h, when the inhibition in the proliferation did not reach a 30%.

4.3.4 GPNMB/OA expression in pancreatic cancer cells is associated with resistance to apoptosis.

4.3.4.1 Analysis of translocation of phosphatidyl serine (PS) to the outer membrane of the cells

To determine whether ectopic GPNMB/OA expression was linked to an enhancement or reduction of the apoptosis, we evaluated the presence of PS on the cell surface using APC-conjugated Annexin-V. Here we changed from FITC-conjugated Annexin-V (used in section 4.1.4.1) to APC-conjugated Annexin-V to avoid any interference of the GFP with the FITC signal.

The wild type Panc-1, GPNMB+ and GPNMB- cell lines subjected either to no treatment or to the Gemcitabine + Erlotinib combined therapy were analyzed. Besides, analysis of the scramble negative Sh cell line was performed as a control. Dot plots showing the percentages of APC and/or IP positive cells are shown in Figure 4.68.

As expected, the wild type Panc-1 cell line without being subjected to any treatment was negative for both Annexin V and PI, indicating that there was not much cell damage. Regarding the GPNMB+ cell line, results were very similar and no significantly different from the former (See Figure 4.70 for specific data referring to the statistical analyses). However, the GPNMB- cell line resulted in a high percentage of Annexin-V positive cells (49.34±5.2). Also as expected, the scramble negative Sh sample showed again very similar and no significantly different results from the wild type Panc-1 cell line.

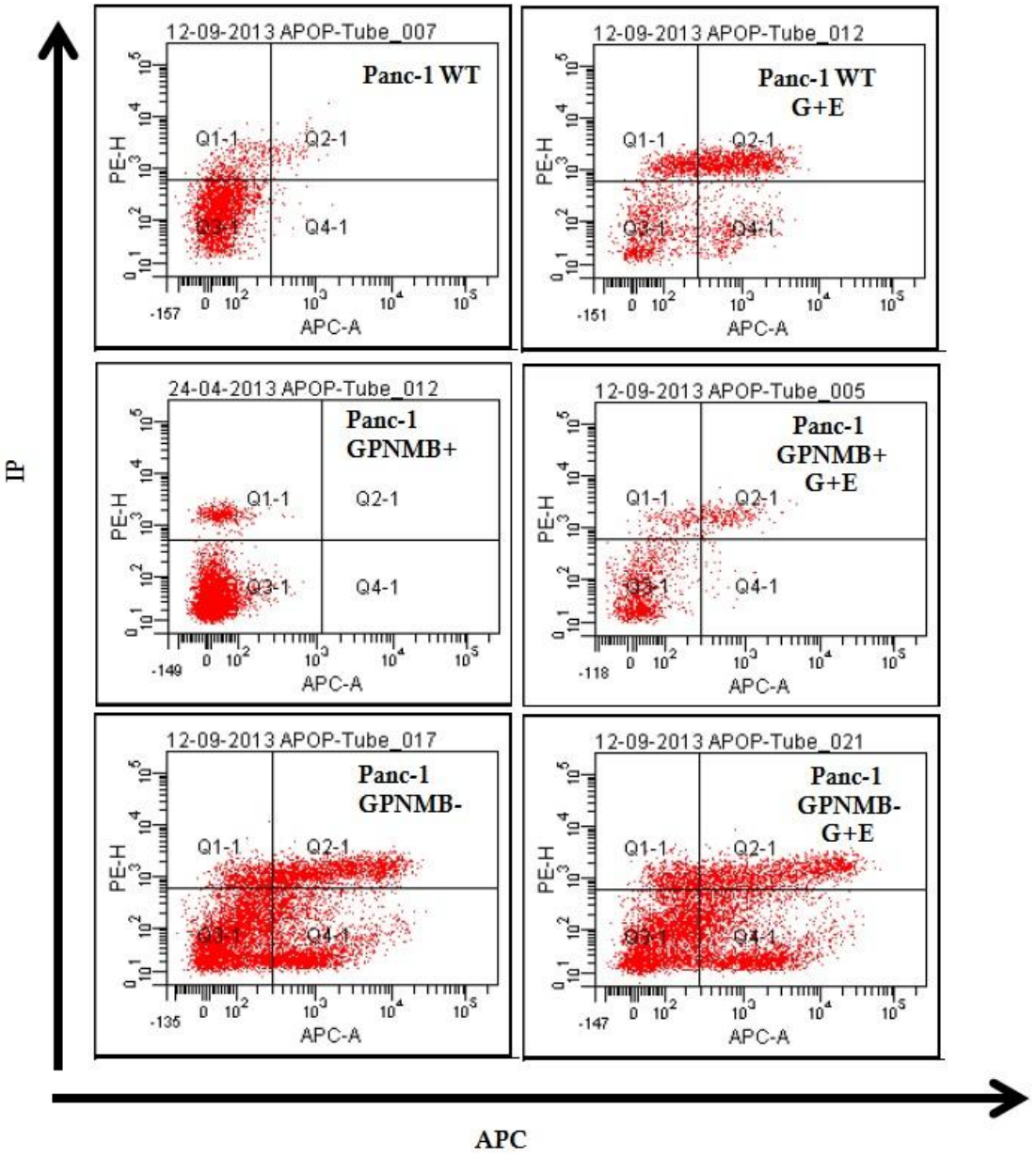

Figure 4.68 Bivariate PI/Annexin V analyses. Apoptotic effect of GPNMB/Osteoactivin ectopic expression on the wild type Panc-1, GPNMB+ and GPNMB- cell lines. Using the Annexin V-affinity assay, the number of apoptotic cells in suspension was determined.

After 48h of the Gemcitabine and Erlotinib treatment, the wild type Panc-1 cell line achieved 56.94±3.5% of Annexin-V positive cells. The GPNMB+ cell line resulted resistant to the apoptosis induced by the chemicals, with only 17.6 ±2.94 % of the cells undergoing apoptosis. Although the treatment of the GPNMB- cell line resulted in a high percentage of Annexin-V positive cells, it was no significantly different for results obtained for this cell line without the treatment.

Detailed results for the wild type Panc-1, GPNMB+ and GPNMB- cell lines are below summarized in Figure 4.69 and Table 4-21. Figure 4.69 depicts percentages of live, apoptotic and necrotic cells without treatment or after the Gemcitabine + Erlotinib combined treatment. Their corresponding percentages are included in Table 4-21.

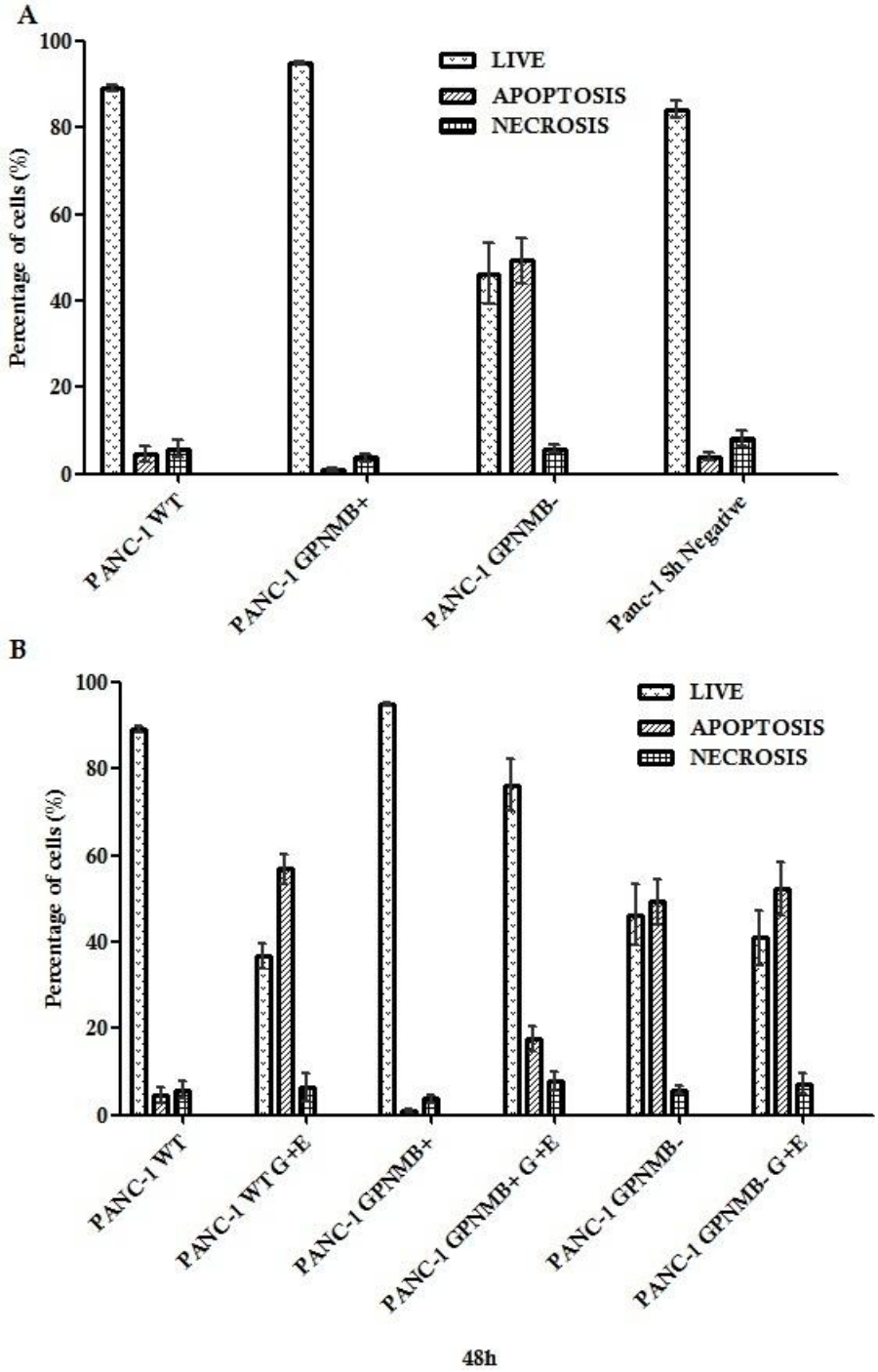

Figure 4.69 Apoptosis was evaluated by cytometric analysis (See Section 3.13 for further details). A shows the percentage of living, apoptotic and necrotic wild type, GPNMB+ and

GPNMB- cell lines without treatment. B shows the percentage of living, apoptotic and necrotic wild type, GPNMB+ and GPNMB- cell lines without and after 48h of the Gemcitabine and Erlotinib combined treatment. Data is expressed as mean ± S.D of at least 4 experiments. Statistical analyses are detailed in Figure 4.70.

Table 4-21 Percentages of the wild type Panc-1, GPNMB+ and GPNMB- cell lines living, apoptotic and necrotic cells after 48h of treatments. Data is expressed as mean ± S.D of at least 4 experiments.

	Live	Apoptosis	Necrosis
Panc-1 WT	89.07±0.7	4.6±1.83	5.79±2.01
Panc-1 WT Gem+Erl	36.62±2.88	56.94±3.5	6.33±3.16
Panc-1 GPNMB+	95.23±1.08	0.97±0.46	3.78±0.85
Panc-1 GPNMB+ Gem+Erl	76.30±5.98	17.63±2.94	7.96±2.14
Panc-1 GPNMB-	46.26±7.1	49.34±5.2	5.83±0.86
Panc-1 GPNMB- Gem+Erl	40.94±6.28	52.37±6.05	7.23±2.23
Panc-1 GPNMB- Negative	84.31±2.05	3.96±0.96	8.07±1.82

Statistically significant changes between the cell lines are shown in Figure 4.70.

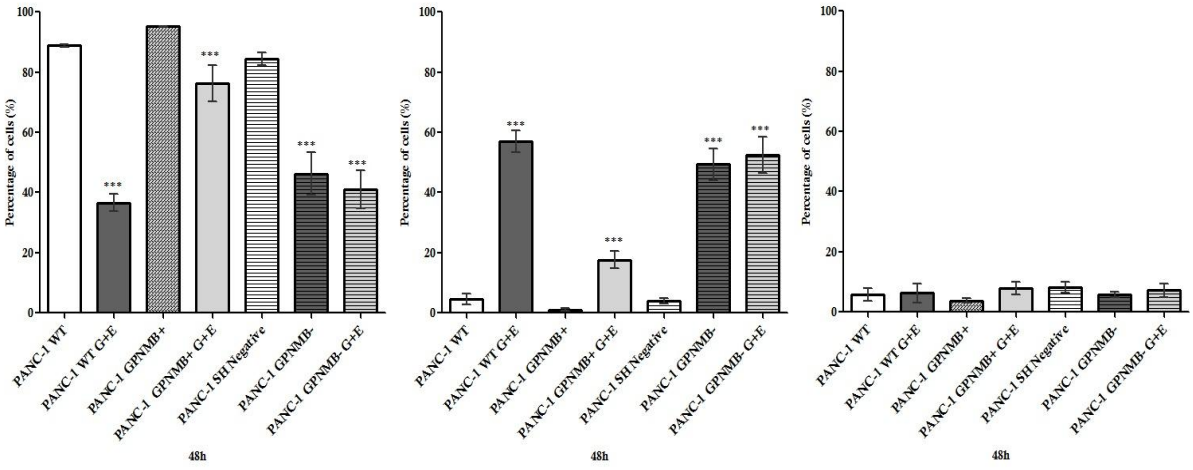

Figure 4.70 GraphPath Prism 5 plots representing the differences in living, apoptotic and

necrotic cell percentages between cell lines. ***: P< 0.0001; **: P<0.01; *: P<0.05 (one-way ANOVA).

As described before for the cell cycle analysis, the Gemcitabine and Erlotinib treatment exerted minimal effect over apoptosis in the GPNMB+ and the GPNMB- cell lines.

4.3.4.2 PCR array of genes related to apoptosis

To widen our knowledge about apoptosis induction in our models, we analyzed the expression of genes related to this procedure. As the treatment failed to show any significant results, only the non-treated wild type Panc-1, GPNMB+ and GPNMB- cell lines were subjected to gene expression analyses.

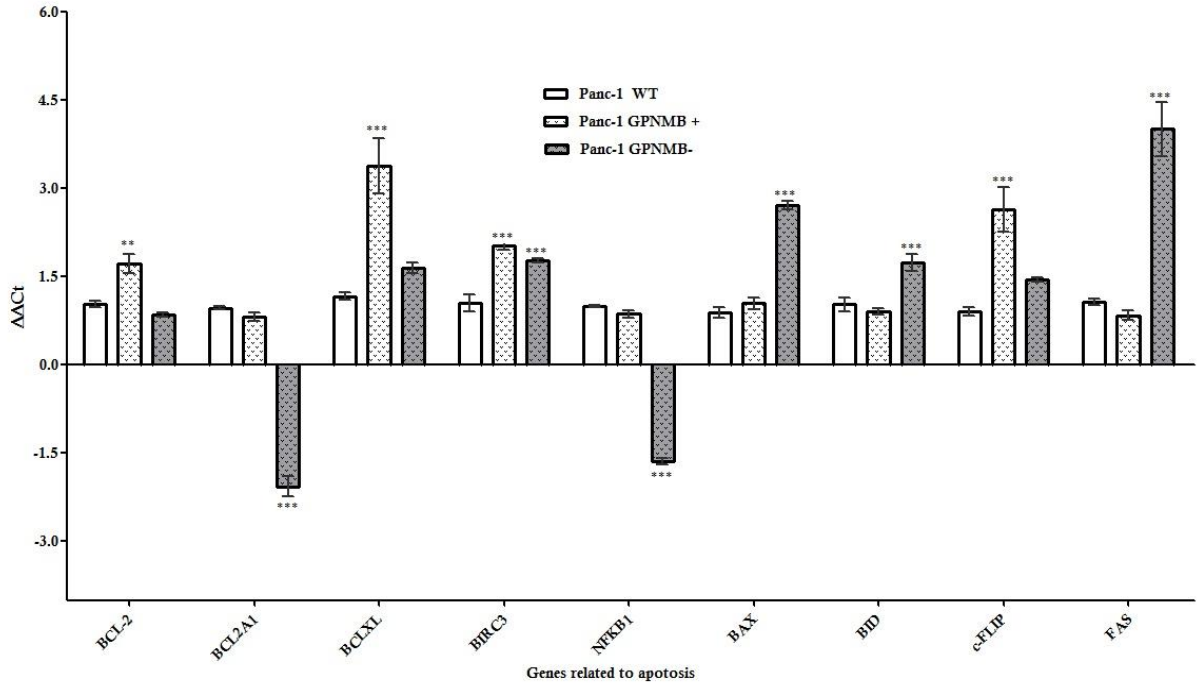

Figure 4.71 Up and down-regulation of genes related to apoptosis. Analysis of relative gene expression data using real-time quantitative PCR and the $2^{(-\Delta\Delta Ct)}$ Method.

Figure 4.71 depicts relative expression of genes related to the apoptotic process. Ectopic expression of GPNMB/Osteoactivin is related to a significantly enhancement of anti-apoptotic genes, such as Bcl-2, Bcl-X_L, c-FLIP and BIRC3. c-

FLIP is a master anti-apoptotic regulator and resistance factor that suppresses tumour necrosis factor-α (TNF-α), Fas-L and TNF-related apoptosis-inducing ligand (TRAIL)-induced apoptosis, as well as apoptosis triggered by chemotherapy agents in malignant cells [118]. BIRC3, also known as cIAP-1, belongs to the inhibitor of apoptosis protein (IAP) family, a family of anti-apoptotic regulators that block cell death in response to diverse stimuli through interactions with inducers and effectors of apoptosis [340].

On the other hand, regarding pro-apoptotic genes, ectopic expression of GPNMB/Osteoactivin did not show any significant change in these genes. However, suppression of GPNMB protein through the Sh vector did enhance expression of pro-apoptotic genes such as Bax and BID. BID is a substrate of caspase-8. Caspase-8 cleaves Bid into tBid which initiates the mitochondrial apoptosis pathway leading to release of cytochrome c (Cyt. C) and Smac/DIABLO from the mitochondria [341]. Besides, suppression of GPNMB expression restored initial expression values of pro-apoptotic genes, which were up-regulated by GPNMB expression. Interestingly, the anti apoptotic gene BCL2A1 was remarkably down-regulated after GPNMB expression suppression. BCL2A1 is overexpressed in a variety of cancer cells, including hematological malignancies and solid tumours and may contribute to tumour progression[342]. Another significantly down-regulated gene after GPNMB gene silence was NF-κB which could be related to the GPNMB- cell line attenuated proliferation and induced apoptosis.

Lastly, the expression on Fas was remarkably induced after GPNMB knockdown. This could mean that apoptosis could be induced via the extrinsic pathway, through cell surface death receptor stimulation.

Taken together, these results imply that GPNMB knockdown activates both extrinsic and intrinsic apoptotic pathways, exhibiting apoptotic effects against pancreatic cancer cells.

4.3.4.3 Analysis of proteins implicated in apoptosis by western blot

In order to complete the analysis of the apoptosis, we further studied apoptotic proteins expression alteration by western blot. Bcl-2, Bcl-X_L and Bax protein expression and Bcl-2/Bax and BCL-X_L ratios were also determined.

Cell lysates were prepared from wild type Panc-1, GPNMB+ and GPNMB- cell without any treatment or treated with the Gemcitabine plus Erlotinib (1+5μM) combined therapy for 48h and used for western blot studies. Figure 4.72 depicts representative western blot images for the Bcl-2 family proteins studied

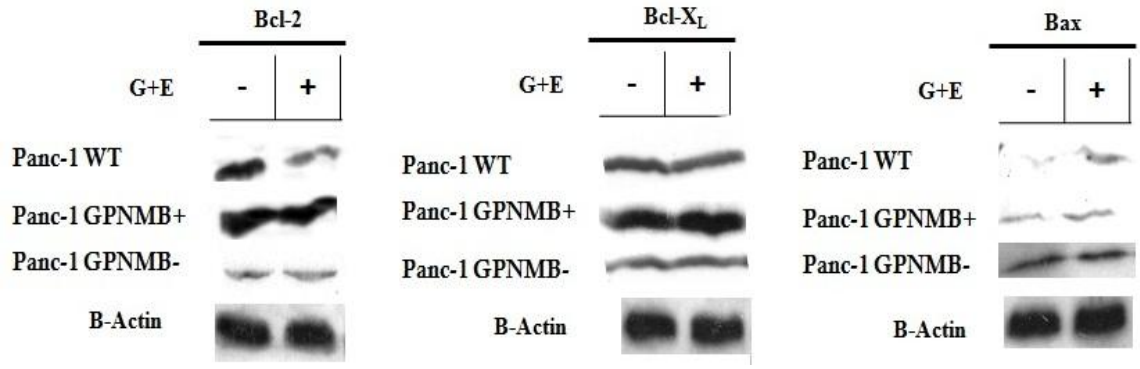

Figure 4.72 The effects of ectopic expression or knockdown of GPNMB/Osteoactivin over the expression of BCL-2 family proteins were analyzed by western blot. For further details see section 3.17. Beta-actin was used as a loading control.

Ectopic expression of the GPNMB (GPNMB+ cell line) resulted in an induction of the BCL-2 protein expression of 1.7±0.05 (Figure 4.73). This was also accompanied by an enhancement in the Bcl-X_L protein expression, very similar to the former. Finally, the Bax expression, although present and measurable, was not enough to compensate the induction of the antiapoptotic proteins. Indeed, the Bcl-2/Bax and Bcl-X_L /Bax ratios were bigger than 1 which implied resistance to apoptosis (Table 4-22).

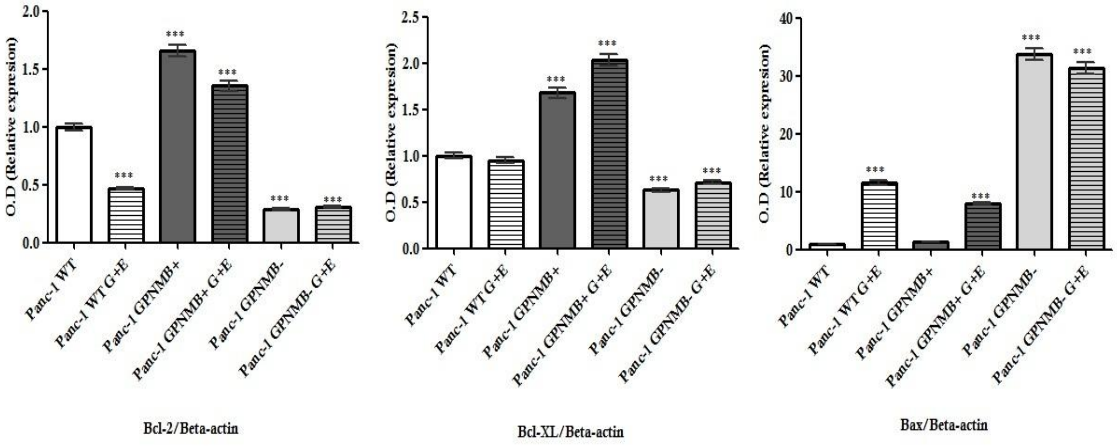

Figure 4.73 Quantitative analysis of the immunoreactive Bcl-2, Bcl-X_L and Bax proteins in the wild type Panc-1, GPNMB+ and GPNMB- cell lines without treatment and after 48h of the Gemcitabine and Erlotinib combined treatment. The autoradiographs were scanned and the level of each protein expression was quantified by densitometry. Results are expressed as optical density relative to the beta-actin. Each value is represented as mean ± S.D of 3 independent determinations. Asterisks indicate significant differences from control values (*: P< 0.0001; **: P<0.01; *: P<0.05).**

On the contrary, GPNMB/Osteoactivin knockdown resulted in a remarkable inhibition of the expression of antiapoptotic proteins, Bcl-2 and Bcl-X_L (Figure 4.73). Besides, there was a notorious induction of Bax expression (33.71±1.03). Indeed, Bcl-2/Bax and Bcl-X_L /Bax ratios were lower than 1 which implied sensitivity to apoptosis (Table 4-22).

Table 4-22 Disruption of Bcl-2/Bax and Bcl-X_L/Bax balances.		
	Bcl-2 /Bax ratio	**Bcl-X_L/Bax ratio**
Panc-1 WT	1.06±0.04	1.024±0.04
Panc-1 WT G+E	0.04±0.004	0.08±0.004
Panc-1 GPNMB+	1.25±0.02	1.25±0.019
Panc-1 GPNMB+ G+E	0.17±0.006	0.27±0.01
Panc-1 GPNMB-	0.01±0.0003	0.02±0.005
Panc-1 GPNMB- G+E	0.009±0.0001	0.02±0.006

4.3.5 GPNMB/Osteoactivin enhanced invasion and migration

4.3.5.1 Migration assay through basement membrane

We examined the influence of increased and decreased GPNMB/Osteoactivin expression over cell motility, invasion and metastasis. The invasion process consists of the secretion of matrix metalloproteases (MMP) to degrade basement membrane, the activation of endothelial cells and the migration across the basement membrane. Cell migration may be evaluated through several different methods, the most widely accepted of which is the Boyden Chamber assay. The Boyden Chamber system uses two-chamber system in which a porous membrane provides an interface between the two chambers. Cells are seeded in the upper chamber and chemoattractants placed in the lower chamber. Cells in the upper chamber migrate toward the chemoattractants by passing through the porous membrane to the lower chamber. Migratory cells are then stained and quantified.

Millipore's QCM Endothelial Cell Invasion Assay was applied to provide an in vitro model to screen whether GPNMB/Osteoactivin can regulate invasion. After removing non-invading cells, invading cells were stained and quantified. Results are depicted in Figure 4.74.

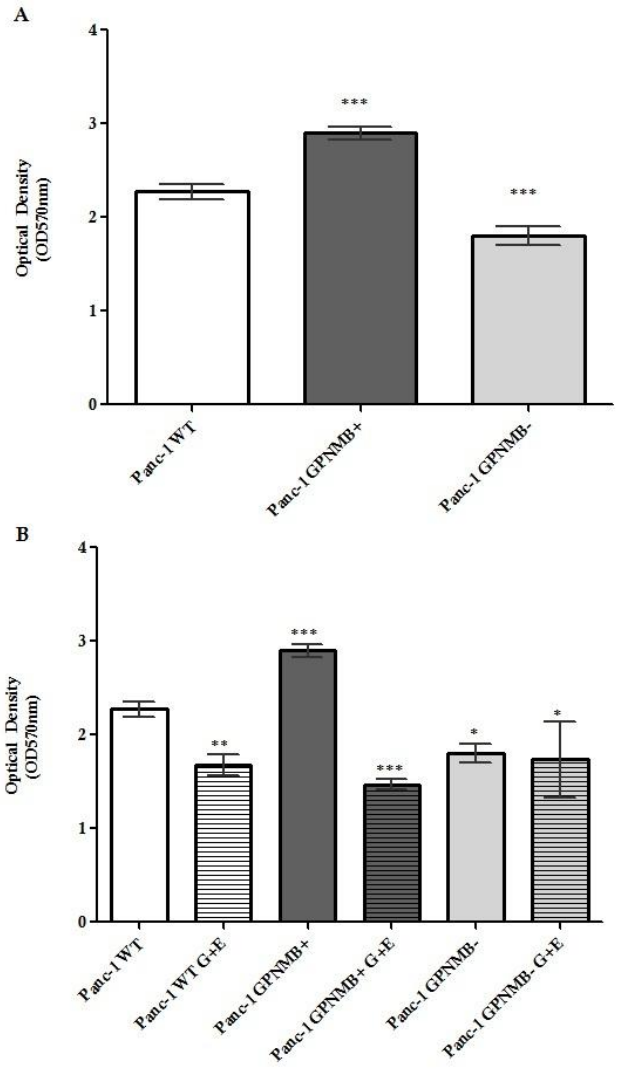

Figure 4.74 Pancreatic cancer cells were seeded on top of Millipore Endothelial Invasion chambers. 300 µL of 10^6 0% FBS-DMEM suspension cells was applied on the top of the chamber while 10% FBS-DMEM was applied to stimulate pancreatic cancer cell invasion. Cells were allowed to invade through basal membrane for 48 hours at 37ºC 5% CO_2 incubator before being subjected to staining. A shows results for the wild type, GPNMB- and GPNMB+ cell lines without any treatment. B shows results for the wild type, GPNMB- and GPNMB+ cell lines without treatment and with 48h of the Gemcitabine and Erlotinib combined treatment. Each value is represented as mean ± S.D of 3 independent determinations. Asterisks indicate significant differences from control values (*: P< 0.0001; **: P<0.01; *: P<0.05).**

Our results showed that ectopic expression of GPNMB/Osteoactivin in the pancreatic cancer cell line Panc-1 significantly increased the number of cells that migrated into the lower compartment. This meant that overexpression of

GPNMB/Osteoactivin enhanced cell migration and invasion when compared against untransfected cells.

On the other hand, knockdown of GPNMB/Osteoactivin in the pancreatic cancer cell line Panc-1 significantly decreased (although in a lower level than before) the number of cells that migrated into the lower compartment. This meant that silence of GPNMB/Osteoactivin attenuated cell migration and invasion when compared against untransfected cells.

Regarding the treatments, Gemcitabine + Erlotinib combined therapy did inhibit cell migration and invasion when compared against control samples. This inhibition was especially significant in the wild type Panc-1 and in the GPNMB+ cell line. In the GPNMB- cell line, differences between treated and non-treated samples were no significant. Indeed, if we compared the treated wild type Panc-1 cell line and the GPNMB+ cell lines against the untreated GPNMB- cell line, differences are, once again, no significant. The silence of GPNMB/Osteoactivin exerted the same effect in terms of inhibition of the invasion that Gemcitabine + Erlotinib combined therapy over the wild type and the GPNMB+ Panc-1 cell lines.

4.3.5.2 PCR arrays of genes related to invasion and metastasis

To further characterize the effect of GPNMB/Osteoactivin over cell motility, invasion and metastasis, we analyzed the expression modulation of some genes related to that processes. Figure 4.75 depicts those genes that were up or down regulated as a consequence of altering GPNMB/Osteoactivin expression.

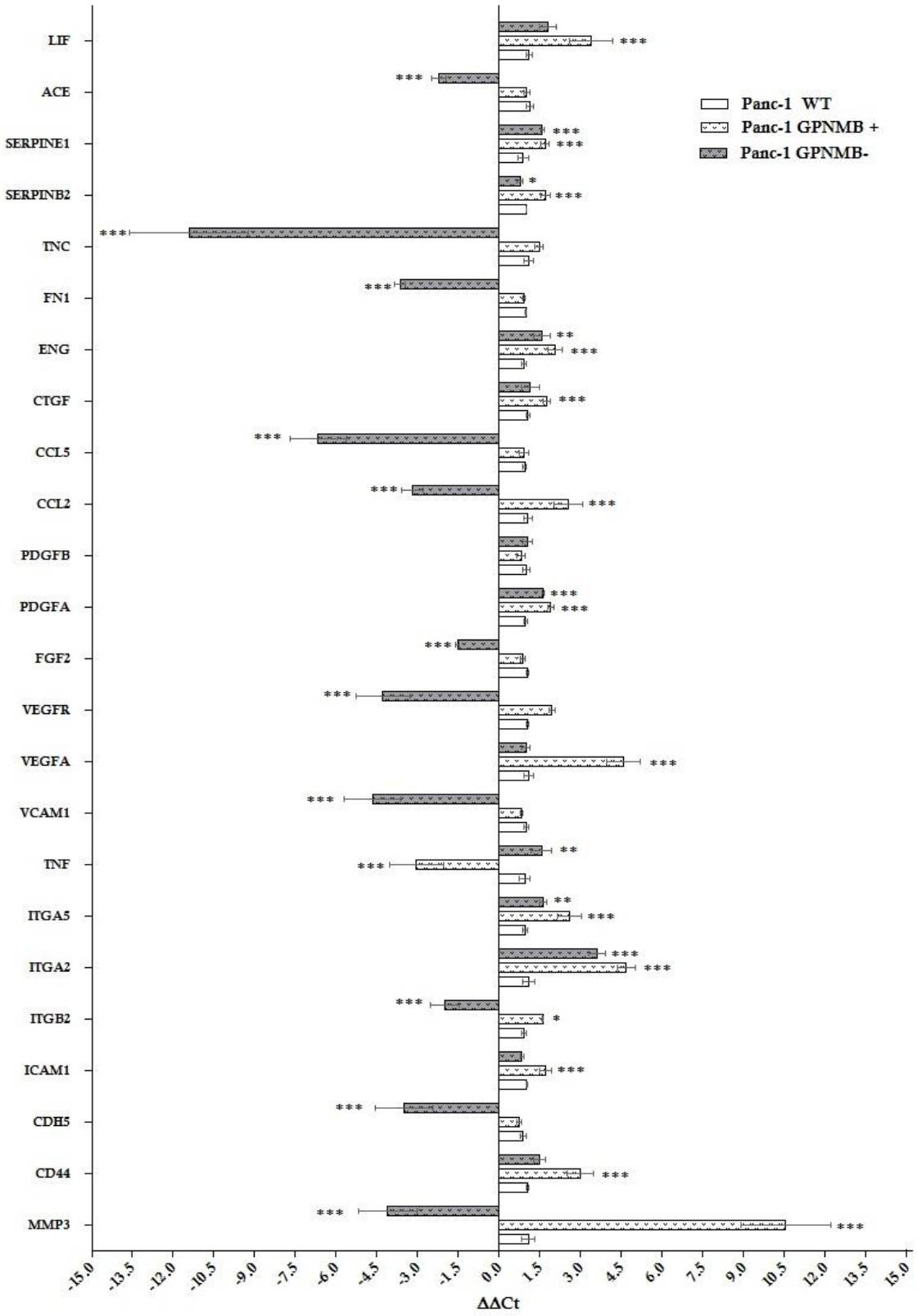

Figure 4.75 Up and down regulation of genes related to migration and metastasis. Analysis of relative gene expression data using real-time quantitative PCR and the $2^{(-\Delta\Delta Ct)}$ Method.

Ectopic expression of GPNMB/OA was followed by the overexpression of positive regulators of the invasion: MMP3, CD44, ICAM1, ITGB2, ITGA5, VEGFA, PDGFA, CCL2, CTGF, ENG, SERPINB2, SERPINE1 and LIF. The only gene that was found to be repressed after GPNMB overexpression was TNF (-3.043±0.45).

Silence of GPNMB/OA was followed by the repression of positive regulators of the invasion: MMP3, CDH5, ITGB2, VCAM1, VEGFR, FGF2, CCL2, CCL5, FN1, TNC and ACE. On the other hand, some positive regulator of the invasion were found to be less expressed when compared against the GPNMB+ cell line but still induced when compared against the wild type Panc-1 cell line: ITGA2, ITGA5, PDGFA, ENG, SERPINB2 and SERPINE1. TNF was overexpressed when compared against both the GPNMB+ and the wild type Panc-1 cell lines.

Taking all these result into consideration, our results pointed that GPNMB/Osteoactivin could represent a novel modulator of the invasion a metastasis in pancreatic cancer cells.

5

DISCUSSION

In order to follow the same structure of results, the discussion section of our work will be also structured in the same three subsections:

i. Interplay between the Gemcitabine and Erlotinib treatments on pancreatic ductal adenocarcinoma cells.
ii. Biomarkers identification in pancreatic ductal adenocarcinoma patients.
iii. Role of the GPNMB/Osteoactivin (highlighted in the former section as predictive biomarker of PDAC) in the carcinogenesis of PDAC.

5.1 INTERPLAY BETWEEN GEMCITABINE AND ERLOTINIB OVER PANCREATIC DUCTAL ADENOCARCINOMA CELLS

Pancreatic ductal adenocarcinoma is one of the most lethal cancers. Although there has been remarkable progress in the chemotherapy for gastrointestinal tract cancer, PDAC remains one with the less response to the conventional chemotherapy. All the efforts are focused on finding more effective therapies and new molecular targets to improve the clinical management and outcome of these patients. In the first objective of this thesis we aimed to analyze the molecular effects of the standard chemotherapy Gemcitabine alone or in combination with Erlotinib *"in vitro"* on pancreatic cancer cells cultures in the attempt to determine what makes this type of cancer so resistant to the available chemotherapy.

Monotherapy on pancreatic cancer with Gemcitabine has only had marginal survival benefits [343]. Combinations of antimetabolites and other drugs are commonly used not only in cancer chemotherapy, but also in many other diseases. The selection of combinations is often based on the efficacy of each agent separately, but the prior identification of a mechanistic basis for a combination may optimize scheduling and dosing of the combination [344].

Considerable resources have been channeled to the development of novel therapies that target the molecular aberrations of the disease. These targeted therapies are designed to disable the cellular pathways that are essential for cancer to survive. Targeted therapies could also be used in a multimodal treatment regimen in combination with standard radiotherapy and chemotherapy to improve outcomes and combat drug resistance. In 2008, detailed, global, genomic analyses found that a large number of genetic alterations affect only a core set of signalling pathways and processes that are genetically altered in 67–100% of cases of pancreatic cancer [5]. These data suggest that treatments for pancreatic cancer should target these complex and overlapping signalling pathways, rather than just the products of a single gene. In pancreatic cancer, only the combination of Gemcitabine and Erlotinib exhibited modest (6.24 vs. 5.91 months) but statistically

significant improvement in overall survival [152].

All the analyses were performed in two different pancreatic cancer cells, Panc-1 and BxPC-3 in order to analyze the role of *k-ras* mutation in any possible difference in responses (being BxPC-3 of wild type genotype).

Monotherapy analyses of Gemcitabine and Erlotinib on pancreatic cancer cell growth showed an inhibition of the proliferation that was dose and time-dependent after 48h of the treatment on pancreatic cancer cells Panc-1, Miapaca-2 and BxPC-3. The Panc-1 and Miapaca-2 cell lines were considered as a Gemcitabine chemoresistant cell lines whereas the BxPC-3 was considered as a Gemcitabine sensitive cell line. These results coincided with others [345-352].

Both Gemcitabine and Erlotinib have been shown to target a broad spectrum of signalling pathways, which are likely to contribute to their ability to inhibit proliferation and sensitize cells to apoptosis [353-354]. In order to analyze the "in vitro" combined effect of Gemcitabine and Erlotinib isobolograms were constructed on the basis of IC_{50} values to indicate any synergistic or antagonistic interactions between these drugs on the Panc-1 and BxPC-3 cell lines. While the treatment with a combination of Gemcitabine and Erlotinib produced a synergistic effect in the Panc-1 cells, such a combination produced antagonistic effects in the BxPC-3 cell line. These findings are supported by the quantification method proposed by Chou and Talalay, which is based at an inhibition level of 50% and establishes synergism with values of CI lower than 1[344].

Thus, the effects of Erlotinib in combination with Gemcitabine were considered, as others [355], additive in *k-ras*-mutated pancreatic cancer cells (Panc-1) whereas the effects of Erlotinib in combination with Gemcitabine were considered antagonistic in *k-ras* -wild type pancreatic cancer cells (BxPC-3).

Recently, the sequence-specific interactions of Erlotinib and chemotherapeutic drug combinations were found to influence the efficacy of regimens in non-small cell lung cancer cells (NSCLC) [356]. The order of the Erlotinib and Gemcitabine

treatment also affected the combination effects. Gemcitabine followed by Erlotinib enhances the antitumour effects of each drug alone, while Erlotinib followed by Gemcitabine has antagonistic effects [357]. The importance of the order seems to be a result of effects on the cell cycle progression. The antagonism could be associated with the Erlotinib-induced arrest of cells in G1. As S-phase entry is crucial for Gemcitabine mediated cytotoxicity, the G1 arrest could be protective. In contrast, if cells are exposed to Gemcitabine first, they entered S-phase and, after the Erlotinib treatment, undergo apoptosis.

In our model, it is possible that the Gemcitabine and Erlotinib combined treatment in the BxPC-3 cell line harbouring wild type *k-ras* exerted antagonistic effects because Erlotinib is able to efficiently block *k-ras* proliferating signalling pathways, hampering S-phase entry and limiting Gemcitabine effects. In the case of the *k-ras* mutated cell line Panc-1, as *k-ras* signalling is constantly active despite the Erlotinib treatment, combination treatments enhance antiproliferative responses.

Next we aimed to discern if the inhibition in the cell proliferation observed after Gemcitabine and Erlotinib, either as single agents or in combination, was accompanied by induction of apoptosis.

In the Panc-1 cell line, Gemcitabine caused a decrease in cell growth and its inhibition increased the level of apoptosis suggesting that the Gemcitabine effect may be inhibiting cell growth by inducing apoptosis. At molecular level, apoptosis induction was demonstrated by induction of proteins related to this process. In order to cause cell death, it is absolute necessary for Gemcitabine to upregulate pro-apoptotic proteins for Gemcitabine to trigger cell death [358]. Indeed, we observed a remarkable induction of the pro-apoptotic proteins Bax and Bak expression after the Gemcitabine treatment. The Bax induction after the Gemcitabine treatment has been previously described [358-359]. Although only a slight induction of the anti-apoptotic proteins Bcl-2 and Bcl-X_L were assessed after the Gemcitabine treatment, the Bcl-2/Bax and Bcl-X_L/Bax expression ratios were under 1 confirming that Gemcitabine harbours ability to induce caspase-mediated apoptosis in the pancreatic cancer cells Panc-1.

The BxPc-3 cancer cell exhibited limited induction of apoptosis after the Gemcitabine treatment. Analysis at molecular level showed remarkable induction of the proapoptotic protein Bak although no increase in Bax levels was determined. It is likely that the induction of Bak by Gemcitabine is responsible, in part, for the Gemcitabine induced apoptosis in the pancreatic tumour cells BxPC-3. This shows that Bak does have a function in pancreatic cancer cells apoptosis induced by Gemcitabine, albeit to a lesser extent compared with Bax. A major role in inducing apoptosis has also been assigned to Bax in other diseases [360]. Gemcitabine also induced expression of the anti-apoptotic protein Bcl-2 and Bcl-X_L. However, despite what happened in the Panc-1 cell line, absence of induction of Bax protein led to Bcl-2/Bax and Bcl-X_L/Bax expression ratios being over 1, confirming that Gemcitabine harbours limited ability to induce caspase-mediated apoptosis in the pancreatic cancer cells BxPC-3.

In the Panc-1 cell line, Erlotinib caused a decrease in cell growth although it exhibited limited induction of apoptosis. Interestingly, in BxPC-3, Erlotinib also caused a decrease in cell growth which was accompanied by the highest induction of apoptosis. The occurrence of somatic *k-ras* mutations is a highly predictive marker of resistance to anti-EGFR chemotherapies. In colorectal cancer, *k-ras* mutations were associated with resistance to anti-EGFR therapies in patients with metastatic diseases, while *k-ras* wild type predicted efficacy in terms of tumour response and patient survival [361-363]. Previous studies in non–small-cell lung cancer have demonstrated that patients carrying *k-ras* mutations are resistant to epidermal growth factor receptor (EGFR) tyrosine kinase inhibitors. [364-365]. Thus, it is clear that constitutive expression of EGFR and its inhibition by an antibody or a small molecule may not always be sufficient to produce a response in the presence of other activated pathways.

The activation of BAX and BAK, including BAX translocation, BAX and BAK conformational changes and oligomerization, plays a crucial role in the initiation of Erlotinib-induced apoptosis in non–small-cell lung cancer cells. Erlotinib-induced apoptosis has been described as dependent on the mitochondrial-mediated pathway, but independent of the extrinsic pathway [366]. Our results agreed with

this and we observed an induction of the pro-apoptotic protein Bax and Bak both in the Panc-1 and BxPC-3 cell lines. However, the main difference here is that, while in the Panc-1 cell line there was no modification of the Bcl-2 protein expression, in the BxPC-3 cell line we observed a marked repression of its expression, which has also been described on hepatocellular and pancreatic cancer [367-368]. In addition to the activation of the pro-apoptotic proteins and to the induction of cytochrome c release, a decrease of antiapoptotic Bcl-2, as demonstrated by western blot, may account for the induction of apoptosis using Erlotinib. This effect over Bcl-2 could be mediated by the inhibition of any of the proliferating signalling pathways activated by EGFR, such as PI3K/AKT or NF-κB.

The Gemcitabine and Erlotinib combined therapy caused a decrease in cell growth in both the Panc-1 and BxPC-3 cell lines. However, in the Panc-1 cell line, this decrease in cell growth also increased the level of apoptosis suggesting that the effects of Gemcitabine in combination with Erlotinib may be inhibiting cell growth by inducing apoptosis. In the BxPC-3 cell line, combined therapy exerted levels of apoptosis very similar to those registered with Gemcitabine as a single agent. These results could be a consequence of the synergic and antagonist interaction of the Gemcitabine and Erlotinib in the Panc-1 and BxPC-3 cell lines respectively.

In order to describe the molecular pathways related to the induction of the apoptosis, an extensive genetic analysis was performed using the RT^2 Profiler PCR Array System. In the Panc-1 cell line, PCR arrays demonstrated that the combined treatment exerted a remarkable induction of pro-apoptotic genes such as *Bax*, *Apaf-1*, *caspase 8*, *Fas*, *DR5* and *DR3*. On the other hand, some anti-apoptotic genes were also found to be overexpressed, such as *Bcl-2*, *Bcl-X$_L$*, *c-Flip* and *Tert*. Bcl-2 and Bcl-X$_L$ overexpressions were also assessed by western blot.

In the Panc-1 cell line, the genes *Bcl-2*, *Bcl-X$_L$*, *c-Flip* and *Tert* could contribute to the chemoresistance to the Gemcitabine and Erlotinib combined treatment in vitro, as the important roles of BCL-2 family members in chemoresistance have already been proven [117, 369-370]. Overexpression of cellular FLICE-like inhibitory protein (cFLIP) is reported to confer chemoresistance in pancreatic cancer cells

[371-372]. Lastly, hTERT expression also enhances the chemoresistance of cancer cells and marker for PDAC [373-374]. These genes could represent novel target to overcome the Gemcitabine and Erlotinib chemoresistance.

In the Panc-1 cell line, the Gemcitabine and Erlotinib combined treatment exerted induction of the pro-apoptotic Bax, both at gene and protein level. Besides, genetic analysis of genes related to apoptosis seemed to reflect an induction of apoptotic mediated by death receptor (*Fas*, *DR3* and *DR5*). Note that pancreatic cancer were defined initially as type II cells which meant that, besides the apoptosis induced by surface receptor, they needed the signal enhancing-effect of mitochondria to induce apoptosis [112]. In the death receptor pathway, the apoptotic events are initiated by engaging the tumour necrosis factor (TNF)-family receptors, including TNFR1, Fas, DR3, DR4 and DR5. After ligand binding or when overexpressed in cells, TNF receptor family members aggregate, resulting in the recruitment of an adapter protein called FADD. The receptor–FADD complex then recruits procaspase-8. This allows proteolytic processing and activation of the receptor-associated procaspase-8, thereby initiating the subsequent cascade of additional processing and activation of downstream effector caspases [109]. Indeed, we also found an induction of *caspase 8* expression.

When compared against BxPC-3, PCR arrays showed that, although there was induction of *Bax* and *DR5*, the modulation was much more limited and agreeing with the low induction of apoptosis obtained in this pancreatic cancer cells. *Htatip2* was also found to be slightly induced after the combined treatment in the BxPC-3 cell line. *Htatip2* is a putative metastasis suppressor that promotes apoptosis and inhibits angiogenesis [375]. Once again, the overexpression of the *Bcl-2 gene* could be associated to chemoresistance of pancreatic cancer cells to Gemcitabine and Erlotinib. However, the Gemcitabine and Erlotinib combined treatment sharply diminished the expression of *Tert* in the BxPC-3 cell line.

Once we checked the role of apoptosis in the Gemcitabina and/or Erlotinib treatment on pancreatic cancer cells, we analyzed any possible modulation in the cell cycle progression. At basal level, proliferative fractions of the Panc-1 cell line

(percentage of cells in the S and G2/M phases) doubled those of the BxPC-3 cell line, so the Panc-1 cell line had a higher rate of proliferation than the BxPC-3. In the Panc-1 cell line, the Gemcitabine, Erlotinib and combined treatments induced a halt in the cell cycle progression in the G0/G1 phase. In the same way, in the BxPC-3 cell line, the Gemcitabine, Erlotinib and combined treatments exerted similar effects although the proliferative fractions were almost undetectable.

In the Panc-1 cell line, the Gemcitabine and the combined treatments affected cancer cell proliferation inhibiting S-phase progression of the cell cycle and this was accompanied by an induction of the apoptosis. On the other hand, the Erlotinib treatment affected cancer cell proliferation inhibiting S-phase progression of the cell cycle but the effect over apoptosis was minimal.

In BxPC-3 cell line, the Erlotinib treatment affected cancer cell proliferation inhibiting S-phase progression of the cell cycle and it was followed by a severe induction of apoptosis. On the other hand, the Gemcitabine and the combined treatments affected cancer cell proliferation inhibiting S-phase progression of the cell cycle but the effect over apoptosis was modest.

The molecular mechanisms underlying this inhibition in the cell cycle were studied by western blot and PCR arrays. A link between EGFR signalling and alterations in normal cell cycle progression has been suggested in several reports. Externally, signalling pathways such as the Ras/Raf/Mek/Erk and the PI3K/Akt pathway can control cyclin concentrations. D-type cyclins and their associated kinases act as sensors of the external stimuli elicited by membrane-bound receptors and permit cells to proceed through the G1 phase of the cell cycle[376]. Cyclin D-CDK4/6, cyclin E-cdk2 and cyclin A-cdk2 operate consecutively in the progression through the G1 and S-phases [377]. CDKs phosphorylate retinoblastoma (Rb), which is the limiting factor in the G1/S transition. When Rb is phosphorylated, it releases E2F factors allowing S-phase progression. The activity of the CDKs is regulated at different levels. Important CDK regulators are the INK (p15, p16, p18, and p19) and Cip/Kip (p21, p27, and p57) families of CDK inhibitors [378].

We analyzed the role of the protein p27Kip1 in the suppression of the cell cycle progression. Our results demonstrated that the Erlotinib and the combined treatments caused cells to accumulate at the G1/S phase accompanied by and induction of the CDK inhibitor p27KIP1 in both pancreatic cancer cell lines, although the effect was higher in the wild type *k-ras* pancreatic cancer, BxPC-3. These findings are consistent with reports in which the overexpression of the p27Kip1 protein led to apoptosis in various cancer cell lines [379-380]. However, details of the mechanism of apoptosis induced by overexpression of the p27Kip1 protein are still unclear [381].

The Gemcitabine treatment reduced the expression of the protein p27Kip1 in the Panc-1 cell line while had no effect on the BxPC-3 cell line. As Gemcitabine is not acting on *k-ras* signalling pathway, Ras may play important roles in the downregulation of the p27Kip1, possibly through the MAPK-mediated phosphorylation of p27Kip1, which prevents binding of the CDK2 inhibitor and may induce the p27Kip1 degradation [382-384]. In the Panc-1 cell line, G0/G1 block has to follow a different path from p27Kip1. Gemcitabine seemed to induce differentiation markers in the Panc-1 cell line [385].

PCR arrays also comprised information of genes related to the cell cycle and control of DNA damage which could help to understand the molecular mechanisms implicated in the suppression of the proliferation in pancreatic cancer cell after the Gemcitabine and Erlotinib combined treatment.

In the BxPC-3 cell line, PCR array of genes related to the cell cycle control showed a general inhibition of genes related to phase S transition. These results agreed with the G0/G1 block of the cell cycle progression as a result of the p27kip overexpression previously observed. Besides, a remarkable repression of the gene *S100A4* was assessed. The protein encoded by the gene S100A4 is now known to be capable of regulating the cell cycle progression, modulating not only intercellular adhesion but also the invasive and metastatic properties of cancer cells. The S100A4 protein appears to be able to sequester and disable the p53 suppressor protein which controls the G1-S transition of cells [386-387]. Its role in

the invasion will be further discussed.

On the other hand, diametrically opposite results regarding the cell cycle regulation were obtained in the Panc-1 cell line. They were lead by an extensive induction of the *e2f1* and *rb1* expression. This was also accompanied by an induction of *atm* and *chek* genes.

A number of E2F family members are known to be responsive to DNA damage. More than 10 years ago, it was shown that E2F1 is induced in response to various DNA-damaging agents, including ionizing radiation, UV radiation and a number of chemotherapeutic drugs [388-390]. This response primarily involves an increase in the stability of the E2F1 and is associated with the induction of apoptosis [391] through p53-dependent [392-394] and –independent pathways [395].

ATM was found to phosphorylate E2F1 on serine-31[391]. Checkpoint kinase 2 (CHK2), which is downstream of ATM in the DNA damage response, phosphorylates E2F1 on serine-364 [396]. These phosphorylations seem to contribute to the stabilization of E2F1 [397]. The retinoblastoma protein (pRB) tumour suppressor blocks cell proliferation by repressing the E2F transcription factors. However, recent data now establish a second role for pRB as a stress-induced activator of apoptosis. Notably, the ability of pRB to promote either arrest or apoptosis seems to be context dependent, with apoptosis being favoured in proliferating cells [398]. The E2F1–RB complexes formed following DNA damage not only participate in the transcriptional repression of cell-cycle genes like cyclin A2 but also in the activation of proapoptotic genes [397]. Note that we have previously described an induction of apoptosis in the Panc-1 cell line after the Gemcitabine and Erlotinib treatment which was comprised by the induction of *Apaf-1*, *caspase-8* and *bax* genes (amongst others). All of them are direct targets of E2F transcription [399].

Even though there is a block in the cell cycle progression in the Panc-1 cell line after the Gemcitabine and Erlotinib treatment, we observed gene induction of *cdc25a*, *cdk2* and *cdk4* which are implied in the cell cycle progression [400].

Besides, also an induction of p27 and p21 was reported. Recent studies have shown that p21WAF/CIP1 and p27KIP1 are necessary for the assembly of the cyclin A/CDK4 or CDK6 and the formation of the cyclins A/CDK2 or E/CDK2 complexes. Thus, an increase in the expression of the p21WAF/CIP1 and p27KIP1 proteins could facilitate assembly of the complexes and result in the suppression of the activity of cyclin/CDKs and thereby in the delay of the cell cycle progression [401].

E2F implication in inducing apoptosis in the Panc-1 cell line is depicted in Figure 5.1.

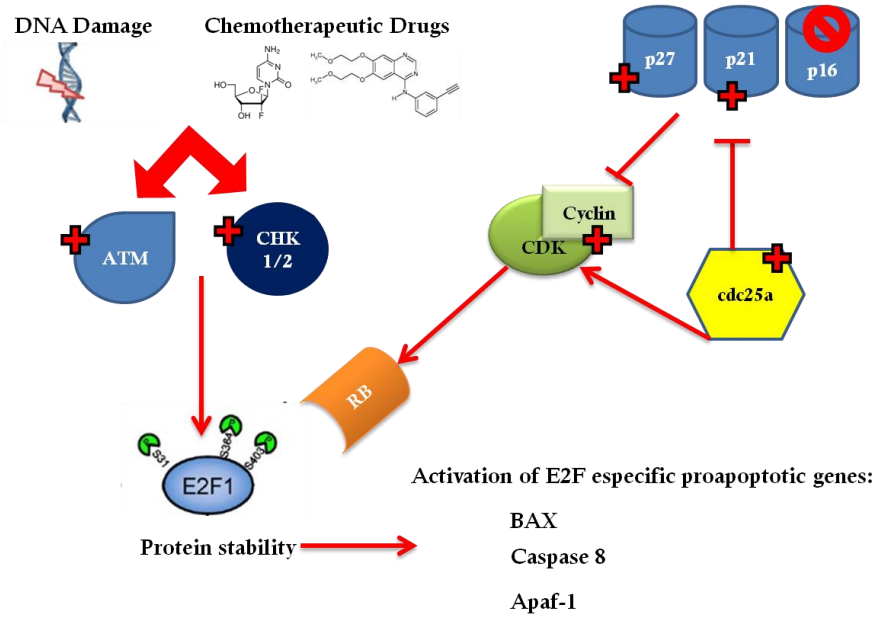

Figure 5.1 Upregulation of activator E2F transcription factor is part of the DNA damage response machinery. Cytotoxic drugs stimulate DNA damage sensor kinase ATM and CHK1/2 which in turn phosphorylate E2F1 causing rapid protein stabilization which leads to the activation of proapoptotic genes. Hence, E2F1 is the unique executor of the death program in response to DNA damage inflicting drugs.

Intracellular pathways with a role in the pathogenesis of PDAC are associated with the resistance to Gemcitabine induced cell death as they block drug induced death signalling. These pathways start from surface molecules such as receptor tyrosine kinases and adhesion mediators and also include down-stream kinases, other

modulators and transcription factors [402]. Amongst them, NF-κB pathways are key regulators of numerous cellular events such as proliferation, differentiation, and apoptosis, and they are also related to tumour development and progression. NF-κB pathways are activated in many cases of pancreatic cancer [85, 403] and might be involved in the resistance against Gemcitabine. Bandala et al [404] showed that the Gemcitabine treatment increased the activity of the NF-κB and Alexader et al [405] showed that the induction of the NF-κB by Gemcitabine was dose-dependent in five pancreatic cancer cell lines. Elevated NF-κB activity in cancer cells provides a survival mechanism by up-regulating anti-apoptotic genes, thereby representing a major causative factor for drug resistance [406-408].

In order to analyze the role of NF-κB in the chemoresistance to apoptosis of the pancreatic cancer cell lines, we studied the induction/repression of NF-κB signalling components. In light of the western blot analysis, Gemcitabine, Erlotinib nor the combined therapy induced expression of the NF-κB (p65) in the Panc-1 cell line. Very similar results were obtained in the BxPC-3 cell line although in the Gemcitabine treated cells a slightly induction of this nuclear factor was determined.

Interestingly, Gemcitabine exerted a huge modulation of IκB expression. In the Panc-1 cell line, IκB-α expression was barely detected. On the contrary, the phosphorylated protein p-IκB-α was found highly overexpressed. This meant that in the Panc-1 cell line after the Gemcitabine treatment, the only presence of the inhibitor IκB-α was in its phosphorylated form, so it was marked to be proteolytically degraded by the proteasome, freeing NF-κB to translocate to the nucleus and to activate its target genes. In the BxPC-3 cell line, Gemcitabine exerted similar results, although there was more expression of active (inhibiting NF-κB) IκB-α. In our study, we determined that the Gemcitabine augmentation of NF-κB translocation to the nucleus was followed by an induction of the binding activity of NF-κB to Bcl-2, Bcl-X_L and MMP-9 promoters in the Panc-1 cell line together with an inhibition of the binding activity of NF-κB to IκB-α promoter. We also determined that Gemcitabine augmentation of NF-κB translocation to the nucleus was followed by an induction of the binding activity of NF-κB to Bcl-2 and

IκB-α promoters in theBxPC-3 cell line.

Erlotinib exerted similar effects in both cell lines, a reduction in the phosphorylated form of IκB-α and an induction of the active IκB-α, sequestering NF-κB in the cytoplasm, thus preventing it from translocate to the nucleus. In our study, we determined that although Erlotinib diminished NF-κB translocation to the nucleus, it was still able to induce the binding activity of NF-κB to Bcl-2 and IκB-α promoters in the Panc-1 cell line. In the same sense, the NF-κB translocation to the nucleus was followed by an induction of the binding activity of NF-κB to IκB-α promoter although it was accompanied by a repression of the binding activity of NF-κB to Bcl-2 and MMP9 in the BxPC-3 cell line. The protective effects of sequestering NFκB in cytoplasm by IκB-α were more important in the *k-ras* wild type pancreatic cancer cell line.

Lastly, we analyzed induction/repression of NF-κB signalling components after the combined treatment. In the Panc-1 cell line, the combined treatment halved the expression of IκB-α protein. Not only did it exert this inhibition but it also induced phosphorylation of the remaining IκB-α protein, leading to a bigger flux of the transduction factor to the nucleus. We determined that the Gemcitabine and Erlotinib combined treatment augmentation of NF-κB translocation to the nucleus was followed by an induction of the binding activity of the NF-κB to the Bcl-2, Bcl-X_L and MMP-9 gene promoters in the Panc-1 cell line. On the contrary, a huge induction of the IκB-α protein was assessed after the Gemcitabine and Erlotinib combined treatment although it was followed also by an induction of its phosphorylated form. We determined that the NF-κB translocation to the nucleus after the Gemcitabine and Erlotinib combined treatment was followed by an induction of the binding activity of the NF-κB to the Bcl-2 and IκB-α gene promoters together with a repression of the binding activity of the NF-κB to the MMP-9 gene promoter in the BxPC-3 cell line.

PCR arrays also comprised information of genes related to signal transduction and transcription factors. In the Panc-1 cell line PCR arrays after the combined treatment exhibited a downregulation of the IκB-α gene expression. In the BxPC-3

cell line, PCR arrays after combined treatment exhibited an induction of the IκB-α gene expression. These results agreed with the previous ones and attribute a central role to the NF-κB regulation in the response to the Gemcitabine and Erlotinib combined treatment in pancreatic cancer cells.

PCR arrays results of genes related to signal transduction and transcription factors have provided light to the possible mechanism of drug resistance in pancreatic cancer cell lines. In the Panc-1 cell line, we observed overexpression of the genes *c-fos*, *map2k1*, *raf1* and *sncg*. C-Fos overexpression has been linked to chemotherapeutic drug resistance as it elevates its target multidrug resistance 1 (MDR1). Knockdown of c-Fos or MDR1 has been shown to sensitize Gemcitabine-resistant cells to the Gemcitabine treatment [409]. Besides, the overexpression of the gene *map2k1* (MEK) could also be related to chemoresistance. A relationship between MEK overexpression and the Gemcitabine chemoresistance in the Panc-1 cell lines has been demonstrated. Besides, constitutively active MEK reduces Gemcitabine sensitivity in the MiaPAca-2 cell line [347]. *Raf1*, being part of the Ras/Raf/ERK signalling pathway, is the best-characterized effector of K-Ras [410]. A correlation between high Raf-1 activity and chemoresistance has been reported in early passage human cervical tumours [411], leukemia and breast cancer [412]. The *sncg* overexpression has been correlated to cancer invasion and infiltration in esophageal cancer [413], breast cancer[414] and gastrointestinal carcinomas[415].

When compared with results of the wild type *k-ras* cell line BxPC-3, results showed a downregulation or maintenance of the previously highlighted genes, also a reduction of PI3K, together with a remarkable induction of IκB-α gene.

Taking all these results into account, we could conclude that *k-ras* mutation, occurring early and in a 90% of the PDAC[29], is responsible for the downstream activation of Raf1/MAPK and NF-κB signalling pathways and chemoresistance to Gemcitabine and Erlotinib observed in the Panc-1 cell line.

To conclude our in vitro analysis about the molecular mechanism underlying the different responses of Gemcitabine and Erlotinib in the *k-ras* mutated or the wild

type pancreatic cell lines, PCR arrays of genes related to invasion, adhesion and angiogenesis were studied. We observed that the Gemcitabine and Erlotinib combined therapy elicited induction of genes related to invasion, adhesion and angiogenesis. This phenotype was a result of either the constantly activated oncogene *k-ras* or the Raf/MEK/ERK and NF-κB signalling pathways induced after this regimen of treatment in the Panc-1 cell line. This induction of the invasion, adhesion and angiogenesis was reverted in the *k-ras* wild type BxPC-3 cell line, in which neither the oncogene *k-ras* or Raf/MEK/ERK not NF-κB signalling pathways were found to be active after the Gemcitabine and Erlotinib treatment.

The c-*met* proto-oncogene plays a prominent role during tumour cell growth and metastasis elicited by the ras oncogene [416]. It has been suggested that stimulation of the Ras-Raf-mitogen-activated protein kinase (MAPK) pathway induces Met expression through the activation of the AP-1, SP-1, and possibly Ets transcription factors [417-418]. *C-met* also presents a NF-κB binding site in its promoter region that may control the *c-met* expression [419]. Recently, inhibitors of c-met signalling have been proven to increase the efficacy of Gemcitabine and overcome chemoresistance together with an inhibition of metastasis in PDAC [420].

We demonstrated that MMP9 overexpression was, in part, due to the enhanced binding of NF-κB MMP9 promoter. MMP9 and other target genes of NF-κB have been associated with chemoresistance [421-422]. Besides, MAPKs are intricately involved in the expression of the components involved in MMP promoter induction via AP-1 and its association with *c-jun* and *c-fos.* They act synergistically to upregulate MMP expression in response to a variety of stimuli (e.g., cytokines, growth factors, and cellular stress) [423]. Besides the overexpression of MMP1 and MMP9, there was a repression of the expression of TIMP3, which antagonizes matrix metalloproteinase activity and can suppress tumour growth, angiogenesis, invasion and metastases. Its reduced expression contributed to tumour growth and tumour invasion by allowing increased activity of MMPs in the extra cellular matrix [424].

The urokinase-type plasminogen activator system consists of uPA (also known as PLAU), the uPA receptor (uPAR; also known as PLAUR), the substrate plasminogen (Plg), the plasminogen activator inhibitor 1 (PAI1; also known as SERPINE1) and PAI2 (also known as SERPINE2). uPA converts plasminogen to plasmin, which in turn can degrade a wide variety of ECM components and enable the tumour cells to penetrate the basement membrane [425-426]. In addition, uPA, by binding to its cell surface receptor (uPAR), also modulates cell adhesion, proliferation and migration [427-428]. TGF-β, together with Plau and PlauR were upregulated in the Panc-1 cell after the Gemcitabine and Erlotinib combined therapy. These effects were reversed in the BxPC-3 cell line. TGF-β modulates the uPA expression in different types of transformed cells: one of the first studies was performed by Keski-Oja et al. [429], showing that TGF-β regulates the expression of uPA in A549 human lung carcinoma. This study helped the understanding of the capacity of TGF-β to enhance migration and invasion of transformed cells. TGF-β has been demonstrated to regulate uPA expression in both tumour cells and normal cells [430-432], suggesting important roles of uPA regulation in normal cell differentiation, angiogenesis and cell development, among other cellular functions, although the underlying mechanisms remain unclear. A Ras-ERK1,2-MAPK signalling implication in TGF-β-enhanced uPA expression has been described [433-434]. Furthermore, signalling through uPAR activates the Ras-MAPK pathway [435]. In order to keep this system active, we also observed an inhibition of the type-1 inhibitor of plasminogen activator, PAI1. PAI-1-overexpression has been linked to enhanced migration of pancreatic cancer cells [436].

As described before, the most remarkable repression in the wild type *k-ras* cell line BxPC-3 after Gemcitabine and Erlotinib was S100A4. In pancreatic cancer cells, knockdown of S1004 resulted in reduced phospho-IκB-α levels, repressing NF-κB activity. This determined that S100A4 activated NF-κB [437]. The effect of the Gemcitabine and Erlotinib combined treatment on the NF-κB could be enhancing the antitumour activity of these drugs. Indeed, the effect could be a result of inhibiting the MMP-9 expression, as we observed in the BxPC-3 cell line and which agreed with others [438-440].

Overexpression of IL-8 plays an important role in tumour angiogenesis and contributes significantly to the aggressive biology of human pancreatic cancer [441-444]. Besides, VEGF is important in angiogenesis and the promotion of tumour growth in many cancers including pancreatic cancer. VEGF and its receptors are overexpressed in pancreatic cancer [445-446]. The Angiopoietin/Tie2 (TEK) system with VEFG is known to be important for the initiation of angiogenesis in tumours [447]. Recently, the angiopoietins have been shown to be important mediators of angiogenesis by regulating of endothelial cell survival in malignant and non-malignant tissues. Among them, Ang-1 has been identified as a major activator of the tyrosine kinase receptor Tie2, leading to receptor autophosphorylation on binding. Ang-1 also stimulates endothelial cell migration in vitro [448-449]. Ang-2 is the naturally occurring antagonist to Ang-1 and inhibits Ang-1-mediated Tie2 phosphorylation. This effect leads to vessel destabilization, a necessary step in the initiation of angiogenesis [450-451]. The prevention of IL-8, VEGF and or Angiopoietin-1expression may function to prevent aggressiveness and invasion in pancreatic cancer.

In summary, our results showed that the effect of the Gemcitabine and Erlotinib combined therapy on the *k-ras* mutated cell did not affect or even induce some of the hallmarks of this aggressive cancer, such as invasion and angiogenesis related genes. On the other hand, in the wild type *k-ras* cell line BxPC-3, a remarkable repression of signalling pathways leading to proliferation and metastasis were found.

We have observed relative insensitivity of pancreatic cancers to EGFR inhibitors, agreeing with others [452] and we hypothesized that this could be explained first, because of the presence of mutant *k-ras* in pancreatic cancers, which makes cells resistant to EGFR inhibition [453-454] and secondly, by the induction of survival pathways and angiogenic pathways such as MAPK and NF-κB signalling pathways. Although this is not the case in the BxPC-3 cell line, which bears wild-type *k-ras*, the BxPC-3 cell line has been reported to express constitutively active Ras [455] that is also insensitive to EGFR inhibitors treatment. Furthermore, BxPC-3 cells have been shown to express elevated levels of ErbB3 (relative to other pancreatic

cancer cells) and constitutively phosphorylated ErbB3 [456]. It has been suggested that this ErbB3 expression results in the heterodimerization of EGFR with ErbB3 and in the recycling of the heterodimer complex back to the cell surface, which may explain resistance to EGFR inhibitors.

As *k-ras* is always almost present in the pancreatic cancer cell lines, combinational therapies of Gemcitabine with specific inhibitors of angiogenesis or directed target therapies against MAPKs and NF-κB signalling pathways would increase the effectiveness of Gemcitabine.

5.2 BIOMARKERS IDENTIFICATION IN PANCREATIC DUCTAL ADENOCARCINOMA PATIENTS

Although the last few years have witnessed important breakthroughs in the comprehension of the molecular biology of PDAC as well as in diagnosis, staging and treatment, there are more deaths from this disease than from any other type of cancer. Amongst the reasons for this dramatic death rate of PDAC stands out that tumours are usually detected at a late stage, at which point the cancer has already metastasized. Furthermore, available chemotherapy does not have positive enough effects. This chemoresistance is associated not only with the panel of genetic alterations presented in PDAC cancer cells but also with the active dense collagen-rich fibrotic tumour microenvironment which resembles a shelter that acts as preclusion to the chemotherapy being delivered within the cancer cells [457]. The need for new diagnosis biomarkers for PDAC and novel targets improving chemotherapy efficiency are beyond dispute.

Due to the main roles the stroma and inflammation have in development, progression and therapeutic response of PDAC [458], we hypothesized that cytokines released to blood by the tumour microenvironment or by the cancer cells could represent novel diagnosis and predictive biomarkers and predictors of cancer outcomes as they can be considered as a reflection of the complex tumour immunosuppressive network underlying PDAC.

We have performed a novel cytokine antibody array from RayBiotech (RayBio® Human Cytokine Array) as a method to identify 507 cytokines in serum of PDAC patients and healthy controls, including cytokines, chemokines, adipokines, growth factors, angiogenic factors, proteases, soluble receptors, soluble adhesion molecules and other proteins. Simultaneous detection of multiple cytokines provides a firm tool in biomedical discovery. Through this we can simultaneously detect key molecules important in cancer development [459].

Deciding which proteomic measurements to include in a model is called feature selection and is a crucial step in developing a class predictor. In order to filter the 507 cytokines, the filter Mann-Whitney U test was applied. For assessing prediction error, in the absence of a large, independent test set, a LOOCV model was developed as a technique to implement partitioning of the original observed data set [303].

The first goal of this part of the study was to determine ***diagnostic biomarkers*** in sera of PDAC patients. We first compared the protein profile between PDAC patients who had not undergone any doses of treatment with healthy controls. After feature selection and LOOCV analyses, PDAC was associated with serum alteration of FGF-10/KGF-2, I-TAC/CXCL11, OSM, Osteoactivin/GPNMB and SCF cytokines. These five cytokines, independently, appeared to be highly discriminatory for PDAC patients with sensitivities ranging from 69-77% and with 75% of specificity for a precise cut-off. The combination of the five cytokines obtained the best results in discriminating PDAC from healthy subjects.

Tumour marker carbohydrate antigen CA 19-9 has been widely used in PDAC diagnosis and is still the current standard serum tumour marker. Nevertheless there are some limitations in the usefulness of this marker. For example, it is elevated in only about 65% of individuals with resectable pancreatic cancer, it has no role in screening asymptomatic populations, it does not discern between pancreatic cancer patients and those with chronic pancreatitis and that it appears in other malignances. In this way, the European Group of Tumour Markers (EGTM) the National academy of Clinical Biochemistry (NACB) recommend that CA 19-9 should not be the only indicator used for diagnosing PDAC [158-159]. Given that serum CA 19-9 reaches sensitivity of 70–80% but with less than 50% of specificities [160] and that our panel of cytokines reaches a specificity of 84.6% and a sensitivity of 67%, we consider that the combination of both measurements would improve the specificity in the diagnosis.

To the best of our knowledge, this is the first time that this combination of cytokines has been associated with diagnosis of PDAC. Although OSM and SCF have

recently been bond to pancreatic cancer processes, the link of the remaining cytolines with the PDAC is original and has not been described elsewhere.

Here follows a summary of their roles and any possible connection with cancer.

FGF-10/KGF-2: this factor has been described as a promoter of pancreatic morphogenesis at primary stages of the organogenesis as well as a regulator of the pancreatic epithelial progenitor cells proliferation [460]. Recently, a link between FGF10/FGFR2-IIIb-signalling and migration and invasion of pancreatic cancer cells through the induction of membrane type 1-matrix metalloproteinase and transforming growth factor TGF-β1, which is an important regulator of the epithelial mesenchymal transition, has also been described [461]. A overexpression of FGF-10 and its receptor, FGFR2 IIIb has also been linked to growth in colorectal adenocarcinoma [462].

I-TAC/CXCL11: CXCL11 is a CXC chemokine that interacts specifically with CXCR3 receptor. It stimulates the phosphorylation of MAPK kinases pathways leading to proliferation and prevention of apoptosis [463]. Besides, a role in several types of cancer tumorigenesis has been described [464-465]. Although here we present CXCL11 as a possible biomarker in PDAC patients for the first time, it has been recently proposed as a serum biomarker for prostate adenocarcinoma [466].

OSM: Oncostatin M belongs to the interleukin-6 cytokine and prompts a variety of functions implicated in wound repair. Although initially it was described as a growth inhibitor of leukemia cells [467] it may harbor a dual role also as a promoter of proliferation, cell migration and invasion, as has been recently reported [468-471]. Besides, high levels of OSM have been found in the stroma of the murine PDAC model [472]. Once OSM binds its receptor, it promotes reciprocal phosphorylation and activation of the Janus kinase family (JAK)/STAT pathway. Several transcriptional targets of STAT3 are important contributors to PDAC biology [473].

Osteoactivin: Glycoprotein non-metastatic melanoma protein B (GPNMB), also known as Osteoactivin (OA), Dendritic Cell–Heparin Integrin Ligand (DC-HIL) or Hematopoietic Growth Factor Inducible Neurokinin-1 type (HGFIN) is a type I transmembrane protein which was first described as low to undetectable in malignant cells [189]. However, more recently studies have describe GPNMB/osteoactivin as a promoter of metastasis and invasion [202] in several cancers such as melanoma [183-184], uveal melanoma [185] glioma, [186] hepatocellular carcinoma [187] and breast cancer in which it has been described also as a prognosis indicator of recurrence [188]. An induction of GPNMB in the spinal cords of amyotrophic lateral sclerosis patients as an inductor of motor neuron degeneration has recently been described [338].

SCF: Stem cell factor, SCF, is the main ligand for the receptor tyrosine kinase *c-kit* (KIT). Their binding supports proliferation, differentiation and survival in KIT-expressing cells, both in normal and tumours cells, including pancreatic cancer cells [474] through activation of (PI3K)/Akt; MAPK and STAT pathways [475]. Previous analyses have described elevated levels of SCF in sera of PDAC and colorectal cancer [476-478].

These five cytokines, being part of the tumour microenvironment, could enhance PDAC development and progression and they represent novel perspectives for treating the dreadful disease. As PDAC harbors multiple genetic and epigenetic alterations and implicates several signalling pathways, a combination of CA 19–9 with diverse biomarkers could represent the most realistic approach to establish new diagnostic biomarkers. FGF-10/KGF-2, I-TAC/CXCL11, OSM, Osteoactivin/GPNMB and SCF could be considered as a novel diagnostic panel of the PDAC disease and could be directed towards a better diagnosis.

The second goal of this study was to determine ***predictive biomarkers***. Predictive biomarkers are those related to the response to the treatment. If an altered cytokine profile in PDAC patients after treatment predicts therapeutic responses to the available chemotherapy it will be of major importance in patient clinical management and outcome. Serum cytokine analysis can also provide new insights into the molecular mechanisms of drug resistance. Understanding the mechanisms by which a treatment may regulate the serum cytokine profile in cancer patients would be fundamental for suggesting alternative, innovative or targeted therapies and for discerning developed chemoresistance.

In the course of our evaluation, we identified 7 cytokines that differ significantly in the sera of pre and post-treated PDAC patients and healthy controls. CD30 Ligand/TNFSF8, Chordin-Like 2, FGF-10/KGF-2, GDF-15, I-TAC/CXCL11, OSM and SCF levels were altered by the chemotherapy and/or the cancer itself. FGF-10/KGF-2, I-TAC/CXCL11, OSM and SCF have been described before.

CD30 Ligand/TNFSF8: Abnormalities of the tumour necrosis factor (TNF) family members have been linked to several human diseases, including cancer. CD30L is a type II transmembrane protein that belongs to the TNF family. Levels of soluble CD30 or CD30L are high in serum or tissue samples of patients with atopic dermatitis, systemic sclerosis, inflammatory bowel disease, systemic lupus erythematosus, rheumatoid arthritis and other diseases, correlating with disease severity in some instances [479]. TNFSF8 has also been found to be expressed and upregulated in some tumour cells, such as mast cells and basal cell carcinoma[480]. TNFSF8 binds exclusively to CD30 and activates the CD30 receptor that engages the MAP kinase in the NF-κB pathway and involves cell differentiation, apoptosis and immune response [481]. High expression of TNFSF8 has been linked to lung cancer [482-483]. Because CD30 expression is restricted to a small number of normal cells, its expression in malignant cells makes it a good target for antibody therapy [484].

Chordin-Like 2: Also known as breast tumour novel factor 1 (BNF-1), encodes a putative extracellular matrix protein. Upregulation of BNF-1 has been detected in

breast, lung and colon tumour tissues [485].

GDF-15: Also known as MIC-1 or NAG-1 is a distant member of the transforming growth factor β (TGF-β) family of cytokines that was originally identified as a gene expressed in the context of macrophage activation [486]. GDF-15 expression is substantially increased during cancer development and progression especially in gastrointestinal, prostate, pancreatic, colorectal, breast, melanoma, and glioblastoma brain tumours. Aberrant increases in the serum levels of secreted NAG-1 correlate with poor prognosis and patient survival rates in some cancers[487]. It has been recently described as a biomarker in the diagnosis of lethal PDAC [488].

Only in the case of Chordin-Like 2 and SCF, the Gemcitabine and Erlotinib treatment restored normal values. For the rest of cytokines, chemotherapy may not be contributing to fight against the disease. All these unbalanced cytokines appear to be promising prime targets for novel therapies or chemoresistance. We propose that this panel of cytokines could constitute emerging predictive biomarkers of response/nonresponse to Gemcitabine and Erlotinib chemotherapy in PDAC patients. They may offer a high level of clinical utility assessing usefulness of treatment in PDAC patients. Consequently, these could be considered as novel targets to new therapeutic approaches. There is a soaring need for new therapeutic strategies and by targeting the tumour stroma in combination with chemotherapy would be a promising option for the treatment of PDAC [489-490].

The last goal of the *in vivo* analysis was to investigate the prognosis significance of serum cytokines as a reflection of the host response to the tumour in PDAC patients (***prognosis biomarkers***).

To assess the impact of altered cytokine profiles on overall survival (OS), Cox's proportional hazard modeling and Kaplan–Meier curves were developed. The effect of serum cytokines levels on OS was dually explored. Initially, a univariate analysis of the cytokines along with some clinicopathologic features was carried out to determine possible significant explanatory variables to model a prognosis index (PI). Whilst univariate analysis returned those highly significant markers to be used as independent prognosis factors, it does not mean that the combination of these outcomes would represent the best performance for the multivariate model. Furthermore, univariate selection methods have certain restrictions and may lead to less accurate classifiers [491]. Hence, the most adequate approach to define the multivariate model would be independent from the former, so disregarded variables could also be considered to complete the multivariate model. Then, as some variables may not be significant in univariate analysis but become significant in multivariate analysis, a multivariate approach was used in this study to identify jointly measurable factors that could be used to model the risk of PDAC mortality. To overcome the noise and overfitting problem derived from the fact that there were more candidate features than samples, a robust feature selection model was carried out [491]. As long as feature selection is performed reasonably, accurate prediction is possible even with the simplest of the predictive models [492].

In the course of our evaluation, we first identified 2 cytokines that correlated with patients' prognosis in univariate analysis, IL-24 and IL-29. Following, a panel of 5 cytokines clearly demonstrated a remarkably better overall performance for modeling OS. Therefore the multivariate model consisting of B7-1/CD80, EG-VEGF/PK1, IL-29, NRG1-beta1/HRG1-beta1 and PD-ECGF proved to be more accurate than the univariate model, which considers the most significant markers. The effectiveness of our model is clearly demonstrated with the evaluation performed by the LOOCV.

Although roles for B7-1/CD80, EG-VEGF/PK1 and NRG1-beta1/HRG1-beta1 have been individually linked to PDAC, to the best of our knowledge this is the first time that this combination of serum cytokines has been collectively described as prognosis factors for PDAC.

An overview of these biomarkers is subsequently given:

B7-1/CD80: The B7 system is one of the most important secondary signalling mechanisms and is essential in maintaining the delicate balance between immune potency and suppression of autoimmunity. B7-1 (CD80) and B7-2 (CD86) are ligands expressed on antigen-presenting cells and they are responsible of the co-stimulatory signalling whereby T cell priming, growth, maturation and tolerance is regulated. Upon binding to their receptors, T cell activation and survival is promoted. On the other hand, they can also deliver co-inhibitory signalling binding to their inhibitory receptors and blocking T cell response [493]. An inadequate co-stimulation has been suggested to contribute to the progressive growth of tumours [494]. The combination of B7-1 and B7-H1 has been proposed as prognosis factor for PDAC [495-496]. Although the role of B7-1 seems to be antitumoral, overall emerging picture is that the aberrant or unbalanced expression of B7 family members can contribute to its lack of detection by the immune system.

EG-VEGF/PK1: This molecule was first described as an example of a class of highly specific mitogen that acts to regulate proliferation and differentiation of the vascular endothelium in a tissue-specific manner. Although this protein does not show any structural homology to the VEGF family, they do share multiple regulatory functions related to proliferation and migration [497]. EG-VEGF/PK1 has been described to be related to ovarian [498], colorectal [499], prostate [500], hepatocellular [501], pancreatic cancer [502] and neuroblastoma [503]. It has also been described as a factor for placenta angiogenesis [504].

IL-29: Also referred as IFN-λ1, belongs to the type III INF family and it has been described as inducing similar biological activities to type I INF family (INT-α and β) Although both are able to induce antiproliferative responses in many cell types,

IFN-λ1 appears to be more limited. Signalling via the IFN-λ1 results in the activation of STAT1, STAT2, STAT3 and STAT5 pathways, the three major mitogen-activated protein kinase (MAPK) cascades and the phosphorylation of Akt through the phosphatidylinositol 3-kinase (PI3K) pathway [505-507]. However, the ability of IFN-λ1 to trigger these alternative pathways could be cell-type specific or altered in cancer cells. Contrasting conclusion has been derived from another study that suggests growth induction in human multiple myeloma cells through MAPK activation [508]. The precise role of IL-29 in host responses and immune surveillance has yet to be defined in the context of cancer in general and in PDAC in particular.

NRG1-beta1/HRG1-beta1: Neuregulin-1 or heregulin-1 is an extracellular protein ligand meant to bind to the ErbB receptors family members, ErbB3 and ErbB4. Upon interaction with their receptor, a wide range of biological events including the induction and progression of several epithelial cancers are prompted. The NRG1/HRG1 proteins play essential roles in the nervous system, heart, and breast and are involved in the development of human diseases, including schizophrenia and breast cancer [509-510]. An up-regulation of the angiogenic factor VEGF by NRG1/HRG1 has also been described [511]. Their proliferative affects are likely to be achieved through the combined action of multiple pathways, including PI3K, MAPK and p38MAPK pathways [512] which has been specifically described in PDAC cells. A lower survival rate was related to those PDAC patients with higher expression of HRG-β mRNA [513]. ErbB3 has a pivotal role in pancreatic tumorigenesis promoting in vitro and in vivo cancer cell proliferation [514]. It has been recently described that cancer-associated fibroblasts release NRG1/HRG1 ligand, activating PDAC cells by ErbB3/AKT-mediated signalling and enhancing tumorigenesis. This could be related to the insufficient effect of Erlotinib (EGFR inhibitor) when combined with Gemcitabina in the treatment of PDCA patients [515].

PD-ECGF: Also known as thymidine phosphorylase, its activity and expression of in carcinomas of the esophagus, stomach, colorectum, pancreas, and lung are significantly higher than in the adjacent non-neoplastic tissue, and may have an

important role in the proliferation of these solid tumours. PD-ECGF is expressed not only in tumour cells but also in tumour associated stromal cells [516-517]. Regression analyses in bladder, colorectal, gastric, renal and pancreatic carcinoma have marked PD-ECGF as a prognosis factor for poor outcome [518].

It may not be possible for one single biomarker to provide the necessary prognosis information about the patient to base treatment options on. For this reason, panels of biomarkers should be advisable to accurately predict the stage of disease and how it will progress. Previous studies have indicated that tumour prognosis is closely associated with immune escape by tumour cells. A dynamic relationship between the host immune system and cancer is emerging [519]. Present prognosis scoring system, based on serum cytokines, has been developed to identify patients at the highest risk of cancer progression and death. Due to the emerging role of tumour microenvironment on cancer progression and aggressiveness, cytokines could represent successfully predictors of cancer outcomes as they can be considered as a reflection of the complex tumour immunosuppressive network underlying PDAC. The worsened prognosis associated with tumours harboring this cytokine panel could be associated to a deregulation of growth factor-mediated paracrine loops, particularly in relation to proliferation and angiogenesis. Giver the interplay between B7-1/CD80, EG-VEGF/PK1, IL-29, NRG1-beta1/HRG1-beta1 and PD-ECGF and poor prognosis, this cytokines could be considered as novel molecular targets that may lead to more successful therapeutic modalities for PDAC patients.

5.3 THE ROLE OF GPNMB/OSTEOACTIVIN IN THE CARCINOGENESIS OF PDAC

We have determined an "in vivo" predictive role for GPNMB/Osteoactivin in pancreatic cancer. Its expression was elevated in serum of PDAC patients when compared against healthy volunteers and it did not show any modulation after Gemcitabine and Erlotinib therapy. We have conducted "in vitro" analyses in order to determine its role in proliferation, apoptosis and migration in the pancreatic cancer cell line Panc-1 using the wild type Panc-1, the GPNMB+ (Panc-1 cell line transfected with the pCMV6-GPNMB-GFP plasmid) and the GPNMB- (Panc-1 cell line transfected with the HuSH p-GFP-V-RS plasmid) cell lines. We selected the Panc-1 cell line as it harbours *k-ras* mutation and most of the pancreatic cancers harbour this mutation [29]. We selected GPNMB/Osteoactivin amongst the five predictive cytokines because its expression pattern, especially expressed in extracellular membrane of cancerous cells, makes GPNMB/Osteoactivin an excellent target for cancer therapies, and also because its role in PDAC was unknown and could represent a novel approach against this disease.

First we analyzed the subcellular localization of GPNMB/Osteoactivin. Ectopic expression of GPNMB/Osteoactivin showed a right processing and its location was, overall, in extracellular membrane. This extracellular expression pattern is what makes GPNMB most attractive as a target in cancer cells [236].

Next, we analyzed the effect of GPNMB over proliferation. Our results showed that ectopic expression of GPNMB/Osteoactivin enhanced proliferative fractions in pancreatic cancer cell. These proliferative fractions were remarkably lowered in the GPNMB- cell line, obtaining a blockade of the cell cycle progression in the G0/G1 phase. These results were recently described in the HepG2 cell line [520]. Regarding treatments, although the Gemcitabine and Erlotinib combined treatment affected proliferation in the GPNMB+ cell line, reducing it, the rate of inhibition was lower compared with the wild type Panc-1 cell line. In the GPNMB- cell line, a mere effect of the treatment was determined. The ectopic expression of

GPNMB/Osteoactivin diminished the potential for the inhibition of the proliferation of these drugs.

Next we analyzed the effect of GPNMB over apoptosis. Although Rose et al described a reduced apoptosis in GPNMB/Osteoactivin-expressing melanomas, due to the dual role that GPNMB/Osteoactivin presents in various cancers, especially in melanoma where it was first described [202], our results showed that ectopic expression of GPNMB/Osteoactivin did not have any significant effect on apoptosis. These results were also obtained in the HepG2 cell line [520]. However, suppression of GPNMB/Osteoactivin expression achieved remarkable levels of apoptosis. The treatment of cells with the GPNMB- genotype did not enhance cell death and results were very similar to the apoptosis obtained in the wild type Panc-1 cell line after the Gemcitabine and Erlotinib treatment which could mean that silence of GPNMB mimics Gemcitabine and Erlotinib effects.

The expression of BCl-2, Bcl-X_L and Bax resembled that GPNMB+ showed increased levels of BCl-2 and Bcl-X_L which can be related to the resistance to apoptosis. Knockdown of the gene had the opposite effect, the anti-apoptotic genes Bcl-2 and Bcl-X_L were diminished and the pro-apoptotic gene Bax was induced. The Bcl-2/Bax and Bcl-X_L/Bax ratios corroborate that the GPNMB+ cell line was resistant to apoptosis, by means of ratios above 1, and that the GPNMB- cell line was sensitive to the apoptotic stimuli.

Genetic analyses of genes related to the apoptosis confirmed this situation. The GPNMB- cell line presented a downregulation in the anti-apoptotic genes *Bcl-2* and Bcl-X_L. Besides, the anti-apoptotic *BCL2A1* gene, which is a highly regulated NF-κB target gene, was remarkably repressed in the GPNMB- cell line. The GPNMB- cell line also showed an induction of the pro-apoptotic gen *Bax* and a string induction of Fas. These results pointed that apoptosis in the GPNMB- cell line was mediated by both, extracellular and mitochondrion pathways. Moreover, the GPNMB silence repressed the NF-κB expression and at least, one target gene, *BCL2A1*, contributed to the cell death. This trend was opposite in the GPNMB+ cell line.

In the event of treating with Gemcitabine and Erlotinib, we observed an apoptotic response confirmed by BCl-2/Bax and Bcl-X_L/Bax ratios being below 1, which meant the cell lines were susceptible to apoptosis, although at a lower degree than in the GPNMB+ cell line. The GPNMB- cell line did not reflect any significant change regarding the induced-apoptosis suggesting that Gemcitabine and Erlotinib induction of apoptosis and Osteoactivin pathway converge at some common point.

Our in vitro results suggested that GPNMB/Osteoactivin can enhance the migratory and invasive characteristics of pancreatic cancer cells. Indeed, the GPNMB+ cell line had greater ability to migrate in the Boyden chamber analyses. The GPNMB- cell line had lower ability to degrade basement membrane. Similarly to our previous results, the treatment in the GPNMB- cell line did not affect the migratory capabilities.

The genetic analyses of genes related to invasion revealed that ectopic GPNMB expression was concomitant with the overexpression of several genes that promoted metastasis. On the other hand, silence of GPNMB/Osteoactivin expression was concomitant with the repression of those genes. An extensive study of invasion genes is subsequently described:

MMPs are the principal matrix-degrading proteinases that play key roles in embryonic development, organ morphogenesis and wound healing. Abnormal activation of MMPs has been implicated in numerous diseases including arthritis, atherosclerosis and tumorigenesis, cleaving many components of the ECM [521]. In the GPNMB+ cell line, our results showed an upregulation of **MMP-3** of ten times. On the contrary, knockdown of GPNMB/Osteoactivin diminished MMP-3 expression when compared against the wild type Panc-1 cell line. Previous studies have suggested that osteoactivin expression is capable of inducing the expression of matrix metalloproteinases (MMP), including MMP-3 and MMP-9[230]. Indeed, ectopic expression of GPNMB/Osteoactivin in poorly metastatic 66cl4 mouse mammary carcinoma cells was sufficient to induce MMP-3 expression and increases their invasion in vitro and promotes bone metastasis in vivo [238].

CD44 has been described as a pancreatic cancer stem cell marker[522]. CD44 is the principal transmembrane adhesion receptor for hyaluronan (HA) and plays a central role in the remodeling and degradation of HA that leads to cell migration, as well as to cancer invasion and metastasis. Upregulation of CD44 and downregulation of CD44 seem to be involved in the EMT process and the acquisition of invasive and metastatic potential [523]. The GPNMB+ cell line showed increased levels of the CD44.

VE-cadherin/**CDH5** plays a role in tumour-associated angiogenesis. CDH5 promotes cell survival and inhibits apoptosis by interacting with β-catenin, phosphoinositide-3 kinase and VEGFR-2 and modulating their signalling. CDH5 is also important for tumour angiogenesis and blocking the CDH5 function with monoclonal antibodies in mouse tumour models leading to an inhibition of tumour angiogenesis and growth [524]. Although the GPNMB+ cell line did not show any significant modulation of this gen when compared against the wild type Panc-1 cell line, the GPNMB- cell line did, being its expression reduced three times.

ICAM-1 plays an important role in cell-cell and cell-extracellular matrix interactions, especially tumour invasion. Increased ICAM-1 expression correlates with poor prognosis in pancreatic cancer [525]. The GPNMB+ cell line significantly induced the expression of the ICAM-1 which could be related with an enhancement of tumour invasion.

The integrins are an important family of adhesion receptors that play key roles in cell migration, environmental sensing and tissue organization [526]. **ITGB2** was found to be overexpressed in the GPNMB+ cell line when compared against the wild type Panc-1 cell line whilst it was repressed in the GPNMB- cell line when compared against the control cell line. Other members of the same family, **ITGA2** and **ITGA5** showed very similar expression pattern in the GPNMB+ cell line, being significantly overexpressed. However, although in the GPNMB- cell line a reduction in the gene expression was also found, it did not reach the wild type Panc-1 cell line levels.

TNF (Tumour necrosis factor) is a double edge sword. TNF exerts many important physiological and pathological actions. TNF activates both cell-survival and cell-death mechanisms simultaneously. TNF has emerged as an important risk factor for tumorigenesis, tumour progression, invasion and metastasis[527]. Ectopic expression of GPNMB/Osteoactivin led to the repression of TNF in the GPNMB+ cell line. On the contrary, the silence of this protein led to the enhancement of TNF expression. Due to the induction of apoptosis seen after GPNMB silence we hypothesized that TNF should be directing apoptosis in the GPNMB- cell line.

Recent studies demonstrate that **VCAM-1** has multiple roles in promoting metastasis by facilitating immune evasion of metastatic cells and promoting recruitment of metastasis-promoting stromal cells, in addition to adhesion of metastatic cells [528]. Knockdown of GPNMB/Osteoactivin reduced its expression.

In order to progress to a larger size, incipient neoplasias must develop angiogenic ability. The angiogenesis-initiating signals are exemplified by vascular endothelial growth factor (**VEGF**) and acidic and basic fibroblast growth factors (FGF1, **FGF2**). Besides, VEGF and its receptors (VEGFR) have been identified as major mediators of tumour angiogenesis. Our model over expressing GPNMB/Osteoactivin resulted in significant upregulation of VEGFA. However, neither the receptor nor the FGF2 significantly changed when compared against the wild type Panc-1 cell line. Regarding these genes in the GPNMB- cell line, VEGFR and FGF2 did show significant repression when compared against the wild type Panc-1 cell line. VEGFA levels returned to that obtained in the wild type cell line.

Other growth factor found to be overexpressed in the GPNMB+ cell line was **PDGFA** whilst **PDGFB** did not show any significant modulation. Upon activation of the PDGF pathway, signalling occurs via the use of the PI3K/AKT complex pathway but there are also MAPK molecules involved alongside proteins of the Src family and Phospholipase C-γ. Other molecules related to the PDGF signalling include the Ras protein, STAT proteins, and guanine-5'-triphosphate (GTPase) activating protein. PDGF has been shown to interfere with the stroma formation and also act as a substrate for angiogenesis. It has also been shown to act in concert with VEGF

in order to promote new vessel formation and stabilize newly synthesized vessels [529]. After GPNMB/Osteoactivin knockdown, PDGFA failed to achieve the same levels as the wild type Panc-1 cell line, being also significantly induced.

Chemokines are a superfamily of secreted proteins involved in immunoregulatory and inflammatory processes. **CCL2** seems to be a key player in mediating STAT3 activation and epithelial–mesenchymal transition (EMT) and tumour metastasis [530]. **CCL5**, besides, up-regulates the release of matrix-degrading enzymes [531]. Both chemokines resulted inhibited in the GPNMB- cell line. Only CCL2 resulted significantly induced in the GPNMB+ cell line when compared against the wild type model.

CTGF is a cysteine-rich matricellular secreted protein that regulates diverse cell functions including adhesion, migration, proliferation, differentiation, survival, senescence and apoptosis. In the pancreas, CTGF regulates critical functions including β cell replication during embryogenesis, stimulation of fibrogenic pathways in pancreatic stellate cells during pancreatitis and regulation of the epithelial and stromal components in pancreatic ductal adenocarcinoma. CTGF seems to have a role in development of desmoplasia in PDAC and in invasion [532]. This gene was found to be significantly induced in the GPNMB+ cell line while the suppression of the GPNMB/Osteoactivin led to the restoration of the wild type values.

Endoglin (**End**) is well acknowledged as being the most reliable marker of proliferation of endothelial cells and it is overexpressed on tumour neovasculature. Human endoglin is a type I integral membrane protein with large extracellular domain, regular hydrophobic transmembrane domain and short cytoplasmic domain. Elevated expression of endoglin correlates with the proliferation of tumour endothelial cell and it seems to be a potent marker of solid tumours vasculature in the mammary gland, prostate, cervix, colon and rectum, lung, head and neck, kidney, esophagus and uterus [533-534]. This gene presented a doubled expression in the GPNMB+ cell line. The expression was slightly reduced after GPNMB/Osteoactivin knockdown but level did not reach the wild type Panc-1

cell line.

Tenascin (**TNC**) and fibronectin (**FN1**) are ECM proteins and key players in tumour angiogenesis and metastasis [535]. It has previously been demonstrated that tenascin can regulate the expression of proangiogenic factors relevant to cancer outcome, including the prototypic angiogenic cytokine VEGFA. Hypoxic stress is a hallmark of tumour stroma that can foster the angiogenic switch of tumours by inducing a genetic reprogramming of stromal and tumour cells leading to increased production of proangiogenic factors. One study had reported that tenascin expression can be induced by hypoxic stress. Interestingly, tenascin expression was recently correlated with hypoxia and lymph node metastasis of medullary thyroid carcinomas. Wnt signalling represents a proangiogenic pathway that seems to be triggered by tenascin. Wnt emerged as prominent morphogenic signal controlling sprouting angiogenesis in a wide array of physiopathological contexts [536]. Tenascin and fibronectin were both significantly down regulated in the GPNMB- cell line.

Serpine1 and **Serpinb2** belong to the urokinase plasminogen activator system. Both are plasminogen activator inhibitors (PAIs, PAI-1 and PAI-2 respectively). The urokinase plasminogen system is particularly associated with the process of metastasis, the spread of primary tumours to distant organs which is always associated with poor prognosis and high mortality. The role of PAI-1 in various tumours and malignancies is rather unconventional. Instinctively one would be inclined to believe that PAI-1, by virtue of inhibiting uPA, would serve as a factor negatively influencing the proliferation of cancers. This does hold true in many cases but it is increasingly being realized that PAI-1 also positively influences the tumour invasion and angiogenesis and has been correlated with poor prognosis [537]. Genetic analysis in the GPNMB+ cell line revealed an induced expression in both genes. Although Serpinb2 returned to wild type gene expression values after knockdown of GPNMB/Osteoactivin, Serpine1 maintained those induced values.

Angiotensin converting enzyme (**ACE**) is responsible of convert the decapeptide angiotensin I (produced from cleavage of angiotensinogen by renin) to the

octapeptide angiotensin II, in the renin angiotensin system (RAS). ACE inhibition in combination with other therapies has been found to improve outcome in certain tumours such as pancreatic and nonsmall lung cancer. However, there are also abundant studies that suggest neutral or even negative impact of ACE inhibitor or RAS blocker use on specific cancers in clinical models [538]. Our model showed a downregulation of this gene in the GPNMB- cell line.

Leukemia inhibitory factor (**LIF**) is a pleiotropic cytokine, which plays an important role in inducing cancer cachexia and promoting cell proliferation in pancreatic human carcinoma cells through c-fos, jun-B and cyclin E expression [539]. This gene was found to be overexpressed in the GPNMB+ cell line. Its value in the GPNMB- cell line was not significantly different of that of the wild type Panc-1 cell line.

All in all, we have described a possible role for GPNMB/Osteoactivin protein in pancreatic cancer. GPNMB/Osteoactivin protein expression prevents cells from apoptosis enhancing proliferation and invasion.

In background section, we described the possible transcription factors responsible for GPNMB/Osteoactivin expression. Microphthalmia-associated transcription factor (MITF) is the master regulator of melanocyte differentiation and of the expression of melanogenic proteins [540]. In melanoma, MITF has critical roles in cell proliferation, survival and invasion [541]. Recently, knockdown of MITF has been linked to inhibition of the invasion in melanoma cells [542], probably by dysregulation of target genes involved in cell invasion. However MITF relationship with invasion is limited to melanoma.

GPNMB/Osteoactivin is a downstream effector of BMP-2 signalling. Bone Morphogenetic Proteins (BMPs) represent the largest subset within the TGF-β superfamily. They are now known to be involved in such a wide variety of processes that several investigators even suggested to change their name from “Bone” to “Body” Morphogenetic Proteins. Although they share some fundamental similarities with other members of the TGF-β superfamily, the pleomorphic

functions of BMPs led to their signalling functions being regulated at such complex levels that far exceed those imposed on the other members of the TGF-β superfamily [543].

GPNMB/Osteoactivin is regulated by BMP-2 [544] and this regulation is mediated through the Smad-1 signalling pathway. Smad1 is an essential intracellular component that is specifically phosphorylated by BMP receptors and translocated into the nucleus upon ligand stimulation [545]. Compared with the normal pancreas, PDAC has been shown to express induced BMP-2 which was concomitant with shorter postoperative survival. Expression of wild-type Smad4 abolished the BMP-2-mediated growth stimulation [546]. Besides, BMP pathway has been described as important for the induction of epithelia-to-mesenchymal transition (EMT) in the Panc-1 cell line, one of the most extensively studied pancreatic cancer cell lines and the most established and robust model for pancreatic cancer cell EMT. This EMT is led by Smad1 signalling, MMP-2-induction and increases invasion[547]. BMP-2 has also been related to metastasis in bladder [548-549], gastric [550], lung [551], breast [552] and pancreatic cancer[553].

The molecular mechanism by which BMP-2 signalling regulates cell motility and invasiveness seems to be through phosphorylation of Smad1 and activation of BMP target genes [554]. Recent studies have implicated multiple non-Smad pathways, including PI3K/AKT, RAS, ERK or NF-κB in mediating BMP-signal transduction [555-557]. Indeed, we obtained a repression of NF-κB after knockdown of GPNMB/Osteoactivin. Furthermore, these pathways are constitutively activated in a variety of metastatic human cancers and are also best understood in the context of a major cascade stimulating cell migration and invasion. Regarding Bmp2 expression, it has been described as directly dependent on continued Sonic hedgehog expression [558-559].

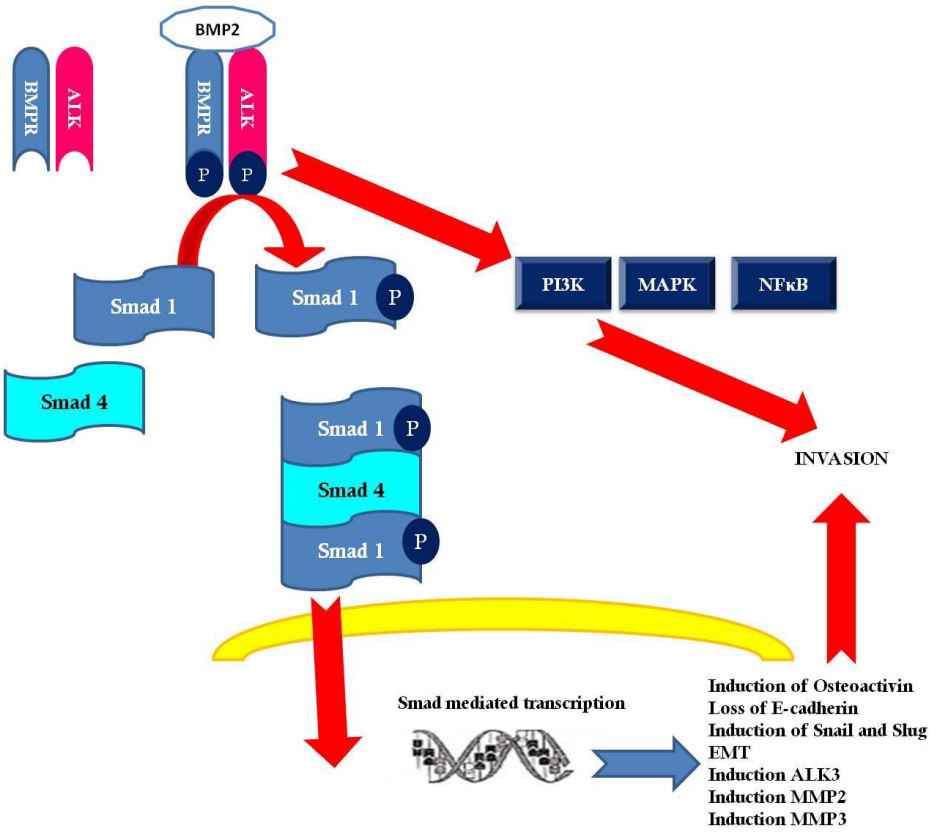

Figure 5.2 Bone morphogenetic proteins (BMPs) regulate developmental EMT and a role for BMP signalling in promoting the metastatic cascade is emerging. BMPs signal by binding an oligomeric receptor complex consisting of a type I receptor [activin-receptor like kinase (ALK)-2, ALK3 or ALK6] and a type II receptor [activin type II receptor, activin type II receptor B or BMP type II receptor (BMPR2)]. The constitutively active type II receptor transphosphorylates and activates the kinase activity of the type I receptor. Once active, the type I receptor phosphorylates the intracellular effector proteins, Smad1, 5 and 8, which complex with Smad4 to accumulate in the nucleus and mediate target gene transcription. Osteoactivin is a target gene of BMP-2 [544].

The malignant phenotypes mediated by GPNMB/Osteoactivin likely involve multiple mechanisms at the molecular level, with the induction of MMP-3 expression as an important component [560] (Figure 5.3). A possible mechanism of GPNMB/Osteoactivin mediated expression of MMP-3 in fibroblasts has been recently proposed trough ERK signalling [561]. Only the inhibition of ERK1/2 resulted in the suppression of MMP-3 expression. ERK signalling is an important pathway that mediates extracellular signals, such as cytokines and growth factors, to nuclear transcription of MMP-3. For example, FGF-2 and EGF induced MMP-3 expression in endothelial cells and fibroblasts, respectively, through the activation of the ERK pathway [562-563]. The biological effects of ERK1/2 are mediated by downstream phosphorylation of nuclear transcription factors. Among them, AP-1 is one of the most important downstream substrates of ERK1/2 signalling that mediate MMP-3 expression induced by osteoactivin, since there are at least two AP-1 binding sites at promoter region of mouse MMP-3 gene [564]. This is very interesting as AP-1 is a critical transcriptional regulator of invasion [565] and could underlie the induction of the invasion in the GPNMB+ cell line.

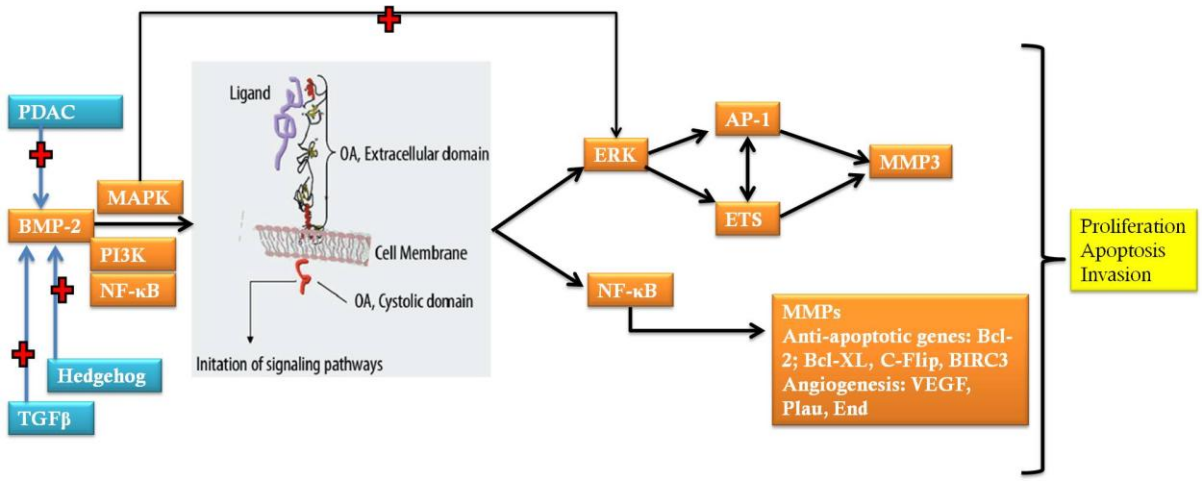

Figure 5.3 Possible mechanisms by which GPNMB/Osteoactivin mediates the expression of genes related to proliferation and invasion. It has been described that Osteoactivin is a downstream effector of BMP-2 signalling. In PDAC, several components of the BMP family have been described to be constitutively active [547]. Signalling pathways such as Hedgehog and TGF-β (both implicated in PDAC) have been described as activators of BMP-2 [566]. BMP-2 activation of the transcription can be mediated by Smad-1 or by non-Smad pathways,

including PI3K/AKT, RAS, ERK or NFκB. ERK seems to induce expression of MMP-3 after Osteoactivin expression by a mechanisms regulated by AP-1. ETS could drive this expression as well or could enhance AP-1 transcription. As we found repression in the GPNMB- cell line of NF-κB, we suggest that aggressive phenotype of the GPNMB+ cell line could also be mediated by it.

GPNMB/Osteoactivin binds to heparin/heparan sulfate and adheres to endothelial cells via its RGD motif [218]. GPNMB/Osteoactivin expressed by antigen-presenting cells (APC) serves as an inhibitor of T cell activation by binding syndecan-4 on activated T cells [223, 567]. An understanding of critical GPNMB/Osteoactivin binding motifs will help to provide an understanding of how GPNMB/Osteoactivin mechanistically enhances cancer cell invasion. Additionally, it will be important to discover the integrins, which may bind the RGD motif in GPNMB/Osteoactivin to confer the invasive phenotype. It is possible that GPNMB/Osteoactivin may bind proteins, such as integrins, on the cell surface and act in an autocrine manner or GPNMB/Osteoactivin may interact with proteins on adjacent stromal cells acting in a paracrine manner. It is also possible that cleaved GPNMB/Osteoactivin may interact with full-length, cell surface tethered GPNMB in an autocrine fashion to promote invasion.

As we have shown in this thesis, the Gemcitabine and Erlotinib combined therapy did not affect expression, proliferation or apoptosis in the GPNMB cell lines. We hypothesized that Gemcitabine and Erlotinib-induced apoptosis and the knockdown of GPNMB gene should converge at some common point, exerting similar effects. This could represent novel therapies strategies focus to those patients who develop resistance to former chemotherapy or it could be possible to combine GPNMB/Osteoactivin targeting therapies with other drugs in the search of better and saver combinations to treat this disease.

Further studies are necessary to elucidate the mechanism of action of GPNMB/Osteoactivin in pancreatic cancer progression, invasion and metastasis.

6

CONCLUSIONS/ CONCLUSIONES

1) In vitro analyses have shown that Gemcitabine and Erlotinib, either as single agents or in combination, exert antiproliferative effects on the Panc-1 and BxPC-3 cell lines in a time and dose-dependent manner. Gemcitabine and Erlotinib exert their effects through different pathways. The interaction between them results in a synergistic effect for the Panc-1 cell line. The combination produces antagonistic effects in the BxPC-3 cell line. The antagonism could be related to the inability of Gemcitabine to exert its toxic effect over S phase cycle due to the efficient block of the G0/G1 phase exerted by Erlotinib.

2) The inhibition of tumour cell growth after the Gemcitabine and Erlotinib treatment is related to the cell cycle arrest in both cell lines. Gemcitabine and its combination with Erlotinib exert cell cycle arrest followed by an induction of the apoptosis in the *k-ras* mutated cell line Panc-1. Gemcitabine and its combination with Erlotinib exert cell cycle arrest however it is not followed by significant apoptotic induction in the wild type *k-ras* cell line BxPC-3. Erlotinib, as a single agent, stops the cell cycle progression in the Panc-1 cell line without inducing apoptosis. On the contrary, Erlotinib exerts both cell cycle arrest and huge induction of apoptosis in the BxPC-3 cell line. The Erlotinib blockade of the cell cycle is mediated by the p27KIP expression. Gemcitabine blockade is associated with induced differentiation as it is shown by CAII and cytokeratin 7 markers.

3) Gemcitabine-induced apoptosis is dependent on the mitochondrial-mediated pathway, through the Bax and Bak expression in the Panc-1 cell line but it is only mediated by Bak in the BxPC-3 cell line. Although Gemcitabine induces expression of the Bcl-2 and Bcl-X_L proteins, the Bcl-2/Bax and Bcl-X_L/Bax expression ratios being under 1 confirm that Gemcitabine harbours ability to induce caspase-mediated apoptosis. In the BxPC-3 cell line, Gemcitabine also induces expression of the anti-apoptotic proteins Bcl-2 and Bcl-X_L. However, in this case, absence or limited presence of the Bax protein leads to the Bcl-2/Bax and Bcl-X_L/Bax expression ratios being over 1, confirming that Gemcitabine harbours

limited ability to induce caspase-mediated apoptosis in the pancreatic cancer cells BxPC-3.

4) Erlotinib-induced apoptosis is dependent on the mitochondrial-mediated pathway by the Bax and Bak expression in both cell lines. Erlotinib represes the Bcl-2 expression only in the wild type *k-ras* cell line, BxPC-3, which could be mediated by the inhibition of the proliferating signalling pathways activated by EGFR, such as PI3K/AKT or NF-κB.

5) The Gemcitabine + Erlotinib-induced apoptosis in the Panc-1 cell line is dependent on the mitochondrial-mediated pathway by the expression of Bax, Bak and Apaf-1 and also on the extrinsic cell death-dependant pathway, mediated by the overexpression of the caspase 8, Fas, DR5 and DR3. The Gemcitabine + Erlotinib-induced apoptosis in the Panc-1 cell line is also dependent on the E2F overexpression which may contribute to the induction of the expression of *Apaf-1*, *caspase-8* and *bax* genes. The Gemcitabine + Erlotinib-induced apoptosis in the BxPC-3 cell line is dependent on the mitochondrial-mediated pathway by the expression of Bax and also on the extrinsic cell death-dependant pathway, mediated by the overexpression of DR5. However, this effect is much more limited than in the Panc-1 cell line.

6) In the Panc-1 cell line, the Gemcitabine and the combined treatments are associated with overexpression of the phosphorylated form of the IκB-α protein, resulting in an enhanced binding activity of the NF-κB to the promoters of the Bcl-2, Bcl-X_L and MMP-9 genes and in an inhibition of the binding activity of the NF-κB to the IκB-α promoter. In the BxPC-3 cell line, the Gemcitabine and the combined treatments enhance binding activity of the NF-κB to the promoters of the Bcl-2 and IκB-α genes. However, the combined treatment also represses the binding activity of the NF-κB to the MMP-9 gene. Erlotinib exerts protective effects sequestering and inhibiting the NF-κB in the cytoplasm by the IκB-α protein in both cell lines although these effects are more important in the *k-ras* wild type pancreatic cancer

cell line.

7) The Gemcitabine and Erlotinib chemoresistance in the Panc-1 cell line could be mediated by the overexpression of the c-FOS, MAP2K1, RAF1 and SNCG transcription factors. The wild type *k-ras* cell line BxPC-3 shows a downregulation or maintenance of those transcription factors, together with a reduction of the PI3K gene and a remarkable induction of the IκB-α gene. K-RAS mutation is responsible of the downstream activation of Raf1/MAPK and NF-κB signalling pathways and of the chemoresistance to Gemcitabine and Erlotinib observed in the Panc-1 cell line.

8) The Gemcitabine and Erlotinib combined therapy over *k-ras* mutated cell induces invasion and angiogenesis related genes such as MMPs, Plau, PlauR IL-8 or VEGFA. On the other hand, in the wild type *k-ras* cell line BxPC-3, a remarkable repression of the signalling pathways leading to proliferation and metastasis is found.

9) We have indentified for the first time a panel of five serum cytokines comprising FGF-10/KGF-2, I-TAC/CXCL11, OSM, Osteoactivin/GPNMB and SCF that are significantly overexpressed in the serum of PDAC patients compared with healthy controls. These five cytokines have been associated with PDAC and represents novel diagnostic biomarkers of PDAC disease.

10) We have found 7 differentially expressed cytokines in PDAC patients after the Gemcitabine and Erlotinib treatment. CD30 Ligand/TNFSF8, Chordin-Like 2, FGF-10/KGF-2, GDF-15, I-TAC/CXCL11, OSM and SCF might represent novel predictive biomarkers for Gemcitabine and Erlotinib response of PDAC patients. They may offer a high level of clinical utility assessing usefulness of treatment in PDAC patients. Consequently, these could be considered as novel targets to new therapeutic approaches.

11) We have identified for the first time a panel of five serum cytokines comprising B7-1/CD80, EG-VEGF/PK1, IL-29, NRG1-beta1/HRG1-beta1 and

PD-ECGF with prognosis significance in PDAC. Not only might these molecules allow a more accurate prediction of prognosis of patients with PDAC, but they may also represent novel targets for therapeutic agents. Studies in prognosis biomarkers achieving true clinical impact and improving patient management and outcome are a matter of the utmost importance in PDAC. Besides, being able to foresee the prognosis of a PDAC patient may help to avoid futile therapy approaches and to improve quality of life of those whose long-term survival is unpromising.

12) Overexpression of the GPNMB/Osteoactivin protein induces cell growth in the Panc-1 cell line indicating that GPNMB-mediated effects on PDAC could be attributed to the enhancement of cell growth. It is accompanied by an abrogation of the apoptosis in the Panc-1 cell line. This inhibition of the apoptosis is mediated by overexpression of the Bcl-2, Bcl-X_L and c-FLIP anti-apoptotic members.

13) Knockdown of the GPNMB/Osteoactivin protein reduces cell growth in the Panc-1 cell line which is followed by an induction of apoptosis led by repression of anti-apoptotic genes such as *Bcl2a1* and by an induction of pro-apoptotic genes such as *Bax*, *Bid* and *Fas*. The apoptosis-induced seems to be a result of the inhibition of the NF-κB transcription factor.

14) Gemcitabine and Erlotinib do not enhance the tumour growth suppression or apoptosis in the GPNMB/Osteoactivin knockdown cell line, so we speculate that suppression of the GPNMB/Osteoactivin and the Gemcitabine and Erlotinib combined treatment could converge at some common point.

15) The ectopic expression of GPNMB/Osteoactivin enhances invasion in the pancreatic cancer cell lines. BMP-2, via Smad1, regulates GPNMB/Osteoactivin expression. Invasion is mediated by MMP-3 and could be associated with induction of ERK or NF-κB signalling pathways.

A better understanding of pancreatic cancer biology, earlier diagnosis and a better selection of patients on the basis of specific bio-pathological characteristics will help to improve the clinical management and outcome of these patients.

1) Los análisis in vitro han demostrado que la Gemcitabina y el Erlotinib, usados tanto en monoterapia como usados en combinación, ejercen efectos antiproliferativos sobre las líneas celulares de cáncer de páncreas Panc-1 y BxPC-3 y este efecto es dependiente del tiempo y de la concentración. Ambos fármacos ejercen su acción a través de diferentes rutas moleculares. La interacción entre ambos fármacos es considerada sinérgica para la línea celular Panc-1 mientras que se considera ligeramente antagónica para la línea celular BxPC-3. El antagonismo podría asociarse a la incapacidad de la Gemcitabina para ejercer su efecto tóxico en la fase S del ciclo celular debido al previo y eficaz bloqueo del ciclo celular en las fases G0/G1 producido por el Erlotinib.

2) La inhibición del crecimiento de las células tumorales tras la incubación con Gemcitabina y Erlotinib está relacionada, en ambas líneas, con una parada del ciclo celular. La Gemcitabina, y su combinación con Erlotinib, produce inhibición del crecimiento celular que va acompañada de una parada del ciclo celular en la fase G0/G1 y una inducción de muerte celular por apoptosis, en la línea celular de cáncer de páncreas Panc-1, la cual porta mutación en el gen *k-ras*. La Gemcitabina, y su combinación con Erlotinib, produce inhibición del crecimiento celular que va acompañada de una parada del ciclo celular en la fase G0/G1 pero sin inducción de muerte celular por apoptosis en la línea celular BxPC-3, de genotipo salvaje para *k-ras*. El Erlotinib, usado en monoterapia, inhibe la progresión del ciclo celular en la línea celular Panc-1 pero esta inhibición no está acompañada de muerte celular por apoptosis. Por el contrario, en la línea BxPC-3, el Erlotinib induce inhibición del crecimiento celular, parada del ciclo celular y muerte celular por apoptosis. El bloqueo de la progresión del ciclo celular provocado por el Erlotinib es debida a una sobreexpresión del inhibidor del ciclo celular p27Kip. El bloqueo de la progresión del ciclo celular provocado por Gemcitabina es debido a una inducción de marcadores de diferenciación como son CAII y la citoqueratina 7.

3) La apoptosis inducida por Gemcitabina es dependiente de la vía apoptótica mitocondrial y está mediada por la expresión de Bax y Bak en la línea celular Panc-1 y sólo por la expresión de Bak en la línea BxPC-3. La Gemcitabina es capaz de inducir la expresión de miembros anti-apoptóticos como BCL-2 y BCL-X_L. Sin embargo, los cocientes BCL-2/Bax y BCL-X_L/Bax son mayores que 1 lo que confirma que la Gemcitabina tiene capacidad para inducir apoptosis mediada por caspasas. En el caso de la línea de cáncer de páncreas BxPC-3, la Gemcitabina también induce la expresión de los miembros anti-apoptóticos como BCL-2 y BCL-X_L. Sin embargo, en este caso, dada la escasa expresión de Bax, los cocientes BCL-2/Bax y BCL-X_L/Bax son menores que 1 lo que confirma que la Gemcitabina tiene una capacidad limitada para inducir la apoptosis mediada por caspasas en la línea celular BxPC-3.

4) La apoptosis inducida por Erlotinib es dependiente de la vía apoptótica mitocondrial y está mediada por la expresión de Bax y Bak tanto en la línea celular Panc-1 como en la BxPC-3. El Erlotinib, sin embargo, sólo reprime la expresión del miembro anti-apoptótico BCL-2 en la línea celular salvaje para *k-ras*, BxPC-3, lo cual debe estar asociado a la inhibición de las rutas de señalización activadas por EGFR: PI3K/AKT y/o NF-κB.

5) La apoptosis inducida por el tratamiento combinado de Gemcitabina y Erlotinib en la línea celular Panc-1 es dependiente de la vía apoptótica mitocondrial y está mediada por la expresión de Bax, Bak y Apaf-1 pero también está implicada la vía extrínseca apoptótica, dependiente de receptores extracelulares de muerte, y está mediada por la sobreexpresión de la caspasa 8, Fas, DR5 y DR3. La apoptosis inducida por el tratamiento combinado de Gemcitabina y Erlotinib en la línea celular Panc-1 es también dependiente de la sobreexpresión del factor de transcripción E2F, el cual contribuye a la expresión de Apaf-1, caspasa 8 y Bax. La apoptosis inducida por el tratamiento combinado de Gemcitabina y Erlotinib en la línea celular BxPC-3 es dependiente de la vía apoptótica mitocondrial mediada por la expresión de Bax y también de la vía extrínseca apoptótica mediada por la

sobreexpresión de DR5. Sin embargo, el efecto de los fármacos en la inducción apoptótica es mucho más limitado en BxPC-3 que en Panc-1.

6) Para la línea Panc-1, el tratamiento de la Gemcitabina como agente individual y la terapia combinada con Erlotinib, se asocia con una sobreexpresión de la forma fosforilada del inhibidor IκB-α, lo que resulta en un aumento de la unión del factor de transcripción NF-κB a sus secuencias de unión en los promotores de los genes BCL-2, BCL-X_L y MMP9, así como en una disminución de la unión del factor de transcripción NF-κB a su secuencia de unión en el promotor de su propio inhibidor, el IκB-α. En la línea BxPC-3, el tratamiento de la Gemcitabina como agente individual y la terapia combinada con Erlotinib se asocia con un aumento de la unión del factor de transcripción NF-κB a sus secuencias de unión en los promotores de los genes BCL-2 e IκB-α aunque se determinó una disminución de la unión del factor de transcripción NF-κB a su secuencia de unión en el promotor de MMP9. El Erlotinib, usado en monoterapia, presenta efectos protectores en tanto en cuanto produce un aumento del bloqueo e inhibición del factor de transcripción NF-κB en el citoplasma mediado por IκB-α en ambas líneas celulares. Sin embargo los efectos son más notables en la línea celular salvaje para *k-ras*, BxPC-3.

7) La quimioresistencia al tratamiento con Gemcitabina y Erlotinib podría estar mediada, en la línea celular Panc-1, por la sobreexpresión de los factores de transcripción c-Fos, MAP2K1, RAF1 y SNCG. Sin embargo, la línea celular salvaje para *k-ras*, BxPC-3, muestra una inhibición o no modificación de estos factores de transcripción junto con una inhibición de PI3K y una notable inducción del inhibidor IκB-α. La mutación en el gen *k-ras* es responsable de la activación de las cascadas de señalización corriente abajo Raf1/MAPK y NF-κB y por tanto responsable de la quimioresistencia observada en la línea Panc-1.

8) El tratamiento combinado de Gemcitabina y Erlotinib induce la expresión de genes relacionados con la invasión y la metástasis tales como MMPs,

Plau, PlauR, IL-8 y VEGFA en la línea de cáncer de páncreas Panc-1. En la línea BxPC-3, el tratamiento produce una importante represión de las vías conducentes a la proliferación y la metástasis.

9) Hemos descrito, por primera vez, el papel de las citoquinas FGF-10/KGF-2, I-TAC/CXCL11, OSM, Osteoactivin/GPNMB y SCF como posibles biomarcadores de diagnóstico de cáncer de páncreas basándonos en la diferencia de su patrón de expresión en suero de pacientes diagnosticados de cáncer de páncreas respecto al de voluntarios sanos.

10) Hemos identificado 7 citoquinas diferencialmente expresadas en el suero de pacientes de PDAC tras el tratamiento con Gemcitabina y Erlotinib. CD30 Ligand/TNFSF8, Chordin-Like 2, FGF-10/KGF-2, GDF-15, I-TAC/CXCL11, OSM y SCF podrían representar marcadores predictivos de respuesta a Gemcitabina y Erlotinib. Podrían albergar una gran utilidad clínica indicando la utilidad y eficacia del tratamiento en pacientes de PDAC. Además podrían constituir nuevas dianas terapéuticas en la lucha contra esta enfermedad.

11) Hemos identificado un panel de 5 citoquinas del suero que comprenden B7-1/CD80, EG-VEGF/PK1, IL-29, NRG1-beta1/HRG1-beta1 y PD-ECGF con utilidad en el pronóstico de PDAC. Los biomarcadores de pronóstico conllevan un gran impacto clínico ya que la capacidad de predecir si una terapia va a ser eficaz o no para un paciente con un determinado patrón de expresión de citoquinas nos permitiría evitar terapias y efectos secundarios innecesarios e ineficaces así como intentar terapias alternativas o más enfocadas al tipo de paciente con el que estemos tratando.

12) La sobreexpresión de GPNMB/Osteoactivin induce el crecimiento celular en la línea de cáncer de páncreas Panc-1 indicando que los efectos mediados por GPNMB en PDAC podrían atribuirse a una inducción de la proliferación celular. El efecto de GPNMB sobre PDAC está acompañado por una resistencia a la apoptosis mediada por la sobreexpresión de factores anti-

apoptóticos como BCL-2, BCL-X_L y C-FLIP.

13) El silenciamiento de GPNMB/Osteoactivin reduce el crecimiento celular en la línea celular Panc-1 lo que va acompañado por una inducción de muerte celular por apoptosis mediada por la represión de genes anti-apoptóticos como *Bcl2a1* y por la inducción de genes pro-apoptóticos como *Bax*, *Bid* y *Fas*. La apoptosis inducida por el silenciamiento de GPNMB/Osteoactivin parece estar ligada a la inhibición del factor de transcripción NF-κB.

14) El tratamiento combinado de Gemcitabina y Erlotinib no aumenta la inhibición de la proliferación ni la apoptosis en la línea celular de cáncer de páncreas Panc-1 silenciada para el gen *gpnmb/osteoactivin*, de manera que estimamos que la supresión de la expresión de este gen y el tratamiento de Gemcitabina y Erlotinib podrían converger en algún punto en común.

15) La expresión ectópica de GPNMB/Osteoactivin induce la invasión en las células de cáncer de páncreas. BMP-2, vía Smad 1, regula la expresión de GPNMB/Osteoactivin. La invasión está mediada por la expresión de múltiples factores entre los que destaca la expresión de MMP-3 la cual podría ser debida a la inducción de las rutas ERK o NF-κB.

Un conocimiento más profundo de la biología del cáncer de páncreas, un diagnóstico más temprano y certero así como la selección de los pacientes en base a sus características biopatológicas podría ayudar a la mejora del tratamiento clínico y del desenlace de los pacientes con esta enfermedad.

7

ACKNOWLEDGEMENTS

Me gustaría empezar esta ardua parte de la tesis doctoral pidiendo disculpas si olvido nombrar a alguien ya que por suerte he contado con muchas personas que han contribuido a que este trabajo salga a la luz.

La realización de esta tesis no habría sido posible sin la valiosa ayuda de mis directoras: Ana y Sonia. A ambas, mi sincero agradecimiento no sólo por la formación académica, la cual sin duda fue muy importante, sino también por la confianza depositada en mí y por vuestro ejemplo de trabajo y dedicación. Las dos habéis creado un espacio de confianza y cariño en el que ha sido un gusto trabajar. Ana, desde el principio me abriste las puertas de tu laboratorio y del mundo de la investigación dándome la oportunidad de empezar esta carrera, te has volcado siempre conmigo para que consiguiera todo lo que me propusiera y al final parece que lo has conseguido. Sonia, te admiro profundamente, como investigadora, como profesora y como persona. He tenido la mayor suerte del mundo teniéndote como directora de tesis y todo lo que sé y soy a nivel investigador ha sido gracias a ti, todo lo he aprendido de ti. Te agradezco de todo corazón todo el trabajo que has realizado con mi tesis, especialmente en este último año y todo lo que me has aportado, a nivel personal y profesional.

A mi familia y en especial a mis padres. Me habéis enseñado con el ejemplo y de vosotros he aprendido que en la vida hay que trabajar muy duro por los sueños y que todo trabajo tiene su recompensa. Gracias por todos los sacrificios y esfuerzos que habéis hecho por nosotras y por estar siempre dispuestos a hacerlos. A mi abuelo porque siempre me decía lo importante que era mi trabajo en la sociedad.
Muy especialmente a Curro, tendría que escribir otra tesis entera para darte las gracias por todo lo que representas para mí. Siempre has creído y confiado en mí hasta el punto de querer pasar la vida entera junto a mí. No puedo agradecerle lo suficiente a Dios que te pusiera en mi camino dándome el regalo más preciado que tengo.

A mis compañeros del Departamento de Bioquímica por formar una gran familia, con sus más y sus menos, pero a la que siempre se puede acudir llegado el momento. Desde que empecé mi trabajo allí me he sentido muy acogida y ayudada

por todos, especialmente por los miembros de mi grupo de investigación. A Patricia porque tu sola presencia da confianza, siempre estás dispuesta a ayudar con lo que sea. A María, también por tu ayuda en el laboratorio y por los raticos de cháchara por la mañana que hacen que uno afronte el día de otra manera. A Marichu porque siempre que he tenido algún problema estabas allí para solucionar mis dudas. A Mª Paz por tu cercanía y tu trato. A Eva por esa alegría que desprendes, por los ratos de camino de la casa a la facultad arreglando el mundo. A Miguel, que desde que has llegado has puesto a mi disposición todo lo que necesitara. A Pablo, por ser mi "compi", el ejemplo a seguir de cómo conseguir las metas que uno se plantea. Me has ayudado mucho con todo el papeleo de la tesis. Has ido abriendo un camino que no ha hecho más que facilitar el paso de los que vamos detrás. Me gusta compartir contigo la pasión por la docencia y la investigación. A Esther, por el tiempo que estuvo en mi laboratorio ayudándome. Gracias por todo el trabajo que me quitabas. Por último, muy especialmente a Xiomara, por su amistad, por su cariño y por su ayuda en todos los aspectos, profesionales y laborales. Te admiro, eres una luchadora y sólo espero que la vida te dé pronto toda la felicidad que mereces y que vivamos muchas más cosas juntas.

No puedo ni quiero olvidarme de Jaime y de Nieves porque sin su trabajo y ayuda no habría podido realizar esta tesis. La citometría me ha dado unos pocos quebraderos de cabeza pero también qué buenos ratos y risas.

Quiero agradecer también a todos los que han colaborado en el proyecto de páncreas, a José Ramón Delgado, por toda su ayuda económica y profesional.

To professor Kemmner, for welcoming me so warmly in his lab and giving me the opportunity to learn of his broad experience. My research stay was an important boost for my PhD and a very enriching experience. I would like to also thank Qing for all her help in the lab and for teaching me so well.

A todos, sinceramente… ¡¡¡Muchas gracias!!!

8

BIBLIOGRAPHY

1. Schwartz, S.I.B.F.C., *Schwartz's principles of surgery*. 2010, New York: McGraw-Hill, Medical Pub. Division.
2. Egerbacher, M. and P. Bock, *Morphology of the pancreatic duct system in mammals.* Microsc Res Tech, 1997. **37**(5-6): p. 407-17.
3. Bardeesy, N. and R.A. DePinho, *Pancreatic cancer biology and genetics.* Nat Rev Cancer, 2002. **2**(12): p. 897-909.
4. Hezel, A.F., et al., *Genetics and biology of pancreatic ductal adenocarcinoma.* Genes Dev, 2006. **20**(10): p. 1218-49.
5. Jones, S., et al., *Core signaling pathways in human pancreatic cancers revealed by global genomic analyses.* Science, 2008. **321**(5897): p. 1801-6.
6. Wood, L.D. and R.H. Hruban, *Pathology and molecular genetics of pancreatic neoplasms.* Cancer J, 2012. **18**(6): p. 492-501.
7. Siegel, R., D. Naishadham, and A. Jemal, *Cancer statistics, 2013.* CA Cancer J Clin, 2013. **63**(1): p. 11-30.
8. Raimondi, S., P. Maisonneuve, and A.B. Lowenfels, *Epidemiology of pancreatic cancer: an overview.* Nat Rev Gastroenterol Hepatol, 2009. **6**(12): p. 699-708.
9. Stolzenberg-Solomon, R.Z., et al., *Dietary and other methyl-group availability factors and pancreatic cancer risk in a cohort of male smokers.* Am J Epidemiol, 2001. **153**(7): p. 680-7.
10. Klein, A.P., et al., *Prospective risk of pancreatic cancer in familial pancreatic cancer kindreds.* Cancer Res, 2004. **64**(7): p. 2634-8.
11. Klein, A.P., *Identifying people at a high risk of developing pancreatic cancer.* Nature Reviews Cancer, 2013. **13**(1): p. 66-74.
12. Klein, A.P., et al., *Familial pancreatic cancer.* Cancer J, 2001. **7**(4): p. 266-73.
13. Maitra, A. and R.H. Hruban, *Pancreatic cancer.* Annu Rev Pathol, 2008. **3**: p. 157-88.
14. Kopinke, D., et al., *Ongoing Notch signaling maintains phenotypic fidelity in the adult exocrine pancreas.* Dev Biol, 2012. **362**(1): p. 57-64.
15. Stanger, B.Z. and Y. Dor, *Dissecting the cellular origins of pancreatic cancer.* Cell Cycle, 2006. **5**(1): p. 43-6.
16. Sergeant, G., et al., *Role of cancer stem cells in pancreatic ductal adenocarcinoma.* Nat Rev Clin Oncol, 2009. **6**(10): p. 580-6.
17. Balic, A., et al., *Stem cells as the root of pancreatic ductal adenocarcinoma.* Experimental Cell Research, 2012. **318**(6): p. 691-704.
18. Li, C., et al., *Identification of pancreatic cancer stem cells.* Cancer Res, 2007. **67**(3): p. 1030-7.
19. Hermann, P.C., et al., *Distinct populations of cancer stem cells determine tumor growth and metastatic activity in human pancreatic cancer.* Cell Stem Cell, 2007. **1**(3): p. 313-23.
20. Penchev, V.R., et al., *Heterogeneity and targeting of pancreatic cancer stem cells.* Clin Cancer Res, 2012. **18**(16): p. 4277-84.
21. Abel, E.V. and D.M. Simeone, *Biology and clinical applications of pancreatic cancer stem cells.* Gastroenterology, 2013. **144**(6): p. 1241-8.
22. Ischenko, I., et al., *Pancreatic cancer stem cells: new understanding of tumorigenesis, clinical implications.* Langenbecks Arch Surg, 2010. **395**(1): p. 1-10.
23. Maitra, A., et al., *Multicomponent analysis of the pancreatic adenocarcinoma progression model using a pancreatic intraepithelial neoplasia tissue microarray.* Mod Pathol, 2003. **16**(9): p. 902-12.
24. Hidalgo, M., *New insights into pancreatic cancer biology.* Annals of Oncology, 2012. **23**: p. 135-138.
25. Hingorani, S.R., et al., *Trp53R172H and KrasG12D cooperate to promote chromosomal instability and widely metastatic pancreatic ductal adenocarcinoma in mice.* Cancer Cell, 2005. **7**(5): p. 469-83.
26. Bardeesy, N., et al., *Both p16(Ink4a) and the p19(Arf)-p53 pathway constrain progression of pancreatic adenocarcinoma in the mouse.* Proceedings of the National Academy of Sciences

of the United States of America, 2006. **103**(15): p. 5947-5952.
27. Guerra, C., et al., *Chronic pancreatitis is essential for induction of pancreatic ductal adenocarcinorna by k-Ras Oncogenes in adult mice.* Cancer Cell, 2007. **11**(3): p. 291-302.
28. Giovinazzo, F., et al., *Clinical implications of biological markers in Pancreatic Ductal Adenocarcinoma.* Surg Oncol, 2012. **21**(4): p. e171-82.
29. Hidalgo, M., *Pancreatic cancer.* N Engl J Med, 2010. **362**(17): p. 1605-17.
30. Hanahan, D. and R.A. Weinberg, *The hallmarks of cancer.* Cell, 2000. **100**(1): p. 57-70.
31. Mitin, N., K.L. Rossman, and C.J. Der, *Signaling interplay in Ras superfamily function.* Curr Biol, 2005. **15**(14): p. R563-74.
32. Malumbres, M. and M. Barbacid, *RAS oncogenes: the first 30 years.* Nat Rev Cancer, 2003. **3**(6): p. 459-65.
33. Klimstra, D.S. and D.S. Longnecker, *K-ras mutations in pancreatic ductal proliferative lesions.* Am J Pathol, 1994. **145**(6): p. 1547-50.
34. Deramaudt, T. and A.K. Rustgi, *Mutant KRAS in the initiation of pancreatic cancer.* Biochim Biophys Acta, 2005. **1756**(2): p. 97-101.
35. Ren, Y.X., et al., *Detection of point mutation in K-ras oncogene at codon 12 in pancreatic diseases.* World Journal of Gastroenterology, 2004. **10**(6): p. 881-884.
36. Shaw, A.T., et al., *Selective killing of K-ras mutant cancer cells by small molecule inducers of oxidative stress.* Proc Natl Acad Sci U S A, 2011. **108**(21): p. 8773-8.
37. Knafo, S. and J.A. Esteban, *Common pathways for growth and for plasticity.* Current Opinion in Neurobiology, 2012. **22**(3): p. 405-411.
38. Adjei, A.A., *Blocking oncogenic Ras signaling for cancer therapy.* J Natl Cancer Inst, 2001. **93**(14): p. 1062-74.
39. Mihaljevic, A.L., et al., *Molecular mechanism of pancreatic cancer--understanding proliferation, invasion, and metastasis.* Langenbecks Arch Surg, 2010. **395**(4): p. 295-308.
40. Santarpia, L., S.M. Lippman, and A.K. El-Naggar, *Targeting the MAPK-RAS-RAF signaling pathway in cancer therapy.* Expert Opin Ther Targets, 2012. **16**(1): p. 103-19.
41. McCubrey, J.A., et al., *Roles of the Raf/MEK/ERK pathway in cell growth, malignant transformation and drug resistance.* Biochim Biophys Acta, 2007. **1773**(8): p. 1263-84.
42. Sun, C., et al., *The role of phosphatidylinositol 3-kinase signaling pathways in pancreatic cancer.* Pancreatology, 2011. **11**(2): p. 252-60.
43. Eser, S., et al., *Selective requirement of PI3K/PDK1 signaling for Kras oncogene-driven pancreatic cell plasticity and cancer.* Cancer Cell, 2013. **23**(3): p. 406-20.
44. Altomare, D.A. and A.R. Khaled, *Homeostasis and the Importance for a Balance Between AKT/mTOR Activity and Intracellular Signaling.* Current Medicinal Chemistry, 2012. **19**(22): p. 3748-3762.
45. Preis, M. and M. Korc, *Kinase signaling pathways as targets for intervention in pancreatic cancer.* Cancer Biology & Therapy, 2010. **9**(10): p. 754-763.
46. Vivanco, I. and C.L. Sawyers, *The phosphatidylinositol 3-Kinase AKT pathway in human cancer.* Nat Rev Cancer, 2002. **2**(7): p. 489-501.
47. Martin, T.D. and C.J. Der, *Differential involvement of RalA and RalB in colorectal cancer.* Small GTPases, 2012. **3**(2): p. 126-30.
48. Lim, K.H., et al., *Divergent roles for RalA and RalB in malignant growth of human pancreatic carcinoma cells.* Curr Biol, 2006. **16**(24): p. 2385-94.
49. Deleo, A.B., et al., *Detection of a Transformation-Related Antigen in Chemically-Induced Sarcomas and Other Transformed-Cells of the Mouse.* Proceedings of the National Academy of Sciences of the United States of America, 1979. **76**(5): p. 2420-2424.
50. Qian, Y. and X. Chen, *Senescence regulation by the p53 protein family.* Methods Mol Biol, 2013. **965**: p. 37-61.
51. Talar-Wojnarowska, R. and E. Malecka-Panas, *Molecular pathogenesis of pancreatic adenocarcinoma: Potential clinical implications.* Medical Science Monitor, 2006. **12**(9): p.

Ra186-Ra193.
52. Scarpa, A., et al., *Pancreatic Adenocarcinomas Frequently Show P53 Gene-Mutations.* American Journal of Pathology, 1993. **142**(5): p. 1534-1543.
53. Gnoni, A., et al., *Carcinogenesis of Pancreatic Adenocarcinoma: Precursor Lesions.* Int J Mol Sci, 2013. **14**(10): p. 19731-19762.
54. Garcea, G., et al., *Molecular prognostic markers in pancreatic cancer: A systematic review.* European Journal of Cancer, 2005. **41**(15): p. 2213-2236.
55. Shin, S.H., et al., *Genetic Alterations of K-ras, p53, c-erbB-2, and DPC4 in Pancreatic Ductal Adenocarcinoma and Their Correlation With Patient Survival.* Pancreas, 2013. **42**(2): p. 216-222.
56. Dong, M., et al., *Clinicopathological significance of p53 and mdm2 protein expression in human pancreatic cancer.* World Journal of Gastroenterology, 2005. **11**(14): p. 2162-2165.
57. Singh, P., R. Srinivasan, and J.D. Wig, *Major Molecular Markers in Pancreatic Ductal Adenocarcinoma and Their Roles in Screening, Diagnosis, Prognosis, and Treatment.* Pancreas, 2011. **40**(5): p. 644-652.
58. Holland, E.C., *Gliomagenesis: genetic alterations and mouse models.* Nat Rev Genet, 2001. **2**(2): p. 120-9.
59. Matthaios, D., et al., *Molecular Pathogenesis of Pancreatic Cancer and Clinical Perspectives.* Oncology, 2011. **81**(3-4): p. 259-272.
60. Ohtsubo, K., et al., *Abnormalities of tumor suppressor gene p16 in pancreatic carcinoma: immunohistochemical and genetic findings compared with clinicopathological parameters.* Journal of Gastroenterology, 2003. **38**(7): p. 663-671.
61. Hu, Y.X., et al., *Frequent loss of p16 expression and its correlation with clinicopathological parameters in pancreatic carcinoma.* Clin Cancer Res, 1997. **3**(9): p. 1473-7.
62. Drabsch, Y. and P. ten Dijke, *TGF-beta signalling and its role in cancer progression and metastasis.* Cancer Metastasis Rev, 2012. **31**(3-4): p. 553-68.
63. Truty, M.J. and R. Urrutia, *Basics of TGF-beta and pancreatic cancer.* Pancreatology, 2007. **7**(5-6): p. 423-35.
64. Ross, S. and C.S. Hill, *How the Smads regulate transcription.* International Journal of Biochemistry & Cell Biology, 2008. **40**(3): p. 383-408.
65. Shi, Y. and J. Massague, *Mechanisms of TGF-beta signaling from cell membrane to the nucleus.* Cell, 2003. **113**(6): p. 685-700.
66. Krantz, S.B., et al., *Contribution of epithelial-to-mesenchymal transition and cancer stem cells to pancreatic cancer progression.* J Surg Res, 2012. **173**(1): p. 105-12.
67. Nicolas, F.J. and C.S. Hill, *Attenuation of the TGF-beta-Smad signaling pathway in pancreatic tumor cells confers resistance to TGF-beta-induced growth arrest.* Oncogene, 2003. **22**(24): p. 3698-711.
68. Yang, G. and X. Yang, *Smad4-mediated TGF-beta signaling in tumorigenesis.* Int J Biol Sci, 2010. **6**(1): p. 1-8.
69. Liu, F., *SMAD4/DPC4 and pancreatic cancer survival. Commentary re: M. Tascilar et al., The SMAD4 protein and prognosis of pancreatic ductal adenocarcinoma. Clin. Cancer Res., 7: 4115-4121, 2001.* Clin Cancer Res, 2001. **7**(12): p. 3853-6.
70. Oliveira-Cunha, M., W.G. Newman, and A.K. Siriwardena, *Epidermal Growth Factor Receptor in Pancreatic Cancer.* Cancers, 2011.
71. Brand, T.M., et al., *The nuclear epidermal growth factor receptor signaling network and its role in cancer.* Discov Med, 2011. **12**(66): p. 419-32.
72. Durkin, A.J., et al., *Defining the role of the epidermal growth factor receptor in pancreatic cancer grown in vitro.* Am J Surg, 2003. **186**(5): p. 431-6.
73. Yamanaka, Y., et al., *Coexpression of Epidermal Growth-Factor Receptor and Ligands in Human Pancreatic-Cancer Is Associated with Enhanced Tumor Aggressiveness.* Anticancer Research, 1993. **13**(3): p. 565-570.

74. Friess, H., M. Korc, and M.W. Buchler, *Growth factors and growth factor receptors in benign pancreatic disorders.* Digestive Surgery, 1994. **11**(3-6): p. 138-142.
75. Von Marschall, Z., et al., *Vascular endothelial growth factor-D induces lymphangiogenesis and lymphatic metastasis in models of ductal pancreatic cancer.* International Journal of Oncology, 2005. **27**(3): p. 669-679.
76. Korc, M., *Pathways for aberrant angiogenesis in pancreatic cancer.* Mol Cancer, 2003. **2**: p. 8.
77. Ferrara, N., H.P. Gerber, and J. LeCouter, *The biology of VEGF and its receptors.* Nat Med, 2003. **9**(6): p. 669-76.
78. Seo, Y., et al., *High expression of vascular endothelial growth factor is associated with liver metastasis and a poor prognosis for patients with ductal pancreatic adenocarcinoma.* Cancer, 2000. **88**(10): p. 2239-2245.
79. Fukasawa, M. and M. Korc, *Vascular endothelial growth factor-trap suppresses tumorigenicity of multiple pancreatic cancer cell lines.* Clin Cancer Res, 2004. **10**(10): p. 3327-32.
80. Kurahara, H., et al., *Impact of vascular endothelial growth factor-C and -D expression in human pancreatic cancer: its relationship to lymph node metastasis.* Clin Cancer Res, 2004. **10**(24): p. 8413-20.
81. Rhim, A.D. and B.Z. Stanger, *Molecular Biology of Pancreatic Ductal Adenocarcinoma Progression Aberrant Activation of Developmental Pathways.* Development, Differentiation and Disease of the Para-Alimentary Tract, 2010. **97**: p. 41-78.
82. Turner, N. and R. Grose, *Fibroblast growth factor signalling: from development to cancer.* Nat Rev Cancer, 2010. **10**(2): p. 116-29.
83. Napetschnig, J. and H. Wu, *Molecular basis of NF-kappaB signaling.* Annu Rev Biophys, 2013. **42**: p. 443-68.
84. Chandler, N.M., J.J. Canete, and M.P. Callery, *Increased expression of NF-kappa B subunits in human pancreatic cancer cells.* J Surg Res, 2004. **118**(1): p. 9-14.
85. Wang, W.X., et al., *The nuclear factor-kappa B RelA transcription factor is constitutively activated in human pancreatic adenocarcinoma cells.* Clinical Cancer Research, 1999. **5**(1): p. 119-127.
86. Liptay, S., et al., *Mitogenic and antiapoptotic role of constitutive NF-kappa B/Rel activity in pancreatic cancer.* International Journal of Cancer, 2003. **105**(6): p. 735-746.
87. Zhang, H., et al., *Epidermal growth factor promotes invasiveness of pancreatic cancer cells through NF-kappaB-mediated proteinase productions.* Pancreas, 2006. **32**(1): p. 101-9.
88. Fujioka, S., et al., *Function of nuclear factor kappaB in pancreatic cancer metastasis.* Clin Cancer Res, 2003. **9**(1): p. 346-54.
89. Trauzold, A., et al., *CD95 and TRAIL receptor-mediated activation of protein kinase C and NF-kappaB contributes to apoptosis resistance in ductal pancreatic adenocarcinoma cells.* Oncogene, 2001. **20**(31): p. 4258-69.
90. Trauzold, A., et al., *CD95 and TRAF2 promote invasiveness of pancreatic cancer cells.* FASEB J, 2005. **19**(6): p. 620-2.
91. Arlt, A., H. Schafer, and H. Kalthoff, *The 'N-factors' in pancreatic cancer: functional relevance of NF-kappaB, NFAT and Nrf2 in pancreatic cancer.* Oncogenesis, 2012. **1**: p. e35.
92. Hayden, M.S. and S. Ghosh, *Shared principles in NF-kappaB signaling.* Cell, 2008. **132**(3): p. 344-62.
93. Ramalho-Santos, M., D.A. Melton, and A.P. McMahon, *Hedgehog signals regulate multiple aspects of gastrointestinal development.* Development, 2000. **127**(12): p. 2763-72.
94. Thayer, S.P., et al., *Hedgehog is an early and late mediator of pancreatic cancer tumorigenesis.* Nature, 2003. **425**(6960): p. 851-856.
95. Kayed, H., et al., *Indian hedgehog signaling pathway: expression and regulation in pancreatic cancer.* Int J Cancer, 2004. **110**(5): p. 668-76.
96. Morton, J.P., et al., *Sonic hedgehog acts at multiple stages during pancreatic tumorigenesis.*

Proceedings of the National Academy of Sciences of the United States of America, 2007. **104**(12): p. 5103-5108.
97. Ranganathan, P., K.L. Weaver, and A.J. Capobianco, *Notch signalling in solid tumours: a little bit of everything but not all the time.* Nat Rev Cancer, 2011. **11**(5): p. 338-51.
98. Gordon, W.R., K.L. Arnett, and S.C. Blacklow, *The molecular logic of Notch signaling--a structural and biochemical perspective.* J Cell Sci, 2008. **121**(Pt 19): p. 3109-19.
99. Demarest, R.M., F. Ratti, and A.J. Capobianco, *It's T-ALL about Notch.* Oncogene, 2008. **27**(38): p. 5082-5091.
100. Garcia, A. and J.J. Kandel, *Notch: a key regulator of tumor angiogenesis and metastasis.* Histol Histopathol, 2012. **27**(2): p. 151-6.
101. Bao, B., et al., *Notch-1 induces epithelial-mesenchymal transition consistent with cancer stem cell phenotype in pancreatic cancer cells.* Cancer Letters, 2011. **307**(1): p. 26-36.
102. De La, O.J. and L.C. Murtaugh, *Notch and Kras in pancreatic cancer: at the crossroads of mutation, differentiation and signaling.* Cell Cycle, 2009. **8**(12): p. 1860-4.
103. Yabuuchi, S., et al., *Notch signaling pathway targeted therapy suppresses tumor progression and metastatic spread in pancreatic cancer.* Cancer Letters, 2013. **335**(1): p. 41-51.
104. Lowe, S.W., E. Cepero, and G. Evan, *Intrinsic tumour suppression.* Nature, 2004. **432**(7015): p. 307-15.
105. Luttges, J., et al., *Lack of apoptosis in PanIN-1 and PanIN-2 lesions associated with pancreatic ductal adenocarcinoma is not dependent on K-ras status.* Pancreas, 2003. **27**(3): p. e57-62.
106. Fiandalo, M.V. and N. Kyprianou, *Caspase control: protagonists of cancer cell apoptosis.* Exp Oncol, 2012. **34**(3): p. 165-75.
107. Ola, M.S., M. Nawaz, and H. Ahsan, *Role of Bcl-2 family proteins and caspases in the regulation of apoptosis.* Mol Cell Biochem, 2011. **351**(1-2): p. 41-58.
108. Adams, J.M. and S. Cory, *Bcl-2-regulated apoptosis: mechanism and therapeutic potential.* Curr Opin Immunol, 2007. **19**(5): p. 488-96.
109. Guicciardi, M.E. and G.J. Gores, *Life and death by death receptors.* FASEB J, 2009. **23**(6): p. 1625-37.
110. Trauzold, A., et al., *CD95 and TRAIL receptor-mediated activation of protein kinase C and NF-kappa B contributes to apoptosis resistance in ductal pancreatic adenocarcinoma cells.* Oncogene, 2001. **20**(31): p. 4258-4269.
111. Hinz, S., et al., *Bcl-XL protects pancreatic adenocarcinoma cells against CD95- and TRAIL-receptor-mediated apoptosis.* Oncogene, 2000. **19**(48): p. 5477-86.
112. Hamacher, R., et al., *Apoptotic pathways in pancreatic ductal adenocarcinoma.* Mol Cancer, 2008. **7**: p. 64.
113. Roder, C., A. Trauzold, and H. Kalthoff, *Impact of death receptor signaling on the malignancy of pancreatic ductal adenocarcinoma.* Eur J Cell Biol, 2011. **90**(6-7): p. 450-5.
114. Muerkoster, S.S., et al., *Acquired chemoresistance in pancreatic carcinoma cells: induced secretion of IL-1beta and NO lead to inactivation of caspases.* Oncogene, 2006. **25**(28): p. 3973-81.
115. Ungefroren, H., et al., *FAP-1 in pancreatic cancer cells: functional and mechanistic studies on its inhibitory role in CD95-mediated apoptosis.* J Cell Sci, 2001. **114**(Pt 15): p. 2735-46.
116. Egberts, J.H., et al., *Anti-tumor necrosis factor therapy inhibits pancreatic tumor growth and metastasis.* Cancer Research, 2008. **68**(5): p. 1443-1450.
117. Arlt, A., S.S. Muerkoster, and H. Schafer, *Targeting apoptosis pathways in pancreatic cancer.* Cancer Lett, 2013. **332**(2): p. 346-58.
118. Safa, A.R., *c-FLIP, a master anti-apoptotic regulator.* Exp Oncol, 2012. **34**(3): p. 176-84.
119. Trauzold, A., et al., *Multiple and synergistic deregulations of apoptosis-controlling genes in pancreatic carcinoma cells.* Br J Cancer, 2003. **89**(9): p. 1714-21.
120. Magistrelli, P., et al., *Apoptotic index or a combination of Bax/Bcl-2 expression correlate with survival after resection of pancreatic adenocarcinoma.* J Cell Biochem, 2006. **97**(1): p. 98-

108.
121. Evans, J.D., et al., *Detailed tissue expression of bcl-2, bax, bak and bcl-x in the normal human pancreas and in chronic pancreatitis, ampullary and pancreatic ductal adenocarcinomas.* Pancreatology, 2001. **1**(3): p. 254-262.
122. Friedl, P. and S. Alexander, *Cancer Invasion and the Microenvironment: Plasticity and Reciprocity.* Cell, 2011. **147**(5): p. 992-1009.
123. Walsh, N., et al., *Alterations in integrin expression modulates invasion of pancreatic cancer cells.* J Exp Clin Cancer Res, 2009. **28**: p. 140.
124. Mareel, M.M., M.E. Bracke, and E.R. Boghaert, *Tumor Invasion and Metastasis - Therapeutic Implications.* Radiotherapy and Oncology, 1986. **6**(2): p. 135-142.
125. Seyfried, T.N. and L.C. Huysentruyt, *On the origin of cancer metastasis.* Crit Rev Oncog, 2013. **18**(1-2): p. 43-73.
126. Waghray, M., et al., *Deciphering the role of stroma in pancreatic cancer.* Curr Opin Gastroenterol, 2013. **29**(5): p. 537-43.
127. Luo, G., et al., *Stroma and pancreatic ductal adenocarcinoma: an interaction loop.* Biochim Biophys Acta, 2012. **1826**(1): p. 170-8.
128. Dangi-Garimella, S., et al., *Epithelial-mesenchymal transition and pancreatic cancer progression.* 2012.
129. Lonardo, E., et al., *Pancreatic stellate cells form a niche for cancer stem cells and promote their self-renewal and invasiveness.* Cell Cycle, 2012. **11**(7): p. 1282-90.
130. Hamada, S., et al., *Pancreatic stellate cells enhance stem cell-like phenotypes in pancreatic cancer cells.* Biochem Biophys Res Commun, 2012. **421**(2): p. 349-54.
131. Apte, M.V., et al., *A starring role for stellate cells in the pancreatic cancer microenvironment.* Gastroenterology, 2013. **144**(6): p. 1210-9.
132. Tod, J., et al., *Tumor-stromal interactions in pancreatic cancer.* Pancreatology, 2013. **13**(1): p. 1-7.
133. Feig, C., et al., *The pancreas cancer microenvironment.* Clin Cancer Res, 2012. **18**(16): p. 4266-76.
134. Phillips, P., *Pancreatic stellate cells and fibrosis.* 2012.
135. Apte, M.V., R.C. Pirola, and J.S. Wilson, *Pancreatic stellate cells: a starring role in normal and diseased pancreas.* Front Physiol, 2012. **3**: p. 344.
136. Alexakis, N., et al., *Current standards of surgery for pancreatic cancer.* Br J Surg, 2004. **91**(11): p. 1410-27.
137. Krug, S. and P. Michl, *New developments in pancreatic cancer treatment.* Minerva Gastroenterol Dietol, 2012. **58**(4): p. 427-43.
138. Bouffard, D.Y., J. Laliberte, and R.L. Momparler, *Kinetic studies on 2',2'-difluorodeoxycytidine (Gemcitabine) with purified human deoxycytidine kinase and cytidine deaminase.* Biochem Pharmacol, 1993. **45**(9): p. 1857-61.
139. Ueno, H., K. Kiyosawa, and N. Kaniwa, *Pharmacogenomics of gemcitabine: can genetic studies lead to tailor-made therapy?* Br J Cancer, 2007. **97**(2): p. 145-51.
140. Heinemann, V., et al., *Cellular elimination of 2',2'-difluorodeoxycytidine 5'-triphosphate: a mechanism of self-potentiation.* Cancer Res, 1992. **52**(3): p. 533-9.
141. Mini, E., et al., *Cellular pharmacology of gemcitabine.* Ann Oncol, 2006. **17 Suppl 5**: p. v7-12.
142. Crul, M., et al., *DNA repair mechanisms involved in gemcitabine cytotoxicity and in the interaction between gemcitabine and cisplatin.* Biochem Pharmacol, 2003. **65**(2): p. 275-82.
143. Morgan, M.A., et al., *Role of checkpoint kinase 1 in preventing premature mitosis in response to gemcitabine.* Cancer Res, 2005. **65**(15): p. 6835-42.
144. Hertel, L.W., et al., *Evaluation of the antitumor activity of gemcitabine (2',2'-difluoro-2'-deoxycytidine).* Cancer Res, 1990. **50**(14): p. 4417-22.
145. Veltkamp, S.A., J.H. Beijnen, and J.H. Schellens, *Prolonged versus standard gemcitabine infusion: translation of molecular pharmacology to new treatment strategy.* Oncologist,

2008. **13**(3): p. 261-76.
146. Bergman, A.M., H.M. Pinedo, and G.J. Peters, *Determinants of resistance to 2',2'-difluorodeoxycytidine (gemcitabine).* Drug Resist Updat, 2002. **5**(1): p. 19-33.
147. Ruiz van Haperen, V.W., et al., *2',2'-Difluoro-deoxycytidine (gemcitabine) incorporation into RNA and DNA of tumour cell lines.* Biochem Pharmacol, 1993. **46**(4): p. 762-6.
148. Gmeiner, W.H., et al., *Structural basis for topoisomerase I inhibition by nucleoside analogs.* Nucleosides Nucleotides Nucleic Acids, 2003. **22**(5-8): p. 653-8.
149. Pauwels, B., et al., *Combined modality therapy of gemcitabine and radiation.* Oncologist, 2005. **10**(1): p. 34-51.
150. Faller, B.A. and B. Burtness, *Treatment of pancreatic cancer with epidermal growth factor receptor-targeted therapy.* Biologics, 2009. **3**: p. 419-28.
151. Rocha-Lima, C.M., et al., *EGFR targeting of solid tumors.* Cancer Control, 2007. **14**(3): p. 295-304.
152. Moore, M.J., et al., *Erlotinib plus gemcitabine compared with gemcitabine alone in patients with advanced pancreatic cancer: a phase III trial of the National Cancer Institute of Canada Clinical Trials Group.* J Clin Oncol, 2007. **25**(15): p. 1960-6.
153. Miksad, R.A., L. Schnipper, and M. Goldstein, *Does a statistically significant survival benefit of erlotinib plus gemcitabine for advanced pancreatic cancer translate into clinical significance and value?* Journal of Clinical Oncology, 2007. **25**(28): p. 4506-4507.
154. Normanno, N. and A. De Luca, *Erlotinib in pancreatic cancer: Are tumor cells the (only) target?* Journal of Clinical Oncology, 2007. **25**(36): p. 5836-5837.
155. Agarwal, B., A.M. Correa, and L. Ho, *Survival in pancreatic carcinoma based on tumor size.* Pancreas, 2008. **36**(1): p. e15-20.
156. Atkinson, A.J., Jr., et al., *Biomarkers and surrogate endpoints: preferred definitions and conceptual framework.* Clin Pharmacol Ther, 2001. **69**(3): p. 89-95.
157. Henry, N.L. and D.F. Hayes, *Cancer biomarkers.* Mol Oncol, 2012. **6**(2): p. 140-6.
158. Sturgeon, C.M., et al., *National Academy of Clinical Biochemistry Laboratory Medicine Practice Guidelines for use of tumor markers in liver, bladder, cervical, and gastric cancers.* Clin Chem, 2010. **56**(6): p. e1-48.
159. Bhat, K., et al., *Advances in biomarker research for pancreatic cancer.* Curr Pharm Des, 2012. **18**(17): p. 2439-51.
160. Ni, X.G., et al., *The clinical value of serum CEA, CA19-9, and CA242 in the diagnosis and prognosis of pancreatic cancer.* Eur J Surg Oncol, 2005. **31**(2): p. 164-9.
161. Bhattacharyya, S., et al., *Diagnosis of pancreatic cancer using serum proteomic profiling.* Neoplasia, 2004. **6**(5): p. 674-686.
162. Winter, J.M., C.J. Yeo, and J.R. Brody, *Diagnostic, prognostic, and predictive biomarkers in pancreatic cancer.* J Surg Oncol, 2013. **107**(1): p. 15-22.
163. Clark, G.M., *Prognostic factors versus predictive factors: Examples from a clinical trial of erlotinib.* Mol Oncol, 2008. **1**(4): p. 406-12.
164. Jamieson, N.B., et al., *Tissue biomarkers for prognosis in pancreatic ductal adenocarcinoma: a systematic review and meta-analysis.* Clin Cancer Res, 2011. **17**(10): p. 3316-31.
165. Garcea, G., et al., *Molecular prognostic markers in pancreatic cancer: a systematic review.* Eur J Cancer, 2005. **41**(15): p. 2213-36.
166. Luo, Y., et al., *Identification of novel predictive markers for the prognosis of pancreatic ductal adenocarcinoma.* Hum Pathol, 2013. **44**(1): p. 69-76.
167. Mann, C.D., et al., *Notch3 and hey-1 as prognostic biomarkers in pancreatic adenocarcinoma.* PLoS One, 2012. **7**(12): p. e51119.
168. Dallol, A., et al., *Methylation of the polycomb group target genes is a possible biomarker for favorable prognosis in colorectal cancer.* Cancer Epidemiol Biomarkers Prev, 2012. **21**(11): p. 2069-75.
169. Denley, S.M., et al., *Activation of the IL-6R/Jak/Stat Pathway is Associated with a Poor*

Outcome in Resected Pancreatic Ductal Adenocarcinoma. J Gastrointest Surg, 2013.
170. Giovannetti, E., et al., *High-throughput microRNA (miRNAs) arrays unravel the prognostic role of MiR-211 in pancreatic cancer.* PLoS One, 2012. **7**(11): p. e49145.
171. Dima, S.O., et al., *An exploratory study of inflammatory cytokines as prognostic biomarkers in patients with ductal pancreatic adenocarcinoma.* Pancreas, 2012. **41**(7): p. 1001-7.
172. Ekins, R., F. Chu, and E. Biggart, *Development of Microspot Multi-Analyte Ratiometric Immunoassay Using Dual Fluorescent-Labeled Antibodies.* Analytica Chimica Acta, 1989. **227**(1): p. 73-96.
173. Sutandy, F.X., et al., *Overview of protein microarrays.* Curr Protoc Protein Sci, 2013. **Chapter 27**: p. Unit 27 1.
174. Caiazzo, R.J., et al., *Protein microarrays as an application for disease biomarkers.* Proteomics Clinical Applications, 2009. **3**(2): p. 138-147.
175. Huang, R., et al., *A biotin label-based antibody array for high-content profiling of protein expression.* Cancer Genomics Proteomics, 2010. **7**(3): p. 129-41.
176. Mantovani, A., et al., *Cancer-related inflammation.* Nature, 2008. **454**(7203): p. 436-44.
177. Germano, G., P. Allavena, and A. Mantovani, *Cytokines as a key component of cancer-related inflammation.* Cytokine, 2008. **43**(3): p. 374-9.
178. Amedei, A., D. Prisco, and D.E. MM, *The use of cytokines and chemokines in the cancer immunotherapy.* Recent Pat Anticancer Drug Discov, 2013. **8**(2): p. 126-42.
179. Shields, M.A., et al., *Biochemical role of the collagen-rich tumour microenvironment in pancreatic cancer progression.* Biochem J, 2012. **441**(2): p. 541-52.
180. Neesse, A., et al., *Stromal biology and therapy in pancreatic cancer.* Gut, 2011. **60**(6): p. 861-8.
181. Schumacher, M., H. Binder, and T. Gerds, *Assessment of survival prediction models based on microarray data.* Bioinformatics, 2007. **23**(14): p. 1768-74.
182. Smit, S., H.C. Hoefsloot, and A.K. Smilde, *Statistical data processing in clinical proteomics.* J Chromatogr B Analyt Technol Biomed Life Sci, 2008. **866**(1-2): p. 77-88.
183. Tomihari, M., et al., *DC-HIL/glycoprotein Nmb promotes growth of melanoma in mice by inhibiting the activation of tumor-reactive T cells.* Cancer Res, 2010. **70**(14): p. 5778-87.
184. Tse, K.F., et al., *CR011, a fully human monoclonal antibody-auristatin E conjugate, for the treatment of melanoma.* Clin Cancer Res, 2006. **12**(4): p. 1373-82.
185. Williams, M.D., et al., *GPNMB expression in uveal melanoma: a potential for targeted therapy.* Melanoma Res, 2010. **20**(3): p. 184-90.
186. Kuan, C.T., et al., *Glycoprotein nonmetastatic melanoma protein B, a potential molecular therapeutic target in patients with glioblastoma multiforme.* Clin Cancer Res, 2006. **12**(7 Pt 1): p. 1970-82.
187. Onaga, M., et al., *Osteoactivin expressed during cirrhosis development in rats fed a choline-deficient, L-amino acid-defined diet, accelerates motility of hepatoma cells.* J Hepatol, 2003. **39**(5): p. 779-85.
188. Rose, A.A., et al., *Glycoprotein nonmetastatic B is an independent prognostic indicator of recurrence and a novel therapeutic target in breast cancer.* Clin Cancer Res, 2010. **16**(7): p. 2147-56.
189. Weterman, M.A., et al., *nmb, a novel gene, is expressed in low-metastatic human melanoma cell lines and xenografts.* Int J Cancer, 1995. **60**(1): p. 73-81.
190. Owen, T.A., et al., *Identification and characterization of the genes encoding human and mouse osteoactivin.* Crit Rev Eukaryot Gene Expr, 2003. **13**(2-4): p. 205-20.
191. Selim, A.A., *Osteoactivin bioinformatic analysis: prediction of novel functions, structural features, and modes of action.* Med Sci Monit, 2009. **15**(2): p. MT19-33.
192. Bonifacino, J.S. and L.M. Traub, *Signals for sorting of transmembrane proteins to endosomes and lysosomes.* Annu Rev Biochem, 2003. **72**: p. 395-447.
193. Takada, Y., X. Ye, and S. Simon, *The integrins.* Genome Biol, 2007. **8**(5): p. 215.

194. Weston, B.S., A.N. Malhas, and R.G. Price, *Structure-function relationships of the extracellular domain of the autosomal dominant polycystic kidney disease-associated protein, polycystin-1.* FEBS Lett, 2003. **538**(1-3): p. 8-13.
195. Ibraghimov-Beskrovnaya, O., et al., *Strong homophilic interactions of the Ig-like domains of polycystin-1, the protein product of an autosomal dominant polycystic kidney disease gene, PKD1.* Hum Mol Genet, 2000. **9**(11): p. 1641-9.
196. Bezbradica, J.S. and R. Medzhitov, *Role of ITAM signaling module in signal integration.* Current Opinion in Immunology, 2012. **24**(1): p. 58-66.
197. Mocsai, A., J. Ruland, and V.L. Tybulewicz, *The SYK tyrosine kinase: a crucial player in diverse biological functions.* Nat Rev Immunol, 2010. **10**(6): p. 387-402.
198. Maric, G., et al., *Glycoprotein non-metastatic b (GPNMB): A metastatic mediator and emerging therapeutic target in cancer.* Onco Targets Ther, 2013. **6**: p. 839-52.
199. Abdelmagid, S.M., et al., *Osteoactivin, an anabolic factor that regulates osteoblast differentiation and function.* Experimental Cell Research, 2008. **314**(13): p. 2334-2351.
200. Hoashi, T., et al., *Glycoprotein nonmetastatic melanoma protein b, a melanocytic cell marker, is a melanosome-specific and proteolytically released protein.* Faseb Journal, 2010. **24**(5): p. 1616-1629.
201. Furochi, H., et al., *Osteoactivin fragments produced by ectodomain shedding induce MMP-3 expression via ERK pathway in mouse NIH-3T3 fibroblasts.* Febs Letters, 2007. **581**(30): p. 5743-5750.
202. Rose, A.A., et al., *ADAM10 releases a soluble form of the GPNMB/Osteoactivin extracellular domain with angiogenic properties.* PLoS One, 2010. **5**(8): p. e12093.
203. Metz, R.L., et al., *Cloning and characterization of the 5 ' flanking region of the HGFIN gene indicate a cooperative role among p53 and cytokine-mediated transcription factors - Relevance to cell cycle regulation.* Cell Cycle, 2005. **4**(2): p. 315-322.
204. Tian, F., et al., *Upregulation of glycoprotein nonmetastatic B by colony-stimulating factor-1 and epithelial cell adhesion molecule in hepatocellular carcinoma cells.* Oncol Res, 2013. **20**(8): p. 341-50.
205. Bandari, P.S., et al., *Hematopoietic growth factor inducible neurokinin-1 type: a transmembrane protein that is similar to neurokinin 1 interacts with substance P.* Regul Pept, 2003. **111**(1-3): p. 169-78.
206. Chung, J.S., et al., *The DC-HIL/syndecan-4 pathway inhibits human allogeneic T-cell responses.* Eur J Immunol, 2009. **39**(4): p. 965-74.
207. Ogawa, T., et al., *Osteoactivin upregulates expression of MMP-3 and MMP-9 in fibroblasts infiltrated into denervated skeletal muscle in mice.* American Journal of Physiology-Cell Physiology, 2005. **289**(3): p. C697-C707.
208. Abdelmagid, S.M., et al., *Osteoactivin acts as downstream mediator of BMP-2 effects on osteoblast function.* Journal of Cellular Physiology, 2007. **210**(1): p. 26-37.
209. Tomihari, M., et al., *Gpnmb is a melanosome-associated glycoprotein that contributes to melanocyte/keratinocyte adhesion in a RGD-dependent fashion.* Experimental Dermatology, 2009. **18**(7): p. 586-595.
210. Ripoll, V.M., et al., *Microphthalmia transcription factor regulates the expression of the novel osteoclast factor GPNMB.* Gene, 2008. **413**(1-2): p. 32-41.
211. Loftus, S.K., et al., *Gpnmb is a melanoblast-expressed, MITF-dependent gene.* Pigment Cell & Melanoma Research, 2009. **22**(1): p. 99-110.
212. Hershey, C.L. and D.E. Fisher, *Mitf and Tfe3: members of a b-HLH-ZIP transcription factor family essential for osteoclast development and function.* Bone, 2004. **34**(4): p. 689-96.
213. Cheli, Y., et al., *Fifteen-year quest for microphthalmia-associated transcription factor target genes.* Pigment Cell & Melanoma Research, 2010. **23**(1): p. 27-40.
214. Turque, N., et al., *Characterization of a new melanocyte-specific gene (QNR-71) expressed in v-myc-transformed quail neuroretina.* EMBO J, 1996. **15**(13): p. 3338-50.

215. Ogihara, H., et al., *Inhibitory effect of the transcription factor encoded by the mutant mi microphthalmia allele on transactivation of mouse mast cell protease 7 gene.* Blood, 2001. **97**(3): p. 645-651.
216. Marie, P.J., *Transcription factors controlling osteoblastogenesis.* Archives of Biochemistry and Biophysics, 2008. **473**(2): p. 98-105.
217. Ozanne, B.W., et al., *Invasion is a genetic program regulated by transcription factors.* Current Opinion in Genetics & Development, 2006. **16**(1): p. 65-70.
218. Shikano, S., et al., *Molecular cloning of a dendritic cell-associated transmembrane protein, DC-HIL, that promotes RGD-dependent adhesion of endothelial cells through recognition of heparan sulfate proteoglycans.* J Biol Chem, 2001. **276**(11): p. 8125-34.
219. Sheng, M.H.C., et al., *Osteoactivin is a novel osteoclastic protein and plays a key role in osteoclast differentiation and activity.* Febs Letters, 2008. **582**(10): p. 1451-1458.
220. Huang, J.J., W.J. Ma, and S. Yokoyama, *Expression and immunolocalization of Gpnmb, a glioma-associated glycoprotein, in normal and inflamed central nervous systems of adult rats.* Brain Behav, 2012. **2**(2): p. 85-96.
221. Ripoll, V.M., et al., *Gpnmb is induced in macrophages by IFN-gamma and lipopolysaccharide and acts as a feedback regulator of proinflammatory responses.* Journal of Immunology, 2007. **178**(10): p. 6557-6566.
222. Ahn, J.H., et al., *Identification of the genes differentially expressed in human dendritic cell subsets by cDNA subtraction and microarray analysis.* Blood, 2002. **100**(5): p. 1742-54.
223. Chung, J.S., et al., *Syndecan-4 mediates the coinhibitory function of DC-HIL on T cell activation.* J Immunol, 2007. **179**(9): p. 5778-84.
224. Chung, J.S., et al., *DC-HIL is a negative regulator of T lymphocyte activation.* Blood, 2007. **109**(10): p. 4320-4327.
225. Chung, J.S., P.D. Cruz, and K. Ariizumi, *Inhibition of T-cell activation by syndecan-4 is mediated by CD148 through protein tyrosine phosphatase activity.* European Journal of Immunology, 2011. **41**(6): p. 1794-1799.
226. Chung, J.S., et al., *Binding of DC-HIL to Dermatophytic Fungi Induces Tyrosine Phosphorylation and Potentiates Antigen Presenting Cell Function.* Journal of Immunology, 2009. **183**(8): p. 5190-5198.
227. Sheng, M.H.C., et al., *Targeted Overexpression of Osteoactivin in Cells of Osteoclastic Lineage Promotes Osteoclastic Resorption and Bone Loss in Mice.* PLoS One, 2012. **7**(4).
228. Onaga, M., et al., *Osteoactivin expressed during cirrhosis development in rats fed a choline-deficient, L-amino acid-defined diet, accelerates motility of hepatoma cells.* Journal of Hepatology, 2003. **39**(5): p. 779-785.
229. Williams, M.D., et al., *GPNMB expression in uveal melanoma: a potential for targeted therapy.* Melanoma Research, 2010. **20**(3): p. 184-190.
230. Rich, J.N., et al., *Bone-related genes expressed in advanced malignancies induce invasion and metastasis in a genetically defined human cancer model.* Journal of Biological Chemistry, 2003. **278**(18): p. 15951-15957.
231. Rose, A.A., et al., *Osteoactivin promotes breast cancer metastasis to bone.* Mol Cancer Res, 2007. **5**(10): p. 1001-14.
232. Ghilardi, C., et al., *Identification of novel vascular markers through gene expression profiling of tumor-derived endothelium.* Bmc Genomics, 2008. **9**.
233. Tomihari, M., et al., *DC-HIL/Glycoprotein Nmb Promotes Growth of Melanoma in Mice by Inhibiting the Activation of Tumor-Reactive T Cells.* Cancer Research, 2010. **70**(14): p. 5778-5787.
234. Keir, C.H. and L.T. Vahdat, *The use of an antibody drug conjugate, glembatumumab vedotin (CDX-011), for the treatment of breast cancer.* Expert Opinion on Biological Therapy, 2012. **12**(2): p. 259-263.
235. Naumovski, L. and J.R. Junutula, *Glembatumumab vedotin, a conjugate of an anti-*

glycoprotein non-metastatic melanoma protein B mAb and monomethyl auristatin E for the treatment of melanoma and breast cancer. Current Opinion in Molecular Therapeutics, 2010. **12**(2): p. 248-257.
236. Zhou, L.T., et al., *Gpnmb/osteoactivin, an attractive target in cancer immunotherapy.* Neoplasma, 2012. **59**(1): p. 1-5.
237. Bachner, D., D. Schroder, and G. Gross, *mRNA expression of the murine glycoprotein (transmembrane) nmb (Gpnmb) gene is linked to the developing retinal pigment epithelium and iris.* Brain Res Gene Expr Patterns, 2002. **1**(3-4): p. 159-65.
238. Rose, A.A.N., et al., *Glycoprotein Nonmetastatic B Is an Independent Prognostic Indicator of Recurrence and a Novel Therapeutic Target in Breast Cancer.* Clinical Cancer Research, 2010. **16**(7): p. 2147-2156.
239. Qian, X.Z., et al., *Pharmacologically enhanced expression of GPNMB increases the sensitivity of melanoma cells to the CR011-vcMMAE antibody-drug conjugate.* Molecular Oncology, 2008. **2**(1): p. 81-93.
240. Rose, A.A.N. and P.M. Siegel, *Emerging therapeutic targets in breast cancer bone metastasis.* Future Oncology, 2010. **6**(1): p. 55-74.
241. Sievers, E.L. and P.D. Senter, *Antibody-drug conjugates in cancer therapy.* Annu Rev Med, 2013. **64**: p. 15-29.
242. Hwu, P., et al., *A phase I/II study of CR011-vcMMAE, an antibody toxin conjugate drug, in patients with unresectable stage III/IV melanoma.* Journal of Clinical Oncology, 2008. **26**(15).
243. Burris, H., et al., *A Phase (Ph) I/II Study of CR011-VcMMAE, an Antibody-Drug Conjugate, in Patients (Pts) with Locally Advanced or Metastatic Breast Cancer (MBC).* Cancer Research, 2009. **69**(24): p. 855s-855s.
244. Hwu, P., et al., *A phase I/II study of CR011-vcMMAE, an antibody-drug conjugate (ADC) targeting glycoprotein NMB (GPNMB) in patients (pts) with advanced melanoma.* Journal of Clinical Oncology, 2009. **27**(15).
245. Peacock, N., et al., *A phase I/II study of CR011-vcMMAE, an antibody-drug conjugate, in patients (pts) with locally advanced or metastatic breast cancer (MBC).* Journal of Clinical Oncology, 2009. **27**(15).
246. Moore, P.S., et al., *Genetic profile of 22 pancreatic carcinoma cell lines. Analysis of K-ras, p53, p16 and DPC4/Smad4.* Virchows Arch, 2001. **439**(6): p. 798-802.
247. Butz, J., E. Wickstrom, and J. Edwards, *Characterization of mutations and loss of heterozygosity of p53 and K-ras2 in pancreatic cancer cell lines by immobilized polymerase chain reaction.* BMC Biotechnol, 2003. **3**: p. 11.
248. Deer, E.L., et al., *Phenotype and genotype of pancreatic cancer cell lines.* Pancreas, 2010. **39**(4): p. 425-35.
249. Lieber, M., et al., *Establishment of a continuous tumor-cell line (panc-1) from a human carcinoma of the exocrine pancreas.* Int J Cancer, 1975. **15**(5): p. 741-7.
250. Wu, M.C., G.K. Arimura, and A.A. Yunis, *Mechanism of sensitivity of cultured pancreatic carcinoma to asparaginase.* Int J Cancer, 1978. **22**(6): p. 728-33.
251. Yunis, A.A., G.K. Arimura, and D.J. Russin, *Human pancreatic carcinoma (MIA PaCa-2) in continuous culture: sensitivity to asparaginase.* Int J Cancer, 1977. **19**(1): p. 128-35.
252. Tan, M.H., et al., *Characterization of a new primary human pancreatic tumor line.* Cancer Invest, 1986. **4**(1): p. 15-23.
253. Redston, M.S., et al., *p53 mutations in pancreatic carcinoma and evidence of common involvement of homocopolymer tracts in DNA microdeletions.* Cancer Res, 1994. **54**(11): p. 3025-33.
254. Seidman, C.E. and K. Struhl, *Introduction of plasmid DNA into cells.* Curr Protoc Protein Sci, 2001. **Appendix 4**: p. 4D.
255. Mortensen, R.M. and R.E. Kingston, *Selection of Transfected Mammalian Cells*, in *Current*

Protocols in Molecular Biology. 2001, John Wiley & Sons, Inc.
256. Hannon, G.J., *RNA interference.* Nature, 2002. **418**(6894): p. 244-51.
257. Elbashir, S.M., et al., *Analysis of gene function in somatic mammalian cells using small interfering RNAs.* Methods, 2002. **26**(2): p. 199-213.
258. Qin, J.Y., et al., *Systematic comparison of constitutive promoters and the doxycycline-inducible promoter.* PLoS One, 2010. **5**(5): p. e10611.
259. Engebrecht, J., R. Brent, and M.A. Kaderbhai, *Minipreps of plasmid DNA.* Curr Protoc Mol Biol, 2001. **Chapter 1**: p. Unit1 6.
260. Gallagher, S.R., *Quantitation of DNA and RNA with absorption and fluorescence spectroscopy.* Curr Protoc Neurosci, 2011. **Appendix 1**: p. Appendix 1K.
261. Felgner, P.L., et al., *Lipofection: a highly efficient, lipid-mediated DNA-transfection procedure.* Proc Natl Acad Sci U S A, 1987. **84**(21): p. 7413-7.
262. Felgner, J.H., et al., *Enhanced gene delivery and mechanism studies with a novel series of cationic lipid formulations.* J Biol Chem, 1994. **269**(4): p. 2550-61.
263. Wheeler, C.J., et al., *Converting an alcohol to an amine in a cationic lipid dramatically alters the co-lipid requirement, cellular transfection activity and the ultrastructure of DNA cytofectin complexes.* Biochimica Et Biophysica Acta-Biomembranes, 1996. **1280**(1): p. 1-11.
264. Mocellin, S. and M. Provenzano, *RNA interference: learning gene knock-down from cell physiology.* J Transl Med, 2004. **2**(1): p. 39.
265. Yu, J.Y., S.L. DeRuiter, and D.L. Turner, *RNA interference by expression of short-interfering RNAs and hairpin RNAs in mammalian cells.* Proc Natl Acad Sci U S A, 2002. **99**(9): p. 6047-52.
266. Vanitharani, R., P. Chellappan, and C.M. Fauquet, *Short interfering RNA-mediated interference of gene expression and viral DNA accumulation in cultured plant cells.* Proc Natl Acad Sci U S A, 2003. **100**(16): p. 9632-6.
267. van Meerloo, J., G.J. Kaspers, and J. Cloos, *Cell sensitivity assays: the MTT assay.* Methods Mol Biol, 2011. **731**: p. 237-45.
268. Berridge, M.V. and A.S. Tan, *Characterization of the cellular reduction of 3-(4,5-dimethylthiazol-2-yl)-2,5-diphenyltetrazolium bromide (MTT): subcellular localization, substrate dependence, and involvement of mitochondrial electron transport in MTT reduction.* Arch Biochem Biophys, 1993. **303**(2): p. 474-82.
269. Bijnsdorp, I.V., E. Giovannetti, and G.J. Peters, *Analysis of drug interactions.* Methods Mol Biol, 2011. **731**: p. 421-34.
270. Yeh, P. and R. Kishony, *Networks from drug-drug surfaces.* Mol Syst Biol, 2007. **3**: p. 85.
271. Greco, W.R., G. Bravo, and J.C. Parsons, *The search for synergy: a critical review from a response surface perspective.* Pharmacol Rev, 1995. **47**(2): p. 331-85.
272. Zhao, L., M.G. Wientjes, and J.L. Au, *Evaluation of combination chemotherapy: integration of nonlinear regression, curve shift, isobologram, and combination index analyses.* Clin Cancer Res, 2004. **10**(23): p. 7994-8004.
273. Tallarida, R.J., *Revisiting the isobole and related quantitative methods for assessing drug synergism.* J Pharmacol Exp Ther, 2012. **342**(1): p. 2-8.
274. Chou, T.C., *Theoretical basis, experimental design, and computerized simulation of synergism and antagonism in drug-combination studies (vol 58, pg 621, 2006).* Pharmacological Reviews, 2007. **59**(1): p. 124-124.
275. Tallarida, R.J., *An overview of drug combination analysis with isobolograms.* J Pharmacol Exp Ther, 2006. **319**(1): p. 1-7.
276. Chou, T.C., *Drug combination studies and their synergy quantification using the Chou-Talalay method.* Cancer Res, 2010. **70**(2): p. 440-6.
277. Henderson, L., et al., *Classic "broken cell" techniques and newer live cell methods for cell cycle assessment.* Am J Physiol Cell Physiol, 2013. **304**(10): p. C927-38.

278. Pozarowski, P. and Z. Darzynkiewicz, *Analysis of cell cycle by flow cytometry.* Methods Mol Biol, 2004. **281**: p. 301-11.
279. Darzynkiewicz, Z., *Critical aspects in analysis of cellular DNA content.* Curr Protoc Cytom, 2011. **Chapter 7**: p. Unit 7 2.
280. Hanon, E., A. Vanderplasschen, and P.P. Pastoret, *The use of flow cytometry for concomitant detection of apoptosis and cell cycle analysis.* Biochemica, 1996. **2**.
281. Elmore, S., *Apoptosis: a review of programmed cell death.* Toxicol Pathol, 2007. **35**(4): p. 495-516.
282. Yamaji-Hasegawa, A. and M. Tsujimoto, *Asymmetric distribution of phospholipids in biomembranes.* Biol Pharm Bull, 2006. **29**(8): p. 1547-53.
283. Demchenko, A.P., *The change of cellular membranes on apoptosis: fluorescence detection.* Exp Oncol, 2012. **34**(3): p. 263-8.
284. van Engeland, M., et al., *Annexin V-affinity assay: a review on an apoptosis detection system based on phosphatidylserine exposure.* Cytometry, 1998. **31**(1): p. 1-9.
285. Kubista, M., et al., *The real-time polymerase chain reaction.* Mol Aspects Med, 2006. **27**(2-3): p. 95-125.
286. Livak, K.J. and T.D. Schmittgen, *Analysis of relative gene expression data using real-time quantitative PCR and the 2(T)(-Delta Delta C) method.* Methods, 2001. **25**(4): p. 402-408.
287. Ginzinger, D.G., *Gene quantification using real-time quantitative PCR: An emerging technology hits the mainstream.* Experimental Hematology, 2002. **30**(6): p. 503-512.
288. Pfaffl, M.W., *A new mathematical model for relative quantification in real-time RT-PCR.* Nucleic Acids Res, 2001. **29**(9): p. e45.
289. Wong, M.L. and J.F. Medrano, *Real-time PCR for mRNA quantitation.* Biotechniques, 2005. **39**(1): p. 75-85.
290. Das, P.M., et al., *Chromatin immunoprecipitation assay.* Biotechniques, 2004. **37**(6): p. 961-9.
291. Nie, L., A.E. Vazquez, and E.N. Yamoah, *Identification of transcription factor-DNA interactions using chromatin immunoprecipitation assays.* Methods Mol Biol, 2009. **493**: p. 311-21.
292. Chakrabarti, S.K., J.C. James, and R.G. Mirmira, *Quantitative assessment of gene targeting in vitro and in vivo by the pancreatic transcription factor, Pdx1. Importance of chromatin structure in directing promoter binding.* J Biol Chem, 2002. **277**(15): p. 13286-93.
293. Albini, A. and D.M. Noonan, *The 'chemoinvasion' assay, 25 years and still going strong: the use of reconstituted basement membranes to study cell invasion and angiogenesis.* Curr Opin Cell Biol, 2010. **22**(5): p. 677-89.
294. Hartmann, M., et al., *Protein microarrays for diagnostic assays.* Anal Bioanal Chem, 2009. **393**(5): p. 1407-16.
295. Brennan, D.J., et al., *Antibody-based proteomics: fast-tracking molecular diagnostics in oncology.* Nat Rev Cancer, 2010. **10**(9): p. 605-17.
296. Kauffmann, A., R. Gentleman, and W. Huber, *arrayQualityMetrics--a bioconductor package for quality assessment of microarray data.* Bioinformatics, 2009. **25**(3): p. 415-6.
297. Simon, R., *Diagnostic and prognostic prediction using gene expression profiles in high-dimensional microarray data.* Br J Cancer, 2003. **89**(9): p. 1599-604.
298. Bewick, V., L. Cheek, and J. Ball, *Statistics review 13: receiver operating characteristic curves.* Crit Care, 2004. **8**(6): p. 508-12.
299. Warnock, D.G. and C.C. Peck, *A roadmap for biomarker qualification.* Nat Biotechnol, 2010. **28**(5): p. 444-5.
300. Akobeng, A.K., *Understanding diagnostic tests 3: receiver operating characteristic curves.* Acta Paediatrica, 2007. **96**(5): p. 644-647.
301. Simon, R., et al., *Pitfalls in the use of DNA microarray data for diagnostic and prognostic classification.* Journal of the National Cancer Institute, 2003. **95**(1): p. 14-18.

302. Kang, L., A. Liu, and L. Tian, *Linear combination methods to improve diagnostic/prognostic accuracy on future observations.* Stat Methods Med Res, 2013.
303. Molinaro, A.M., R. Simon, and R.M. Pfeiffer, *Prediction error estimation: a comparison of resampling methods.* Bioinformatics, 2005. **21**(15): p. 3301-7.
304. Kaplan, E.L. and P. Meier, *Nonparametric Estimation from Incomplete Observations.* Journal of the American Statistical Association, 1958. **53**(282): p. 457-481.
305. Goel, M.K., P. Khanna, and J. Kishore, *Understanding survival analysis: Kaplan-Meier estimate.* Int J Ayurveda Res, 2010. **1**(4): p. 274-8.
306. Bland, J.M. and D.G. Altman, *The logrank test.* BMJ, 2004. **328**(7447): p. 1073.
307. Cox, D.R., *Regression Models and Life-Tables.* Journal of the Royal Statistical Society. Series B (Methodological), 1972. **34**(2): p. 187-220.
308. Dima, S.O., et al., *An Exploratory Study of Inflammatory Cytokines as Prognostic Biomarkers in Patients With Ductal Pancreatic Adenocarcinoma.* Pancreas, 2012. **41**(7): p. 1001-1007.
309. Anjomshoaa, A., et al., *Reduced expression of a gene proliferation signature is associated with enhanced malignancy in colon cancer.* British Journal of Cancer, 2008. **99**(6): p. 966-973.
310. Haury, A.C., P. Gestraud, and J.P. Vert, *The influence of feature selection methods on accuracy, stability and interpretability of molecular signatures.* PLoS One, 2011. **6**(12): p. e28210.
311. Kale, J., et al., *Shedding light on apoptosis at subcellular membranes.* Cell, 2012. **151**(6): p. 1179-84.
312. Michels, J., et al., *Functions of BCL-XL at the Interface between Cell Death and Metabolism.* International Journal of Cell Biology, 2013. **2013**: p. 10.
313. Wong, W.W. and H. Puthalakath, *Bcl-2 family proteins: the sentinels of the mitochondrial apoptosis pathway.* IUBMB Life, 2008. **60**(6): p. 390-7.
314. Garrido, C., et al., *Mechanisms of cytochrome c release from mitochondria.* Cell Death Differ, 2006. **13**(9): p. 1423-33.
315. Oltvai, Z.N., C.L. Milliman, and S.J. Korsmeyer, *Bcl-2 heterodimerizes in vivo with a conserved homolog, Bax, that accelerates programmed cell death.* Cell, 1993. **74**(4): p. 609-19.
316. Korsmeyer, S.J., et al., *Bcl-2/Bax: a rheostat that regulates an anti-oxidant pathway and cell death.* Semin Cancer Biol, 1993. **4**(6): p. 327-32.
317. Childs, A.C., et al., *Doxorubicin treatment in vivo causes cytochrome C release and cardiomyocyte apoptosis, as well as increased mitochondrial efficiency, superoxide dismutase activity, and Bcl-2:Bax ratio.* Cancer Res, 2002. **62**(16): p. 4592-8.
318. Edlich, F., et al., *Bcl-x(L) retrotranslocates Bax from the mitochondria into the cytosol.* Cell, 2011. **145**(1): p. 104-16.
319. Todt, F., et al., *The C-terminal helix of Bcl-x(L) mediates Bax retrotranslocation from the mitochondria.* Cell Death Differ, 2013. **20**(2): p. 333-42.
320. Darzynkiewicz, Z., H.D. Halicka, and H. Zhao, *Analysis of Cellular DNA Content by Flow and Laser Scanning Cytometry.* Polyploidization and Cancer, 2010. **676**: p. 137-147.
321. Ross, J.S., et al., *DNA ploidy and cell cycle analysis in breast cancer.* Am J Clin Pathol, 2003. **120 Suppl**: p. S72-84.
322. Studzinski, G.P., *Cell growth and apoptosis: a practical approach*. 1995: IRL Press at Oxford University Press.
323. Nunez, R., *DNA measurement and cell cycle analysis by flow cytometry.* Curr Issues Mol Biol, 2001. **3**(3): p. 67-70.
324. Cavanagh, B.L., et al., *Thymidine analogues for tracking DNA synthesis.* Molecules, 2011. **16**(9): p. 7980-93.
325. Iyonaga, K., et al., *Alterations in cytokeratin expression by the alveolar lining epithelial cells in lung tissues from patients with idiopathic pulmonary fibrosis.* Journal of Pathology, 1997. **182**(2): p. 217-24.
326. Moll, R. and W.W. Franke, *Intermediate filaments and their interaction with membranes. The desmosome-cytokeratin filament complex and epithelial differentiation.* Pathol Res Pract,

1982. **175**(2-3): p. 146-61.
327. Purkis, P.E., et al., *Antibody markers of basal cells in complex epithelia.* J Cell Sci, 1990. **97 (Pt 1)**: p. 39-50.
328. Crisera, C.A., et al., *Expression and role of laminin-1 in mouse pancreatic organogenesis.* Diabetes, 2000. **49**(6): p. 936-944.
329. Karin, M. and F.R. Greten, *NF-kappaB: linking inflammation and immunity to cancer development and progression.* Nat Rev Immunol, 2005. **5**(10): p. 749-59.
330. Karin, M., *Nuclear factor-kappa B in cancer development and progression.* Nature, 2006. **441**(7092): p. 431-436.
331. Liptay, S., et al., *Mitogenic and antiapoptotic role of constitutive NF-kappaB/Rel activity in pancreatic cancer.* Int J Cancer, 2003. **105**(6): p. 735-46.
332. Catz, S.D. and J.L. Johnson, *Transcriptional regulation of bcl-2 by nuclear factor kappa B and its significance in prostate cancer.* Oncogene, 2001. **20**(50): p. 7342-7351.
333. Wu, H.T., et al., *Identifying the Regulative Role of NF-kappa B Binding Sites Within Promoter Region of Human Matrix Metalloproteinase 9 (mmp-9) by TNF-alpha Induction.* Applied Biochemistry and Biotechnology, 2013. **169**(2): p. 438-449.
334. Pahl, H.L., *Activators and target genes of Rel/NF-kappaB transcription factors.* Oncogene, 1999. **18**(49): p. 6853-66.
335. Piva, R., G. Belardo, and M.G. Santoro, *NF-kappaB: a stress-regulated switch for cell survival.* Antioxid Redox Signal, 2006. **8**(3-4): p. 478-86.
336. Sung, J., et al., *Molecular signatures from omics data: from chaos to consensus.* Biotechnol J, 2012. **7**(8): p. 946-57.
337. van Persijn van Meerten, E.L., H. Gelderblom, and J.L. Bloem, *RECIST revised: implications for the radiologist. A review article on the modified RECIST guideline.* Eur Radiol, 2010. **20**(6): p. 1456-67.
338. Tanaka, H., et al., *The potential of GPNMB as novel neuroprotective factor in amyotrophic lateral sclerosis.* Sci Rep, 2012. **2**: p. 573.
339. Ripoll, V.M., et al., *Gpnmb is induced in macrophages by IFN-gamma and lipopolysaccharide and acts as a feedback regulator of proinflammatory responses.* J Immunol, 2007. **178**(10): p. 6557-66.
340. Vucic, D., *Targeting IAP (inhibitor of apoptosis) proteins for therapeutic intervention in tumors.* Curr Cancer Drug Targets, 2008. **8**(2): p. 110-7.
341. Kantari, C. and H. Walczak, *Caspase-8 and Bid: Caught in the act between death receptors and mitochondria.* Biochimica Et Biophysica Acta-Molecular Cell Research, 2011. **1813**(4): p. 558-563.
342. Vogler, M., *BCL2A1: the underdog in the BCL2 family.* Cell Death and Differentiation, 2012. **19**(1): p. 67-74.
343. Arbuck, S.G., *Chemotherapy for pancreatic cancer.* Baillieres Clin Gastroenterol, 1990. **4**(4): p. 953-68.
344. Peters, G.J., et al., *Basis for effective combination cancer chemotherapy with antimetabolites.* Pharmacol Ther, 2000. **87**(2-3): p. 227-53.
345. Jiang, Y., et al., *Combinatorial therapies improve the therapeutic efficacy of nanoliposomal ceramide for pancreatic cancer.* Cancer Biol Ther, 2011. **12**(7): p. 574-85.
346. Yang, Y., et al., *Role of fatty acid synthase in gemcitabine and radiation resistance of pancreatic cancers.* Int J Biochem Mol Biol, 2011. **2**(1): p. 89-98.
347. Fryer, R.A., et al., *Mechanisms underlying gemcitabine resistance in pancreatic cancer and sensitisation by the iMiD lenalidomide.* Anticancer Res, 2011. **31**(11): p. 3747-56.
348. Kreutzer, J.N., M. Ruzzene, and B. Guerra, *Enhancing chemosensitivity to gemcitabine via RNA interference targeting the catalytic subunits of protein kinase CK2 in human pancreatic cancer cells.* BMC Cancer, 2010. **10**: p. 440.
349. Guo, Q., Y. Chen, and Y. Wu, *Enhancing apoptosis and overcoming resistance of gemcitabine*

in pancreatic cancer with bortezomib: a role of death-associated protein kinase-related apoptosis-inducing protein kinase 1. Tumori, 2009. **95**(6): p. 796-803.

350. Humbert, M., et al., *Masitinib combined with standard gemcitabine chemotherapy: in vitro and in vivo studies in human pancreatic tumour cell lines and ectopic mouse model.* PLoS One, 2010. **5**(3): p. e9430.
351. Funamizu, N., et al., *Hydroxyurea decreases gemcitabine resistance in pancreatic carcinoma cells with highly expressed ribonucleotide reductase.* Pancreas, 2012. **41**(1): p. 107-13.
352. Rejiba, S., et al., *Gemcitabine-based chemogene therapy for pancreatic cancer using Ad-dCK::UMK GDEPT and TS/RR siRNA strategies.* Neoplasia, 2009. **11**(7): p. 637-50.
353. Mini, E., et al., *Cellular pharmacology of gemcitabine.* Annals of Oncology, 2006. **17 Suppl 5**: p. v7-12.
354. Bareschino, M.A., et al., *Erlotinib in cancer treatment.* Annals of Oncology, 2007. **18 Suppl 6**: p. vi35-41.
355. Furugaki, K., et al., *Antitumor activity of erlotinib in combination with gemcitabine in in vitro and in vivo models of KRAS-mutated pancreatic cancers.* Oncol Lett, 2010. **1**(2): p. 231-235.
356. Mahaffey, C.M., et al., *Schedule-dependent apoptosis in K-ras mutant non-small-cell lung cancer cell lines treated with docetaxel and erlotinib: rationale for pharmacodynamic separation.* Clin Lung Cancer, 2007. **8**(9): p. 548-53.
357. Li, M., et al., *Preclinical pharmacokinetic/pharmacodynamic models to predict schedule-dependent interaction between erlotinib and gemcitabine.* Pharm Res, 2013. **30**(5): p. 1400-8.
358. Hill, R., et al., *Gemcitabine-mediated tumour regression and p53-dependent gene expression: implications for colon and pancreatic cancer therapy.* Cell Death Dis, 2013. **4**: p. e791.
359. Wang, J., et al., *The role of Bax and Bcl-2 in gemcitabine-mediated cytotoxicity in uveal melanoma cells.* Tumour Biol, 2013.
360. Karlberg, M., et al., *Pro-apoptotic Bax is the major and Bak an auxiliary effector in cytokine deprivation-induced mast cell apoptosis.* Cell Death Dis, 2010. **1**: p. e43.
361. De Roock, W., et al., *KRAS wild-type state predicts survival and is associated to early radiological response in metastatic colorectal cancer treated with cetuximab.* Annals of Oncology, 2008. **19**(3): p. 508-15.
362. Di Fiore, F., et al., *Clinical relevance of KRAS mutation detection in metastatic colorectal cancer treated by Cetuximab plus chemotherapy.* Br J Cancer, 2007. **96**(8): p. 1166-9.
363. Lièvre, A., et al., *KRAS Mutations As an Independent Prognostic Factor in Patients With Advanced Colorectal Cancer Treated With Cetuximab.* Journal of Clinical Oncology, 2008. **26**(3): p. 374-379.
364. Pao, W., et al., *KRAS mutations and primary resistance of lung adenocarcinomas to gefitinib or erlotinib.* PLoS Med, 2005. **2**(1): p. e17.
365. Massarelli, E., et al., *KRAS mutation is an important predictor of resistance to therapy with epidermal growth factor receptor tyrosine kinase inhibitors in non-small-cell lung cancer.* Clin Cancer Res, 2007. **13**(10): p. 2890-6.
366. Ling, Y.H., R. Lin, and R. Perez-Soler, *Erlotinib induces mitochondrial-mediated apoptosis in human H3255 non-small-cell lung cancer cells with epidermal growth factor receptorL858R mutation through mitochondrial oxidative phosphorylation-dependent activation of BAX and BAK.* Mol Pharmacol, 2008. **74**(3): p. 793-806.
367. Huether, A., et al., *Signaling pathways involved in the inhibition of epidermal growth factor receptor by erlotinib in hepatocellular cancer.* World J Gastroenterol, 2006. **12**(32): p. 5160-7.
368. Lu, Y.Y., et al., *Anti-tumor activity of erlotinib in the BxPC-3 pancreatic cancer cell line.* World J Gastroenterol, 2008. **14**(35): p. 5403-11.
369. van Oosterwijk, J.G., et al., *Restoration of chemosensitivity for doxorubicin and cisplatin in chondrosarcoma in vitro: BCL-2 family members cause chemoresistance.* Annals of Oncology,

2012. **23**(6): p. 1617-26.
370. Wang, S.J., et al., *Dihydroartemisinin inactivates NF-kappaB and potentiates the anti-tumor effect of gemcitabine on pancreatic cancer both in vitro and in vivo.* Cancer Lett, 2010. **293**(1): p. 99-108.
371. Wang, P., et al., *Inhibition of RIP and c-FLIP enhances TRAIL-induced apoptosis in pancreatic cancer cells.* Cell Signal, 2007. **19**(11): p. 2237-46.
372. Yang, J.K., *FLIP as an anti-cancer therapeutic target.* Yonsei Med J, 2008. **49**(1): p. 19-27.
373. Hiyama, E. and K. Hiyama, *Telomerase as tumor marker.* Cancer Lett, 2003. **194**(2): p. 221-33.
374. Uemura, K., et al., *Comparative analysis of K-ras point mutation, telomerase activity, and p53 overexpression in pancreatic tumours.* Oncol Rep, 2003. **10**(2): p. 277-83.
375. Ito, M., et al., *TIP30 deficiency increases susceptibility to tumorigenesis.* Cancer Research, 2003. **63**(24): p. 8763-8767.
376. Sherr, C.J., *The Pezcoller lecture: cancer cell cycles revisited.* Cancer Res, 2000. **60**(14): p. 3689-95.
377. Sherr, C.J. and J.M. Roberts, *CDK inhibitors: positive and negative regulators of G1-phase progression.* Genes Dev, 1999. **13**(12): p. 1501-12.
378. Bartek, J. and J. Lukas, *Cell cycle. Order from destruction.* Science, 2001. **294**(5540): p. 66-7.
379. Katayose, Y., et al., *Promoting apoptosis: a novel activity associated with the cyclin-dependent kinase inhibitor p27.* Cancer Res, 1997. **57**(24): p. 5441-5.
380. Katner, A.L., et al., *Induction of cell cycle arrest and apoptosis in human prostate carcinoma cells by a recombinant adenovirus expressing p27(Kip1).* Prostate, 2002. **53**(1): p. 77-87.
381. Kudo, Y., et al., *p27Kip1 accumulation by inhibition of proteasome function induces apoptosis in oral squamous cell carcinoma cells.* Clin Cancer Res, 2000. **6**(3): p. 916-23.
382. Kawada, M., et al., *Induction of p27(Kip1) degradation and anchorage independence by Ras through the MAP kinase signaling pathway.* Oncogene, 1997. **15**(6): p. 629-637.
383. Aktas, H., H. Cai, and G.M. Cooper, *Ras links growth factor signaling to the cell cycle machinery via regulation of cyclin D1 and the Cdk inhibitor p27KIP1.* Mol Cell Biol, 1997. **17**(7): p. 3850-7.
384. Mittnacht, S., et al., *Ras signalling is required for inactivation of the tumour suppressor pRb cell-cycle control protein.* Current Biology, 1997. **7**(3): p. 219-221.
385. Harashima, H. and A. Schnittger, *The integration of cell division, growth and differentiation.* Curr Opin Plant Biol, 2010. **13**(1): p. 66-74.
386. Sherbet, G.V. and M.S. Lakshmi, *S100A4 (MTS1) calcium binding protein in cancer growth, invasion and metastasis.* Anticancer Res, 1998. **18**(4A): p. 2415-21.
387. Berge, G. and G.M. Mlandsmo, *Evaluation of potential interactions between the metastasis-associated protein S100A4 and the tumor suppressor protein p53.* Amino Acids, 2011. **41**(4): p. 863-873.
388. Blattner, C., A. Sparks, and D. Lane, *Transcription factor E2F-1 is upregulated in response to DNA damage in a manner analogous to that of p53.* Molecular and Cellular Biology, 1999. **19**(5): p. 3704-3713.
389. Huang, Y., et al., *Role for E2F in DNA damage-induced entry of cells into S phase.* Cancer Res, 1997. **57**(17): p. 3640-3.
390. O'Connor, D.J. and X. Lu, *Stress signals induce transcriptionally inactive E2F-1 independently of p53 and Rb.* Oncogene, 2000. **19**(20): p. 2369-76.
391. Lin, W.C., F.T. Lin, and J.R. Nevins, *Selective induction of E2F1 in response to DNA damage, mediated by ATM-dependent phosphorylation.* Genes Dev, 2001. **15**(14): p. 1833-44.
392. Kowalik, T.F., et al., *E2F1 overexpression in quiescent fibroblasts leads to induction of cellular DNA synthesis and apoptosis.* J Virol, 1995. **69**(4): p. 2491-500.
393. Hsieh, J.K., et al., *Novel function of the cyclin A binding site of E2F in regulating p53-induced apoptosis in response to DNA damage.* Mol Cell Biol, 2002. **22**(1): p. 78-93.

394. Wu, X. and A.J. Levine, *p53 and E2F-1 cooperate to mediate apoptosis.* Proc Natl Acad Sci U S A, 1994. **91**(9): p. 3602-6.
395. Nahle, Z., et al., *Direct coupling of the cell cycle and cell death machinery by E2F.* Nat Cell Biol, 2002. **4**(11): p. 859-64.
396. Stevens, C., L. Smith, and N.B. La Thangue, *Chk2 activates E2F-1 in response to DNA damage.* Nat Cell Biol, 2003. **5**(5): p. 401-9.
397. Biswas, A.K. and D.G. Johnson, *Transcriptional and nontranscriptional functions of E2F1 in response to DNA damage.* Cancer Res, 2012. **72**(1): p. 13-7.
398. Ianari, A., et al., *Proapoptotic function of the retinoblastoma tumor suppressor protein.* Cancer Cell, 2009. **15**(3): p. 184-94.
399. Udayakumar, T., et al., *The E2F1/Rb and p53/MDM2 pathways in DNA repair and apoptosis: understanding the crosstalk to develop novel strategies for prostate cancer radiotherapy.* Semin Radiat Oncol, 2010. **20**(4): p. 258-66.
400. Shen, T. and S. Huang, *The role of Cdc25A in the regulation of cell proliferation and apoptosis.* Anticancer Agents Med Chem, 2012. **12**(6): p. 631-9.
401. Slingerland, J. and M. Pagano, *Regulation of the cdk inhibitor p27 and its deregulation in cancer.* J Cell Physiol, 2000. **183**(1): p. 10-7.
402. Voutsadakis, I.A., *Molecular predictors of gemcitabine response in pancreatic cancer.* World J Gastrointest Oncol, 2011. **3**(11): p. 153-64.
403. Sclabas, G.M., et al., *NF-kappaB in pancreatic cancer.* Int J Gastrointest Cancer, 2003. **33**(1): p. 15-26.
404. Bandala, E., et al., *Inhibitor of apoptosis-1 (IAP-1) expression and apoptosis in non-small-cell lung cancer cells exposed to gemcitabine.* Biochem Pharmacol, 2001. **62**(1): p. 13-9.
405. Arlt, A., et al., *Role of NF-kappaB and Akt/PI3K in the resistance of pancreatic carcinoma cell lines against gemcitabine-induced cell death.* Oncogene, 2003. **22**(21): p. 3243-51.
406. Salem, K., et al., *Combination chemotherapy increases cytotoxicity of multiple myeloma cells by modification of nuclear factor (NF)-kappaB activity.* Experimental Hematology, 2013. **41**(2): p. 209-18.
407. Jiang, X.J., et al., *Synergistic effect of panobinostat and bortezomib on chemoresistant acute myelogenous leukemia cells via AKT and NF-kappaB pathways.* Cancer Lett, 2012. **326**(2): p. 135-42.
408. Oiso, S., et al., *Involvement of NF-kappaB activation in the cisplatin resistance of human epidermoid carcinoma KCP-4 cells.* Oncol Rep, 2012. **28**(1): p. 27-32.
409. Song, B., et al., *Plk1 phosphorylation of orc2 and hbo1 contributes to gemcitabine resistance in pancreatic cancer.* Mol Cancer Ther, 2013. **12**(1): p. 58-68.
410. Li, X., Z. Cheng, and H. Jin, *Dynamics of Ras complexes observed in living cells.* Sensors (Basel), 2012. **12**(7): p. 9411-22.
411. Rasouli-Nia, A., et al., *High Raf-1 kinase activity protects human tumor cells against paclitaxel-induced cytotoxicity.* Clin Cancer Res, 1998. **4**(5): p. 1111-6.
412. Davis, J.M., et al., *Raf-1 and Bcl-2 induce distinct and common pathways that contribute to breast cancer drug resistance.* Clinical Cancer Research, 2003. **9**(3): p. 1161-1170.
413. Luo, J.H., J. Zhou, and Y. Gao, *Correlation between periostin and SNCG and esophageal cancer invasion, infiltration and apoptosis.* Asian Pacific Journal of Tropical Medicine, 2013. **6**(7): p. 516-519.
414. Wu, K.J., et al., *Expression of synuclein gamma indicates poor prognosis of triple-negative breast cancer.* Medical Oncology, 2013. **30**(3).
415. Liu, C.Y., et al., *Elevated Serum Synuclein-Gamma in Patients with Gastrointestinal and Esophageal Carcinomas.* Hepato-Gastroenterology, 2012. **59**(119): p. 2222-2227.
416. Furge, K.A., et al., *Suppression of Ras-mediated tumorigenicity and metastasis through inhibition of the Met receptor tyrosine kinase.* Proc Natl Acad Sci U S A, 2001. **98**(19): p. 10722-7.

417. Seol, D.W., Q.Y. Chen, and R. Zarnegar, *Transcriptional activation of the Hepatocyte Growth Factor receptor (c-met) gene by its ligand (Hepatocyte Growth Factor) is mediated through AP-1.* Oncogene, 2000. **19**(9): p. 1132-1137.
418. Organ, S.L. and M.S. Tsao, *An overview of the c-MET signaling pathway.* Ther Adv Med Oncol, 2011. **3**(1 Suppl): p. S7-S19.
419. Liu, Y., *The human hepatocyte growth factor receptor gene: complete structural organization and promoter characterization.* Gene, 1998. **215**(1): p. 159-69.
420. Hage, C., et al., *The novel c-Met inhibitor cabozantinib overcomes gemcitabine resistance and stem cell signaling in pancreatic cancer.* Cell Death Dis, 2013. **4**: p. e627.
421. Kunnumakkara, A.B., et al., *Curcumin sensitizes human colorectal cancer to capecitabine by modulation of cyclin D1, COX-2, MMP-9, VEGF and CXCR4 expression in an orthotopic mouse model (vol 125, pg 2187, 2009).* International Journal of Cancer, 2010. **126**(3): p. 799-799.
422. Yu, L.L., et al., *Nuclear factor-kappaB p65 (RelA) transcription factor is constitutively activated in human colorectal carcinoma tissue.* World J Gastroenterol, 2004. **10**(22): p. 3255-60.
423. Bloomston, M., E.E. Zervos, and A.S. Rosemurgy, *Matrix metalloproteinases and their role in pancreatic cancer: A review of preclinical studies and clinical trials.* Annals of Surgical Oncology, 2002. **9**(7): p. 668-674.
424. Fendrich, V., et al., *Alterations of the tissue inhibitor of metalloproteinase-3 (TIMP3) gene in pancreatic adenocarcinomas.* Pancreas, 2005. **30**(2): p. e40-5.
425. Duffy, M.J., P.M. McGowan, and W.M. Gallagher, *Cancer invasion and metastasis: changing views.* Journal of Pathology, 2008. **214**(3): p. 283-93.
426. Duffy, M.J., *Urokinase-type plasminogen activator: a potent marker of metastatic potential in human cancers.* Biochemical Society Transactions, 2002. **30**: p. 207-210.
427. Jo, M., et al., *Dynamic assembly of the urokinase-type plasminogen activator signaling receptor complex determines the mitogenic activity of urokinase-type plasminogen activator.* J Biol Chem, 2005. **280**(17): p. 17449-57.
428. Planus, E., et al., *Binding of urokinase to plasminogen activator inhibitor type-1 mediates cell adhesion and spreading.* J Cell Sci, 1997. **110 (Pt 9)**: p. 1091-8.
429. Keskioja, J., et al., *Regulation of the Synthesis and Activity of Urokinase Plasminogen-Activator in A549 Human-Lung Carcinoma-Cells by Transforming Growth Factor-Beta.* Journal of Cell Biology, 1988. **106**(2): p. 451-459.
430. Gerwin, B.I., et al., *Tgf-Beta-1 Modulation of Urokinase and Pai-1 Expression in Human Bronchial Epithelial-Cells.* American Journal of Physiology, 1990. **259**(4): p. L262-L269.
431. Allan, E.H., et al., *Transforming growth factor beta inhibits plasminogen activator (PA) activity and stimulates production of urokinase-type PA, PA inhibitor-1 mRNA, and protein in rat osteoblast-like cells.* J Cell Physiol, 1991. **149**(1): p. 34-43.
432. Arnoletti, J.P., et al., *Thrombospondin and Transforming Growth-Factor-Beta-1 Increase Expression of Urokinase-Type Plasminogen-Activator and Plasminogen-Activator Inhibitor-1 in Human Mda-Mb-231 Breast-Cancer Cells.* Cancer, 1995. **76**(6): p. 998-1005.
433. Santibanez, J.F., et al., *Involvement of the Ras/MAPK signaling pathway in the modulation of urokinase production and cellular invasiveness by transforming growth factor-beta(1) in transformed keratinocytes.* Biochem Biophys Res Commun, 2000. **273**(2): p. 521-7.
434. Kutz, S.M., et al., *TGF-beta1-induced PAI-1 gene expression requires MEK activity and cell-to-substrate adhesion.* J Cell Sci, 2001. **114**(Pt 21): p. 3905-14.
435. Juretic, N., et al., *ERK 1,2 and p38 pathways are involved in the proliferative stimuli mediated by urokinase in osteoblastic SaOS-2 cell line.* J Cell Biochem, 2001. **83**(1): p. 92-8.
436. Lupu-Meiri, M., et al., *Knock-down of plasminogen-activator inhibitor-1 enhances expression of E-cadherin and promotes epithelial differentiation of human pancreatic adenocarcinoma cells.* Journal of Cellular Physiology, 2012. **227**(11): p. 3621-3628.
437. Mahon, P.C., et al., *S100A4 contributes to the suppression of BNIP3 expression,*

chemoresistance, and inhibition of apoptosis in pancreatic cancer. Cancer Res, 2007. **67**(14): p. 6786-95.

438. Zhang, J., et al., *S100A4 regulates migration and invasion in hepatocellular carcinoma HepG2 cells via NF-kappa B-dependent MMP-9 signal.* European Review for Medical and Pharmacological Sciences, 2013. **17**(17): p. 2372-2382.
439. Huang, L., et al., *Downregulation of S100A4 expression by RNA interference suppresses cell growth and invasion in human colorectal cancer cells.* Oncol Rep, 2012. **27**(4): p. 917-22.
440. Dahlmann, M., et al., *Systemic shRNA mediated knock-down of S100A4 in colorectal cancer xenografted mice reduces metastasis formation.* Oncotarget, 2012. **3**(8): p. 783-797.
441. Shi, Q., et al., *Constitutive and inducible interleukin 8 expression by hypoxia and acidosis renders human pancreatic cancer cells more tumorigenic and metastatic.* Clin Cancer Res, 1999. **5**(11): p. 3711-21.
442. Le, X., et al., *Molecular regulation of constitutive expression of interleukin-8 in human pancreatic adenocarcinoma.* J Interferon Cytokine Res, 2000. **20**(11): p. 935-46.
443. He, L., et al., *Hispidulin, a small flavonoid molecule, suppresses the angiogenesis and growth of human pancreatic cancer by targeting vascular endothelial growth factor receptor 2-mediated PI3K/Akt/mTOR signaling pathway.* Cancer Sci, 2011. **102**(1): p. 219-25.
444. Matsuo, Y., et al., *CXCL8/IL-8 and CXCL12/SDF-1α co-operatively promote invasiveness and angiogenesis in pancreatic cancer.* International Journal of Cancer, 2009. **124**(4): p. 853-861.
445. Baker, C.H., C.C. Solorzano, and I.J. Fidler, *Blockade of vascular endothelial growth factor receptor and epidermal growth factor receptor signaling for therapy of metastatic human pancreatic cancer.* Cancer Res, 2002. **62**(7): p. 1996-2003.
446. You, W.K., et al., *VEGF and c-Met blockade amplify angiogenesis inhibition in pancreatic islet cancer.* Cancer Res, 2011. **71**(14): p. 4758-68.
447. Hata, K., et al., *Expression of the angopoietin-1, angopoietin-2, Tie2, and vascular endothelial growth factor gene in epithelial ovarian cancer.* Gynecol Oncol, 2004. **93**(1): p. 215-22.
448. Davis, S., et al., *Isolation of angiopoietin-1, a ligand for the TIE2 receptor, by secretion-trap expression cloning.* Cell, 1996. **87**(7): p. 1161-9.
449. Suri, C., et al., *Requisite role of Angiopoietin-1, a ligand for the TIE2 receptor, during embryonic angiogenesis.* Cell, 1996. **87**(7): p. 1171-1180.
450. Maisonpierre, P.C., et al., *Angiopoietin-2, a natural antagonist for Tie2 that disrupts in vivo angiogenesis.* Science, 1997. **277**(5322): p. 55-60.
451. Holash, J., et al., *Vessel cooption, regression, and growth in tumors mediated by angiopoietins and VEGF.* Science, 1999. **284**(5422): p. 1994-8.
452. Morgan, M.A., et al., *The combination of epidermal growth factor receptor inhibitors with gemcitabine and radiation in pancreatic cancer.* Clin Cancer Res, 2008. **14**(16): p. 5142-9.
453. Benvenuti, S., et al., *Oncogenic activation of the RAS/RAF signaling pathway impairs the response of metastatic colorectal cancers to anti-epidermal growth factor receptor antibody therapies.* Cancer Res, 2007. **67**(6): p. 2643-8.
454. Massarelli, E., et al., *KRAS Mutation Is an Important Predictor of Resistance to Therapy with Epidermal Growth Factor Receptor Tyrosine Kinase Inhibitors in Non–Small-Cell Lung Cancer.* Clinical Cancer Research, 2007. **13**(10): p. 2890-2896.
455. Huang, Z.Q., et al., *Differential responses by pancreatic carcinoma cell lines to prolonged exposure to Erbitux (IMC-C225) anti-EGFR antibody.* J Surg Res, 2003. **111**(2): p. 274-83.
456. Arnoletti, J.P., et al., *Mechanisms of resistance to Erbitux (anti-epidermal growth factor receptor) combination therapy in pancreatic adenocarcinoma cells.* J Gastrointest Surg, 2004. **8**(8): p. 960-9; discussion 969-70.
457. Erkan, M., et al., *The impact of the activated stroma on pancreatic ductal adenocarcinoma biology and therapy resistance.* Curr Mol Med, 2012. **12**(3): p. 288-303.
458. Lunardi, S., R.J. Muschel, and T.B. Brunner, *The stromal compartments in pancreatic cancer:*

Are there any therapeutic targets? Cancer Lett, 2013.
459. Natesan, M. and R.G. Ulrich, *Protein microarrays and biomarkers of infectious disease.* Int J Mol Sci, 2010. **11**(12): p. 5165-83.
460. Bhushan, A., et al., *Fgf10 is essential for maintaining the proliferative capacity of epithelial progenitor cells during early pancreatic organogenesis.* Development, 2001. **128**(24): p. 5109-17.
461. Nomura, S., et al., *FGF10/FGFR2 signal induces cell migration and invasion in pancreatic cancer.* Br J Cancer, 2008. **99**(2): p. 305-13.
462. Matsuike, A., et al., *Expression of fibroblast growth factor (FGF)-10 in human colorectal adenocarcinoma cells.* J Nippon Med Sch, 2001. **68**(5): p. 397-404.
463. Miekus, K., et al., *Role of I-TAC-binding receptors CXCR3 and CXCR7 in proliferation, activation of intracellular signaling pathways and migration of various tumor cell lines.* Folia Histochem Cytobiol, 2010. **48**(1): p. 104-11.
464. Lo, B.K., et al., *CXCR3/ligands are significantly involved in the tumorigenesis of basal cell carcinomas.* Am J Pathol, 2010. **176**(5): p. 2435-46.
465. Furuya, M., et al., *Differential expression patterns of CXCR3 variants and corresponding CXC chemokines in clear cell ovarian cancers and endometriosis.* Gynecol Oncol, 2011. **122**(3): p. 648-55.
466. Klee, E.W., et al., *Candidate serum biomarkers for prostate adenocarcinoma identified by mRNA differences in prostate tissue and verified with protein measurements in tissue and blood.* Clin Chem, 2012. **58**(3): p. 599-609.
467. Zarling, J.M., et al., *Oncostatin M: a growth regulator produced by differentiated histiocytic lymphoma cells.* Proc Natl Acad Sci U S A, 1986. **83**(24): p. 9739-43.
468. Fossey, S.L., et al., *Oncostatin M promotes STAT3 activation, VEGF production, and invasion in osteosarcoma cell lines.* BMC Cancer, 2011. **11**: p. 125.
469. Li, Q., et al., *Oncostatin M promotes proliferation of ovarian cancer cells through signal transducer and activator of transcription 3.* Int J Mol Med, 2011. **28**(1): p. 101-8.
470. Winder, D.M., et al., *Overexpression of the oncostatin M receptor in cervical squamous cell carcinoma cells is associated with a pro-angiogenic phenotype and increased cell motility and invasiveness.* J Pathol, 2011. **225**(3): p. 448-62.
471. Tiffen, P.G., et al., *A dual role for oncostatin M signaling in the differentiation and death of mammary epithelial cells in vivo.* Mol Endocrinol, 2008. **22**(12): p. 2677-88.
472. Benson, D.D., et al., *Activation state of stromal inflammatory cells in murine metastatic pancreatic adenocarcinoma.* Am J Physiol Regul Integr Comp Physiol, 2012. **302**(9): p. R1067-75.
473. Corcoran, R.B., et al., *STAT3 plays a critical role in KRAS-induced pancreatic tumorigenesis.* Cancer Res, 2011. **71**(14): p. 5020-9.
474. Yasuda, A., et al., *The stem cell factor/c-kit receptor pathway enhances proliferation and invasion of pancreatic cancer cells.* Mol Cancer, 2006. **5**: p. 46.
475. Yasuda, A., et al., *Stem cell factor/c-kit receptor signaling enhances the proliferation and invasion of colorectal cancer cells through the PI3K/Akt pathway.* Dig Dis Sci, 2007. **52**(9): p. 2292-300.
476. Mroczko, B., et al., *Hematopoietic cytokines in the sera of patients with pancreatic cancer.* Clin Chem Lab Med, 2005. **43**(2): p. 146-50.
477. Mroczko, B., et al., *Stem cell factor and macrophage-colony stimulating factor in patients with pancreatic cancer.* Clin Chem Lab Med, 2004. **42**(3): p. 256-60.
478. Mroczko, B., et al., *Pretreatment serum levels of hematopoietic cytokines in patients with colorectal adenomas and cancer.* Int J Colorectal Dis, 2007. **22**(1): p. 33-8.
479. Croft, M., C.A. Benedict, and C.F. Ware, *Clinical targeting of the TNF and TNFR superfamilies.* Nat Rev Drug Discov, 2013. **12**(2): p. 147-68.
480. Diaconu, N.C., et al., *Increase in CD30 ligand/CD153 and TNF-alpha expressing mast cells in*

basal cell carcinoma. Cancer Immunol Immunother, 2007. **56**(9): p. 1407-15.
481. Chiarle, R., et al., *CD30 overexpression enhances negative selection in the thymus and mediates programmed cell death via a Bcl-2-sensitive pathway.* Journal of Immunology, 1999. **163**(1): p. 194-205.
482. Florido, M., S.R. McColl, and R. Appelberg, *Delayed recruitment of lymphocytes into the lungs of CD30-deficient mice during aerogenic Mycobacterium avium infections.* Immunobiology, 2009. **214**(8): p. 643-652.
483. Nam, S.Y., et al., *CD30 supports lung inflammation.* International Immunology, 2008. **20**(2): p. 177-184.
484. Younes, A. and M.E. Kadin, *Emerging applications of the tumor necrosis factor family of ligands and receptors in cancer therapy.* J Clin Oncol, 2003. **21**(18): p. 3526-34.
485. Wu, I. and M.A. Moses, *BNF-1, a novel gene encoding a putative extracellular matrix protein, is overexpressed in tumor tissues.* Gene, 2003. **311**: p. 105-10.
486. Bootcov, M.R., et al., *MIC-1, a novel macrophage inhibitory cytokine, is a divergent member of the TGF-beta superfamily.* Proceedings of the National Academy of Sciences of the United States of America, 1997. **94**(21): p. 11514-11519.
487. Wang, X.Y., S.J. Baek, and T.E. Eling, *The diverse roles of nonsteroidal anti-inflammatory drug activated gene (NAG-1/GDF15) in cancer.* Biochemical Pharmacology, 2013. **85**(5): p. 597-606.
488. Kaur, S., et al., *Potentials of Plasma NGAL and MIC-1 as Biomarker(s) in the Diagnosis of Lethal Pancreatic Cancer.* PLoS One, 2013. **8**(2).
489. Erkan, M., et al., *The role of stroma in pancreatic cancer: diagnostic and therapeutic implications.* Nat Rev Gastroenterol Hepatol, 2012. **9**(8): p. 454-67.
490. Vonderheide, R.H. and L.J. Bayne, *Inflammatory networks and immune surveillance of pancreatic carcinoma.* Curr Opin Immunol, 2013.
491. Saeys, Y., I. Inza, and P. Larranaga, *A review of feature selection techniques in bioinformatics.* Bioinformatics, 2007. **23**(19): p. 2507-2517.
492. Simon, R., *Supervised analysis when the number of candidate features (p) greatly exceeds the number of cases (n).* SIGKDD Explor. Newsl., 2003. **5**: p. 31-36.
493. Seliger, B. and D. Quandt, *The expression, function, and clinical relevance of B7 family members in cancer.* Cancer Immunol Immunother, 2012. **61**(8): p. 1327-41.
494. Chen, L., et al., *Tumor immunogenicity determines the effect of B7 costimulation on T cell-mediated tumor immunity.* J Exp Med, 1994. **179**(2): p. 523-32.
495. Wang, L., et al., *Clinical significance of B7-H1 and B7-1 expressions in pancreatic carcinoma.* World J Surg, 2010. **34**(5): p. 1059-65.
496. Wang, L., et al., *Immune sculpting of norepinephrine on MHC-I, B7-1, IDO and B7-H1 expression and regulation of proliferation and invasion in pancreatic carcinoma cells.* PLoS One, 2012. **7**(9): p. e45491.
497. LeCouter, J., et al., *Identification of an angiogenic mitogen selective for endocrine gland endothelium.* Nature, 2001. **412**(6850): p. 877-84.
498. Balu, S., et al., *The immunohistochemical expression of endocrine gland-derived-VEGF (EG-VEGF) as a prognostic marker in ovarian cancer.* Rom J Morphol Embryol, 2012. **53**(3): p. 479-83.
499. Nagano, H., et al., *Endocrine gland-derived vascular endothelial growth factor (EG-VEGF) expression in colorectal cancer.* J Surg Oncol, 2007. **96**(7): p. 605-10.
500. Pasquali, D., et al., *The endocrine-gland-derived vascular endothelial growth factor (EG-VEGF)/prokineticin 1 and 2 and receptor expression in human prostate: Up-regulation of EG-VEGF/prokineticin 1 with malignancy.* Endocrinology, 2006. **147**(9): p. 4245-51.
501. Li, Q., et al., *Correlation of four vascular specific growth factors with carcinogenesis and portal vein tumor thrombus formation in human hepatocellular carcinoma.* J Exp Clin Cancer Res, 2006. **25**(3): p. 403-9.

502. Jiang, X., et al., *Pancreatic islet and stellate cells are the main sources of endocrine gland-derived vascular endothelial growth factor/prokineticin-1 in pancreatic cancer.* Pancreatology, 2009. **9**(1-2): p. 165-72.
503. Ngan, E.S., et al., *Implications of endocrine gland-derived vascular endothelial growth factor/prokineticin-1 signaling in human neuroblastoma progression.* Clin Cancer Res, 2007. **13**(3): p. 868-75.
504. Brouillet, S., et al., *EG-VEGF: a key endocrine factor in placental development.* Trends Endocrinol Metab, 2012. **23**(10): p. 501-8.
505. Kotenko, S.V., *IFN-lambdas.* Curr Opin Immunol, 2011. **23**(5): p. 583-90.
506. Maher, S.G., et al., *IFNalpha and IFNlambda differ in their antiproliferative effects and duration of JAK/STAT signaling activity.* Cancer Biol Ther, 2008. **7**(7): p. 1109-15.
507. Donnelly, R.P. and S.V. Kotenko, *Interferon-lambda: a new addition to an old family.* J Interferon Cytokine Res, 2010. **30**(8): p. 555-64.
508. Novak, A.J., et al., *A role for IFN-lambda1 in multiple myeloma B cell growth.* Leukemia, 2008. **22**(12): p. 2240-6.
509. Falls, D.L., *Neuregulins: functions, forms, and signaling strategies.* Exp Cell Res, 2003. **284**(1): p. 14-30.
510. Hayes, N.V. and W.J. Gullick, *The neuregulin family of genes and their multiple splice variants in breast cancer.* J Mammary Gland Biol Neoplasia, 2008. **13**(2): p. 205-14.
511. Yen, L., et al., *Heregulin selectively upregulates vascular endothelial growth factor secretion in cancer cells and stimulates angiogenesis.* Oncogene, 2000. **19**(31): p. 3460-9.
512. Stove, C. and M. Bracke, *Roles for neuregulins in human cancer.* Clin Exp Metastasis, 2004. **21**(8): p. 665-84.
513. Kolb, A., et al., *Expression and differential signaling of heregulins in pancreatic cancer cells.* Int J Cancer, 2007. **120**(3): p. 514-23.
514. Liles, J.S., et al., *ErbB3 expression promotes tumorigenesis in pancreatic adenocarcinoma.* Cancer Biol Ther, 2010. **10**(6): p. 555-63.
515. Liles, J.S., et al., *Targeting ErbB3-mediated stromal-epithelial interactions in pancreatic ductal adenocarcinoma.* Br J Cancer, 2011. **105**(4): p. 523-33.
516. Bronckaers, A., et al., *The dual role of thymidine phosphorylase in cancer development and chemotherapy.* Med Res Rev, 2009. **29**(6): p. 903-53.
517. Liekens, S., et al., *Targeting platelet-derived endothelial cell growth factor/thymidine phosphorylase for cancer therapy.* Biochem Pharmacol, 2007. **74**(11): p. 1555-67.
518. Wang, L., et al., *Prognostic value of TP/PD-ECGF and thrombocytosis in gastric carcinoma.* Eur J Surg Oncol, 2012. **38**(7): p. 568-73.
519. Dunn, G.P., C.M. Koebel, and R.D. Schreiber, *Interferons, immunity and cancer immunoediting.* Nat Rev Immunol, 2006. **6**(11): p. 836-48.
520. ZHANG Cheng-yan, X.X., ZHANG Chun-xi, GAO Deng-sheng, *Effect of GPNMB on proliferation, apoptosis and invasion of human hepatoma cells.* Chin J Pathophysiol, 2013. **29**(8): p. 1441-1446.
521. Hua, H., et al., *Matrix metalloproteinases in tumorigenesis: an evolving paradigm.* Cell Mol Life Sci, 2011. **68**(23): p. 3853-68.
522. Rasheed, Z.A. and W. Matsui, *Biological and clinical relevance of stem cells in pancreatic adenocarcinoma.* J Gastroenterol Hepatol, 2012. **27 Suppl 2**: p. 15-8.
523. Cho, S.H., et al., *CD44 enhances the epithelial-mesenchymal transition in association with colon cancer invasion.* Int J Oncol, 2012. **41**(1): p. 211-8.
524. Mao, X.G., et al., *CDH5 is specifically activated in glioblastoma stemlike cells and contributes to vasculogenic mimicry induced by hypoxia.* Neuro-Oncology, 2013. **15**(7): p. 865-879.
525. Roland, C.L., et al., *Tumor-derived intercellular adhesion molecule-1 mediates tumor-associated leukocyte infiltration in orthotopic pancreatic xenografts.* Exp Biol Med (Maywood), 2010. **235**(2): p. 263-70.

526. Desgrosellier, J.S. and D.A. Cheresh, *Integrins in cancer: biological implications and therapeutic opportunities.* Nat Rev Cancer, 2010. **10**(1): p. 9-22.
527. Chu, W.M., *Tumor necrosis factor.* Cancer Lett, 2013. **328**(2): p. 222-5.
528. Smith, H.A. and Y. Kang, *The metastasis-promoting roles of tumor-associated immune cells.* J Mol Med (Berl), 2013. **91**(4): p. 411-29.
529. Gavalas, N.G., et al., *Angiogenesis-related pathways in the pathogenesis of ovarian cancer.* Int J Mol Sci, 2013. **14**(8): p. 15885-909.
530. Kudo-Saito, C., et al., *CCL2 is critical for immunosuppression to promote cancer metastasis.* Clinical & Experimental Metastasis, 2013. **30**(4): p. 393-405.
531. Mishra, P., D. Banerjee, and A. Ben-Baruch, *Chemokines at the crossroads of tumor-fibroblast interactions that promote malignancy.* Journal of Leukocyte Biology, 2011. **89**(1): p. 31-39.
532. Charrier, A. and D.R. Brigstock, *Regulation of pancreatic function by connective tissue growth factor (CTGF, CCN2).* Cytokine Growth Factor Rev, 2013. **24**(1): p. 59-68.
533. Bernabeu, C., J.M. Lopez-Novoa, and M. Quintanilla, *The emerging role of TGF-beta superfamily coreceptors in cancer.* Biochim Biophys Acta, 2009. **1792**(10): p. 954-73.
534. Fonsatti, E., et al., *Targeting cancer vasculature via endoglin/CD105: a novel antibody-based diagnostic and therapeutic strategy in solid tumours.* Cardiovasc Res, 2010. **86**(1): p. 12-9.
535. Van Obberghen-Schilling, E., et al., *Fibronectin and tenascin-C: accomplices in vascular morphogenesis during development and tumor growth.* Int J Dev Biol, 2011. **55**(4-5): p. 511-25.
536. Midwood, K.S., et al., *Advances in tenascin-C biology.* Cell Mol Life Sci, 2011. **68**(19): p. 3175-99.
537. Dass, K., et al., *Evolving role of uPA/uPAR system in human cancers.* Cancer Treat Rev, 2008. **34**(2): p. 122-36.
538. Okwan-Duodu, D., et al., *Angiotensin-converting enzyme and the tumor microenvironment: mechanisms beyond angiogenesis.* American Journal of Physiology-Regulatory Integrative and Comparative Physiology, 2013. **305**(3): p. R205-R215.
539. Kamohara, H., et al., *Leukemia inhibitory factor functions as a growth factor in pancreas carcinoma cells: Involvement of regulation of LIF and its receptor expression.* International Journal of Oncology, 2007. **30**(4): p. 977-983.
540. Levy, C., M. Khaled, and D.E. Fisher, *MITF: master regulator of melanocyte development and melanoma oncogene.* Trends Mol Med, 2006. **12**(9): p. 406-14.
541. Carreira, S., et al., *Mitf regulation of Dia1 controls melanoma proliferation and invasiveness.* Genes Dev, 2006. **20**(24): p. 3426-39.
542. Luo, C., et al., *MiR-101 inhibits melanoma cell invasion and proliferation by targeting MITF and EZH2.* Cancer Lett, 2013.
543. Kim, M. and S. Choe, *BMPs and their clinical potentials.* Bmb Reports, 2011. **44**(10): p. 619-634.
544. Singh, M., et al., *Homeodomain transcription factors regulate BMP-2-induced osteoactivin transcription in osteoblasts.* J Cell Physiol, 2012. **227**(1): p. 390-9.
545. Yang, X., et al., *Smad1 domains interacting with Hoxc-8 induce osteoblast differentiation.* J Biol Chem, 2000. **275**(2): p. 1065-72.
546. Kleeff, J., et al., *Bone morphogenetic protein 2 exerts diverse effects on cell growth in vitro and is expressed in human pancreatic cancer in vivo.* Gastroenterology, 1999. **116**(5): p. 1202-1216.
547. Gordon, K.J., et al., *Bone morphogenetic proteins induce pancreatic cancer cell invasiveness through a Smad1-dependent mechanism that involves matrix metalloproteinase-2.* Carcinogenesis, 2009. **30**(2): p. 238-248.
548. Yang, Z.J., et al., *Expression of bone-morphogenetic protein 2 and tumor necrosis factor alpha correlates with bone metastases in bladder urothelial carcinoma.* Ann Diagn Pathol, 2013. **17**(1): p. 51-3.

549. Wen, H., et al., *Med19 promotes bone metastasis and invasiveness of bladder urothelial carcinoma via bone morphogenetic protein 2.* Annals of Diagnostic Pathology, 2013. **17**(3): p. 259-264.
550. Kang, M.H., et al., *BMP2 accelerates the motility and invasiveness of gastric cancer cells via activation of the phosphatidylinositol 3-kinase (PI3K)/Akt pathway.* Exp Cell Res, 2010. **316**(1): p. 24-37.
551. Langenfeld, E.M., et al., *The mature bone morphogenetic protein-2 is aberrantly expressed in non-small cell lung carcinomas and stimulates tumor growth of A549 cells.* Carcinogenesis, 2003. **24**(9): p. 1445-1454.
552. Katsuno, Y., et al., *Bone morphogenetic protein signaling enhances invasion and bone metastasis of breast cancer cells through Smad pathway.* Oncogene, 2008. **27**(49): p. 6322-6333.
553. Chen, X., et al., *Activation of the PI3K/Akt pathway mediates bone morphogenetic protein 2-induced invasion of pancreatic cancer cells Panc-1.* Pathol Oncol Res, 2011. **17**(2): p. 257-61.
554. Lorente-Trigos, A., et al., *BMP signaling promotes the growth of primary human colon carcinomas in vivo.* J Mol Cell Biol, 2010. **2**(6): p. 318-32.
555. Beck, S.E. and J.M. Carethers, *BMP suppresses PTEN expression via RAS/ERK signaling.* Cancer Biol Ther, 2007. **6**(8): p. 1313-7.
556. Fong, Y.C., et al., *BMP-2 increases migration of human chondrosarcoma cells via PI3K/Akt pathway.* J Cell Physiol, 2008. **217**(3): p. 846-55.
557. Graham, T.R., et al., *PI3K/Akt-Dependent Transcriptional Regulation and Activation of BMP-2-Smad Signaling by NF-kappa B in Metastatic Prostate Cancer Cells.* Prostate, 2009. **69**(2): p. 168-180.
558. Laufer, E., et al., *Sonic Hedgehog and Fgf-4 Act through a Signaling Cascade and Feedback Loop to Integrate Growth and Patterning of the Developing Limb Bud.* Cell, 1994. **79**(6): p. 993-1003.
559. Yuasa, T., et al., *Sonic hedgehog is involved in osteoblast differentiation by cooperating with BMP-2.* Journal of Cellular Physiology, 2002. **193**(2): p. 225-232.
560. Rich, J.N., et al., *Bone-related genes expressed in advanced malignancies induce invasion and metastasis in a genetically defined human cancer model.* J Biol Chem, 2003. **278**(18): p. 15951-7.
561. Furochi, H., et al., *Osteoactivin fragments produced by ectodomain shedding induce MMP-3 expression via ERK pathway in mouse NIH-3T3 fibroblasts.* FEBS Lett, 2007. **581**(30): p. 5743-50.
562. Pintucci, G., et al., *Induction of stromelysin-1 (MMP-3) by fibroblast growth factor-2 (FGF-2) in FGF-2-/- microvascular endothelial cells requires prolonged activation of extracellular signal-regulated kinases-1 and -2 (ERK-1/2).* J Cell Biochem, 2003. **90**(5): p. 1015-25.
563. Brogley, M.A., M. Cruz, and H.S. Cheung, *Basic calcium phosphate crystal induction of collagenase 1 and stromelysin expression is dependent on a p42/44 mitogen-activated protein kinase signal transduction pathway.* J Cell Physiol, 1999. **180**(2): p. 215-24.
564. Yee, J., et al., *Identification of promoter activity and differential expression of transcripts encoding the murine stromelysin-1 gene in renal cells.* Kidney Int, 1997. **52**(1): p. 120-9.
565. Ozanne, B.W., et al., *Transcription factors control invasion: AP-1 the first among equals.* Oncogene, 2007. **26**(1): p. 1-10.
566. Lan, Y. and R. Jiang, *Sonic hedgehog signaling regulates reciprocal epithelial-mesenchymal interactions controlling palatal outgrowth.* Development, 2009. **136**(8): p. 1387-96.
567. Chung, J.S., et al., *DC-HIL is a negative regulator of T lymphocyte activation.* Blood, 2007. **109**(10): p. 4320-7.

9

ANNEXES

9.1 LIST OF FIGURES

9.2 LIST OF TABLES

9.3 RT² PROFILER™ PCR ARRAY HUMAN CANCER PATHWAY FINDER GENE TABLE

Position	*GeneBank*	*Symbol*	*Description*
A01	NM_005163	**AKT1**	*V-akt murine thymoma viral oncogene homolog 1*
A02	NM_001146	**ANGPT1**	*Angiopoietin 1*
A03	NM_001147	**ANGPT2**	*Angiopoietin 2*
A04	NM_001160	**APAF1**	*Apoptotic peptidase activating factor 1*
A05	NM_000051	**ATM**	*Ataxia telangiectasia mutated*
A06	NM_004322	**BAD**	*BCL2-associated agonist of cell death*
A07	NM_004324	**BAX**	*BCL2-associated X protein*
A08	NM_000633	**BCL2**	*B-cell CLL/lymphoma 2*
A09	NM_138578	**BCL2L1**	*BCL2-like 1*
A10	NM_007294	**BRCA1**	*Breast cancer 1, early onset*
A11	NM_001228	**CASP8**	*Caspase 8, apoptosis-related cysteine peptidase*
A12	NM_001238	**CCNE1**	*Cyclin E1*
B01	NM_001789	**CDC25A**	*Cell division cycle 25 homolog A (S. pombe)*
B02	NM_001798	**CDK2**	*Cyclin-dependent kinase 2*
B03	NM_000075	**CDK4**	*Cyclin-dependent kinase 4*
B04	NM_000389	**CDKN1A**	*Cyclin-dependent kinase inhibitor 1A (p21, Cip1)*
B05	NM_000077	**CDKN2A**	*Cyclin-dependent kinase inhibitor 2A (melanoma, p16, inhibits CDK4)*
B06	NM_003879	**CFLAR**	*CASP8 and FADD-like apoptosis regulator*
B07	NM_007194	**CHEK2**	*CHK2 checkpoint homolog (S. pombe)*
B08	NM_030582	**COL18A1**	*Collagen, type XVIII, alpha 1*
B09	NM_005225	**E2F1**	*E2F transcription factor 1*
B10	NM_004448	**ERBB2**	*V-erb-b2 erythroblastic leukemia viral oncogene homolog 2, neuro/glioblastoma derived oncogene homolog (avian)*
B11	NM_005239	**ETS2**	*V-Ets erythroblastosis virus E26 oncogene homolog 2 (avian)*
B12	NM_000043	**FAS**	*Fas (TNF receptor superfamily, member 6)*
C01	NM_000141	**FGFR2**	*Fibroblast growth factor receptor 2*
C02	NM_005252	**FOS**	*FBJ murine osteosarcoma viral oncogene homolog*
C03	NM_006144	**GZMA**	*Granzyme A (granzyme 1, cytotoxic T-lymphocyte-associated serine esterase 3)*
C04	NM_006410	**HTATIP2**	*HIV-1 Tat interactive protein 2, 30kDa*

C05	NM_024013	**IFNA1**	*Interferon, alpha 1*
C06	NM_002176	**IFNB1**	*Interferon, beta 1, fibroblast*
C07	NM_000618	**IGF1**	*Insulin-like growth factor 1 (somatomedin C)*
C08	NM_000584	**IL8**	*Interleukin 8*
C09	NM_181501	**ITGA1**	*Integrin, alpha 1*
C10	NM_002203	**ITGA2**	*Integrin, alpha 2 (CD49B, alpha 2 subunit of VLA-2 receptor)*
C11	NM_002204	**ITGA3**	*Integrin, alpha 3 (antigen CD49C, alpha 3 subunit of VLA-3 receptor)*
C12	NM_000885	**ITGA4**	*Integrin, alpha 4 (antigen CD49D, alpha 4 subunit of VLA-4 receptor)*
D01	NM_002210	**ITGAV**	*Integrin, alpha V (vitronectin receptor, alpha polypeptide, antigen CD51)*
D02	NM_002211	**ITGB1**	*Integrin, beta 1 (fibronectin receptor, beta polypeptide, antigen CD29 includes MDF2, MSK12)*
D03	NM_000212	**ITGB3**	*Integrin, beta 3 (platelet glycoprotein IIIa, antigen CD61)*
D04	NM_002213	**ITGB5**	*Integrin, beta 5*
D05	NM_002228	**JUN**	*Jun proto-oncogene*
D06	NM_002755	**MAP2K1**	*Mitogen-activated protein kinase kinase 1*
D07	NM_006500	**MCAM**	*Melanoma cell adhesion molecule*
D08	NM_002392	**MDM2**	*Mdm2 p53 binding protein homolog (mouse)*
D09	NM_000245	**MET**	*Met proto-oncogene (hepatocyte growth factor receptor)*
D10	NM_002421	**MMP1**	*Matrix metallopeptidase 1 (interstitial collagenase)*
D11	NM_004530	**MMP2**	*Matrix metallopeptidase 2 (gelatinase A, 72kDa gelatinase, 72kDa type IV collagenase)*
D12	NM_004994	**MMP9**	*Matrix metallopeptidase 9 (gelatinase B, 92kDa gelatinase, 92kDa type IV collagenase)*
E01	NM_004689	**MTA1**	*Metastasis associated 1*
E02	NM_004739	**MTA2**	*Metastasis associated 1 family, member 2*
E03	NM_014751	**MTSS1**	*Metastasis suppressor 1*
E04	NM_002467	**MYC**	*V-myc myelocytomatosis viral oncogene homolog (avian)*
E05	NM_003998	**NFKB1**	*Nuclear factor of kappa light polypeptide gene enhancer in B-cells 1*
E06	NM_020529	**NFKBIA**	*Nuclear factor of kappa light polypeptide gene enhancer in B-cells inhibitor, alpha*
E07	NM_000269	**NME1**	*Non-metastatic cells 1, protein (NM23A) expressed in*
E08	NM_005009	**NME4**	*Non-metastatic cells 4, protein expressed in*
E09	NM_002607	**PDGFA**	*Platelet-derived growth factor alpha polypeptide*

E10	NM_002608	**PDGFB**	*Platelet-derived growth factor beta polypeptide*
E11	NM_181504	**PIK3R1**	*Phosphoinositide-3-kinase, regulatory subunit 1 (alpha)*
E12	NM_002658	**PLAU**	*Plasminogen activator, urokinase*
F01	NM_002659	**PLAUR**	*Plasminogen activator, urokinase receptor*
F02	NM_002687	**PNN**	*Pinin, desmosome associated protein*
F03	NM_002880	**RAF1**	*V-raf-1 murine leukemia viral oncogene homolog 1*
F04	NM_000321	**RB1**	*Retinoblastoma 1*
F05	NM_002961	**S100A4**	*S100 calcium binding protein A4*
F06	NM_002639	**SERPINB5**	*Serpin peptidase inhibitor, clase B (ovalbumin), member 5*
F07	NM_000602	**SERPINE1**	*Serpin peptidase inhibitor, clase E (nexin, plasminogen activator inhibitor type 1), member 1*
F08	NM_003087	**SNCG**	*Synuclein, gamma (breast cancer-specific protein 1)*
F09	NM_003177	**SYK**	*Spleen tyrosine kinase*
F10	NM_000459	**TEK**	*TEK tyrosine kinase, endothelial*
F11	NM_198253	**TERT**	*Telomerase reverse transcriptase*
F12	NM_000660	**TGFB1**	*Transforming growth factor, beta 1*
G01	NM_004612	**TGFBR1**	*Transforming growth factor, beta receptor 1*
G02	NM_003246	**THBS1**	*Thrombospondin 1*
G03	NM_003254	**TIMP1**	*TIMP metallopeptidase inhibitor 1*
G04	NM_000362	**TIMP3**	*TIMP metallopeptidase inhibitor 3*
G05	NM_000594	**TNF**	*Tumor necrosis factor*
G06	NM_003842	**TNFRSF10B**	*Tumor necrosis factor receptor superfamily, member 10b*
G07	NM_001065	**TNFRSF1A**	*Tumor necrosis factor receptor superfamily, member 1A*
G08	NM_003790	**TNFRSF25**	*Tumor necrosis factor receptor superfamily, member 25*
G09	NM_000546	**TP53**	*Tumor protein p53*
G10	NM_000474	**TWIST1**	*Twist homolog 1 (Drosophila)*
G11	NM_017549	**EPDR1**	*Ependymin related protein 1 (zebrafish)*
G12	NM_003376	**VEGFA**	*Vascular endothelial growth factor A*
H01	NM_004048	**B2M**	*Beta-2-microglobulin*
H02	NM_000194	**HPRT1**	*Hypoxanthine phosphoribosyltransferase 1*
H03	NM_012423	**RPL13A**	*Ribosomal protein L13a*
H04	NM_002046	**GAPDH**	*Glyceraldehyde-3-phosphate dehydrogenase*
H05	NM_001101	**ACTB**	*Actin, beta*
H06	SA_00105	**HGDC**	*Human Genomic DNA Contamination*
H07	SA_00104	**RTC**	*Reverse Transcription Control*
H08	SA_00104	**RTC**	*Reverse Transcription Control*
H09	SA_00104	**RTC**	*Reverse Transcription Control*

H10	SA_00103	**PPC**	*Positive PCR Control*
H11	SA_00103	**PPC**	*Positive PCR Control*
H12	SA_00103	**PPC**	*Positive PCR Control*

9.4 OTHER GENES ANALYZED

GeneBank	*Symbol*	*Description*
NM_000789	**ACE**	*Angiotensin I converting enzyme (peptidyl-dipeptidase A) 1*
NM_004049	**BCL2A1**	*BCL2-related protein A1*
NM_001196	**BID**	*BH3 interacting domain death agonist*
NM_001165	**BIRC3**	*Baculoviral IAP repeat containing 3*
NM_002982	**CCL2**	*Chemokine (C-C motif) ligand 2*
NM_002985	**CCL5**	*Chemokine (C-C motif) ligand 5*
NM_000610	**CD44**	*CD44 molecule (Indian blood group)*
NM_001795	**CDH5**	*Cadherin 5, type 2 (vascular endothelium)*
NM_003879	**CFLAR**	*CASP8 and FADD-like apoptosis regulator*
NM_001901	**CTGF**	*Connective tissue growth factor*
NM_000501	**ELN**	*Elastin*
NM_000118	**ENG**	*Endoglin*
NM_002006	**FGF2**	*Fibroblast growth factor 2 (basic)*
NM_002026	**FN1**	*Fibronectin 1*
NM_000201	**ICAM1**	*Intercellular adhesion molecule 1*
NM_002203	**ITGA2**	*Integrin, alpha 2 (CD49B, alpha 2 subunit of VLA-2 receptor)*
NM_002205	**ITGA5**	*Integrin, alpha 5 (fibronectin receptor, alpha polypeptide)*
NM_000887	**ITGAX**	*Integrin, alpha X (complement component 3 receptor 4 subunit)*
NM_000211	**ITGB2**	*Integrin, beta 2 (complement component 3 receptor 3 and 4 subunit)*
NM_002309	**LIF**	*Leukemia inhibitory factor (cholinergic differentiation factor)*
NM_002422	**MMP3**	*Matrix metallopeptidase 3 (stromelysin 1, progelatinase)*
NM_002607	**PDGFA**	*Platelet-derived growth factor alpha polypeptide*
NM_002608	**PDGFB**	*Platelet-derived growth factor beta polypeptide*
NM_002575	**SERPINB2**	*Serpin peptidase inhibitor, clade B (ovalbumin), member 2*
NM_000602	**SERPINE1**	*Serpin peptidase inhibitor, clade E (nexin, plasminogen activator inhibitor type 1), member 1*
NM_002160	**TNC**	*Tenascin C*
NM_000594	**TNF**	*Tumor necrosis factor*
NM_001078	**VCAM1**	*Vascular cell adhesion molecule 1*
NM_003376	**VEGFA**	*Vascular endothelial growth factor A*

9.5 LIST OF CONTRIBUTIONS

9.5.1 ARTICLES

- **C. Torres**, S. Perales, M.J Alejandre, J. Iglesias, R. Palomino; O. Caba, J.C Prados, A. Aránega, J.R Delgado, A. Irigoyen, F. M. Ortuño I. Rojas, and A. Linares. *"Serum cytokine profile in patients with pancreatic cancer."* Pancreas. Submitted and under second revision (manuscript number Pancreas 13315)

- **C. Torres**, S. Perales, M.J Alejandre, J. Iglesias, R. Palomino; O. Caba, J.C Prados, A. Aránega, J.R Delgado, A. Irigoyen, F. M. Ortuño I. Rojas, and A. Linares. *"Prognosis relevance of serum cytokines in pancreatic cancer."* Submitted and under revision (Manuscript Number PANCREAS 13316)

- O. Caba, J Prados, R. Ortiz, C. Melguizo, C. Jiménez, P. J. Álvarez, J. R. Delgado, A. Irigoyen, I. Rojas, J. P. Florido, S. Perales, **C. Torres**, A. Linares and A. Aránega. "Transcriptional Profiling of Peripheral Blood in Pancreatic Ductal Adenocarcinoma Patients Identifies Potential Diagnostic Biomarkers." American Journal of Gastroenterology. Submitted and under revision (Manuscript Number AJG-13-0544).

9.5.2 PATENTS

- Título: BIOMARCADORES, MÉTODO Y KIT PARA EL DIAGNÓSTICO TEMPRANO DEL ADENOCARCINOMA DUCTAL DE PÁNCREAS
  Inventores: **C. Torres**, S. Perales, M.J Alejandre, J. Iglesias, R. Palomino, O. Caba, J.C Prados, A. Aránega, J.R Delgado, A. Irigoyen, A. Linares.
  Oficina de patente: OEPM Madrid
  Número de solicitud: P201330897
  Número de concesión: Fecha de prioridad: 14 junio 2013, 15:49 (CEST)

- Título: MÉTODO DE OBTENCIÓN DE DATOS ÚTILES PARA PREDECIR O PRONOSTICAR LA RESPUESTA AL TRATAMIENTO DE LOS PACIENTES CON CÁNCER DE PÁNCREAS
  Inventores: **C. Torres**, S. Perales, M.J Alejandre, J. Iglesias, R. Palomino, O. Caba, J.C Prados, A. Aránega, J.R Delgado, A. Irigoyen, A. Linares.
  Oficina de patente: OEPM Madrid
  Número de solicitud: P201330896
  Número de concesión: Fecha de prioridad: 14 junio 2013, 15:22 (CEST)
  Entidad titular:
  Entidad que la explota:

- Título: MÉTODO DE OBTENCIÓN DE DATOS ÚTILES PARA EL DIAGNÓSTICO, PRONÓSTICO Y PREDICCIÓN DE RESPUESTA AL TRATAMIENTO DE ADENOCARCINOMA DE PÁNCREAS
  Inventores: **C. Torres**, S. Perales, M.J Alejandre, J. Iglesias, R. Palomino, O. Caba, J.C Prados, A. Aránega, J.R Delgado, A. Irigoyen, A. Linares.
  Oficina de patente: OEPM Madrid
  Número de solicitud: P201231761
  Número de concesión: Fecha de prioridad: 14 NOVIEMBRE 2012.
  Entidad titular:
  Entidad que la explota: